LBNL-39518
UC-000

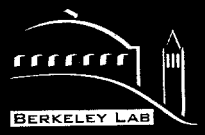

ERNEST ORLANDO LAWRENCE
BERKELEY NATIONAL LABORATORY

Hydrological and Geochemical Investigations of Selenium Behavior at Kesterson Reservoir

P.T. Zawislanski, T.K. Tokunaga, S.M. Benson,
P.W. Johannis, M. Zavarin, C. Wahl, T. Sears,
J. Kengsoontra, L. Tsao, J. Oldfather, and A.W. Yee
Earth Sciences Division

May 1995

LBNL - 39518
UC - 000

HYDROLOGICAL AND GEOCHEMICAL INVESTIGATIONS OF SELENIUM BEHAVIOR AT KESTERSON RESERVOIR

Progress Report

October 1, 1992 through September 30, 1994

Peter T. Zawislanski, Tetsu K. Tokunaga, Sally M. Benson, Paul W. Johannis, Mavrik Zavarin, Carolyn Wahl, Tobin Sears, Jenny Kengsoontra, Leon Tsao, Joan Oldfather, and Andy W. Yee

Earth Sciences Division
Lawrence Berkeley Laboratory
University of California
Berkeley, CA 94720

May 1995

This work was supported by the U.S. Bureau of Reclamation, under U.S. Department of Interior Interagency Agreement 9-AA-20-20, through U.S. Department of Energy Contract No. DE-AC03-76SF00098.

Table of Contents

List of Figures

List of Tables

Acknowledgments

We thank Mike Delamore, Art Tuma, and Bill Greer of the U.S. Bureau of Reclamation for their continued support. We also thank Robert Giauque of Lawrence Berkeley Laboratory for providing chemical analyses; George Hanna and Brenda Royce of California State University, Fresno, for chemical analyses; Mark L. Rivers (Center for Advanced Radiation Sources, The University of Chicago), and the staff at NSLS; George Parks, John Bargar, Singfoong Cheah, Andrea Foster, Ping Liu, Maria Peterson, Hillary Thompson, and Ning Xu of Stanford University for help with data collection, P. Frank and S. Shadle for assistance in obtaining Se standards, and Graham George for helpful discussions and access to his XAS edge-fitting software; Steve Flexser and Jiamin Wan of Lawrence Berkeley Laboratory for helpful comments on the Chapters 3 and 4; Joan Macy of UC Davis and Doug Lipton of Levine•Fricke Inc. for reviews of Chapter 6; Kesterson Field Office personnel for assistance in field activities; Gamani Jayaweera of UC Davis for assistance in sample collection in Pond 2.

The bulk of this work was carried out under U.S. Department of Energy Contract No. DE-AC03-76SF00098, with additional funding under contracts DE-FG02-92BR14244 (SRS), and DE-AC02-76CH00016 (Brookhaven National Laboratory). Research was in part carried out at the National Synchrotron Light Source (NSLS), Brookhaven National Laboratory, which is supported by the U.S. Department of Energy, Division of Materials Sciences and Division of Chemical Sciences, and at the Stanford Synchrotron Radiation Laboratory, which is operated by the DOE, Office of Basic Energy Sciences and is supported by the NIH, Biomedical Research Technology Program, Division of Research Resources.

1.0 Executive Summary

This report describes research relevant to selenium speciation, fractionation, physical redistribution, reduction and oxidation, and spatial distribution as related to Kesterson Reservoir. The work was carried out by scientists and engineers from the Earth Sciences Division of the Lawrence Berkeley Laboratory over a two year period from October 1992 to September 1994. Much of the focus of these efforts was on the effects of two above-average rainfall years (1991/1992 and 1992/1993). These events marked a departure from the previous six years of drought conditions, under which oxidation of Se in the soil profile led to a marked increase in soluble Se. Evidence from the last two years shows that much of the re-oxidized Se was once more reduced due to increased soil moisture content. Also, in areas of high hydraulic conductivity, major vertical displacement of selenium and other solutes due to rainfall infiltration was observed. Such observations underscore the dependence of the future of Se speciation and distribution on environmental conditions.

Chapter 2 contains descriptions of field monitoring of soil processes. This work is primarily a continuation of ongoing monitoring efforts.

In **Section 2.1**, elevated Se concentrations observed in groundwater in the northern part of Pond 9 are investigated. Based on correlations between salinity and Se and rainfall events, it is concluded that in areas of very high hydraulic conductivity, Se and salts can be driven deep into the soil profile and into the groundwater by infiltrating rainwater.

The monitoring of upland areas is described in **Section 2.2**. Continued monitoring of the soluble Se inventory showed Se reduction following the 1992 rainfall events but an increase in soluble Se in 1993 despite even higher rainfall. This result is not easily accounted for, although it stresses the importance of re-oxidation. The proliferation of annual grasses was observed following two years of above-average rainfall.

Physical and chemical redistribution of Se at a filled site in Pond 5 is examined in **Section 2.3**. Pre-1992 trends were ones of Se oxidation and movement into the fill material as a result of evapotranspirative fluxes and diffusion. Following the 1992 and 1993 rains, the Se inventory was reduced and displaced deeper into the soil profile due to higher moisture content and rainfall infiltration, respectively.

In **Section 2.4**, Se and Cl redistribution in sites in Ponds 8 and 9 are examined, with the findings that the 1992 and 1993 rains resulted in the downward displacement of Se and Cl to depths of 0.3 m to below 1.0 m, depending on soil texture. It appears that in areas where soil texture is fine, Se reduction prevents Se displacement to great depths. Similar to findings in

other ponds, the 1992 rainstorms resulted in a more reduced Se inventory than the 1993 rainstorms, despite the greater total rainfall in 1993. An analysis of near-surface soils showed that nearly all Cl was flushed out in 1992, while soluble Se concentrations were reduced to 1988 levels or lower.

Reservoir-wide monitoring of Se, sulfate, and chloride continued and is described in **Section 2.5**. Following a significant decline in total Se in the top 0.15 m of soil from 1989 to 1992, 1993 concentrations were the same as in 1989. Similarly, water-extractable Se and sulfate concentrations increased in 1993. Comparison by habitat showed that the only statistically significant changes in total Se in the Fill and Grassland habitats occurred in 1992 (decline), while in the Open habitat, there was an increase in 1993. Although statistically significant, changes in water-extractable Se were very small in the Fill habitat. In the Grassland habitat, a decreasing trend was observed, while significant fluctuations in the Open habitat did not follow a significant trend, except a marked decline in 1992, likely the result of rainfall infiltration.

Chapters 3 and 4 contain descriptions of experiments utilizing synchrotron X-ray fluorescence microprobe (SXRFM) and absorption spectroscopy (XANES) respectively, to study distribution and speciation of Se on intact samples of soil and plant material. In **Chapter 3**, the former method exposed, in soil samples, localized zones on the scale of 1 mm with significantly elevated levels of Se, indicative of the presence of Se(0) and other solid Se forms. Because of such localization, oxidation rates may be limited by reactions at solid phase surfaces. The presence of such reduced zones around root material shows the importance of decomposing organic matter in Se reduction on a scale of 1 mm. In **Chapter 4**, a laboratory experiment is described, in which Se partitioning and transformations in ponded sediments are observed and modeled. Reduction to elemental Se (as confirmed using X-ray absorption spectroscopy) was found to occur in the top few millimeters of the sediment. Extremely large gradients in Se concentrations on the scale of 1 mm at the sediment surface (as observed via X-ray microprobe analysis) indicate the need for such resolution in order to carry out mechanistic diffusion-redox analyses of such processes.

Results of soil and soil-water monitoring in the Pond 2 Microbial Volatilization Pilot-Scale plot are presented in **Chapter 5**. Agreement between soluble Se and salinity trends suggests that large concentrations of Se have been displaced downward during rain events. The relatively coarser nature of sediments in this area allows for fast transport and Se can be displaced before it is chemically reduced. Soluble Se concentrations in the soil profile are high enough (on the order of 10 ppm) that flushing of pore waters results in measurable declines in the total Se inventory at the soil surface. However, not all of the observed declines in total Se can be accounted for in this fashion and are therefore likely the result of methylation of Se.

Chapter 6 contains the description of experiments designed to accelerate Se transformation rates in soils, for the purpose of estimating such rates and the likely future fractionation of Se. Incubation and sequential extraction of soils showed that the predominant change was the oxidation of refractory Se (primarily Se(0), as shown via X-ray absorption spectroscopy) to selenate under aerobic conditions. Organically-associated Se was also oxidized, but at a slower rate. No losses of total-Se were observed, indicating the relative insignificance of methylation. An apparent plateau in oxidation of the refractory pool suggests heterogeneity of this pool, with some components more readily oxidized than others. In soils incubated at or near saturation, Se was readily reduced. In soils which were exposed to varying moisture and temperature conditions, Se went through oxidation and reduction cycles, with a small but significant net oxidation trend. Over periods of years to decades, currently immobile and leach-resistant Se may become available to the biological system, dependent on field moisture conditions.

The formation of ephemeral pools is examined in **Chapter 7**. It is found that during above-average rainfall years, more than 10% of Kesterson Reservoir may become flooded, as occurred in 1992. Se concentrations were highest in unfilled lowland areas (occasionally up to 500 ppb), but these were primarily research/monitoring sites which comprise a very small areal percentage of the Reservoir. Many of these sites will be filled in the near future. Most measurements in filled areas revealed Se concentrations below 5 ppb, with concentrations occasionally up to 50 ppb. In upland areas, which comprise 15% of the Reservoir, similar ranges of Se concentrations were observed. Recommendations are made to fill in specific areas and to continue regular monitoring at about twenty locations.

The ongoing analytical quality control program is described in **Chapter 8**. This includes the methods for monitoring the performance of both the analytical instrument and the analyst, through the use of blanks, standards, spikes, and duplicates. Selenium standard statistics are presented.

In addition to this report, the following articles have been either published or submitted for publication over the past two years:

- Benson, S.M., T.K. Tokunaga, P.T. Zawislanski, and C. Wahl. 1994. Mechanisms and rates of selenium remobilization and transport in selenium-contaminated soils. Abstract presented at The I&EC Special Symposium, American Chemical Society, Atlanta GA, September 19-21, 1994.

- Benson, S.M., T.K. Tokunaga, P.T. Zawislanski, and C. Wahl. 1994. Mechanisms and rates of selenium remobilization and transport in selenium-contaminated soils. Submitted to American Chemical Society, 1994.

- Frankenberger, W.T., Jr., and S.M. Benson, (eds.). 1994. Selenium in the Environment. Marcel Dekker, Inc. New York.

• Sutton, S.R., S. Bajt, D. Schulze, and T. Tokunaga. 1994. Oxidation state mapping using x-ray absorption near edge structure with synchrotron microbeams. Abstract presented at Am. Geophys. Union, Fall 1994 Meeting, San Francisco, CA.

• Tokunaga, T.K., I.J. Pickering, and G.E. Brown, Jr.. 1995. X-ray absorption spectroscopy studies of selenium transformations in ponded sediments. Submitted to Soil Sci. Soc. Am. J..

• Tokunaga, T.K., S.R. Sutton, and S. Bajt. 1994. Mapping of selenium concentrations in soil aggregates with synchrotron x-ray fluorescence microprobe. Soil Sci. 158:421-434.

• Tokunaga, T.K., S.R. Sutton, and S. Bajt. 1994. Reduction and diffusion of selenium in soil aggregates: Synchrotron X-ray fluorescence microprobe studies of intra-aggregate chemical heterogeneity formation. Am. Geophys. Union, Chapman Conference on Hydrogeologic Processes: Building and Testing Atomistic- to Basin-scale Models. Lincoln, New Hampshire, June, 1994.

• Tokunaga, T.K, P.T. Zawislanski, P.W. Johannis, S. Benson, and D.S. Lipton. 1994. Field investigations of selenium speciation, transformation, and transport in soils from Kesterson Reservoir and Lahontan Valley. In, Selenium in the Environment. W.T. Frankenberger and S. Benson, eds. Marcel Dekker. New York. pp. 119-138.

• Zawislanski, P.T. and M. Zavarin. 1995. Nature and rates of selenium transformations in soils: A laboratory study. Submitted to Soil Sci. Soc. Am. J..

1.1 Recommendations

Given the results of field and laboratory research, a number of recommendations regarding the future management and further investigations of Kesterson Reservoir are made. Broad conclusions are stated, followed by specific recommendations which will help design an effective management strategy.

• Changes in mean total Se concentrations occur very slowly, on the order of a few percent per year. There may be a few scattered sites in which high organic content and favorable moisture conditions, combined with relatively high Se concentrations result in accelerated selenium methylation rates. However, by and large, annual changes in total Se concentrations are smaller than analytical uncertainty.

⇒ *It is recommended, that for the purpose of tracking long-term changes in total Se, a two-year sampling interval be adopted.*

• Although changes in total Se are slow, reduction and oxidation of Se species can be observed over an annual cycle. These changes are strongly influenced by the magnitude and patterns of precipitation. As was the result of heavy rainfall in recent years, Se, which was slowly oxidized

over a number of dry years, was reduced over periods of days as a result of rainfall infiltration and ponding. This has profound implications for the timing of synoptic soil sampling for the purpose of Se speciation.

⇒ *Synoptic soil sampling for the purpose of Se speciation should continue be conducted in the summer in order to minimize the effects of rainfall.*

• A small number of areas within the Reservoir is more susceptible to rainwater infiltration due to coarser texture of sediments, e.g. the northern parts of Pond 9 and Pond 2. This may result in downward displacement of Se toward the water table. However, research has shown that Se is quickly reduced under saturated conditions, thereby severely limiting Se concentrations in shallow groundwater.

⇒ *Groundwater under areas characterized as having high saturated conductivity should continue to be monitored on a seasonal basis. Should Se be found to be increasing in the groundwater, these areas may be filled with lower conductivity soil, or "capped." Nonetheless, the percentage of these areas, relative to the total area of the Reservoir is very small.*

• Periodic ponding of certain areas has been observed. The ponds are a direct result of rainfall: less than 1% of the Reservoir is below the elevation of the highest level of the regional groundwater table. Se concentrations in ephemeral pools are controlled more by the rate of Se dissolution from the soil surface and less by Se concentrations in the vadose zone. Therefore, areas in which surface-Se concentrations are high, tend to have higher ephemeral pool Se concentrations. However, as water is ponded, reducing conditions near the soil surface severely limit the amount of soluble Se. As a result, most ephemeral pool-Se concentrations are below 10 ppb.

⇒ *Since they are the most direct path for Se ingestion by water-fowl, ephemeral pools should continue to be monitored. This applies to pools formed on fill areas, as dissolved Se concentrations have been increasing relative to original Se concentrations in the fill material.*

⇒ *A small number of areas susceptible to ponding with elevated concentrations of Se, should be filled. In particular, former research sites in Ponds 1 (LBL "UZ" sites), 6 (LBL sites P6S6*

and P6S12), 8 (LBL site 8EP), 9 (LBL sites 9C, 9D, 9R, and 9BE), 10 (LBL sites GC, GS) and 11 (UCR).

⇒ *Aerial photography of the Reservoir during the winter and spring should be conducted in order to better estimate the extent of flooding.*

• Long-term re-oxidation of Se will depend to a great degree upon the precipitation pattern. Field and laboratory experiments have shown comparable oxidation rates under dry conditions. However, near-surface soils are easily reduced during and subsequent to rainfall events and especially during ponding. Therefore, long-term trends are not easy to predict.

⇒ *Selected field sites with a long history of monitoring should continue to be maintained, with a focus on Se remobilization as influenced by moisture content. This should include a variety of environments, both filled and unfilled.*

⇒ *Special attention should be paid to areas with high Se concentrations near the soil surface. Should there be a prolonged period of dry weather, followed by heavy rains, ephemeral pools in these areas are likely to exhibit high dissolved Se concentrations.*

2.0 Vadose Zone Monitoring

The following sections describe efforts in soil monitoring at previously established field sites. These include sites in Pond 5, Pond 8, Pond 9, Pond 11, as well as Reservoir-wide monitoring of near-surface soils and soil water. General layout of these sites is shown in Fig. 2.0.1.

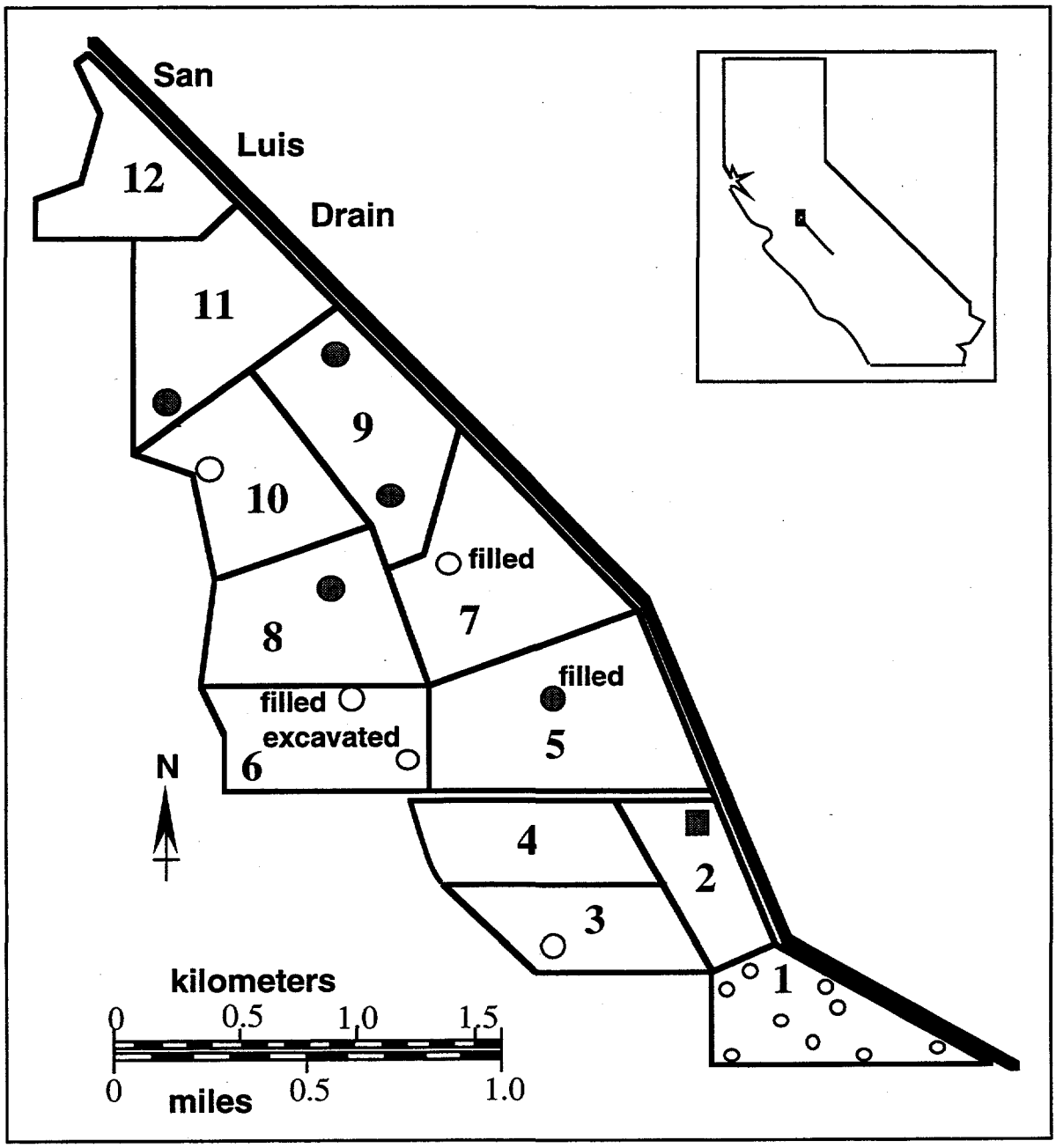

Figure 2.0.1. Distribution of sites described in Chapter 2. See maps within each section for detail.

2.1 Deeper Soil Pore Waters from the Northern Pond 9 Monitoring Area

Tetsu Tokunaga and Paul Johannis
Earth Sciences Division
Lawrence Berkeley Laboratory

In recent years, USBR shallow groundwater monitoring activities have revealed some large periodic increases and decreases in Se concentrations within a limited number of shallow wells (USBR, Kesterson Reservoir 1994 Annual Report). One of the three locations at which such observations were made is in the northern Pond 9 area. (The other two sites at which elevated Se concentrations have been measured are (i) at the intersections of Ponds 2, 3, and 4, and (ii) at the southeast corner of Pond 1.) In view of these findings, more detailed information on soluble Se distributions in deeper soil profiles from the northern Pond 9 monitoring area was obtained in order to improve understanding of Se transport from soils into shallow groundwater. This effort consisted of continued monitoring of existing soil water samplers and installation-monitoring of a new, deeper set of samplers.

2.1.1 Site Description

Soil profile monitoring in a former playa environment in the northern portion of Pond 9 began in February of 1987, about one year after this area last received drainage waters. Locations of LBL soil profile monitoring sites and USBR shallow groundwater monitoring wells (DH9 series) in this area are shown in Figure 2.1.1. The northern Pond 9 study area has recently been supplemented with additional instrumentation to provide information on deeper soil profile and shallow groundwater Se concentrations. A new monitoring site, P9L, provides soil water and shallow groundwater samples at approximately 0.50 m depth intervals down to 3.25 m below the soil surface (Figure 2.1.2). It is located directly between the DH9-5 and DH9-8 wells, which have yielded the highest shallow groundwater Se concentrations from the northern Pond 9 area. The P9L site includes duplicate sets of samplers and tensiometers, and moisture monitoring with a neutron probe. The deeper samplers, centered at the 2.25, 2.75, and 3.25 m depths, are stainless steel drive-point pipes with 0.15 m screened lengths. Based on previous water table records, the 2.75 m and 3.25 m deep samplers are expected to always remain below the water table, while the 2.25 m drive-point sampler is expected to experience short periods of time above the water table. A second set of drive-point samplers (P9M) was installed adjacent to well DH9-5, at depths of 2.30, 2.80, and 3.30 m (Figure 2.2.1).

The depth to groundwater at this former playa area typically varies between about 1.0 and 2.4 m. Seasonal variations in water table elevations measured in well DH9-3 are shown in Figure

2.1.2. The earliest data (1987 to early 1988) include influences of drawdown from pumping of shallow groundwater along a short, northern section of the San Luis Drain (bordering Ponds 5, 7, 9, 11, and 12). The local groundwater was pumped for the purpose of maintaining portions of Kesterson Reservoir (Ponds 1, 2, 5, and 7) flooded with non-seleniferous waters during the interval between termination of drain water deliveries and final de-watering of ponds. During drought years (1988 to 1991), the water table fluctuated between depths of 1.2 to 2.5 m below the soil surface. Note that the water table reached the soil surface during the winters of 1992 and 1993. These years brought above-average rainfalls of 320 mm and 420 mm respectively. The well from which these data were obtained is located in the northern Pond 9 soil monitoring area which would otherwise have been covered with about 0.1 m of fill soil. Also note that the late summer maximum depth of the water table returned to near normal levels in 1992, while it remained about 0.38 m (15 inches) higher in 1993. The shallower depths to groundwater in the summer of 1993 probably resulted from the combined influence of much higher than average rainfall and expansion of wetlands within Kesterson National Wildlife Refuge, a short distance (about 0.5 km, 0.3 mile) to the east.

The shallow groundwater in the northern Pond 9 area is monitored by the USBR through the DH9 series wells. Wells #2, 3, 5, and 8 of the DH9 series are screen over the 3.0-4.6 m (10 to 15 ft). Wells #1, 4, 6, and 7 of the DH9 series are screen over the 7.6-9.2 m (25 to 30 ft) depths. Following the 1992 wet season, the USBR monitoring program reported elevated concentrations of Se in these shallow wells. A recent summary of data from these wells is included in the Appendix D of the USBR 1994 Annual Report for Revised Monitoring and Reporting Program Number 87-149. All of the deeper DH9 series wells (1, 4, 6, and 7) have maintained low Se concentrations ($\leq$ 2 µg/L) throughout the monitored history. Data from the shallower wells showed initial (1988) Se concentrations as high as 21 µg L^{-1}, with gradually declining concentrations. By early 1992, these shallow wells all yielded waters with Se concentrations of $\leq$ 10 µg L^{-1}. However, three out of the four shallower wells have shown periodic increases in Se concentrations following the major rainfall events in 1992 and 1993. The sampled Se concentrations in these shallow wells (DH9, #2, 5, and 8) have fluctuated between 11 and 130 µg L^{-1} since the February 1992 rainstorms. The measured DH9-3 well Se concentrations have remained $\leq$ 6 µg L^{-1}.

Past LBL reports have included information on soil water Se and salinity from three monitored soil profiles, P9C, P9R, and P9D (Fig. 2.1.1). The deepest soil water samplers at these older sites are at 2.12 m (6.95 ft) below the surface. In the previous LBL report (Benson et al., 1992), data on high soil water Se concentrations and on soil textures characteristic of high permeability (sandy) soils were presented from this area. These factors probably permit locally very effective leaching of Se into the underlying shallow groundwater during the wet season.

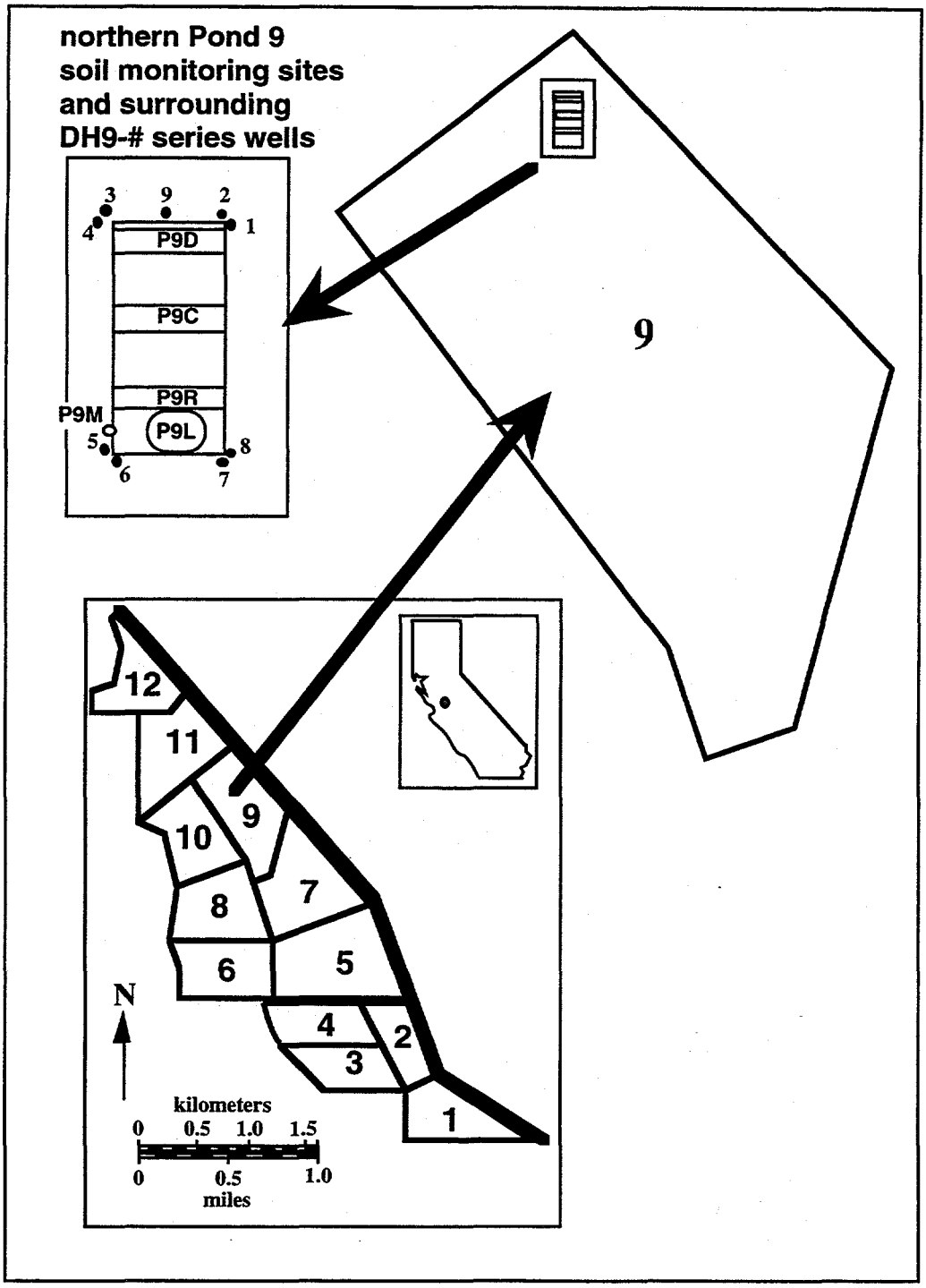

Figure 2.1.1. Locations of northern Pond 9 monitoring sites and shallow monitoring wells.

Additional data from these older soil water samplers were obtained through the 1993 wet season. Information from deeper portions of site P9C will be presented to show seasonal trends in soil solution Se concentrations and salinity during these two above-average rainfall years. Comparisons with soil solution data from the 1991 drought year are included. Data on Se concentrations and salinity from the newer installations during 1993-1994, an average rainfall year, will be presented later in this section.

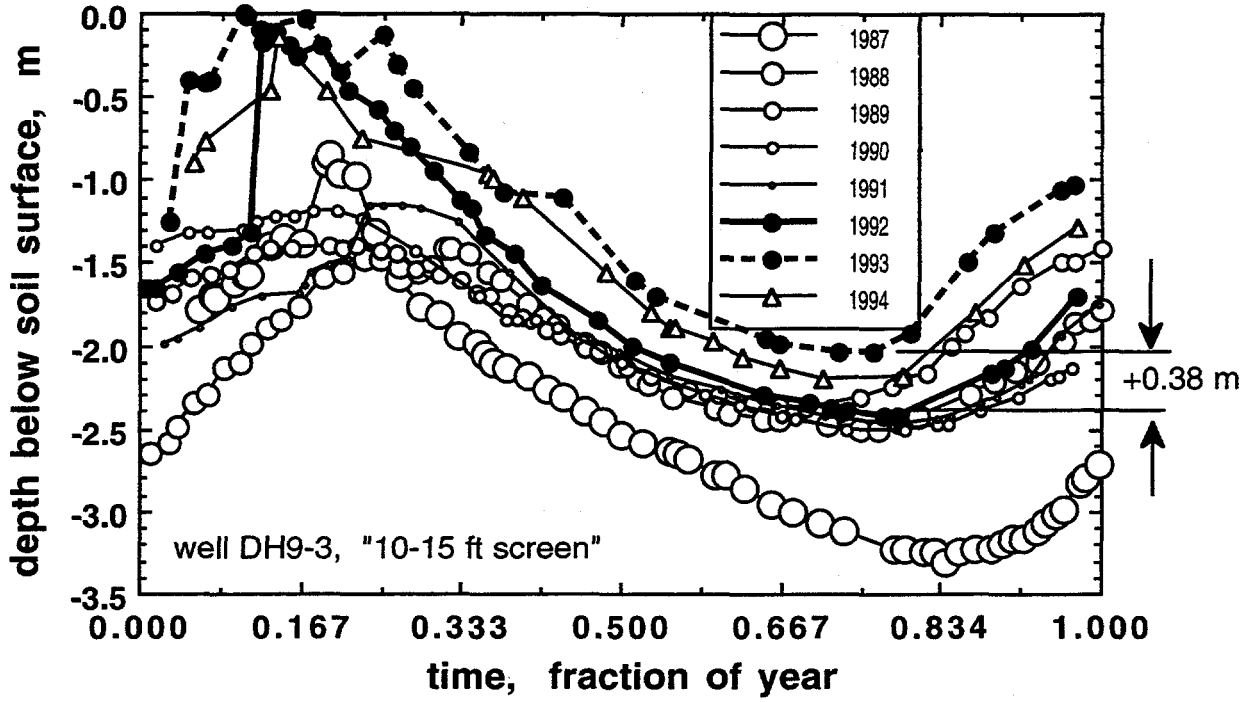

Figure 2.1.2. Seasonal variations in depths to the shallow water table in well DH 9-3, in the northern corner of Pond 9.

2.1.2 Site P9C, Deeper Profile Soluble Selenium Concentrations

Earlier data from this site previously presented in Benson et al. (1992) largely focused on variations in pore water Se profiles during the first 6 months of 1992. During this period, the short-term influence of above-average rainfall events was evident through large decreases in soluble Se inventories and salinities. Since that period, relatively frequent soil pore water samples were collected until late 1993. For the purpose of addressing concerns for Se transport into shallow groundwater, we will be concerned only with data from deeper soil water samplers. The combination of these data with earlier data from the 1991 drought year provides an opportunity to study time trends in Se concentrations within deeper soil pore waters (shallow groundwater) under highly contrasting hydrologic conditions. For this purpose, data from the 1.38, 1.65, 1.87, and 2.12 m deep soil water samplers were compiled into time trends in total solution Se concentrations, solution Se(IV) concentrations, and solution salinities (EC).

Although none of these older samplers overlap into the depth interval represented by the shallow wells (3.0 to 4.6 m), they do provide indicators of solute composition for waters which can leach downwards from the overlying soils. The relatively small (≈50 mm linear dimension), nested samplers provide high spatial resolution of solute distributions. Extremely heterogeneous solution chemical compositions can be anticipated because of the commonly large vertical gradients in total Se inventories, salinities, and redox potentials. The latter variable can be strongly influenced by seasonal water table fluctuations. On average, the shallowest (1.38 m) sampler considered here remains below the water table for about 30% of each year, while the deepest (2.12 m) sampler at P9C remains below the water table during about 90% of each year. Time trends for these variables are plotted over the interval beginning in January 1991, and ending in December 1993.

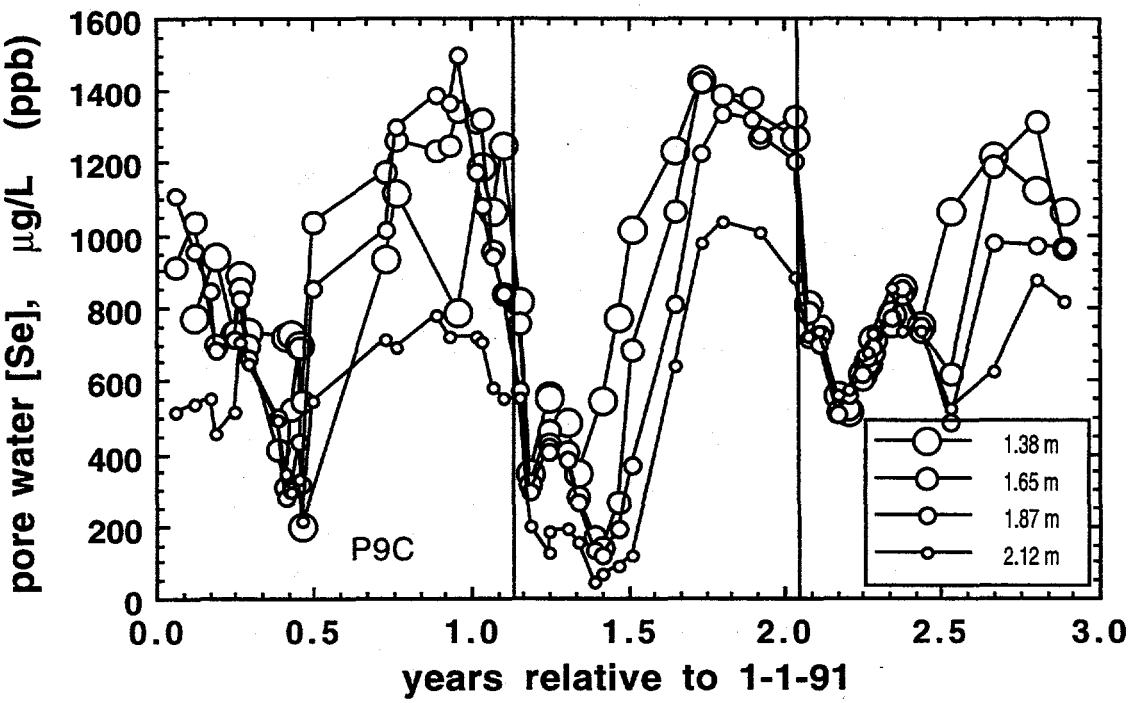

Figure 2.1.3. Trends in deeper soil pore water Se at P9C (1991-1993). Sampler depths are shown in the legend. Vertical lines indicate the start of major rainfall ponding.

In Figure 2.1.3, time trends for total dissolved Se concentrations within these deeper pore waters are provided. Vertical reference lines indicate times of major rainfall and ponding events during 1992 and 1993. Annual cycling in deep soil pore water Se concentrations are clearly visible in these data. Rapid declines in Se concentrations are observed following major rainfall and ponding events. Annual increases in Se concentrations exhibit both phase lags and amplitude damping with respect to depth. Depth trends in phase lags are probably due to the longer duration of reducing conditions deeper in these profiles. Damping of oscillations in

soluble Se concentrations with depth are due to decreasing Se inventories at depth. The local soluble Se concentration minima during 1991 appears to largely result from Se reduction and removal from the aqueous phase. The more distinct minima observed during 1992 and 1993 include influences of dilution from rainfall infiltration through the overlying soil profile. This interpretation is based on trends in deep sampler pore water EC values, which exhibited sharp declines in salinity following the major rainfall events of 1992 and 1993, but not during the 1991 drought year (Figure 2.1.4). The fact that EC time trends do not display the depth-correlated phase lags found in the case of soluble Se concentrations lends support to previously mentioned redox-control interpretation. Along with seasonal variations in total Se concentrations in pore waters, changes in Se speciation are also observed. Seasonal variations in pore waters associated with Se oxidation and reduction may sometimes be inferred from inspections of ratios of Se to

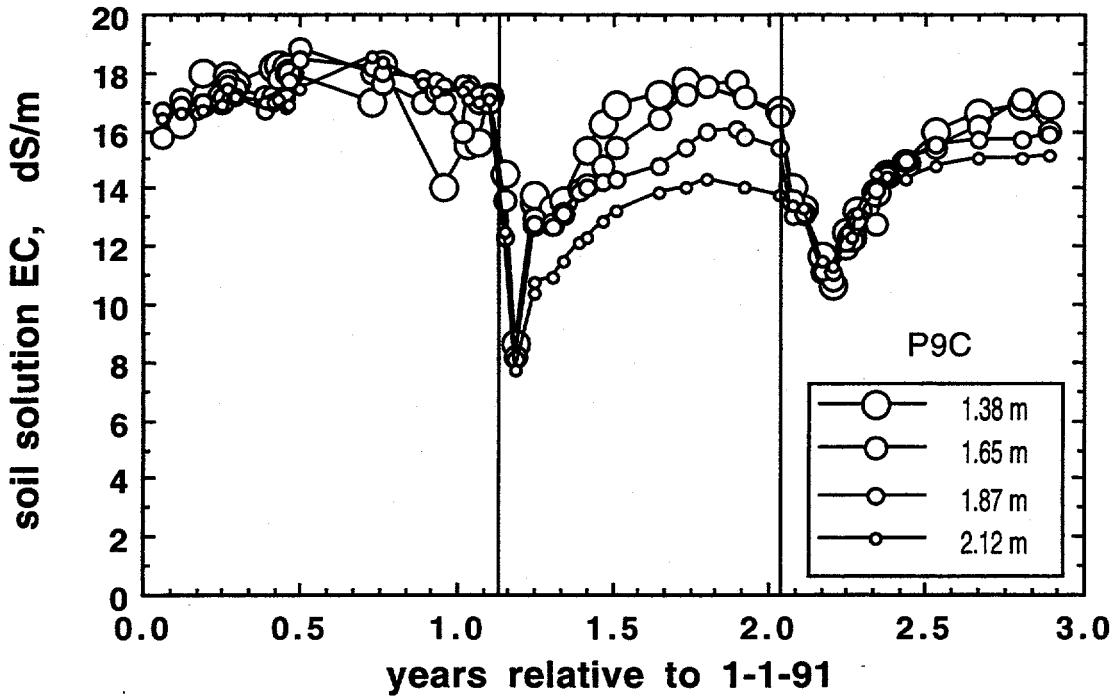

Figure 2.1.4. Trends in deeper soil pore water salinity at P9C (1991-1993). Sampler depths are shown in the legend. Vertical lines indicate the start of major rainfall ponding.

salinity (Figure 2.1.5). Declines and increases in the Se/EC ratio in this figure suggest that Se reduction and re-oxidation are respectively occurring. Using this approach, one may infer that soluble Se (primarily as Se(VI)) is removed from these deep soil solutions from midwinter through spring of each year via reduction to Se(IV) and possibly to Se(0). Re-oxidation of these reduced species would account for seasonal increases in deep soil solution Se concentrations during summer months. This interpretation is strictly applicable only when the solution of interest is (i) effectively unmixed with neighboring pore waters, (ii) diluted with pore waters

having equivalent Se/EC values, or (iii) diluted with rain water (insignificant influxes of Se and TDS). In addition, precipitation reactions involving major ions must be relatively insignificant. A potentially more direct approach to determining when oxidation versus reduction is dominant involves tracking trends on ratios of Se(IV) in solution to total solution Se (denoted ∑Se here). It has been shown by Lindberg and Runnells (1984) and by Runnells and Lindberg (1990) that speciation of aqueous phase Se can not be used quantitatively to characterize equilibrium redox conditions. Nevertheless, time-trends in Se(IV)/∑Se in pore waters can indicate whether solutions are becoming more reducing or more oxidizing. This approach is presented in Figure 2.1.6. Reducing conditions are expected to result in higher ratios of Se(IV)/∑Se relative to oxidizing conditions. A slightly different version of this approach would involve tracking trends

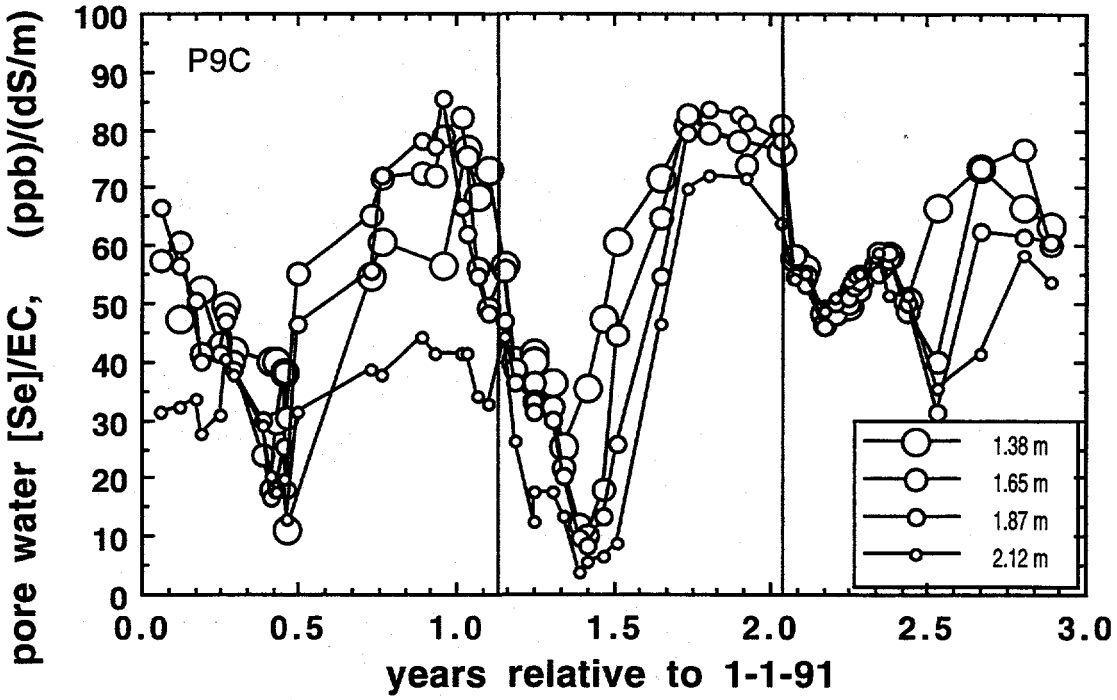

Figure 2.1.5. Trends in deeper soil pore water ratios of Se to EC at P9C (1991-1993). Sampler depths are shown in the legend. Vertical lines indicate start of rainfall ponding.

in the ratio of Se(IV) to Se(VI) in solution. However, this approach is subject to greater analytical uncertainty, especially at low ∑Se concentrations since Se(VI) is calculated as the difference between ∑Se and Se(IV). The trends in Se(IV)/∑Se shown in Figure 2.1.6 indicate minor Se reduction during the 1991 winter to spring, and much stronger reduction in the months following the 1992 rain storms. The lack of significant increases in Se(IV)/∑Se in these soil waters during 1993 indicates that the observed decreases in dissolved Se (Figure 2.1.3) were dominated by dilution rather than by reduction to Se(IV) and Se(0).

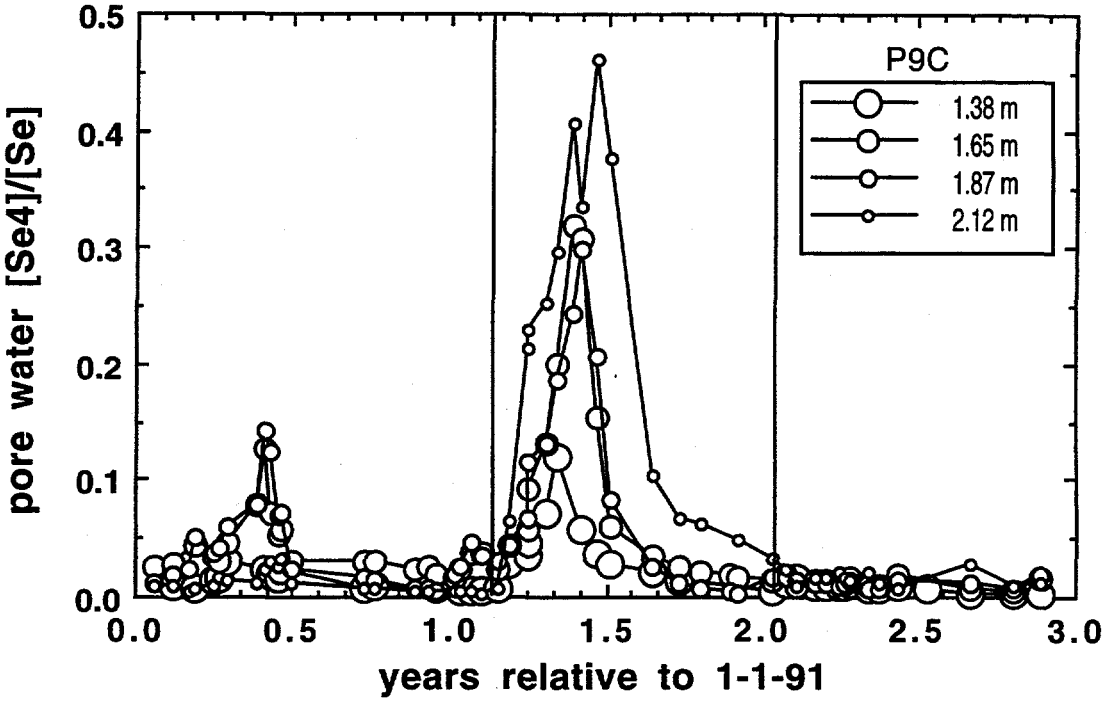

Figure 2.1.6. Trends in deeper soil pore water Se(IV)/Se ratios at P9C (1991-1993). Sampler depths are shown in the legend. Vertical lines indicate start of rainfall ponding.

2.1.3 Site P9L, Deeper Profile Soluble Selenium Concentrations

Depth profile data on soil solution Se concentrations from this site are shown in Figure 2.1.7 for various times from Oct. 1993 through Aug. 1994. Over this interval, the general profile was relatively stable, with the maximum Se concentrations (400 to 700 μg L^{-1}) at the 1.50 m depth. Other Pond 9 samplers (at P9C, P9R, and P9D) currently exhibit maxima in Se concentrations at depths ranging from 0.91 to 1.38 m. Soluble Se concentration profiles in these northern Pond 9 profiles are now more similar to those of the upland Pond 11 saltgrass soil monitoring area, than to earlier (1987 to 1991) Pond 9 playa soils. Time trends of total Se concentrations from site P9L deeper pore waters are shown in Figure 2.1.8. Time trends in Se(IV):ΣSe ratios from this site are shown in Figure 2.1.9. Note that no strongly reducing conditions were detected at this site during the past year, although the deepest samplers maintain moderately high Se(IV):ΣSe values. During the monitored period, Se(VI) accounted for at least 90% of the dissolved Se in all but the deepest samplers. The roughly steady nature of the deeper profile Se concentrations, and the approximately uniform gradient of Se concentration over the 1.50 to 3.25 m depth interval permit estimation of the magnitude of downwards Se diffusion from the deeper soils into the shallow groundwater. A Fick's law calculation of the average rate of Se(VI) diffusion (in the absence of flow) leads to an estimated diffusive flux of about 2 mg m^{-2} y^{-1}, or roughly 0.1% of

the total soil Se inventory per year. This magnitude of Se flux would be equivalent to an advective displacement of waters with a Se concentration of 300 μg L^{-1} of only 7 mm per year.

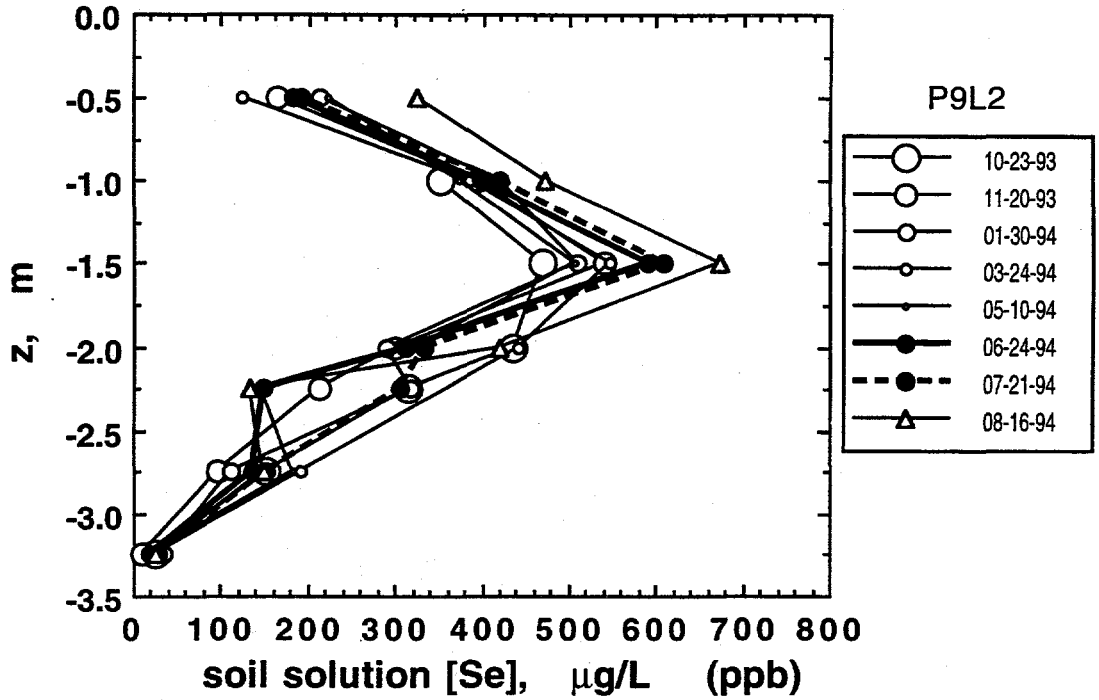

Figure 2.1.7. Depth profiles of pore water Se concentrations at the P9L, deeper soil monitoring site.

The fact that maxima in both soluble Se and salinities in the Pond 9 monitoring area currently occur at depths ranging from 0.9 m down to about 2.5 m below the soil surface indicates that advective transport dominates over diffusion. Lower surface soil salinities (relative to deeper portions of profiles, Figure 2.1.10) currently observed at these sites represent significant changes relative to earlier conditions. The earliest data on soil solution composition from the northern Pond 9 area were obtained in February 1987 (LBL, Dec. 1987). Those data exhibited maxima in soluble Se and dissolved salts within the upper 0.15 m of the soil profile. Displacement of maxima in soluble Se and salts from the soil surface down to the current depths (0.9 to 2.5 m) indicates average annual recharge rates range between 40 and 100 mm (assuming an average volumetric water content of 0.3). In view of the rainfall history and other data from Pond 9 soil water samplers, it is more realistic to assign higher recharge rates for 1992 and 1993, and lower rates for other years. Average rates of downwards Se transport associated with the aforementioned recharge rates would be 12 and 30 mg m^{-2} y^{-1}, when a soluble Se concentration of 300 μg L^{-1} is assumed. However, reduction of Se(VI) and removal of Se(IV) and possibly Se(0) from solution during the course of infiltration significantly diminishes actual

displacements of Se from soils into groundwaters. Without reduction, much higher Se concentrations would be observed in the DH9 shallow groundwater samples.

From the profiles of soluble Se at P9L (Fig. 2.1.7) it is evident that a large gradient in Se concentration persists into the depths sampled by the DH9 wells. The limited overlap between depths sampled by the drive-point well samplers and the shallow DH9 wells makes it impossible to determine the detailed Se concentration distributions averaged by these wells. The best available comparisons can be made between the DH9-5 well (3.0 to 4.6 m slotted interval), and the P9M samplers (0.15 m screened lengths, centered at depths of 2.80 and 3.30 m). Data on Se concentrations from samples collected at similar times of the year by the USBR (DH9-5) and by LBL (P9M) are shown in Fig. 2.1.11. The Se concentration obtained at a given time from the DH9-5 well represents a flow-weighted average of unknown spatial distributions of both soluble Se concentrations and permeabilities along the 3.0 to 4.6 m depth interval (Benson et al., 1991).

Given a lack of information on permeability distributions in the present case, only heterogeneities in Se concentrations along the DH9-5 slotted interval will be considered. If Se concentrations from the 2.80 and 3.30 m samplers were considerably higher than corresponding values obtained from the DH9-5 well, it would suggest that the latter values are strongly influenced by small contributions from the upper portion of the slotted interval. However, the fact that Se concentrations from the DH9-5 well agree reasonably well with those from the 2.80 and 3.30 m samplers indicate that they are representative of most of the slotted interval.

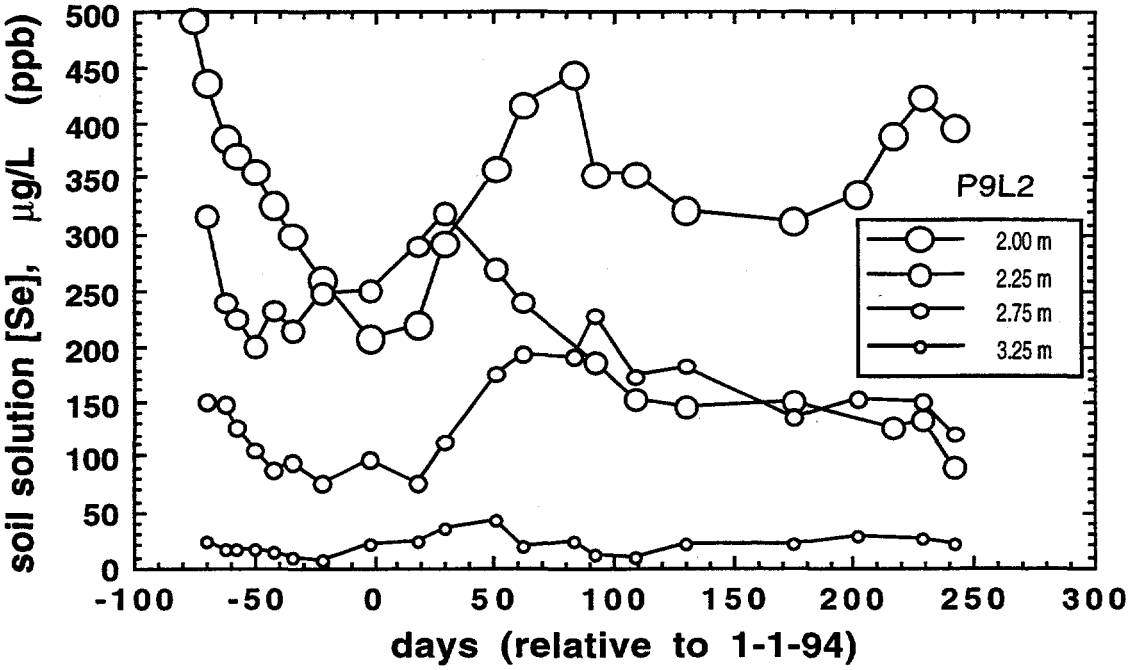

Figure 2.1.8. Time-trends in deep profile soluble Se concentrations at site P9L2.

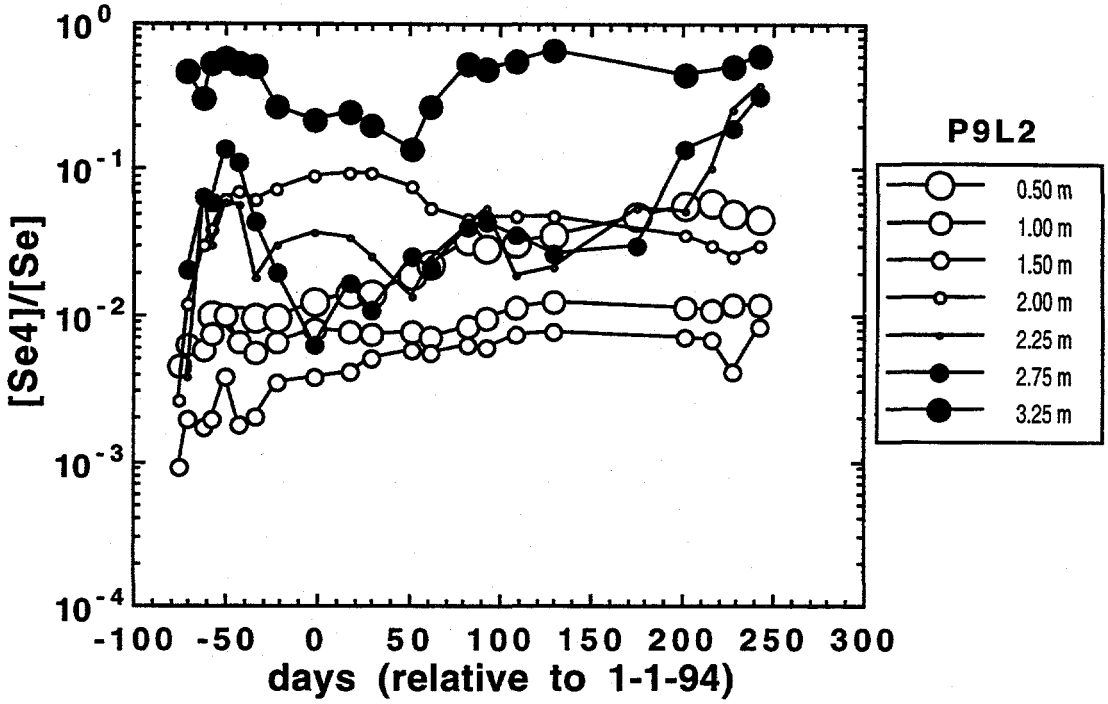

Figure 2.1.9. Time-trends in Se(IV)/∑Se in pore water samples from site P9L2.

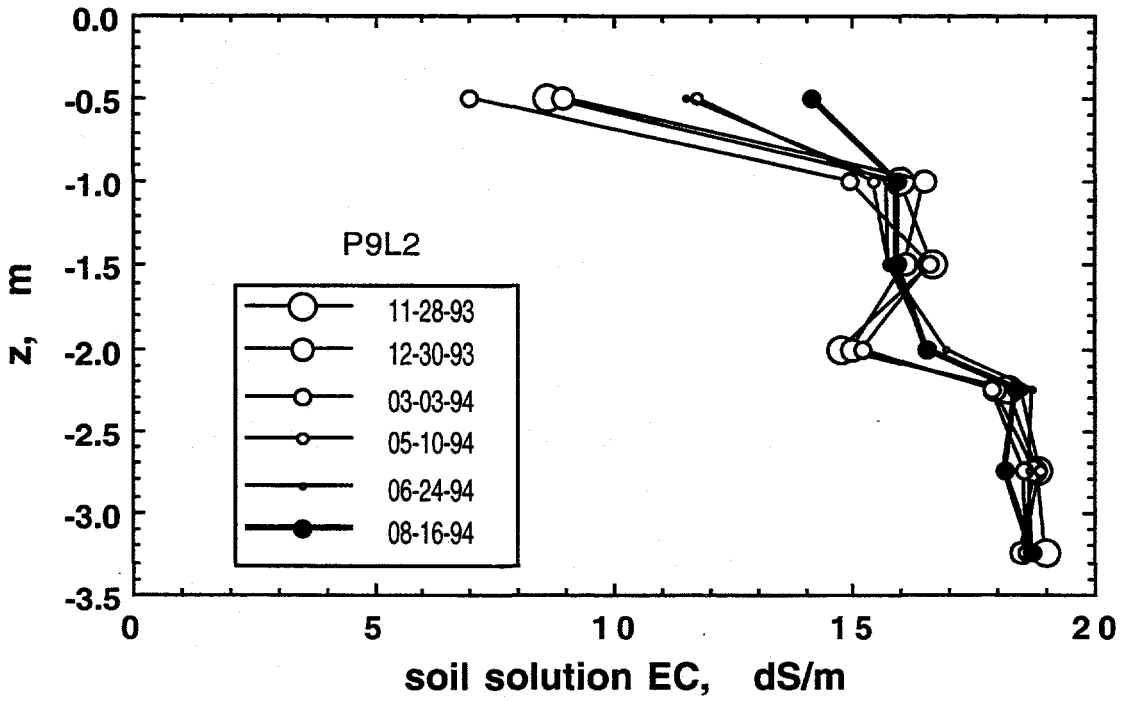

Figure 2.1.10. Depth profiles of pore water salinities (ECs) at the P9L, deeper soil monitoring site.

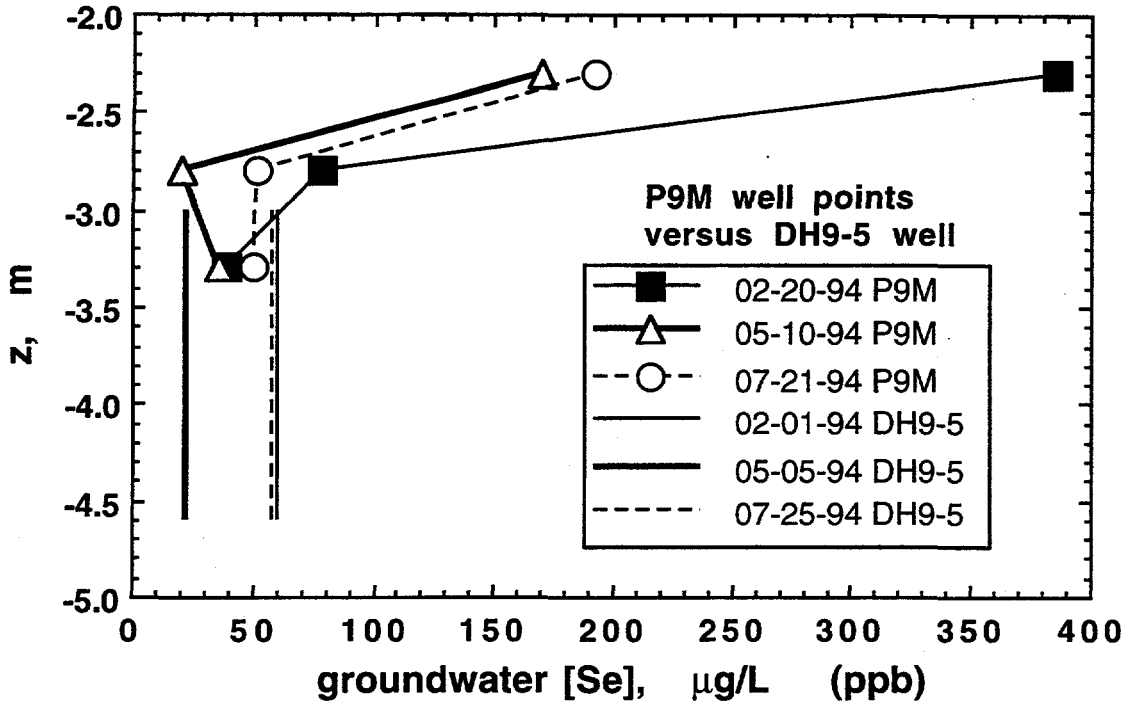

Figure 2.1.11. Comparisons between Se concentrations in shallow groundwaters sampled from the P9M drive-point wells and the USBR DH9-5 monitoring well.

2.2 Pond 11 Upland Monitoring Area

Tetsu Tokunaga and Paul Johannis
Earth Sciences Division
Lawrence Berkeley Laboratory

Three upland monitoring sites are located in the southern portion of Pond 11, about 0.3 km to the east of Mud Slough. These sites, identified as P11C, P11D, and P11H were originally established in late 1986 to observe possible changes in soil Se in response to simple surface soil alteration. The C, D, and H originally referred to control, disked, and vegetation-harvested treatments. Rapid re-establishment of native vegetation in the D and H sites and the decision to discontinue further disking/harvesting activities have permitted monitoring of all three sites as upland control systems. Information on soil and soil water was been collected on a regular basis at these sites since Feb. 1987.

2.2.1 Site Description

Vegetation at these sites has been dominated by salt-tolerant *Distichlis spicata* (saltgrass), *Frankenia grandifolia* (alkali heath), and *Cressa truxillensis* (alkali weed). The prevalence of these species, also common in other upland areas comprised of native Kesterson soil, reflects the high salinity found in these soils. The above-average rainfall received at Kesterson during the 1991-1992 (320 mm) and 1992-1993 (420 mm) wet seasons caused significant decreases in near-surface concentrations of soluble Se and salts. Leaching of solutes deeper into soil profiles was observed, along with chemical reduction of soluble Se(VI) to adsorbable and less soluble Se(IV) and Se(0). Increases in salinity and soluble Se concentrations were observed during late spring through summer months, but not to the extent of building up soil profile inventories of these constituents to levels found prior to the early 1992 rains. The sequence of two years of above-average rainfall is also probably the primary factor resulting in the proliferation of annual grasses in the Pond 11 study area as well as other regions within Kesterson Reservoir. Introduced species of *Bromus, Hordeum*, and *Avena* (which have long been well established throughout many parts of California and other states) have been abundant in 1992 and 1993. Nevertheless, *Distichlis*, *Frankenia* , and *Cressa* persisted, and appeared to regain dominance in the Pond 11 study area during 1994. The 1993-1994 wet season provided 280 mm of rainfall, close to the annual average (270 mm) obtained from available precipitation data (1982 through 1994, with the 1984-1985 wet season missing).

In the following subsections, summary information on soluble Se and salinity distributions will be provided. Year to year comparisons of soluble Se and salts are provided through depth

profiles obtained in September or October of each year. Water-extracts of soils obtained at this time, prior to the onset of significant rainfall, permit clearer year to year comparisons than would be possible from samples collected at any other time of the year. These data will be presented in two forms. In the first form, soluble (water-extracted) concentrations of Se ($C_{Se(wx)}$) are expressed per unit mass of soil solids ($\mu g\ kg^{-1}$ or ppb solids) and salinity is expressed as EC ($dS\ m^{-1}$) of the 1:5 (soil:water) extract. In the second form, soluble Se and salinity are expressed as depth integrals. In this representation, quantities of solutes are presented on the basis of mass (m) per unit horizontal area (A) from the soil surface downwards. This provides cumulative solute masses per unit area, summing downwards through the profile. The two forms of data presentation are shown schematically in Figure 2.2.1. Because solute masses are referenced to soil volume in the second approach, soil bulk densities need to be factored into calculations. For this purpose, depth-dependent bulk densities were estimated from a regression based on similar core samples. The mass of soluble Se per unit bulk area of soil, within a specific sampling depth interval (Δz_i), is given by

$$m_{Se(wx),i} = \rho_{b,i} C_{Se(wx),i} A \Delta z_i \quad , \tag{1}$$

so that the total mass of water-extracted Se found from the soil surface down to the n^{th} depth interval (inclusively) is given by

$$M_{Se(wx),n} = A \sum_{i=1}^{n} \rho_{b,i} C_{Se(wx),i} \Delta z_i \quad . \tag{2}$$

Comparisons of data from one year to another in this representation permit clear determinations of whether or not net increases or net losses of water-extracted Se have occurred within whole profiles (or sections within profiles).

2.2.2 Soluble Selenium Distributions

Depth profiles of soluble (water-extracted) Se at site P11C are presented in Figure 2.2.2(A,B), for samples collected in the late summer or early fall of 1988, 1989, 1991, 1992, and 1993. The legend in this figure includes estimates of depth-integrated soluble Se inventories and also expresses these values relative to the total soil Se inventory. The depth-integrated Se profiles are shown in Figure 2.2.3(A,B). Total soil Se inventories are based upon previously published analyses (Tokunaga et al., 1991). The cumulative error due to the uncertainty in Se analysis is shown as an example in the 10/15/91 data. Up through, and including, the 1991 sampling, these data indicated two general trends. First, net increases in the water soluble Se

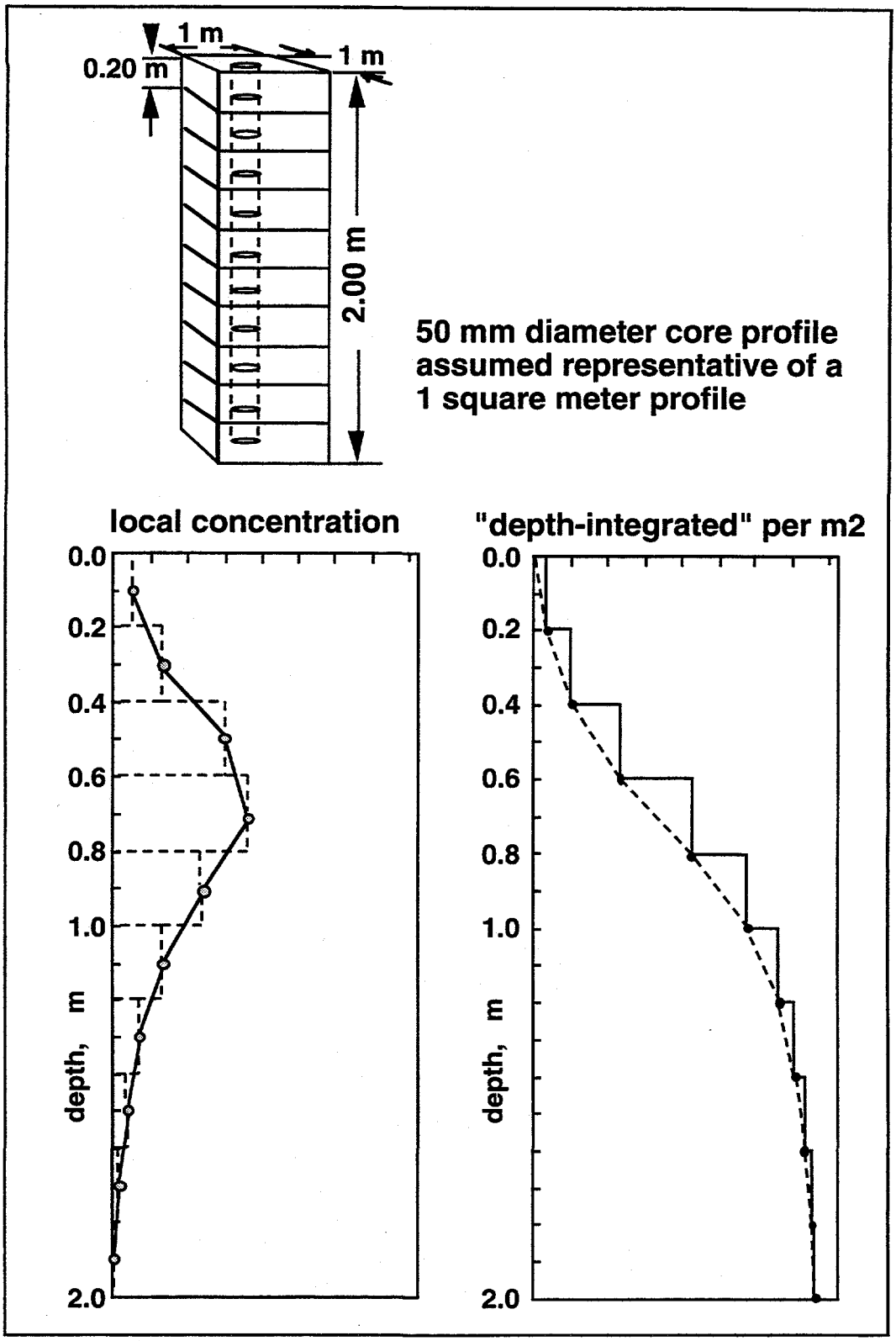

Figure 2.2.1. Illustration of relation between local concentration profiles and "depth-integrated" chemical inventories.

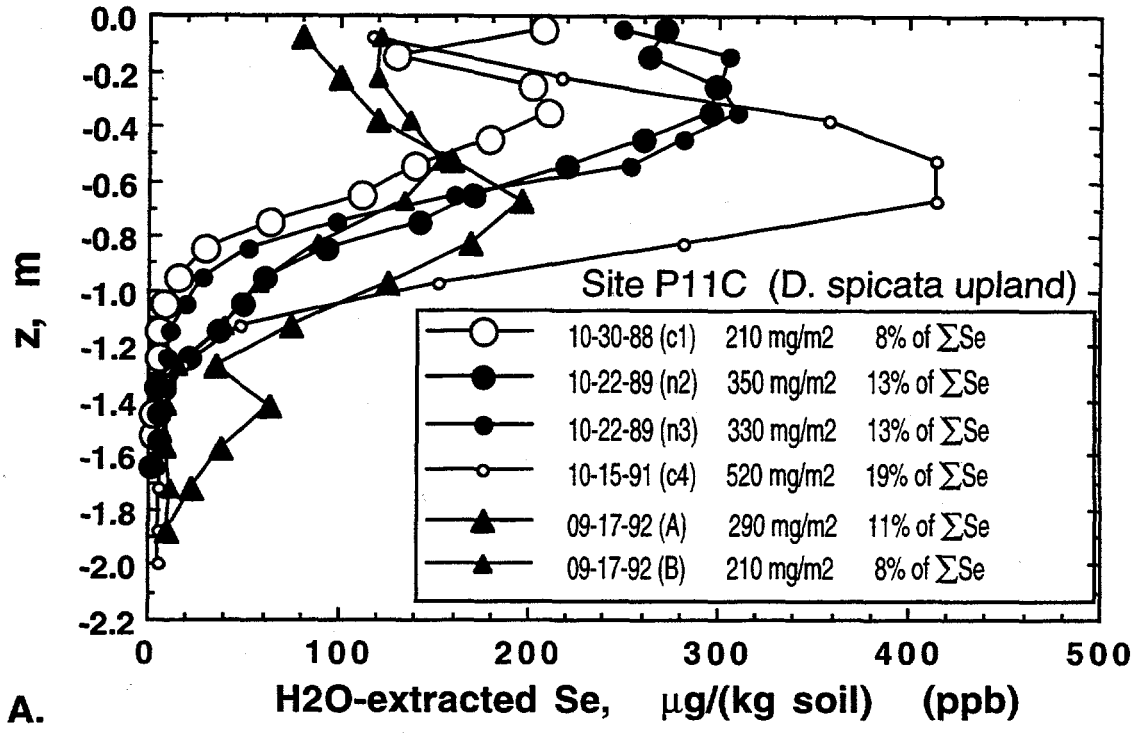

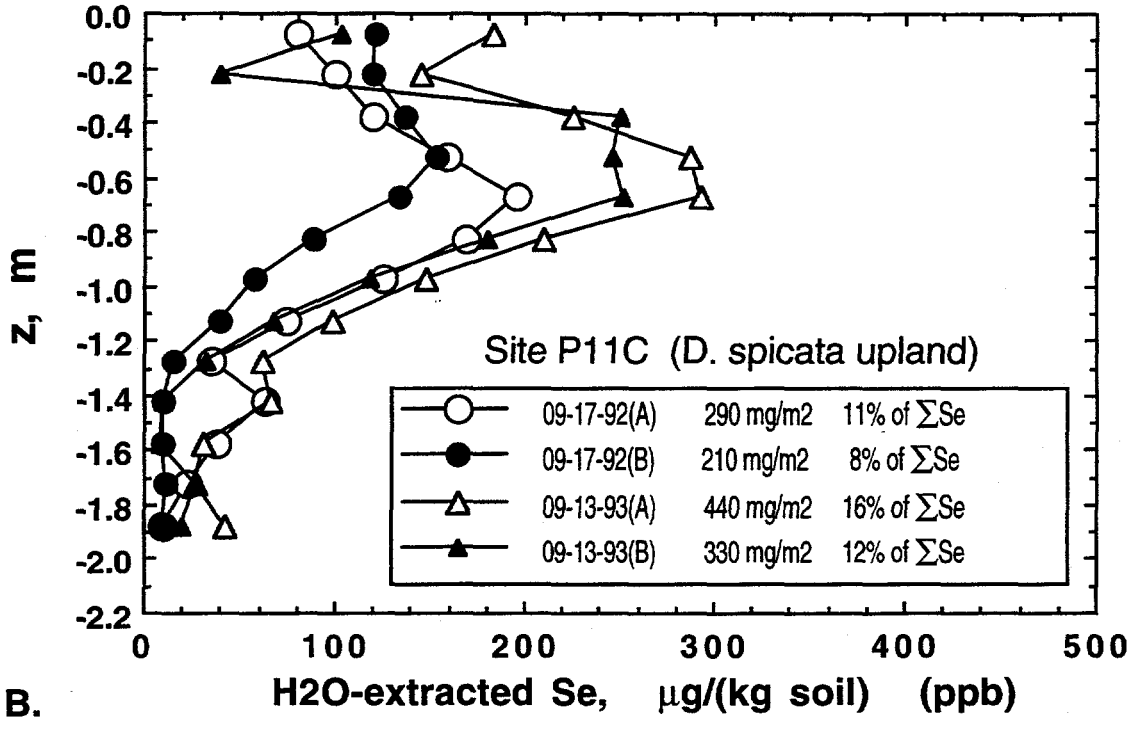

Figure 2.2.2. Depth profiles of water-extractable Se at the Pond 11 upland monitoring site P11C, from samples collected in late summer to early fall. (**A**) for 1988, 1989, 1991, 1992, and (**B**) for 1992 and 1993.

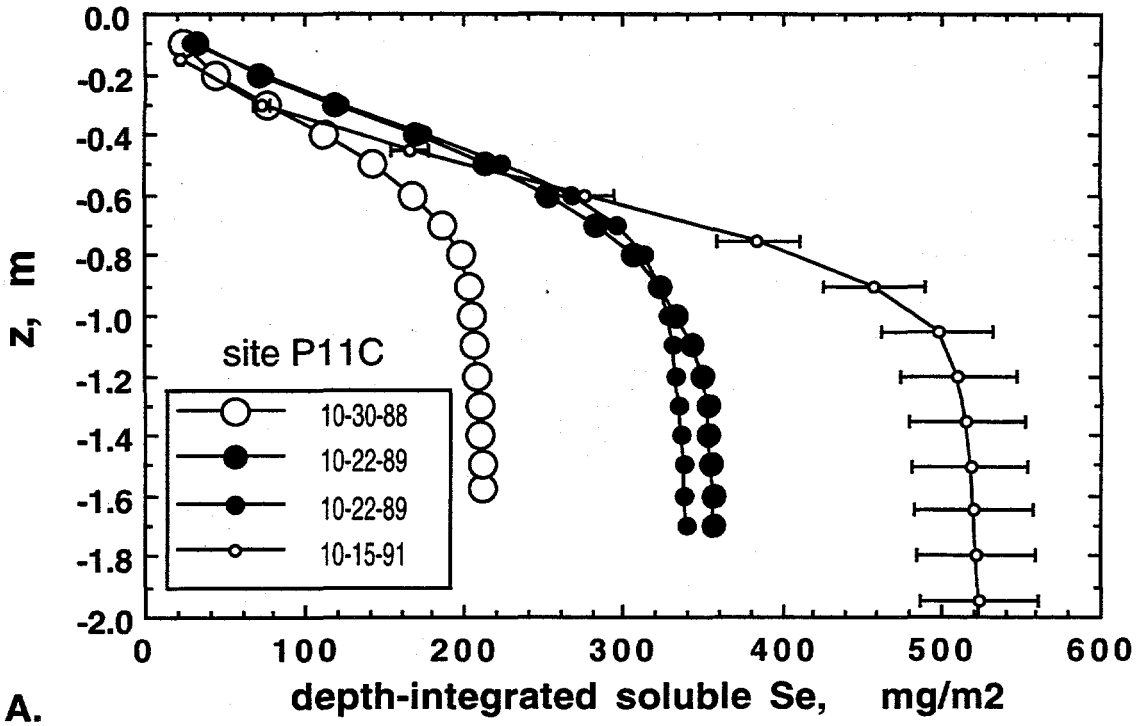

A.

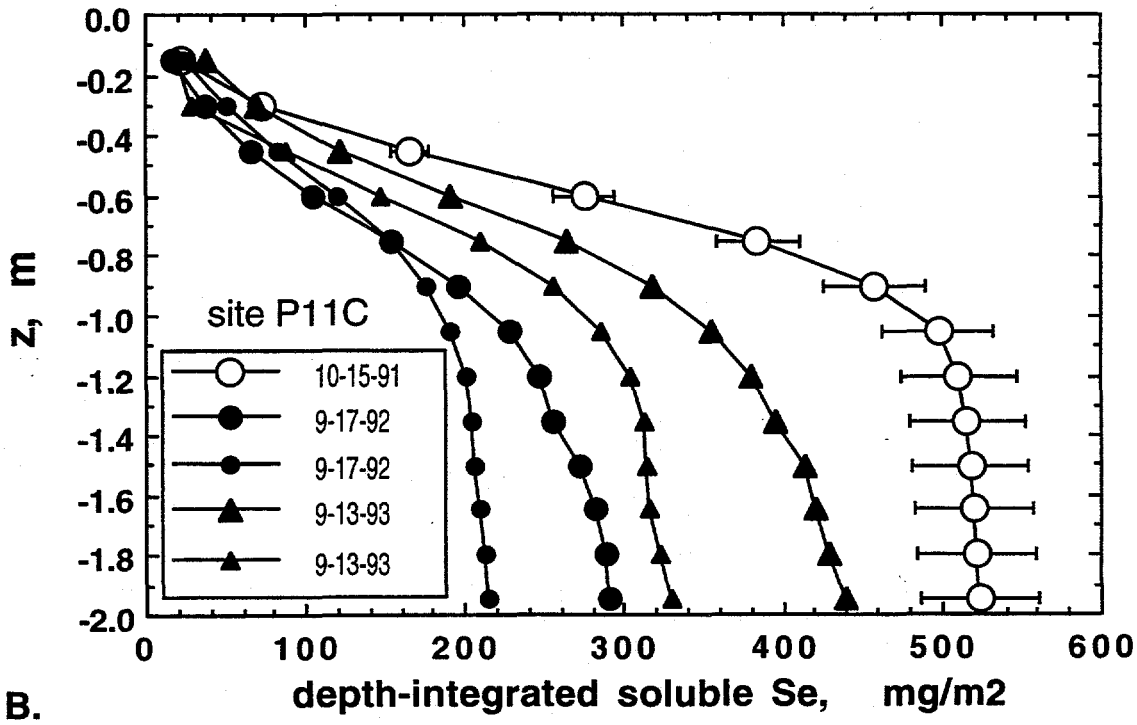

B.

Figure 2.2.3. Depth-integrated inventories of water-extractable Se at the Pond 11 upland monitoring site P11C, from samples collected in late summer to early fall. (**A**) for 1988, 1989, and 1991, and (**B**) for 1991, 1992, and 1993.

inventory were observed. These increases amounted to depletion (oxidation) of the insoluble Se inventory at an average rate of about 5% y^{-1}. The second general trend observed in these data is the movement of soluble Se deeper into the soil profile. This trend is reasonable in view of the presence of densely distributed roots which sustain evapotranspirative removal of soil water in the about 0.2 to 1.0 m depth interval throughout the later spring and summer months. The data from the 1992 core sampling show significant declines in soluble Se, reflecting both leaching and Se(VI) reduction under the above-average rainfall. The summer 1992 soluble Se inventory at this site is only about half that of the summer 1991 amount. The fact that the summer 1993 soluble Se inventory at this site is higher than that of 1992 despite having received even higher rainfall shows that re-oxidation was significant and that its extent is not presently predictable. Similar results were obtained in the P11D and P11H sites, as shown in Table 2.2.1. Another quantifiable feature of these profiles is the depth to the center of mass of the soluble Se inventory. Its movement is useful for tracking net displacements resulting from leaching, evaporation, and transpiration. The center of mass for a given soluble Se inventory coincides with the depth at which half of the total soluble inventory is reached in the depth-integrated profiles. Positions of soluble Se centers of mass during the late summer samplings are summarized in Table 2.2.2. The Pond 11 upland soils had centers of mass for soluble Se at depths ranging from 0.42 to 0.60 m below the surface by 1991. Following two wet seasons in 1992 and 1993, the centers of mass for soluble Se shifted downwards to depths of 0.64 to 0.82 m.

Table 2.2.1. Comparisons of soluble Se inventories in core samples collected in the late summer following a drought year (1991), and following two above-average rainfall years (1992 and 1993).

soluble Se inventories in late-summer soil profile samples					
site	1991	1992		1993	
	mg m^{-2}	mg m^{-2}	% of Sept. '91	mg m^{-2}	% of Sept. '91
P11C, A	520	290		440	
P11C, B		210		330	
P11C			48%		74%
P11D, A	530	359		745	
P11D, B	540	398		494	
P11D			71%		116%
P11H, A	950	671		1079	
P11H, B	1100	661		739	
P11H			65%		89%

Table 2.2.2 Comparisons of depths of centers of mass for soluble Se inventories in core samples collected in the late summer following a drought year (1991), and following two above-average rainfall years (1992 and 1993).

soluble Se center of mass in late-summer soil profile samples					
site	**1991**	**1992**		**1993**	
	m	**m**	**shift relative to Sept. 1991, m**	**m**	**shift relative to Sept. 1991, m**
P11C, A	-0.58	-0.70		-0.68	
P11C, B		-0.58		-0.65	
P11C			-0.06 ±0.06		-0.08 ±0.02
P11D, A	-0.50	-0.70		-0.78	
P11D, B	-0.60	-0.75		-0.82	
P11D			-0.18 ±0.03		-0.20 ±0.02
P11H, A	-0.42	-0.67		-0.71	
P11H, B	-0.42	-0.64		-0.64	
P11H			-0.23 ±0.02		-0.26 ±0.04

2.3 Pond 5, Fill Soil Monitoring Site

Tetsu Tokunaga and Paul Johannis
Earth Sciences Division
Lawrence Berkeley Laboratory

The LBL soil monitoring site P5F located in a filled area in the north-central portion of Pond 5 has been sampled for analyses of selenium and salinity since March 1989. At this site, early field observations and soil analyses indicated that the fill material consisted of imported, non-seleniferous soil. The fill depth is 0.53 m (1.7 ft). The initially barren fill soil was rapidly vegetated by annual grasses (*Avena, Bromus, Hordeum*), *Bassia hyssopifolia*, and *Salsola kali*.. In a previous descriptions of this site (LBL, Oct. 1990; Tokunaga et al., 1994), year-to-year trends in soluble Se and salinity distributions in these soils under drought conditions were provided. The above-average rainfall in 1992 and 1993 provided contrasting hydrologic conditions, much more conducive to leaching and also Se(VI) reduction. During 1992, soil moisture contents (and soil matric potentials) remained high enough throughout even the summer months. This provided an opportunity to directly track soil solution chemistry during a complete spring/summer drying cycle. In previous years, portions of most soil profiles were dry beyond the matric potential limit of soil water samplers ($\approx$ -80 kPa) by late spring. In this section, depth profile trends in soil solution Se and salinity during a single wetting-drying cycle (1992), and year-to-year (summer) comparisons in soluble Se and salinity will be provided.

2.3.1 1992 Soil Solution Se and Salinity Trends

The first major rainfall event resulting in the formation of numerous ephemeral pools occurred on Feb. 12, 1992. Rainfall ponding persisted for several weeks at the P5F site. Before this time, most of the P5F soil profile was too dry to permit collection of soil solution samples. Only the surface (0.20 m depth) and deepest (1.60 m) soil water samplers were functioning in late Jan. 1992, by which time only 90 mm of rainfall was received. Following the Feb. 1992 ponding, soil solution samples were collected at 1 to 3 week intervals through the end of summer. In Figures 2.3.1(A,B), depth profiles of soil solution Se and salinity are presented in approximately monthly intervals. The Se concentrations throughout the upper profile rapidly decreased following the rainstorms. Data from soil solution samples collected shortly after the major rainfall are not included in these figures because of uncertainties arising from possible macropore flow influences. Salinity (EC) data (Fig. 2.3.1B) show the apparent position of the infiltration front at about 1.0 m below the soil surface by Feb. 25, 1992. The steady recovery of the salinity profile with time shows the dominance of evapotranspirative water losses over

gravity drainage, continuing until the following fall. Depth profiles and time trends for soluble Se (Fig. 2.3.1A) are much more complex than those for soil salinity. The initial leaching and Se(VI) reduction to adsorbable and insoluble Se species (primarily Se(IV) and Se(0) respectively), is followed by increases in the soluble Se inventory during the drying cycle. The soluble Se profile evolves primarily through a combination of oxidative generation of Se(VI), advective-diffusive transport, and evapotranspirative re-concentration. Oxidation of Se(0) and Se(IV) to produce high concentrations of soluble Se (primarily as Se(VI)) occurs both within the original Kesterson surface soil and within the fill (Fig. 2.3.1A). Significant re-oxidation of Se in the original Kesterson surface soil is expected following the recession of the water table because this zone typically contains about 75% of the total soil Se inventory. Most of the original Kesterson surface soil Se inventory is currently still in various reduced, insoluble forms, potentially available for re-oxidation. The rapid reappearance of soluble Se at the 0.20 and 0.33 m depths in the P5F fill soil between late April and early May of 1992, followed by steady decreases is more difficult to explain. One possible explanation requires the pre-storm inventory of Se(VI) in the fill to be largely reduced in place instead of being leached downwards. This recently reduced inventory is then rapidly re-oxidized as the drying front moves downwards during the spring months. Recent laboratory experiments have shown that in soils with low available organic carbon contents, Se reduced during short-term flooding can be very rapidly re-oxidized back to Se(VI). The declining soluble Se concentrations in the 0.20 and 0.33 m depths during the rest of the drying cycle might result from evaporative advection of pore waters towards the soil surface. An average evaporation rate of about 1 mm d^{-1}, consistent with rates measured at Kesterson Reservoir by Zawislanski (1990), would be required to produce this result. Although this scenario is consistent with time trends for soluble Se in the 0.20 and 0.33 m depths, an explanation for the persistent low soluble Se concentrations at the 0.46 m depth (Fig. 2.3.1A) is needed. Possible existence of a reducing zone just above the interface between the Kesterson soil and fill could explain this anomaly. This explanation appears plausible since vegetation buried during emplacement of fill soil could provide additional organic matter to sustain Se reduction. The occurrence of the maxima in water-extracted Se(IV) in the Sept. 1993 soil sampling in the vicinity of the 0.46 m depth (Figure 2.3.3A, to be discussed below) may also reflect influences of Se(VI) reduction during the previous year.

2.3.2 Year-to-Year, Late Summer Trends in Soluble Se and Salinity

More long-term patterns in spatial distributions of soluble Se and salts can be studied through comparisons of water-extracts performed on soil samples collected at the end of each summer. Total water-extracted Se concentration profiles from site P5F are shown in Figures 2.3.2A (full profile) and 2.3.2B (close-up of upper fill). Each of these profiles represent averages of 4 to 5

core profiles within the fill, and 2 core profiles within the underlying Kesterson Reservoir soil. Spatial variability over relatively short lateral distances (approx 8 m) limit quantification of year-to-year comparisons, but some important features are clearly displayed. Earlier samplings were

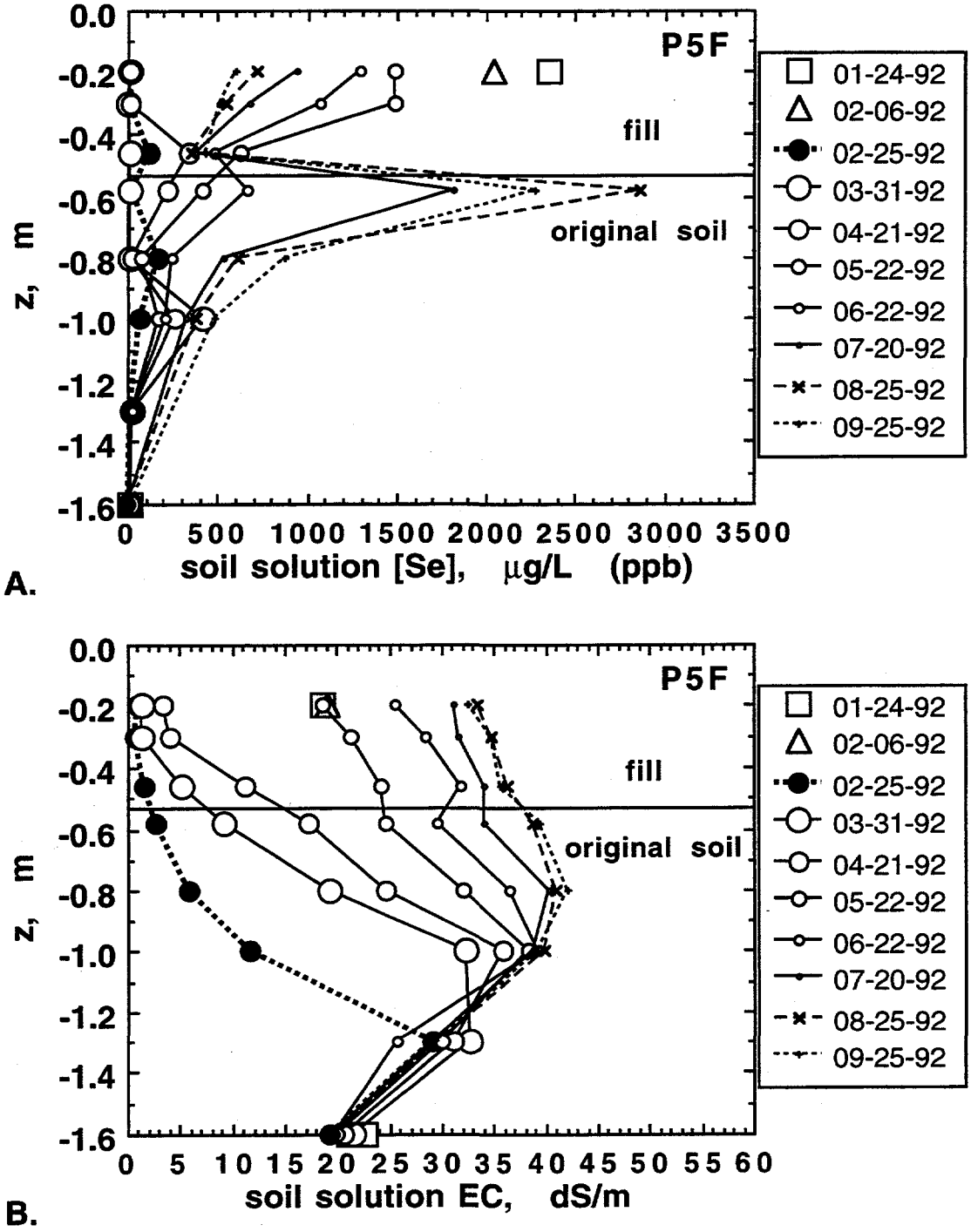

Figure 2.3.1. Soil solution Se concentrations (**A**), and salinities (**B**) at the P5F fill monitoring site during 1992, before and after the Feb. 1992 rainstorms.

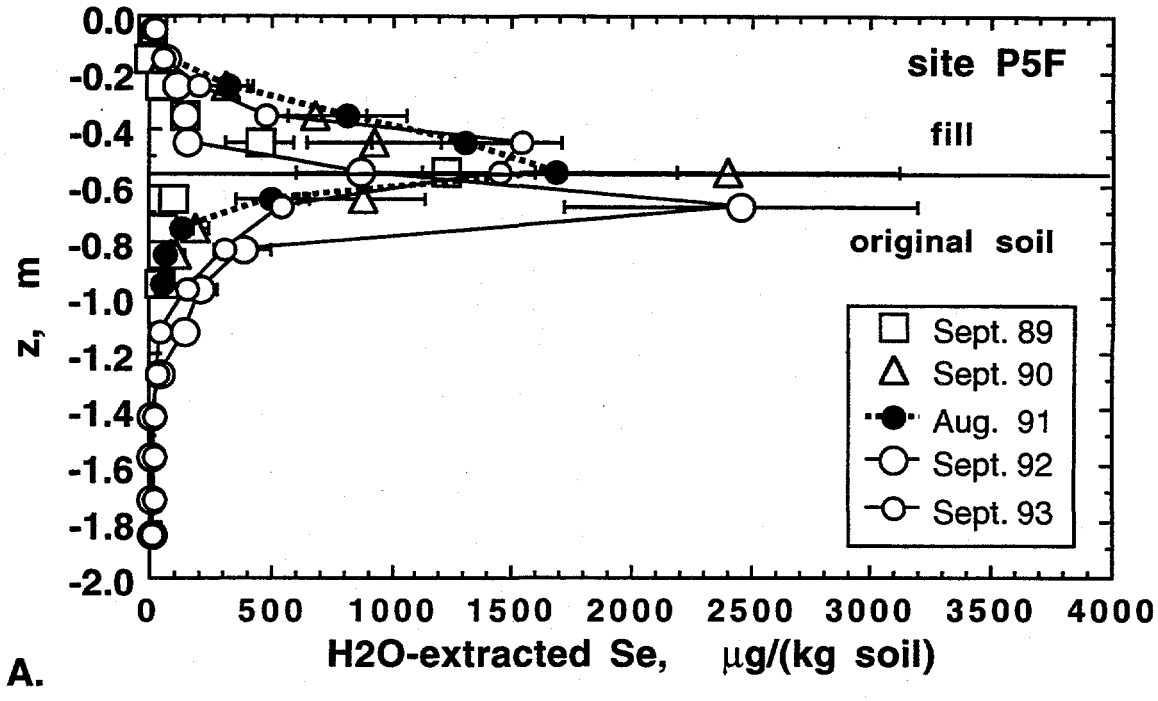

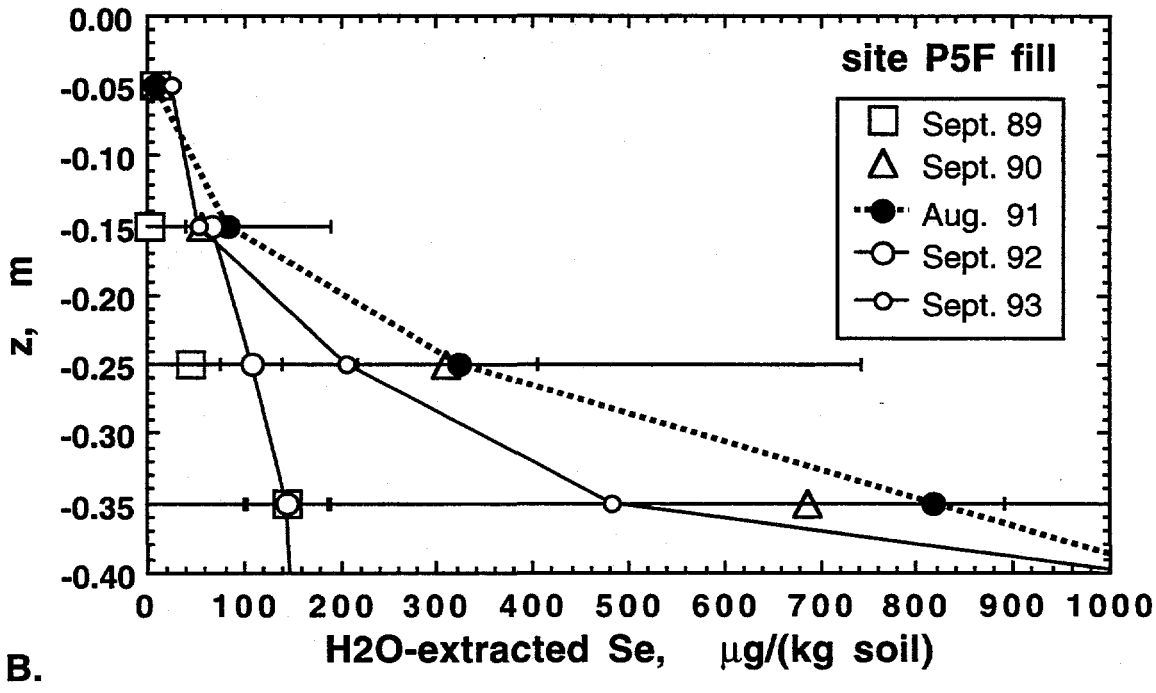

Figure 2.3.2. Water-extractable Se profiles from yearly late summer core sampling of fill site P5F. (**A**) total profile data, and (**B**) near-surface soils.

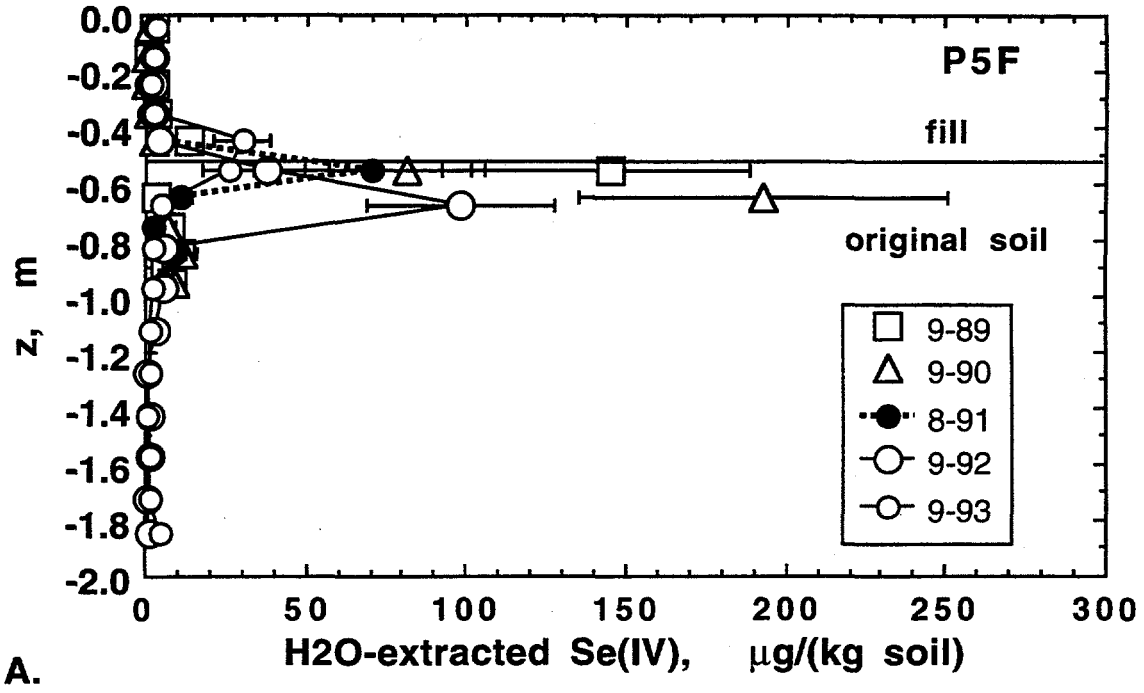

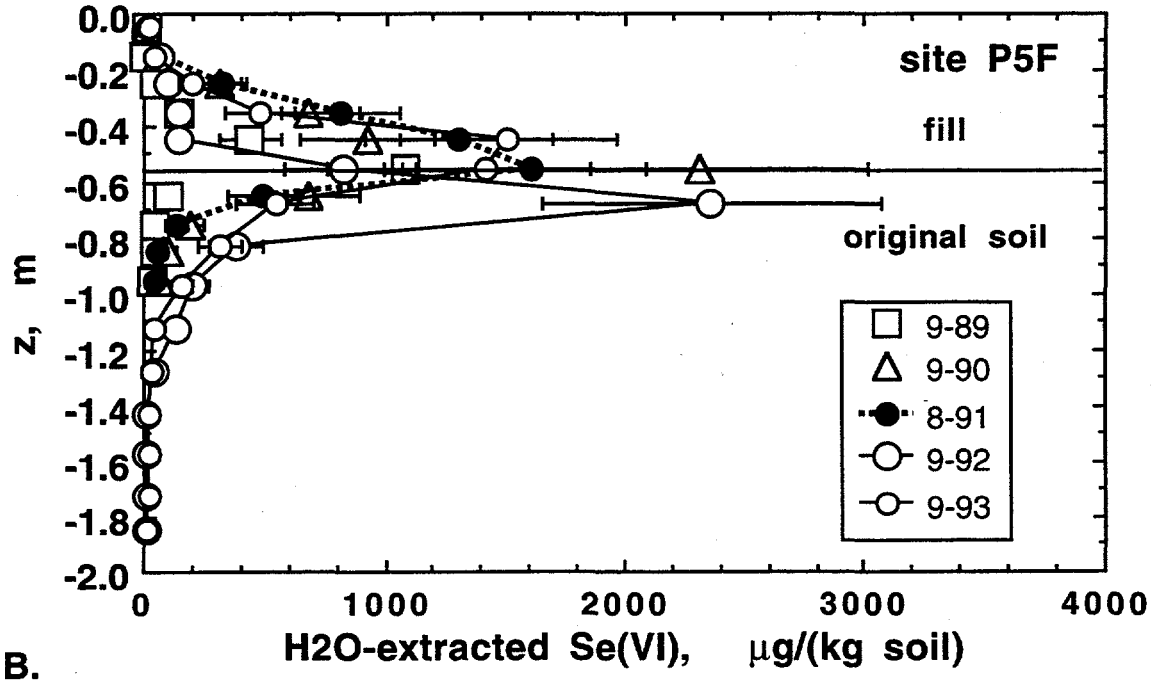

Figure 2.3.3. (**A**) Water-extractable Se(IV), and (**B**) Se(VI) profiles from yearly late summer core sampling of fill site P5F.

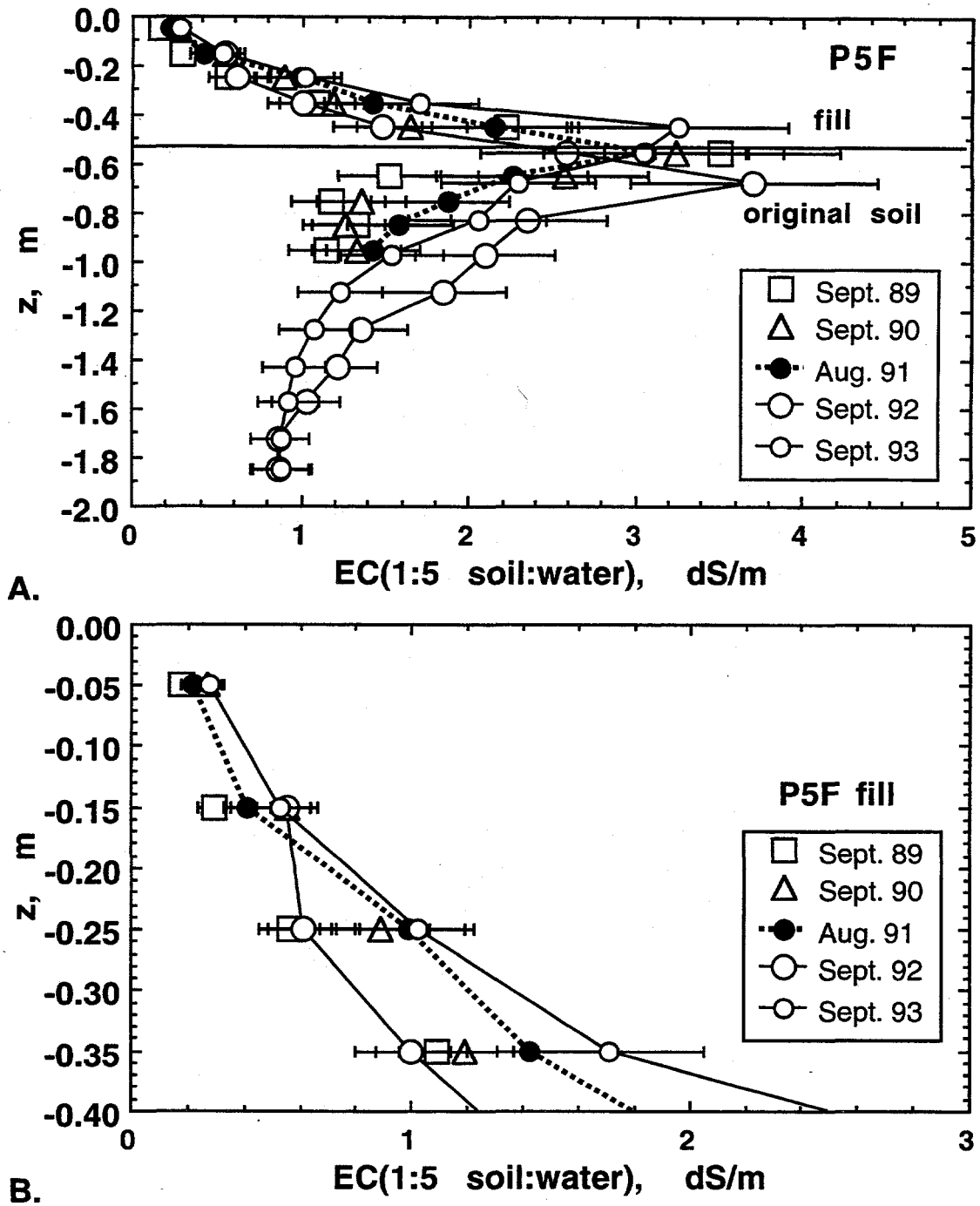

Figure 2.3.4. Salinity (EC of 1:5 soil:water extracts) profiles from yearly late summer core sampling of fill site P5F. (**A**) total profile data, and (**B**) near-surface soils.

obtained during a series of drought years. Up through the summer of 1991, trends indicated net oxidation of soil Se, resulting in increases in the water-soluble Se inventory. Net advective-diffusive movement of soluble Se into the initially clean fill was also shown (Fig. 2.3.2A). The above-average rain seasons in 1992 and 1993 resulted in slowing or reversing of this pattern. The 1992 sampling yielded about the same soluble Se inventory as in 1991, but with the zone of

high concentration displaced downwards by about 0.10 m. The 1993 sampling exhibited about a 15% reduction in the soluble Se inventory, along with an upwards displacement of the high concentration zone. Speciation of the soluble Se inventory into Se(IV) and Se(VI) shows that the former state is largely restricted to remaining within or close to the original Kesterson Reservoir soil surface, while Se(VI) is more widely distributed (Figures 2.3.3 A,B). This pattern is consistent with the lower mobility of Se(IV), due to adsorption and precipitation, the greater probability of Se(IV) oxidation to Se(VI) near the fill surface, and the high mobility of Se(VI). Significant displacement of the water-extracted Se(IV) maximum up into the fill soil occurred in samples collected one year after observing soluble Se profiles consistent with Se(VI) reduction within the lower portion of the fill. Salinity distributions (Figures 2.3.4 A,B) exhibit patterns similar to those found for soluble Se. The few ephemeral pool water samples collected in the vicinity of the P5F site during the 1992 and 1993 winters were low in both Se concentration (less than 5 ppb) and in salinity (EC less than 1 dS m^{-1}). These observations are consistent with pool formation by rain ponding (rather than water table rise), and with water-extract data from the P5F surface fill soils.

2.4 Soil Selenium and Salinity Monitoring in Plots 8EP and 9BE

Peter Zawislanski, Mavrik Zavarin, Tobin Sears, and Jenny Kengsoontra
Earth Sciences Division
Lawrence Berkeley Laboratory

Data from five years of monitoring in sites 8EP and 9BE are described below. Efforts were focused on measuring movement of selenium and salts through the soil profiles as influenced by rainfall and evapotranspiration. Previous reports (LBL, 1992, 1990) described soil profiles dominated by evapotranspiration due to drought conditions. Relatively heavier rains of 1992, 1993, and 1994 resulted in significant downward movement of solutes. Soil cores taken in the late fall through 1993 show the bulk concentrations of water-soluble Se and salts, allowing for mass balance calculations. Soil water samples, taken periodically, show the concentrations of mobile Se and salts, often dominated by macropore flow. Both sets of data contribute to the overall analysis of the chemical and physical redistribution of Se and salts.

2.4.1 Moisture Monitoring

Tensiometers and neutron probes are being used to monitor moisture movement in plots 8EP and 9BE. Neutron probe measurements allow for direct estimates of moisture content, and when normalized to a saturated moisture content, saturation. During 1992, 1993, and 1994, the moisture regime was dominated by heavy rainfall during February and March. This rainfall resulted in ponding in both plots (except 8EP in 1994), often to a depth of close to 1 m. This was possible because of both the rise of the groundwater table and also because the plots occupy depressions which are in turn a result of the filling of the surrounding areas. Figures 2.4.1 through 2.4.6 depict changes in soil saturation as measured using neutron probes. Although in both plots saturation was at or close to 100% during and immediately after ponding, moisture content declined very little in plot 8EP, especially below a depth of 0.5 m as compared with plot 9BE where saturation dropped to as low as 60% at a depth of 1 m during fall months. This suggests that the amount of redistribution taking place in plot 9BE is very much more significant than in plot 8EP, primarily due to the much coarser texture and lower moisture retention of sediments in plot 9BE as compared to plot 8EP.

Ponding usually occurred during a period of about 8-10 weeks between the middle of February and the middle of May. The draining of plot 9BE generally took a little longer due its relatively lower elevation. Changes in draining pattern are also influenced by regional groundwater table elevations. This can be seen in Figure 2.4.5, where the moisture content at 1 m depth in October 1993 exceeds the October 1992 value by 30%, as a result of a higher water

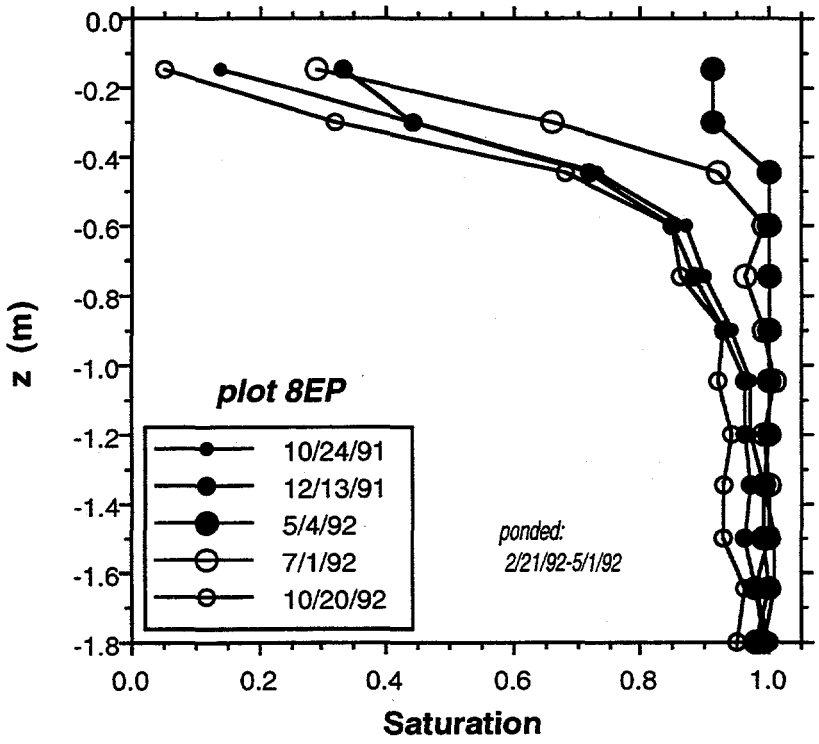

Figure 2.4.1. Changes in soil saturation from 10/91 through 10/92 in plot 8EP.

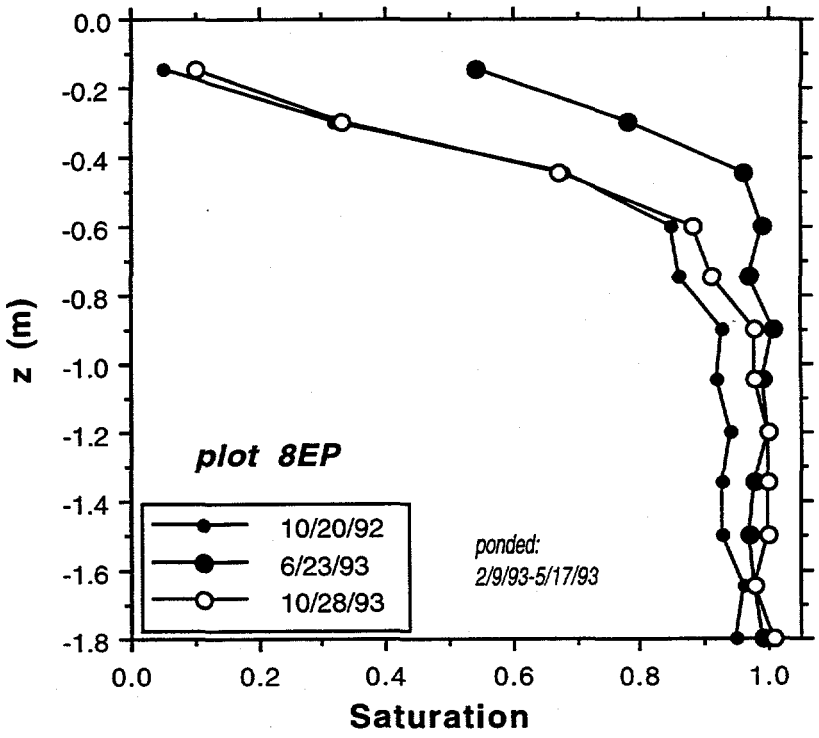

Figure 2.4.2. Changes in soil saturation from 10/92 through 10/93 in plot 8EP.

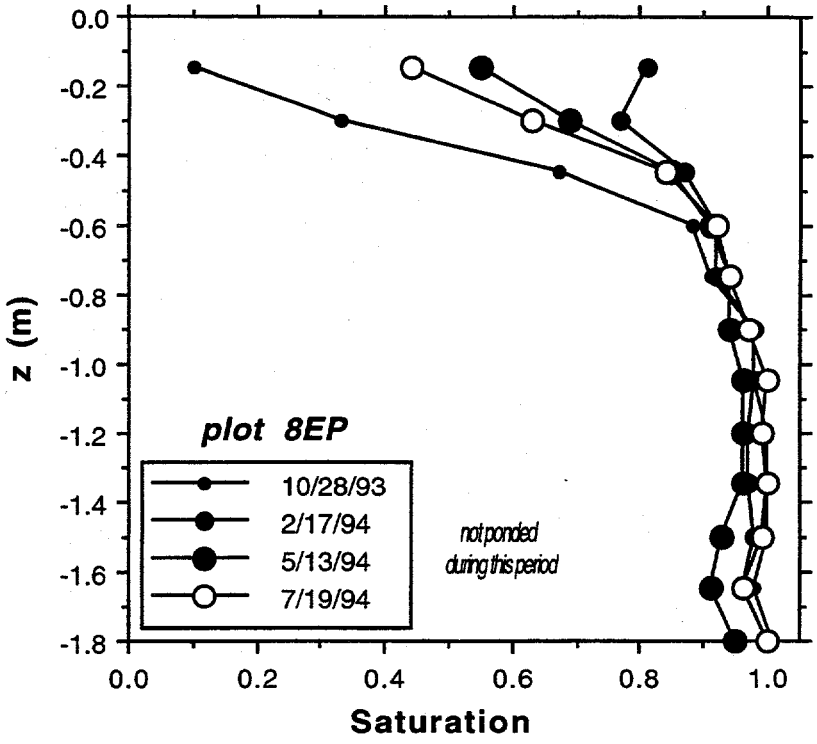

Figure 2.4.3. Changes in soil saturation from 10/93 through 7/94 in plot 8EP.

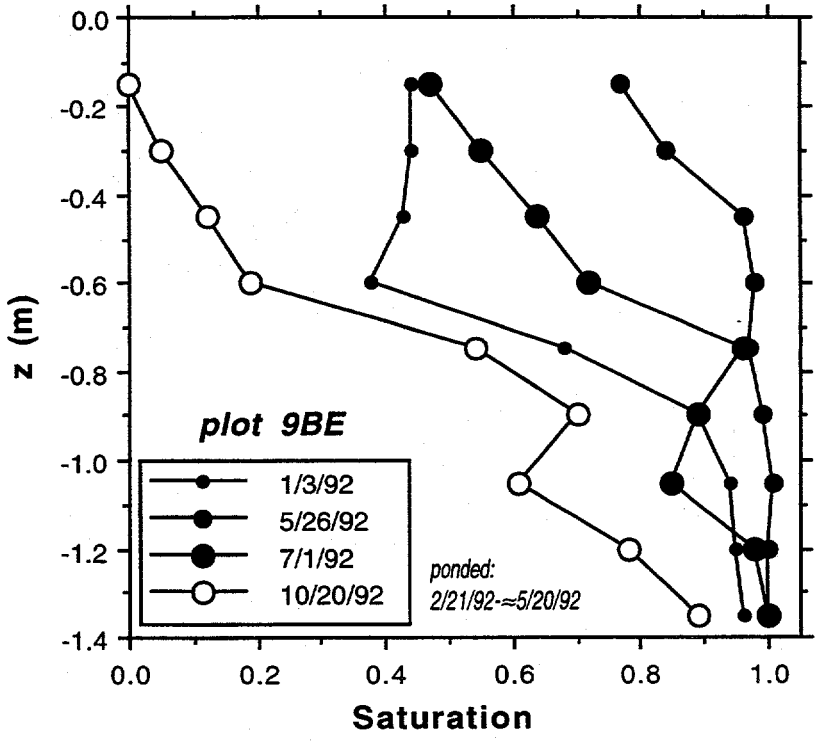

Figure 2.4.4. Changes in soil saturation from 1/92 through 10/92 in plot 9BE.

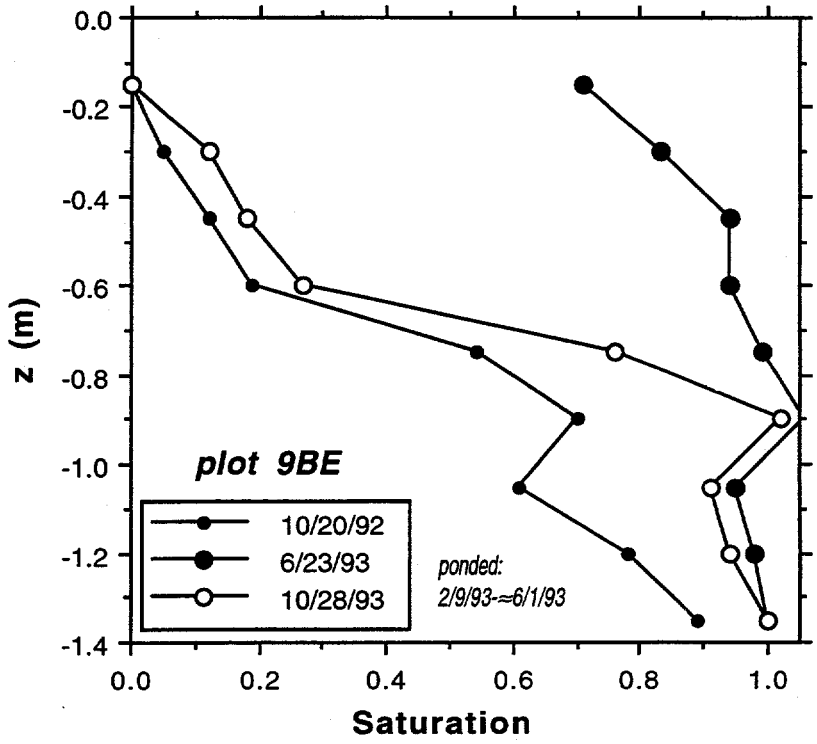

Figure 2.4.5. Changes in soil saturation from 10/92 through 10/93 in plot 9BE.

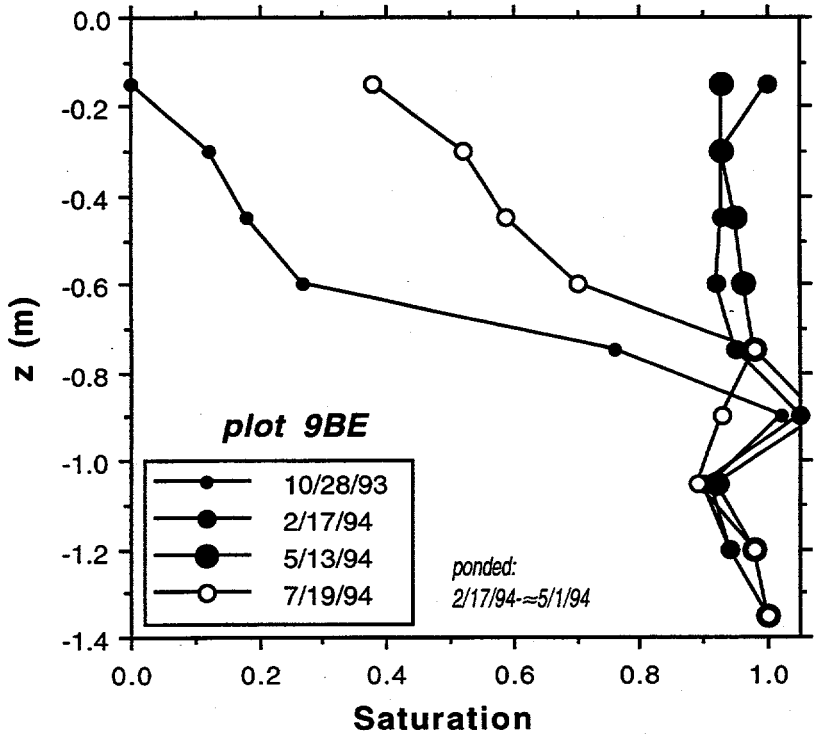

Figure 2.4.6. Changes in soil saturation from 10/93 through 7/94 in plot 9BE.

table. The rains of 1994 were not sufficient to result in ponding in plot 8EP, though moisture content increases were observed down to a depth of 0.70 m.

An additional effect of the spring-time ponding is the reduced density of plants in the summer. Because the plots were inundated during the early growing season, plant growth was limited and as a result the transpirative effect of plants was reduced as compared with the dry years (1988-1991).

2.4.2 Solute Monitoring

Data from soil water samplers and cumulative rainfall are shown in Figures 2.4.7 through 2.4.16. This mode of presentation allows for correlation of Se and salt displacement and Se reduction and oxidation with rainfall patterns.

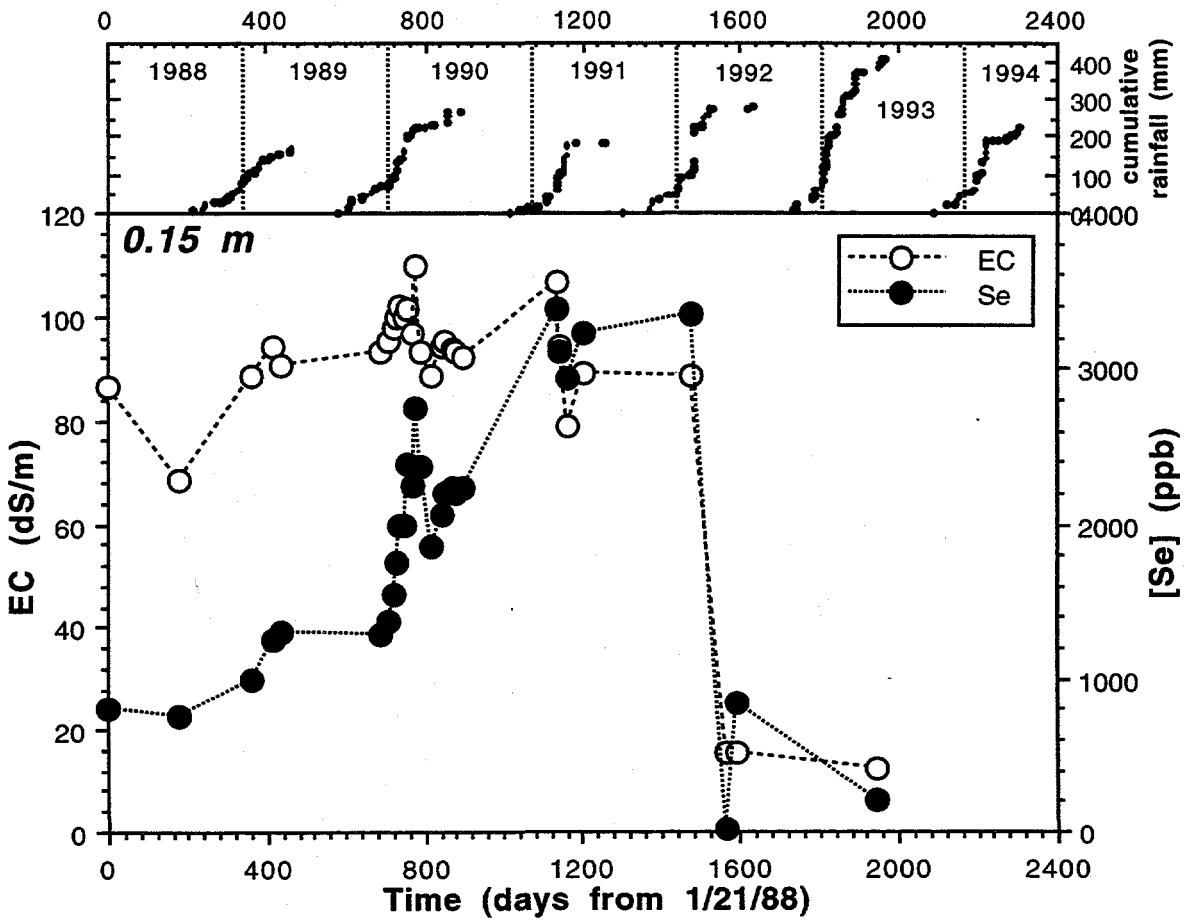

Figure 2.4.7. Changes in Se and EC in soil water at a depth of 0.15 m in plot 8EP and cumulative annual rainfall as measured by local weather stations.

Data from plot 8EP is shown in Figures 2.4.7 through 2.4.10. Because of the unavailability of sample due to dry conditions at these shallow depths during the summer and fall, and ponding

during the spring, data here is sparse and the connecting lines are for visual enhancement and do not necessarily indicate trends.

There is a good correlation between Se and soluble salts (as represented by EC) trends. This is indicative of the dominance of physical redistribution of Se over oxidation or reduction. Again, the lack of data from summer and fall months, when Se oxidation is most likely to occur, makes it difficult to arrive at concrete conclusions. However, over the long term (1988 through 1994), the relative concentration of Se to soluble salts increases at all depths. This suggests that redox-sensitive Se is reduced during wet periods, preventing it from being flushed deeper with infiltrating rainwater, and is subsequently re-oxidized during drier months.

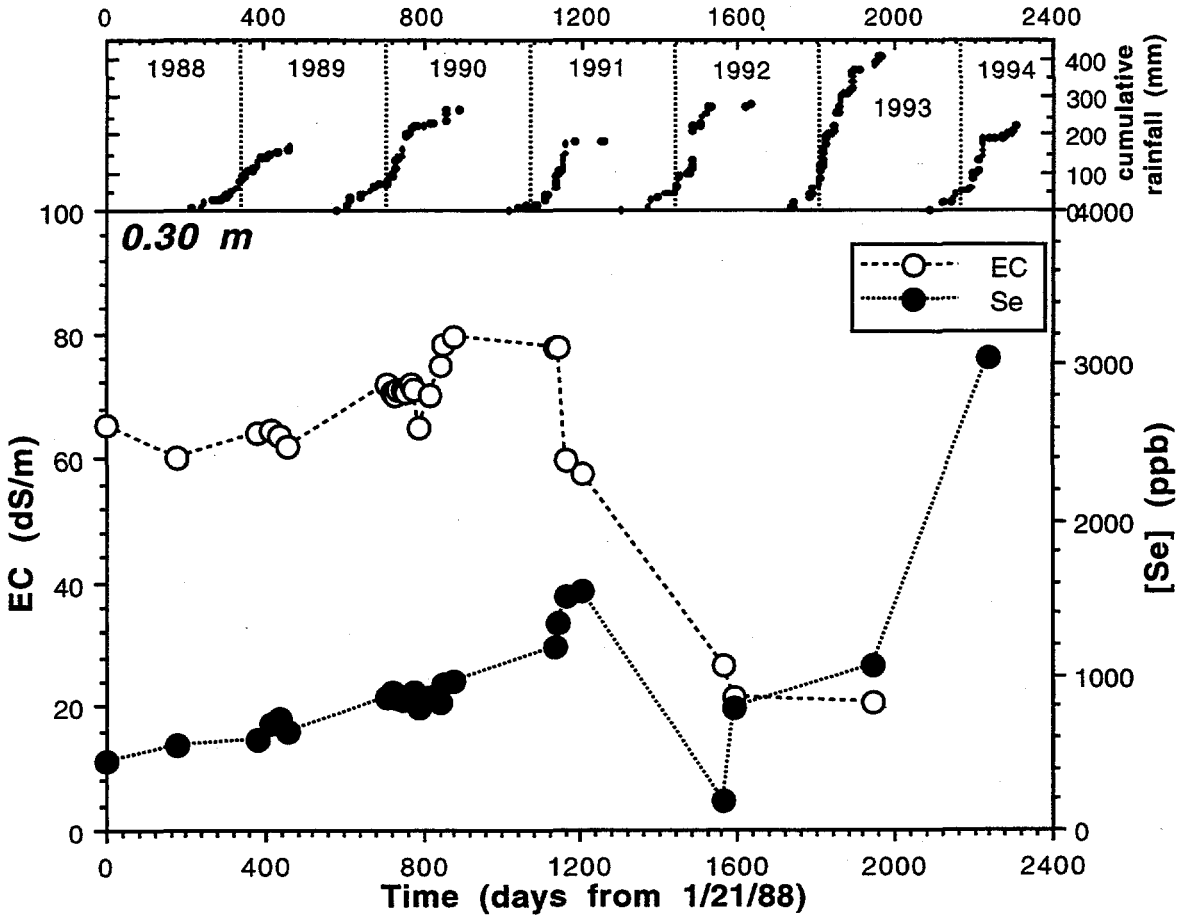

Figure 2.4.8. Changes in Se and EC in soil water at a depth of 0.30 m in plot 8EP and cumulative annual rainfall as measured by local weather stations.

The most significant changes in both Se and salt distribution occur following the 1992 rainfalls and, to a lesser extent, the 1993 storm events. It appears that the intensity of a single rainfall may cause more displacement than several smaller rainfalls of similar cumulative

magnitude. For example, 90 mm of rain fell over the course of 48 hours in early February of 1992. Such events likely caused the major down-flushing of solutes in plot 8EP. Subsequent to the 1992 rainfall, both soluble Se and salts appear to have been mostly flushed out of the 0.15 m depth. This agrees qualitatively with the displacement of water as observed through neutron probe monitoring (Figure 2.4.1).

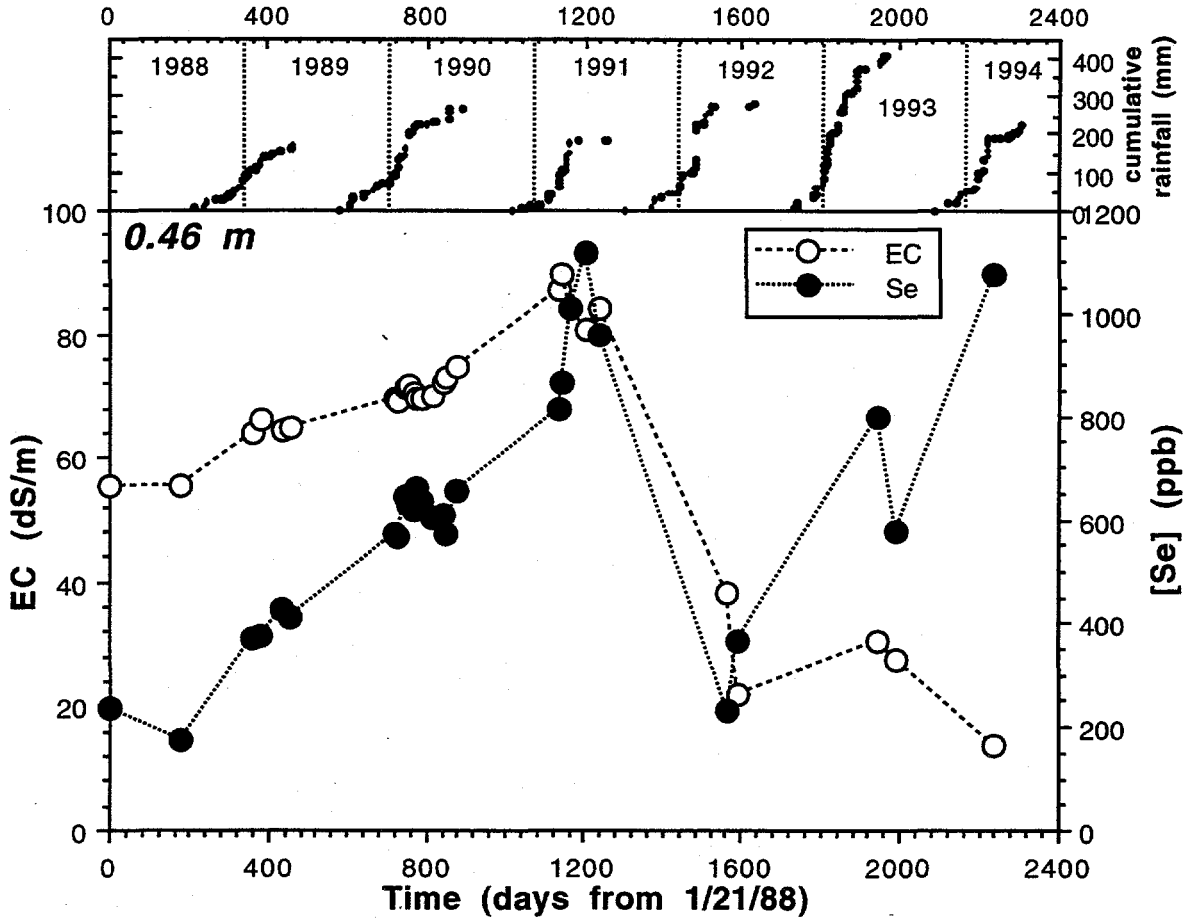

Figure 2.4.9. Changes in Se and EC in soil water at a depth of 0.46 m in plot 8EP and cumulative annual rainfall as measured by local weather stations.

Data from plot 9BE is shown in Figures 2.4.11 through 2.4.16. Samples from this plot are available throughout most of the year due to a shallower water table. During more than six months out of the year, the 0.90 and 1.20 m samplers are below the water table. This results in Se reduction and soluble Se concentrations close to zero (Fig. 2.4.15-16). As in the case of plot 8EP, samples were not available when the plot was ponded.

Several trends are apparent from this data. First, there is a fairly good correlation between Se and EC data, suggesting the importance of physical redistribution of Se. Secondly, there are

strong seasonal responses in both Se and EC, even during the dry years (1988-1991). This is primarily a result of the coarse texture of sediments in this plot, as alluded to in Section 2.4.1. Downward flushing of solutes occurred during every winter season. This, combined with transpirative concentration of solutes in the root zone (LBL, 1992), resulted in overall increases in EC during dry years, at all depths except 0.15 m. The contemporaneous changes in Se are less distinct, but do result in net increases. These trends were reversed following the rains of 1992, with both EC and Se concentrations plummeting and never recovering to pre-1992 levels. Such patterns of physical redistribution, and in the case of Se, reduction under ponded conditions, are consistent with patterns of moisture movement as measured using neutron probe (Fig. 2.4.4-6). Because of the desaturation of the profile during summer and fall months, the potential exists to transport large volumes of water through the profile and with it dissolved salts and Se. Furthermore, the transport through sandy soils can be very rapid, thus allowing for Se displacement before reducing conditions set in.

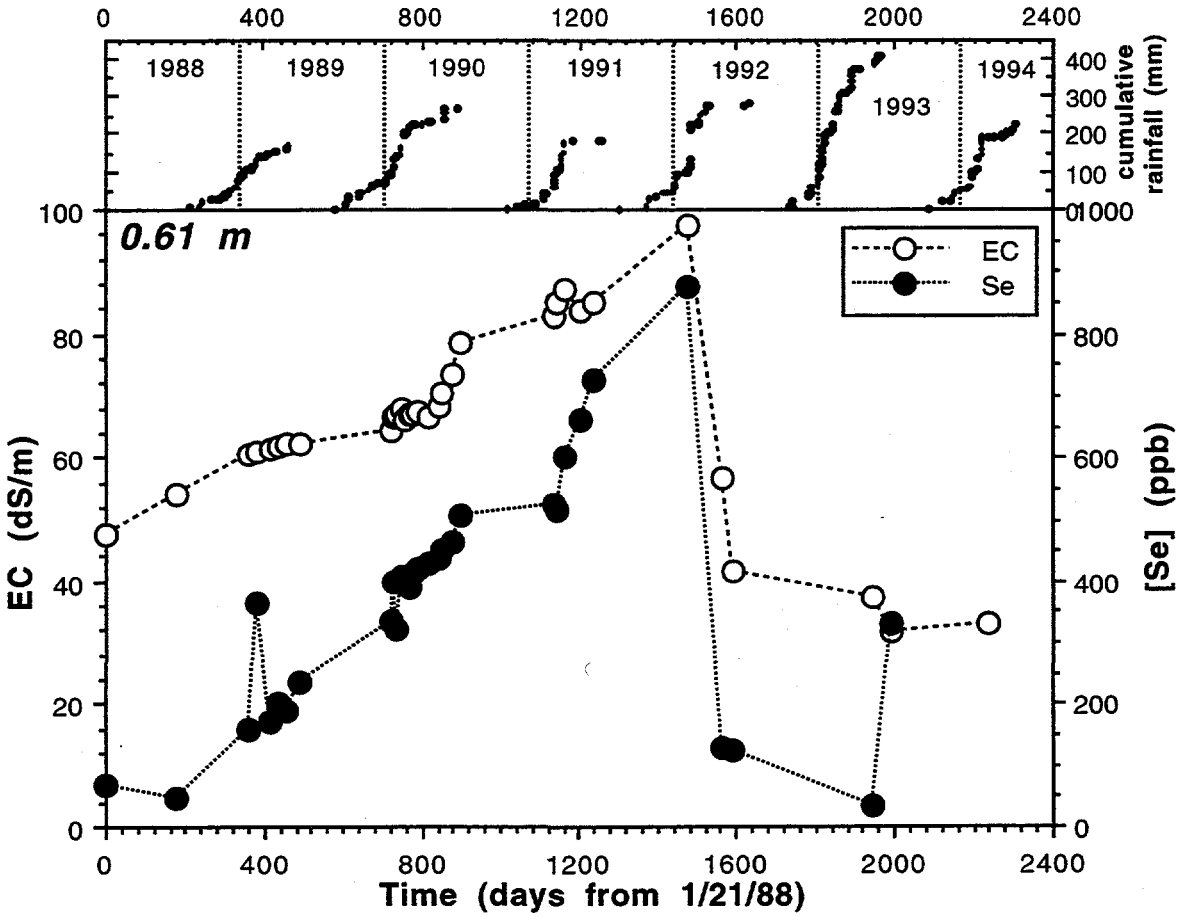

Figure 2.4.10. Changes in Se and EC in soil water at a depth of 0.61 m in plot 8EP and cumulative annual rainfall as measured by local weather stations.

Part of the difficulty in making firm conclusions on the changes in salt and Se concentrations based on soil water sampler data, stems from the fact that soil water samples are usually unavailable during the late summer, when a comparison is most valid. Analysis of soil cores taken at those times provides more quantitative results.

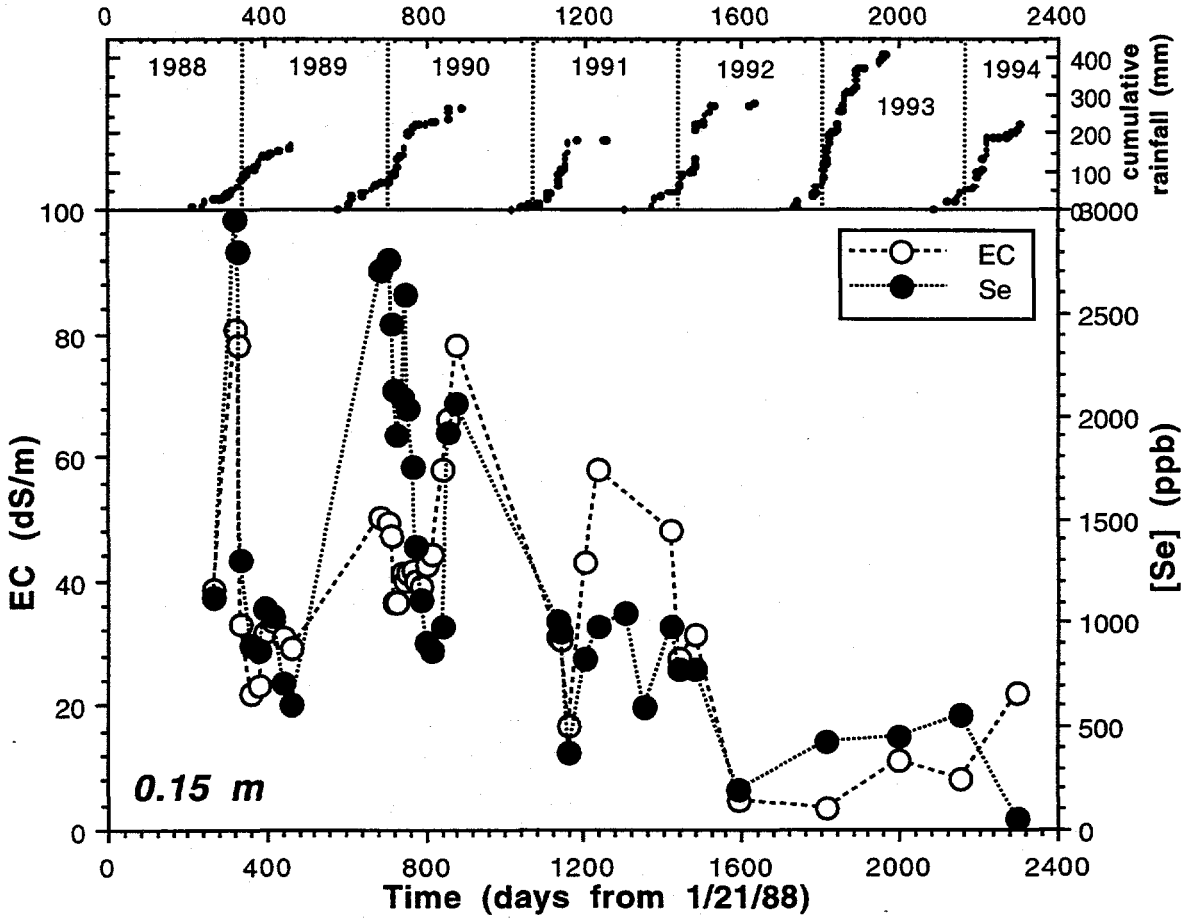

Figure 2.4.11. Changes in Se and EC in soil water at a depth of 0.15 m in plot 9BE and cumulative annual rainfall as measured by local weather stations.

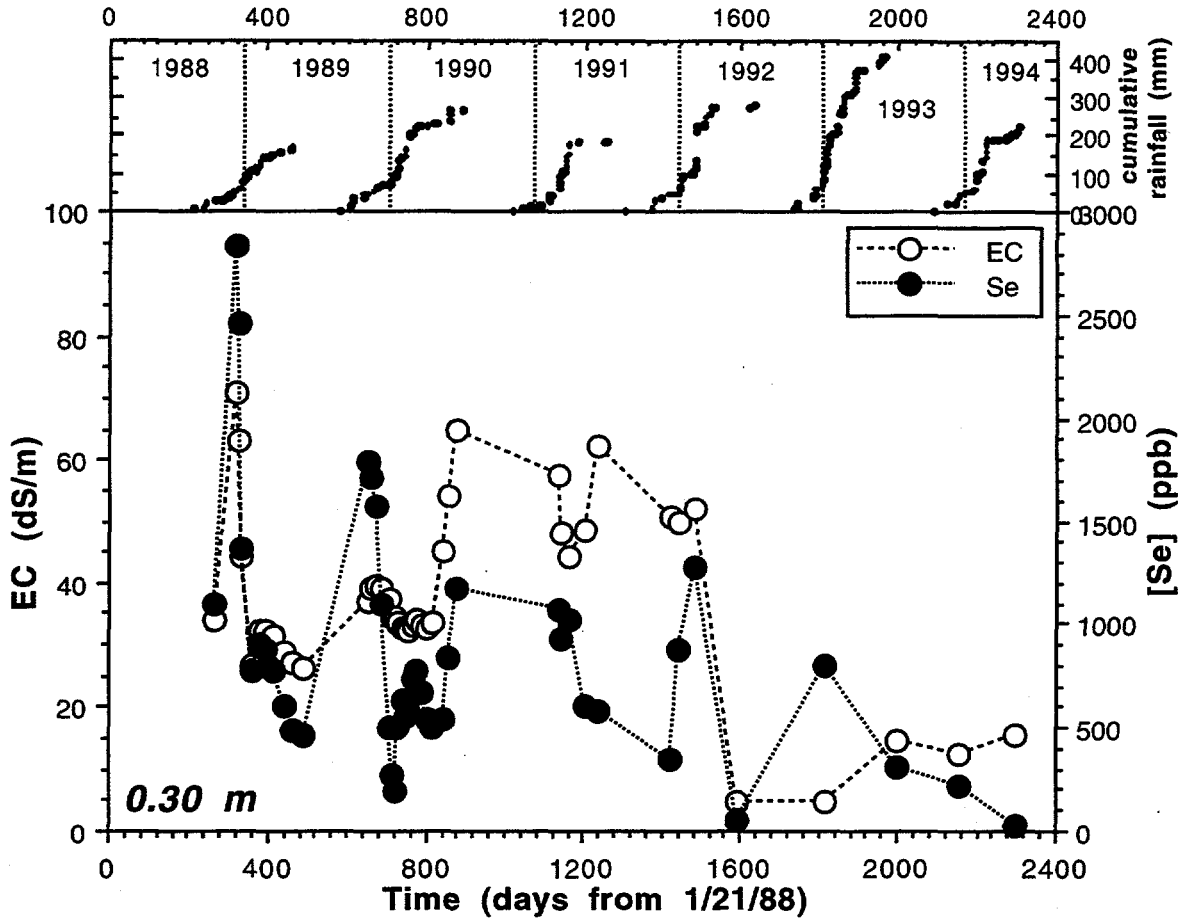

Figure 2.4.12. Changes in Se and EC in soil water at a depth of 0.30 m in plot 9BE and cumulative annual rainfall as measured by local weather stations.

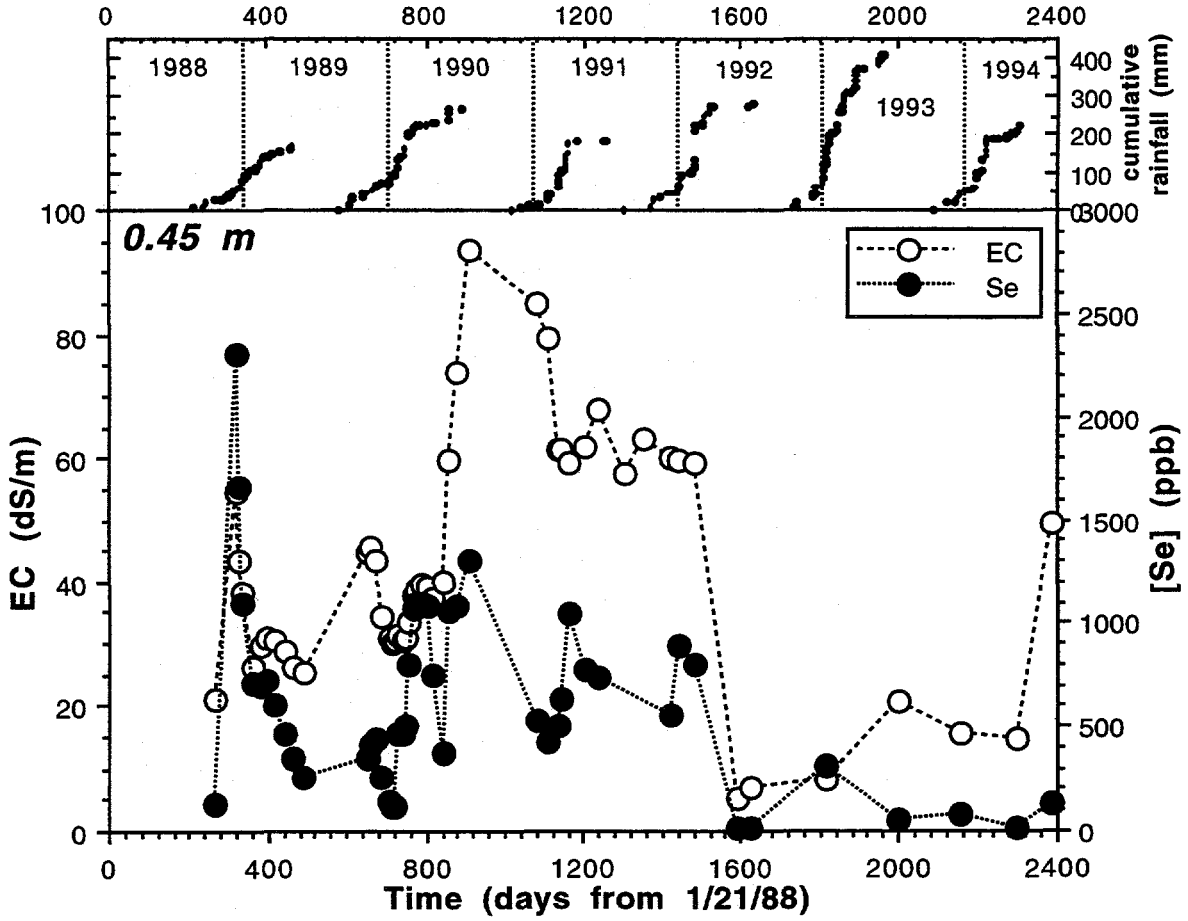

Figure 2.4.13. Changes in Se and EC in soil water at a depth of 0.45 m in plot 9BE and cumulative annual rainfall as measured by local weather stations.

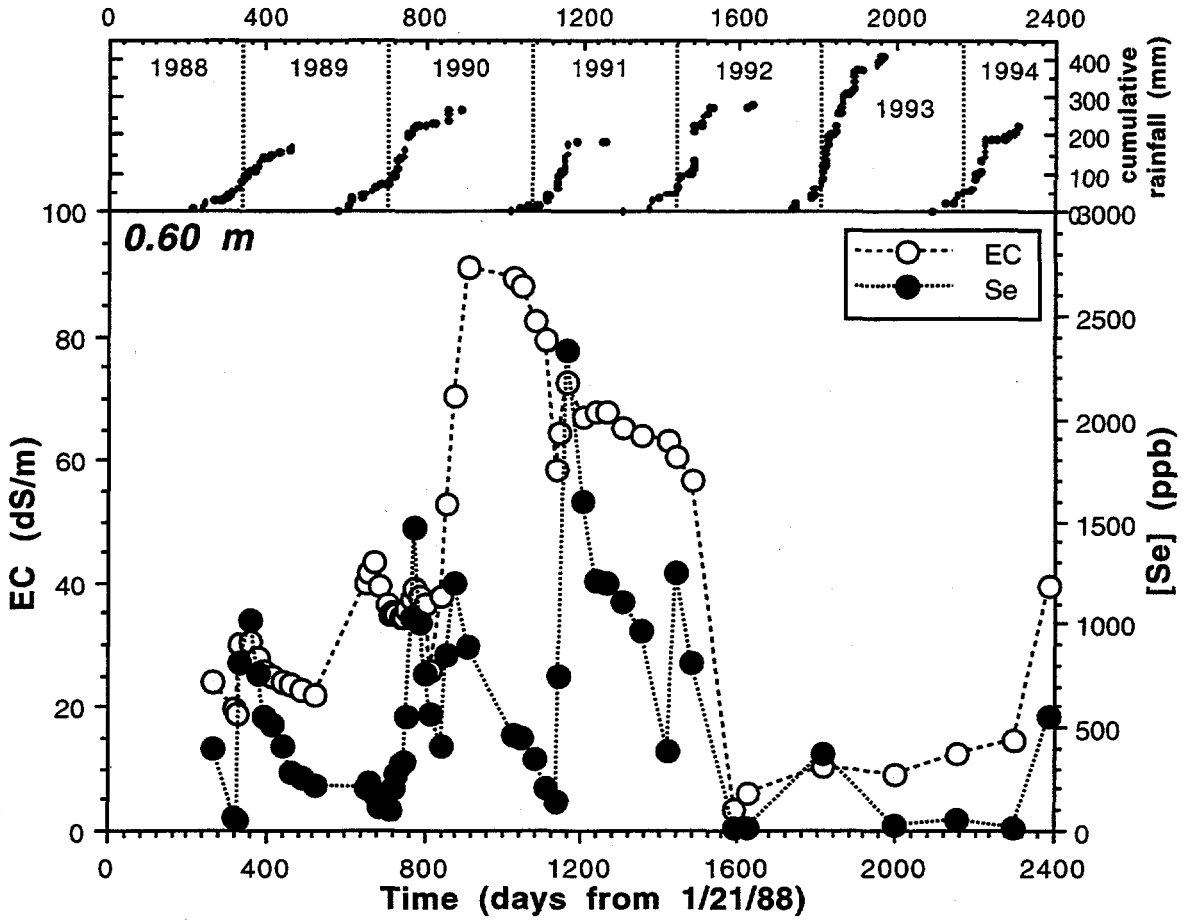

Figure 2.4.14. Changes in Se and EC in soil water at a depth of 0.60 m in plot 9BE and cumulative annual rainfall as measured by local weather stations.

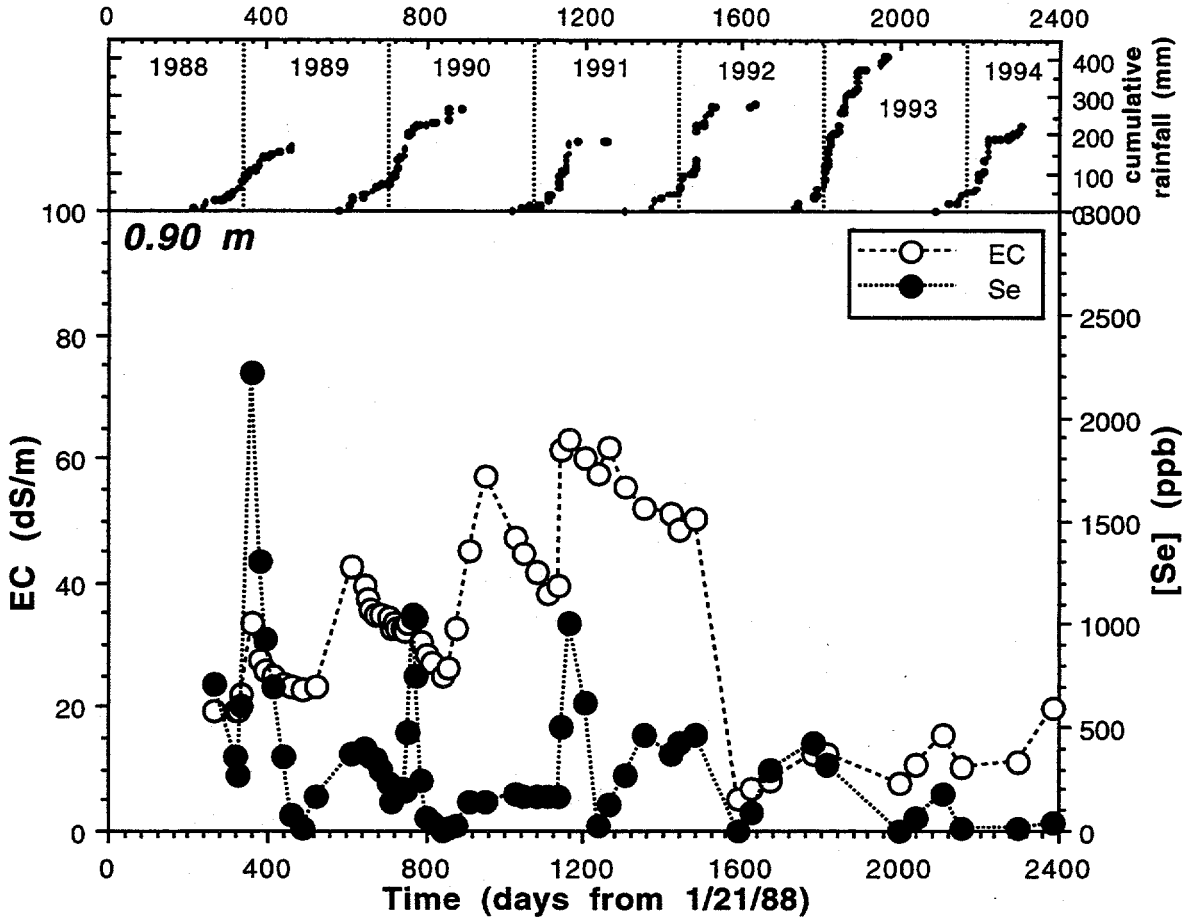

Figure 2.4.15. Changes in Se and EC in soil water at a depth of 0.90 m in plot 9BE and cumulative annual rainfall as measured by local weather stations.

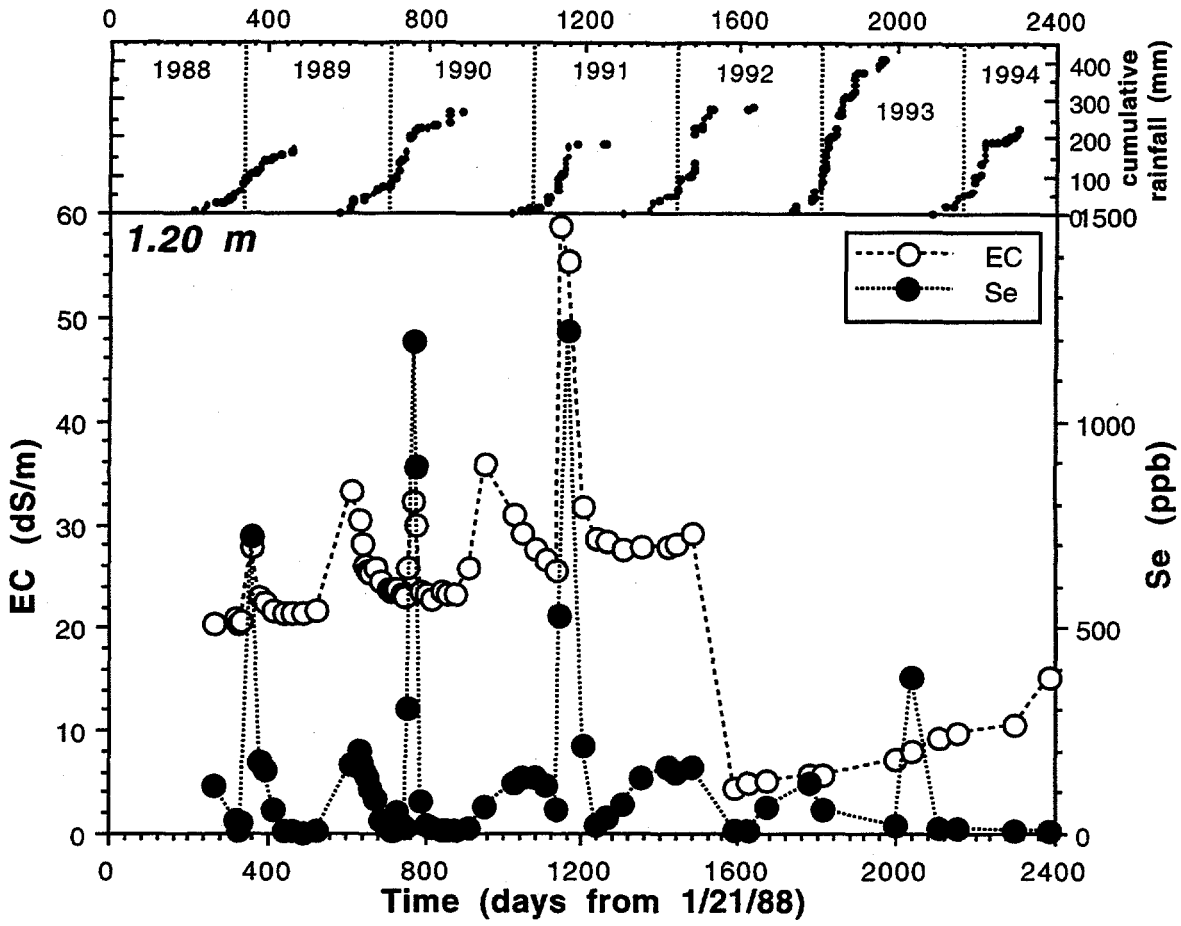

Figure 2.4.16. Changes in Se and EC in soil water at a depth of 1.20 m in plot 9BE and cumulative annual rainfall as measured by local weather stations.

2.4.3. Soil Moisture, Selenium, and Salinity Monitoring

Changes in soil Se and salt distribution are commonly affected by evapotranspiration and rainfall infiltration, as shown in Section 2.4.2. Therefore, when long-term, and not seasonal changes are sought to be observed, it is important to collect samples at roughly the same time of year, and preferably significantly after the rainy season. Soil cores have been collected in plots 8EP and 9BE on the following dates: 7/21/88, 7/25/88, 11/16/89, 11/21/89, 8/15/90, 8/22/90, 9/24/91, 10/10/92, 10/28/93, and 11/1/93. Additional cores have been taken during the rainy season but will not be discussed here in detail.

The following is a brief description of the soil sampling, preparation and analysis procedures. Cores were taken using either a hand-auger with a 2-inch barrel, or a Giddings hydraulic sampling rig. Cores were divided in the field into 10-cm intervals, except the top 20 cm which was divided into 0.5-cm to 5-cm intervals, the top 10 cm being sampled using a 10-cm long, 2-inch diameter pipe, the sample from which was split in the lab. Samples were stored

in heavy-duty freezer bags, with minimal air in the bag. After each sample was homogenized, a subsample of known mass (on the order of 10 to 20 g) was used to prepare a 1:10 soil:water extract which was stirred or shaken for 2 hours. Subsequently, the suspension was centrifuged at between 3000 and 6000 revolutions per minute for 5 to 20 minutes, depending on the texture of the soil. The supernatant liquid was then poured off and filtered through a 0.45 μm filter in preparation for chemical analysis. Selenite and total dissolved Se were analyzed for using atomic absorption spectroscopy (AAS) coupled with a hydride generator. Chloride was analyzed for using Mohr titration, as described by Flaschka and others (1969). Boron and major ions other than Cl were analyzed for using inductively coupled plasma spectrophotometry (ICP). All concentrations presented herein are normalized to the mass of dry soil, thereby providing a reference to a constant mass.

Changes in gravimetric moisture content of the cores are shown in Figures 2.4.17-18. There is an overall trend of decreasing moisture content in both plots, even following wet rainy seasons of 1992 and 1993, although the 1993 cores from plot 9BE are more moist than the previous three years below a depth of 0.80 m. There was also an increase in moisture content in plot 8EP in 1992 relative to the previous two years below a depth of 0.80 m. The net decrease in moisture content over the years is likely the result of plant evapotranspiration (LBL, 1992). The slight increases at depth are likely related to the lower density of plants resulting from ponding, as described in Section 2.4.1.

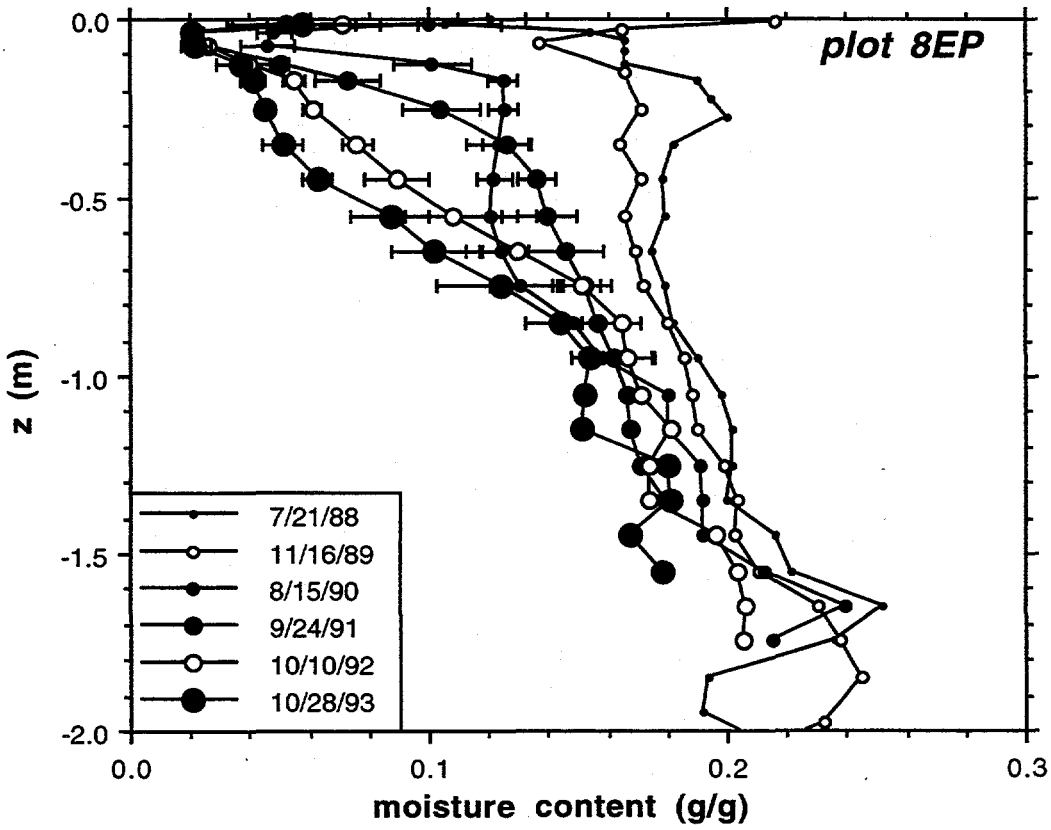

Figure 2.4.17. Changes in gravimetric moisture content in plot 8EP.

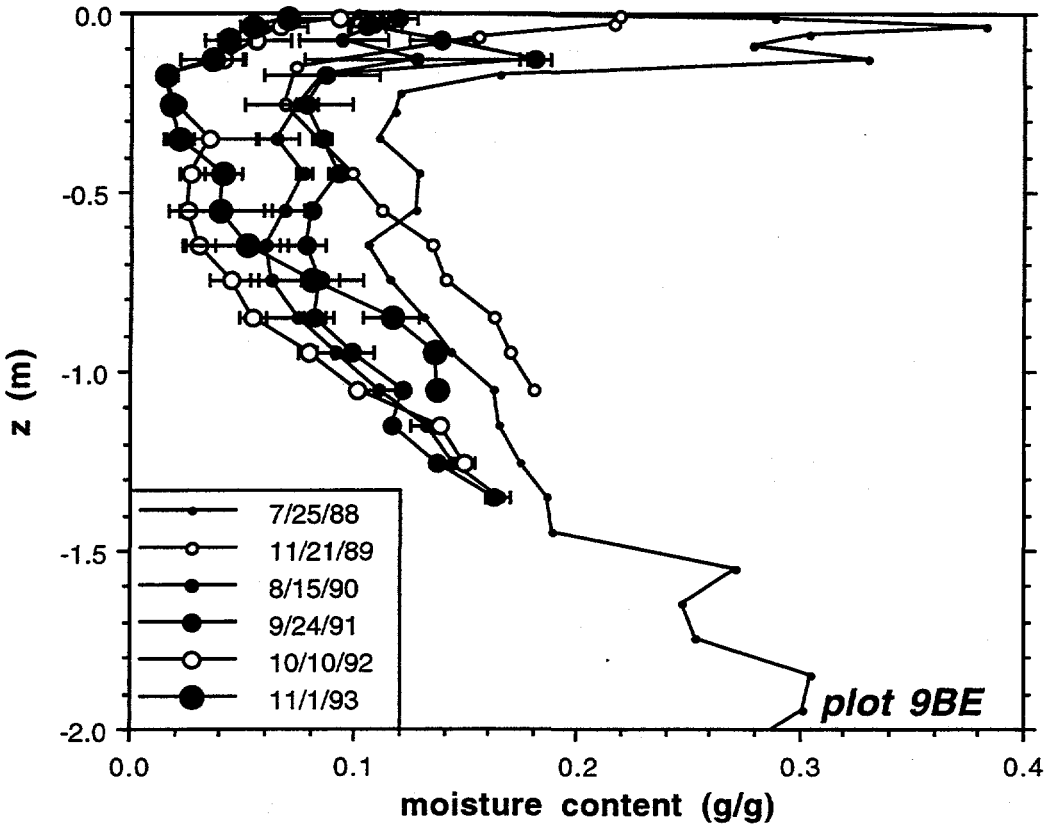

Figure 2.4.18. Changes in gravimetric moisture content in plot 9BE.

Infiltrating rainwater displaces dissolved solutes and also dissolves high solubility salts, such as NaCl. Root extraction of soil water leads not only to loss of moisture but also to an increase in solutes and the possible precipitation of salts. Chloride was chosen to study these effects because of its high solubility and relatively conservative behavior in a soil system. Changes in Cl in the soil profile of plot 8EP are shown in Figure 2.4.19. Cl concentrations at depth increased significantly between 11/89 and 8/90 due to the invasion of the plot by plants. There was also a significant increase in Cl between the depths of 1.0 m and 1.5 m, while a significant decrease in soil moisture was not observed in this interval. This may be due to a more rapid re-wetting of soil in that region due to its proximity to the water table in the spring (depth to water was 1.4 m to 1.8 m). As a result of downward displacement of soil water, Cl concentrations declined in the top 0.40 m and increased below 0.40 m between 8/90 and 9/91. The greatest change occurred between 1991 and 1992, when, as a result of heavy rains in early 1992, Cl concentrations were reduced to close to zero near the surface and most of the Cl was displaced to below a depth of 1.0 m. Cl was displaced a little deeper in 1993. These are however only net changes, with Cl concentrations being even lower immediately following ponding events and

increasing over the course of the summer due to evapotranspiration. As seen in Figure 2.4.20, similar patterns were observed in plot 9BE. After a marked increase in Cl between 1989 and 1990, concentrations were somewhat reduced in 1991 and greatly reduced in 1992. The degree to which Cl was displaced in 1992 is indicative of its mobility in this coarse-textured soil. Cl concentrations in the root zone increased in 1993, likely the result of increased evapotranspiration.

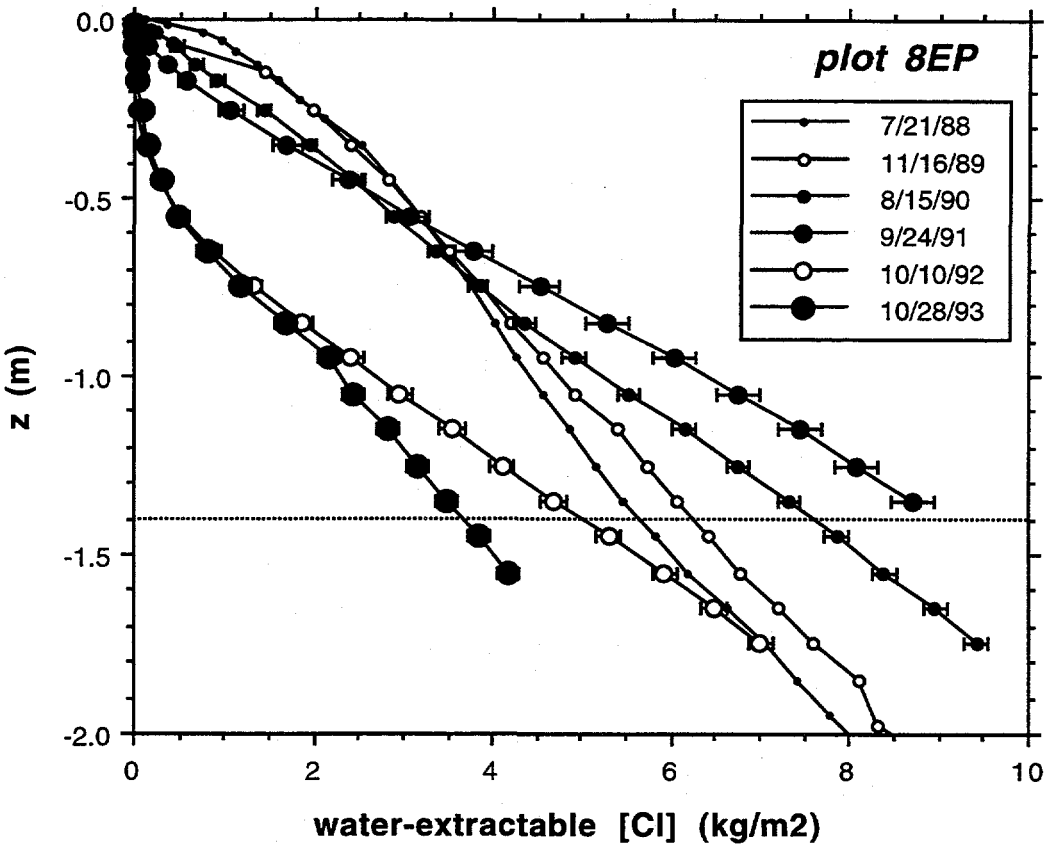

Figure 2.4.19. Depth-cumulative water-extractable Cl concentrations, normalized to area, in plot 8EP.

In contrast to Cl, Se concentrations in the soil profile did not change dramatically from year to year in plot 8EP (Figure 2.4.21). Mechanisms for accumulation in the vadose zone are different for Cl and Se. Cl accumulates due to its transport in water coming up from the water table: concentrations of Cl in groundwater are roughly the same as those in the vadose zone. This, however, is not the case with water-soluble Se. Its concentration in groundwater is very low (usually < 5 ppb) and therefore water coming up from the water table cannot contribute significant amounts of Se. An increase in water-soluble Se (mostly selenate, and to a lesser

extent selenite), is predominantly a result of oxidation of more reduced forms, such as Se(IV), Se_0 and $Se_{organic}$. It has been shown in previous and ongoing studies, that most of the Se inventory is not in its most oxidized forms and is thus subject to oxidation over the long term (LBL, 1990, Section 2.5). The major increase observed between 1988 and 1989 is indicative of such re-oxidation, since Cl concentrations did not change significantly over this period. Aside from this change, the Se inventory in the top 1.4 m remained between 375 mg m^{-2}, and 475 mg m^{-2}. There is, however, a decline in Se in the top 0.30 m and an increase below that depth over the course of the last 4 years, suggesting some displacement with infiltrating rainwater. Downward displacement of Se is much more prominent in plot 9BE (Figure 2.4.22), where, after an increase from 1988 to 1989 to 1990 due to oxidation, Se concentrations decrease dramatically in 1991, 1992, and somewhat in 1993. Although some of these decreases may be due to in-situ reduction, there is definitely significant flushing of Se taking place, as patterns match those of Cl fairly well (cf. Figures 2.4.11-16).

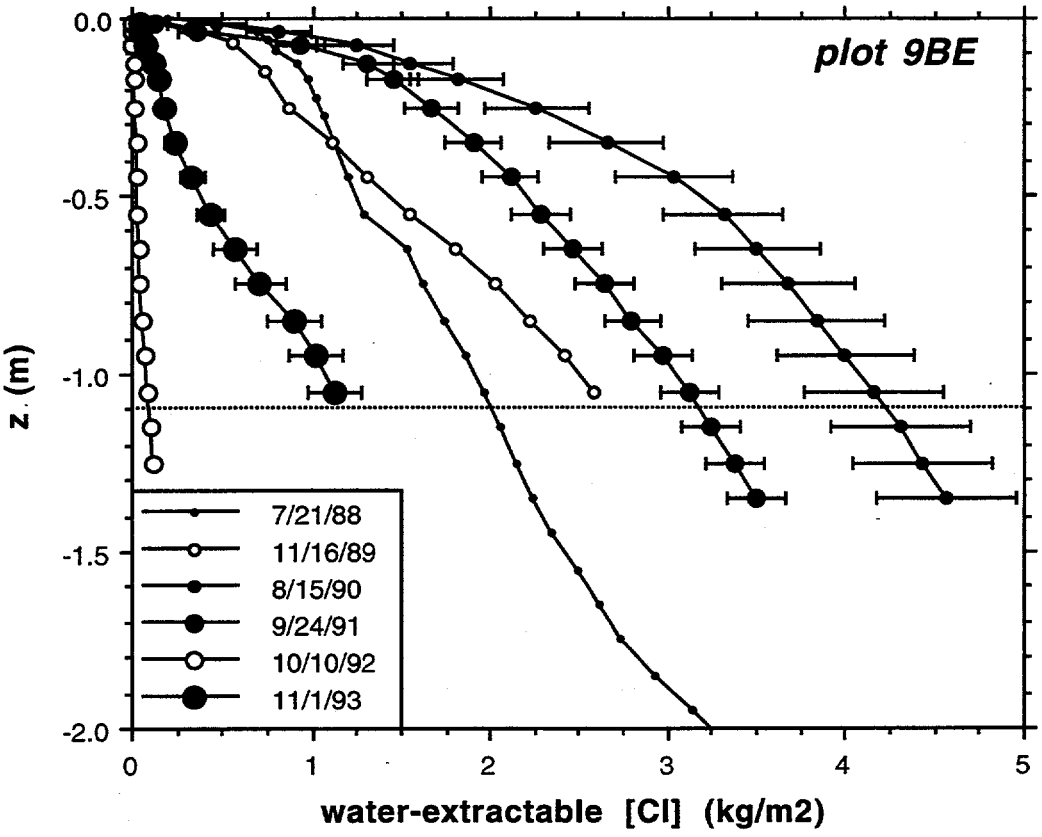

Figure 2.4.20. Depth-cumulative water-extractable Cl concentrations, normalized to area, in plot 9BE.

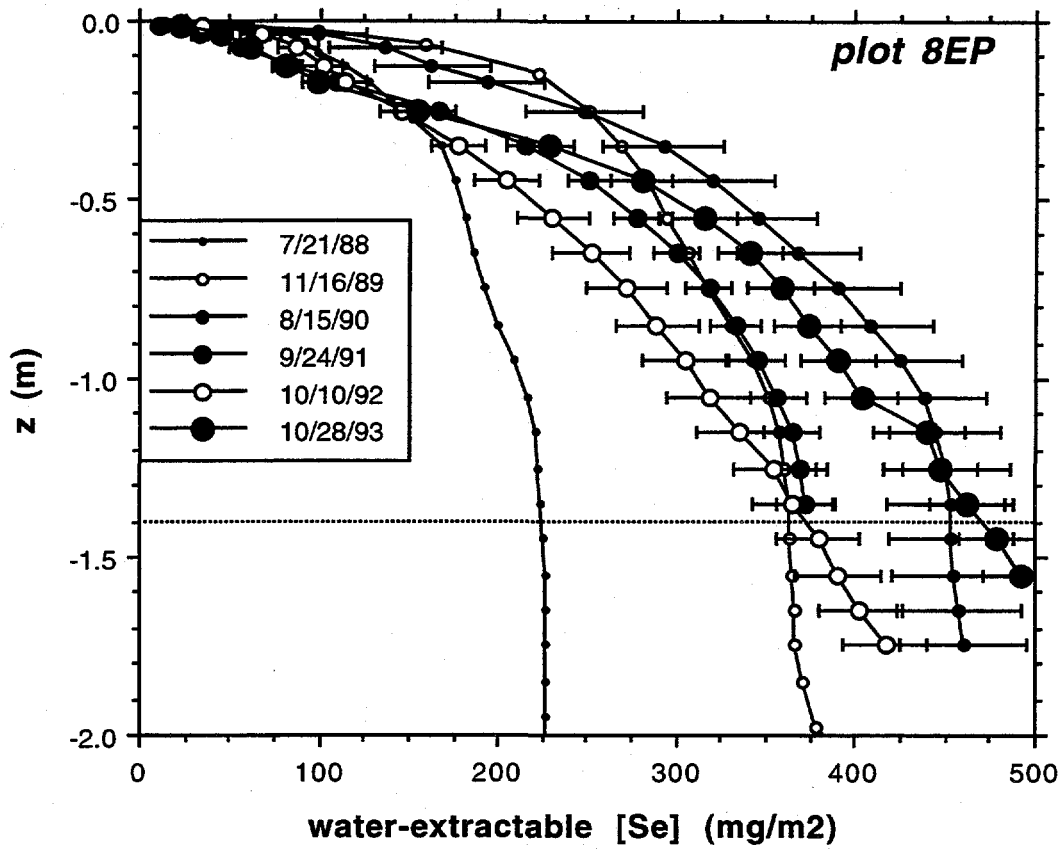

Figure 2.4.21. Depth-cumulative water-extractable Se concentrations, normalized to area, in plot 8EP.

2.4.4 Quantitative Assessment of Chloride and Selenium Concentration Changes

Even though groundwater levels fluctuate seasonally, a nominal vadose zone may be assumed for the purpose of the following analysis. The criteria were: the interval to be unsaturated during part of the year, water-soluble Se concentrations to be non-zero (or more precisely, concentrations to exceed analytical detection limit), and soil sample was available. In plot 8EP, this interval extends down to 1.4 m, in plot 9BE, to 1.1 m. Table 2.4.1 contains the results of calculations of mean profile values for: gravimetric moisture content (θ), Cl concentrations normalized to projected soil area ($[Cl]/m^2$), and water-soluble Se concentrations normalized to projected soil area ($[Se]/m^2$). Also, percentage of change relative to the previous year is shown.

Increases in Se are generally indicative of Se oxidation, because, as pointed out in Section 2.4.3, there is very little Se below this zone to serve as a source for redistribution. Cl increases are generally the result of evapotranspiration. However, Se decreases during the wet years are the result of both chemical reduction and physical displacement. A further complication is that Se will be reduced during rainwater infiltration and thus "retarded" relative to Cl. The rate of reduction is not known a priori, and so the analysis of these processes is beyond the scope of this report. Suffice it to say that significant flushing of Se did occur in plot 9BE in 1992. Samples from 1993 are currently being analyzed for total Se in order to assess the effect of the flushing on the total Se inventory.

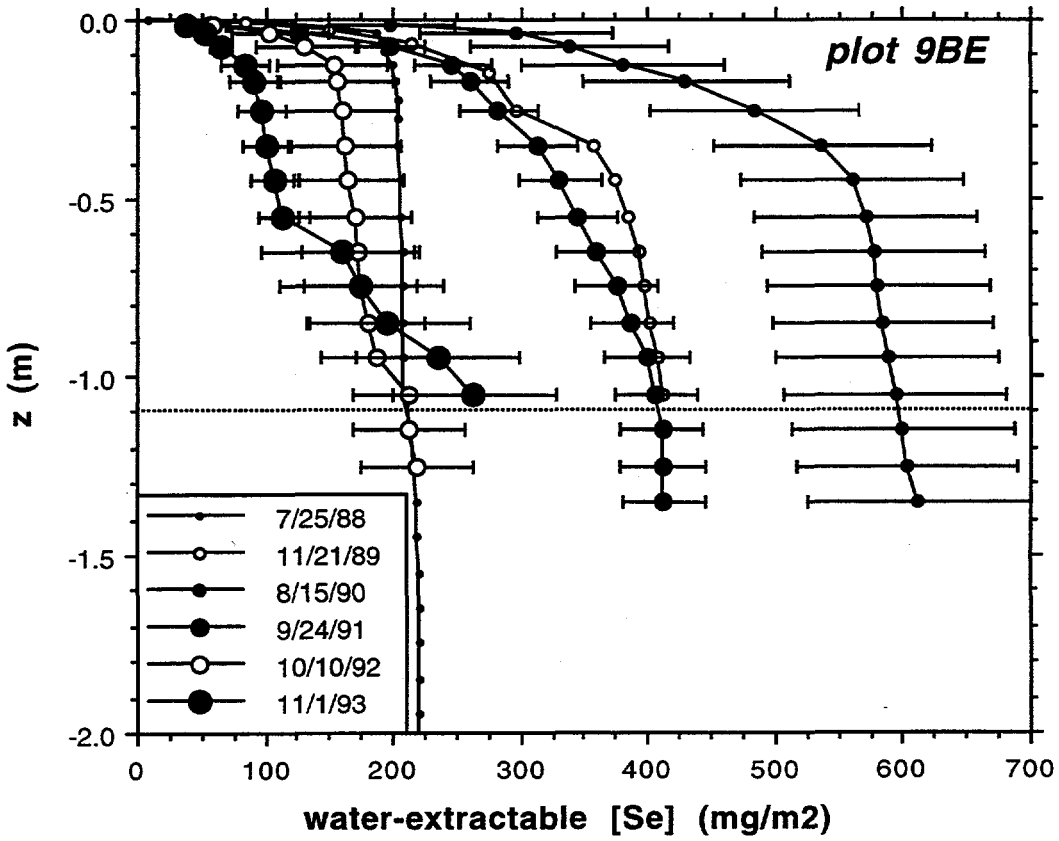

Figure 2.4.22. Depth-cumulative water-extractable Se concentrations, normalized to area, in plot 9BE.

Re-oxidation rates can be estimated based on changes between Se in samples taken shortly after the rainy season (May) and those taken in the late fall. This analysis will be presented in a future publication. Interestingly enough, following the cycles of oxidation and reduction, the

soluble Se inventory in both plot 8EP and 9BE was roughly the same in 1993 as in 1988. This is illustrative of the dynamic nature of the shallow soil environment with respect to Se redox state.

Table 2.4.1. Profile-averaged gravimetric moisture content, Cl and Se concentrations and changes in concentrations from year to year.

Sample Date	θ (g/g)	[Cl]/soil (kg/m^2)	change [Cl] %	[Se]/soil (mg/m^2)	change [Se] %
Plot 8EP					
7/21/88	0.186	5.47	—	223	—
11/16/89	0.178	6.07	*+11%*	363	*+63%*
8/15/90	0.142	7.33	*+21%*	453	*+25%*
5/8/91	0.162	7.82	*+7%*	272	*-40%*
9/24/91	0.137	8.70	*+11%*	372	*+37%*
5/26/92	0.196	3.38	*-61%*	286	*-23%*
10/10/92	0.122	4.69	*+39%*	366	*+28%*
10/28/93	0.114	3.49	*-26%*	462	*+26%*
Plot 9BE					
7/25/88	0.146	1.96	—	209	—
11/21/89	0.125	2.58	*+31%*	412	*+97%*
8/22/90	0.080	4.17	*+61%*	594	*+44%*
9/24/91	0.094	3.12	*-25%*	406	*-31%*
5/26/92	0.144	0.462	*-85%*	121	*-70%*
10/10/92	0.038	0.117	*-75%*	219	*+81%*
11/1/93	0.077	1.127	*+963%*	263	*+20%*

2.4.5 Chloride and Selenium in Near-Surface Soils of Plots 8EP and 9BE

Beginning in July 1988 and ending in July 1989, samples of the top 9 cm of soil were taken from plots 8EP (NE quarter of Pond 8) and 9BE (SW quarter of Pond 9) for analysis on a monthly basis. The impetus for this sampling strategy was to track changes in chemical species concentrations in these surface soils as affected by bare soil evaporation and rainfall infiltration. The 1988/89 series of samples yielded data which suggested that while seasonal fluctuations in this interval were significant (species flushed down deeper into the soil profile during the wet season, and evaporatively concentrated during the dry season), the net differences over a twelve

month period were very small; these changes were recognized to be strongly dependent on atmospheric conditions, especially rainfall amount and intensity. In summary, salt concentrations over that twelve month period dropped slightly, while water-extractable Se concentrations did not change significantly (for a full discussion see LBL, 1989). This twelve month period was representative of drought conditions which were prevalent in California since 1986. Since July 1989, seven more sets of samples have been taken from the experimental plots (9/89, 4/90, 10/90, 5/91, 10/91, 5/92, 10/92).

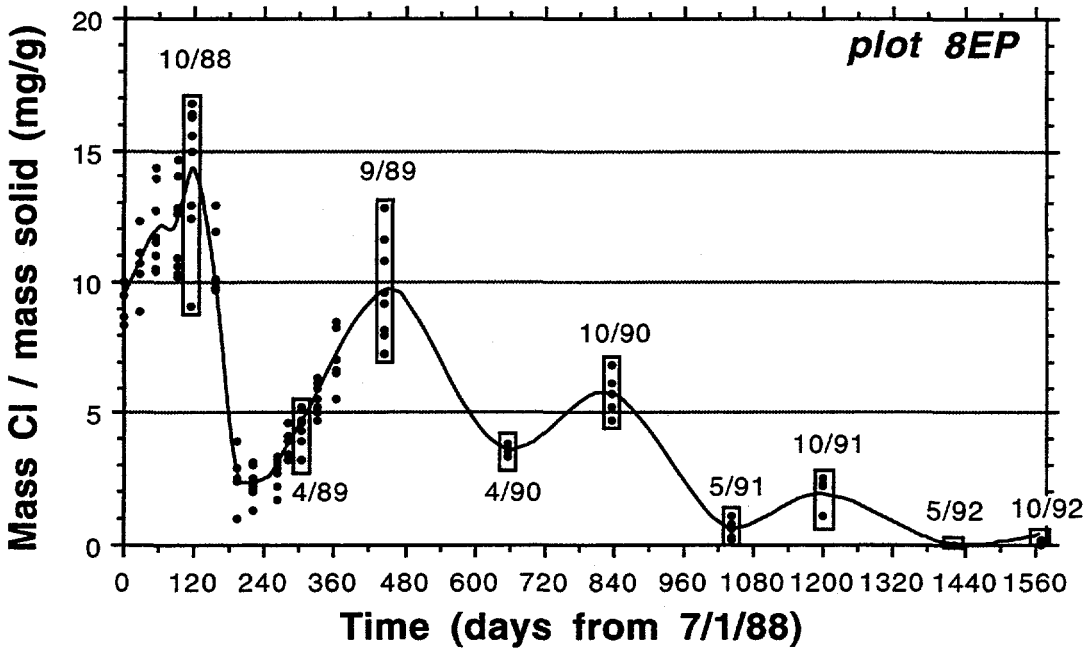

Figure 2.4.23. Changes in chloride concentration in the top 9 cm of soil in plot 8EP: July 1988 - October 1992.

Figure 2.4.23 shows changes in Cl concentrations in the top 9 cm of soil in plot 8EP. A pattern of higher concentrations at the end of the summer and lower concentrations at the end of the winter corresponds to the evaporative accumulation of salts at the surface during dry months and the flushing down of solutes deeper into the profile during the rainy season, respectively. Overall, Cl concentrations have been declining over the last four years, suggesting a solute gradient toward the root zone of plants (predominantly *Bassia*) which have become more dominant over the last three years. Salt distribution is never in equilibrium from year to year due to varying rainfall patterns. Even after relatively dry winters of 88/89 and 89/90, there were marked decreases in Cl concentration. After a somewhat wetter winter of 90/91, Cl concentrations were drastically reduced. The plot was flooded after relatively intense rainfall events in February, March, and April of 1992, resulting in almost complete flushing of soluble

salts out of the surface soils. A comparison of water-soluble Se concentrations (Figure 2.4.24) reveals a similar overall pattern through 1991, but not in 5/92 or 10/92. Although ponded rainwater in 1992 flushed Cl out, the decline in Se concentrations was much less pronounced. This agrees qualitatively with trends observed by, among others, Long et. al. (1990). Soluble Se becomes rather quickly reduced under ponded conditions and immobilized in shallow sediments. On the other hand, very low Se concentrations in May 1991 are likely due to soluble Se being flushed deeper into the soil profile with infiltrating but not ponded rainwater. Further discussion of Se oxidation in the soil profile may be found in Section 6.

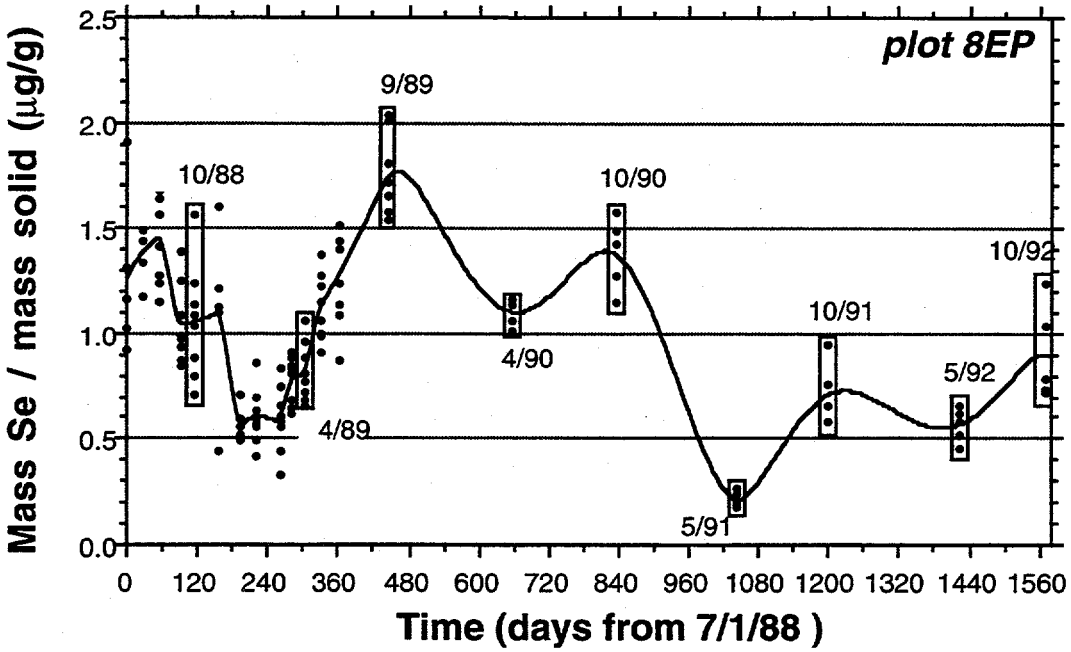

Figure 2.4.24. Changes in water-extractable selenium in the top 9 cm of soil in plot 8EP: July 1988 - October 1992.

Surface salt and Se concentration changes in plot 9BE are more difficult to discern given their preponderant spatial variability. Changes in Cl concentrations in the top 9 cm of this plot are shown in Figure 2.4.25. The pattern here differs from plot 8EP in that in April 1990 concentrations did not decline significantly. This may be due to the fact that ≈75% of the rainfall of that season occurred by the end of February, while in 1989 and 1991, much of the rainfall occurred in March and April. In contrast to plot 8EP, where the groundwater table is usually no shallower than 140 cm below the soil surface, the groundwater table in plot 9BE is within 50 cm of the soil surface during the late winter and early spring, wetting up the soil profile, and allowing for more rapid accumulation of solutes near the soil surface. Similar to plot 8EP, Cl concentrations were drastically reduced as a result of ponding in 1992. Se patterns are

qualitatively similar to Cl. As in plot 8EP, Se was not flushed as much as Cl in 1992, although 10/92 concentrations were lower than in any other fall sampling period.

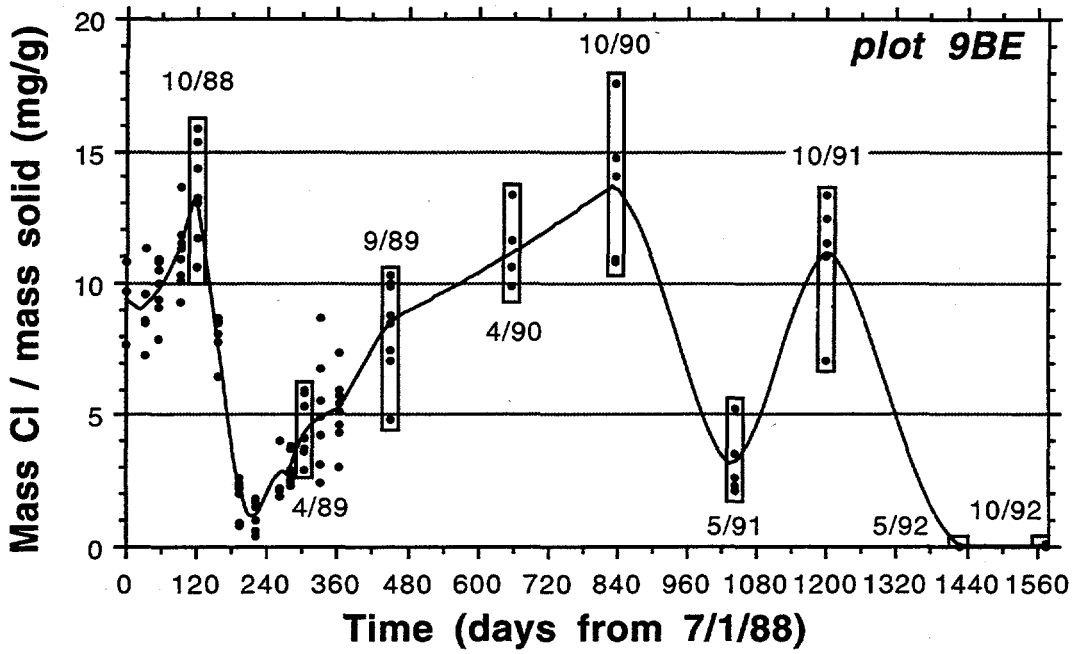

Figure 2.4.25. Changes in chloride concentration in the top 9 cm of soil in plot 9BE: July 1988 - October 1992.

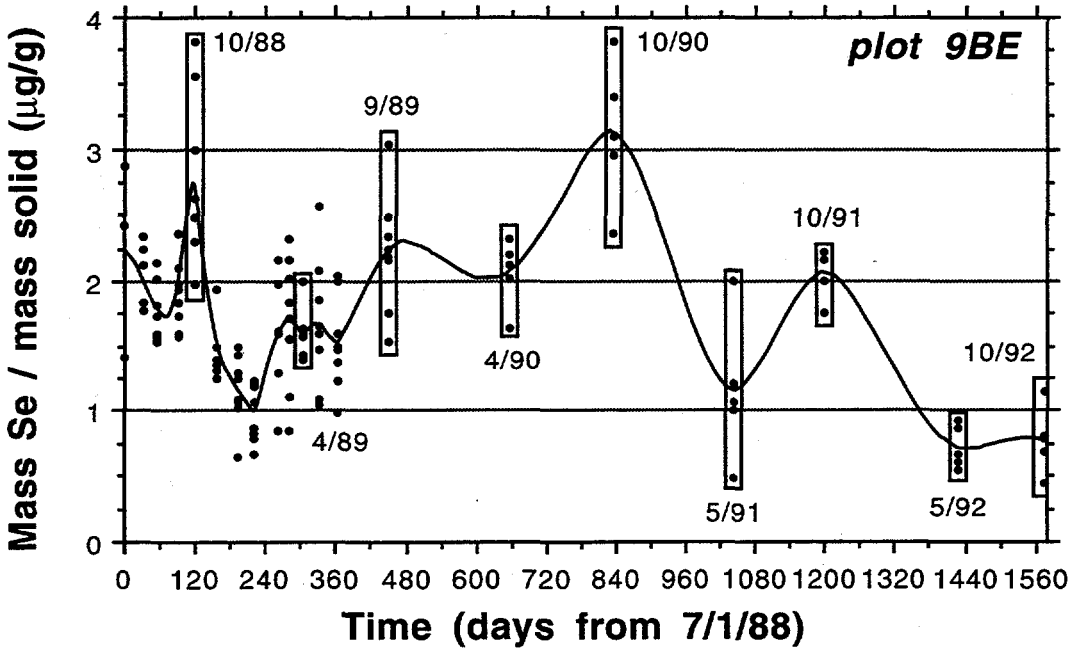

Figure 2.4.26. Changes in water-extractable selenium in the top 9 cm of soil in plot 9BE: July 1988 - October 1992.

Overall trends in both plots are characterized by extreme reductions of chloride and other soluble salts near the soil surface and much less pronounced declines of water-extractable selenium due to infiltrating rainwater. The absolute amount of selenium which was displaced deeper into the profile cannot be known without the quantification of selenium re-oxidation.

The 10/92 data was the final data set collected as part of this study.

2.5 Reservoir-Wide Monitoring of Soil Selenium

Carolyn Wahl, Peter Zawislanski, and Sally Benson
Earth Sciences Division
Lawrence Berkeley Laboratory

Since 1989, LBL and CH2M Hill researchers have cooperated to provide a data set on the overall status of the selenium inventory at Kesterson Reservoir. The data presented herein describe and summarize the results of five years of such research.

2.5.1 Site Description

Kesterson Reservoir is divided into three distinct habitat types: Fill (F), Grassland (G), Open (O) and three trisections (T1, T2, T3) (Figure 2.5.1). Fill areas represent areas where the soil surface was previously below the maximum height of the annual groundwater rise. The fill areas were frequently flooded with drain waters. An organic-rich ooze was deposited in the pond bottoms. Fill habitat is presently vegetated with annual vegetation dominated by *Bassia hyssopifolia* and annual grasses. Fill habitat covers about 56 percent of the Reservoir.

Grassland areas, although present in patches throughout the Reservoir, dominate the relatively dry, upland northern ponds and contain large areas covered by saltgrass (*Distichlis spicata*). This habitat normally remained above water most of the year, and a loose deposit of organic detritus accumulated under the canopy of the living vegetation. Grassland sites are dominated by saltgrass and cover 31 percent of the Reservoir.

Open habitats represent areas above high groundwater levels which were flooded during the winter and remained damp during the summer and fall. These areas were dominated by cattails (*Typha sp.*) which accumulated large amounts of selenium. As flow ceased, and the Reservoir dried, loose thick organic deposits of selenium-rich material accumulated and presently remain in these areas. Open areas are former cattail areas that were de-watered and disked in 1988 to eliminate nesting for tri-colored blackbirds. Open sites are sparsely vegetated with *Bassia*, prickly lettuce (*Lactuca serriola*), and clover (*Medicago, Melilotus, Trifolium spp.*). Open habitat covers about 13 percent of the Reservoir (CH2M Hill, 1991).

Trisection 1 (T1) consists of the southern Ponds 1, 2, 3, and 4; Trisection 2 (T2) consists of the central Ponds (5, 6, 7, and 9); and Trisection 3 (T3) consists of the northern Ponds (8, 10, 11, and 12). Ponds 1 and 2 of T1 received the largest amounts of agricultural drainage water from the San Luis Drain during 1978-1986, as water flowed by gravity from south to north, with Ponds 1 through 5 being used most extensively. The ponds in this trisection have the highest

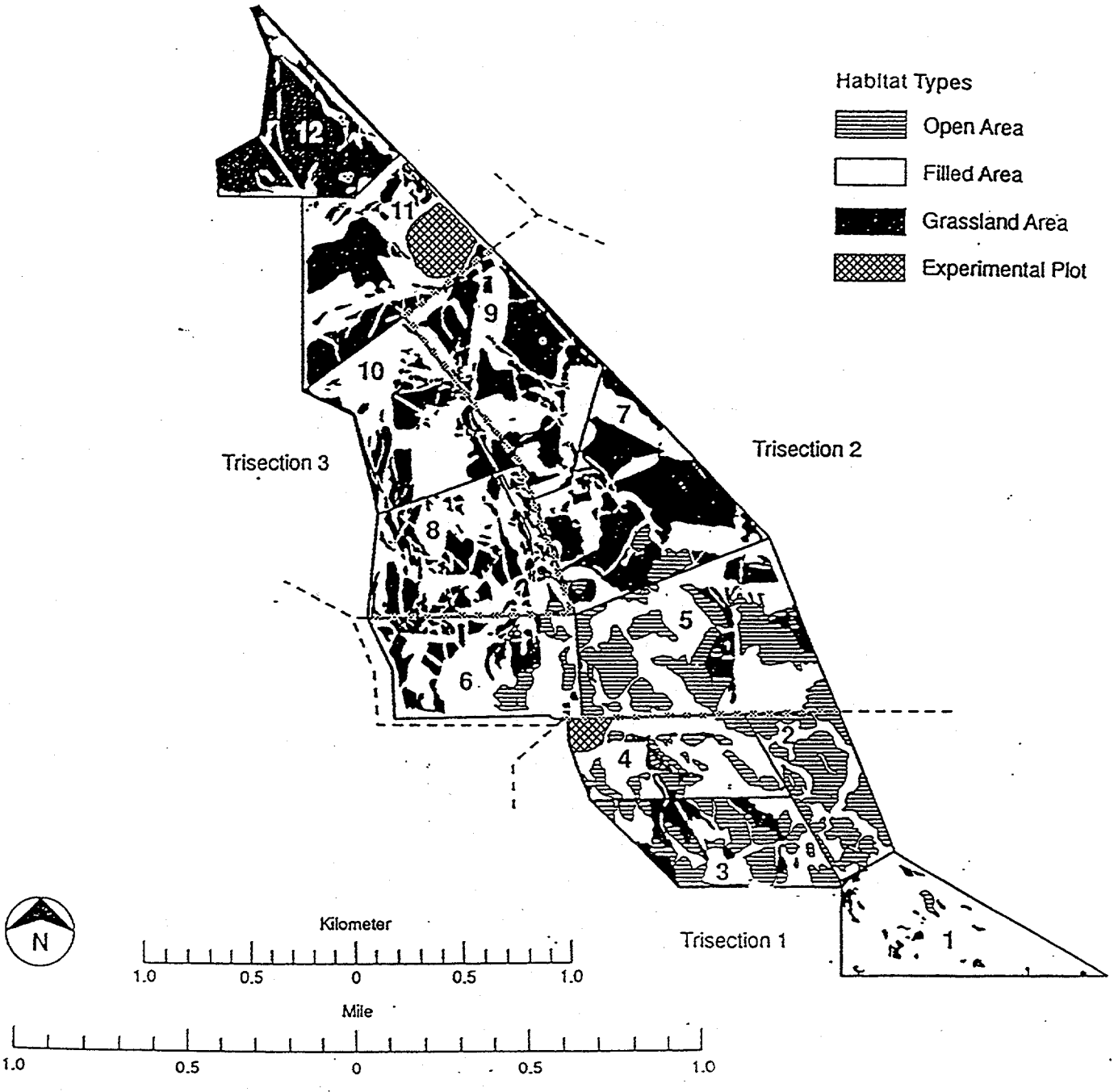

Figure 2.5.1. Map of habitat and trisection delineations at Kesterson Reservoir (CH2MHill, 1991).

reported soil selenium levels (LBL, 1990; CH2M Hill, 1991), and contained mostly open water and cattail areas in the past, and presently contain mostly open and fill habitats.

The ponds in T2 also received substantial amounts of drainwater in the past (LBL, 1990; CH2M Hill, 1991). However, these ponds generally have lower soil selenium levels than those in T1. Although only open water, and cattail areas were characteristic of T2 in the past, today open, grassland and fill habitats are all found in the trisection. Trisection 3 received the least amount of drainwater and ponds in this trisection have the lowest reported soil selenium levels (LBL, 1990; CH2M Hill, 1991). Trisection 3 is dominated by large areas of grassland and fill habitats.

2.5.2. Sampling, Extraction, and Analysis

Within each trisection, six sites of each habitat type were chosen for long-term monitoring of soils for a total of 54 sampling sites. Soil samples were collected by inserting a 2.54 cm diameter push-tube sampler to a depth of 15 cm from six stations in each habitat type of each trisection, for a total of 18 stations per trisection. The samples were collected at each site within a radius of about 1 m of the stations center. In the 1992 sampling event, depth samples were collected using a hydraulic drill rig at intervals of 0-15, 15-50, and 50-100 cm. The sampling dates for the soils over the three-year period were as follows: 1989 (May 8, 9); 1990 (March 7); 1991 (Feb. 20, 26, 27); 1992 (July 15, 16, 17, 20); 1993 (July 26, 27); and 1994 (August 19, 20). Data from the 1994 sampling are currently not available.

Soil samples were homogenized at field-moist conditions by hand chopping and passed through a 4.75-mm sieve. A known mass (between 20 and 30 g) of the homogenized subsample was then placed into an open stainless steel can and oven dried at 105°C for 24 hours. The common practice of air drying samples prior to extraction was not employed in order to minimize possible accelerated oxidation of selenium during sample processing (Tokunaga and Benson, 1992). At the end of the 24-hour period, the subsample was weighed and the gravimetric moisture content of the soil (mass of water per mass of dry soil) was calculated. Approximately two grams of the subsample was pulverized in a ball mill and pressed into a pellet for energy dispersive X-ray fluorescence (XRF) analysis which measures the total selenium concentrations of the sample (Giauque et al., 1976).

For the water-soluble selenium determination, another subsample of the homogenized soil (20 to 25 g) was used to prepare a 5:1 water to soil extract (distilled water:dry soil). After being placed on a reciprocating shaker table and agitated for 60 minutes the mixtures were centrifuged at 7800 revolutions per minute for 15 minutes and the supernatant solution was filtered through a 0.45 micron membrane filter prior to analysis. For the phosphate-extractable selenium determination, a prepared phosphate solution was added to the remaining soil mixture (20:1

1mM Na2HPO4 to soil mass ratio). The mixtures were placed on a reciprocating shaker table and agitated for 24 hours. After which, the samples were centrifuged at 7800 revolution per minute for 15 minutes and the supernatant solution was filtered through a 0.45 micron membrane filter prior to analysis.

Soil water extracts were analyzed for water-extractable and phosphate-extractable selenium, water-extractable and phosphate-extractable selenite; and the two major anions: sulfate and chloride. Sulfate was analyzed using an Inductively Coupled Plasma Spectrophotometer (ICP). Chloride was analyzed using a Mohr titration, as described by Flaschka et al. (1969). Water-extractable selenium and selenite were analyzed using atomic absorption spectroscopy (AAS) coupled with a hydride generator (see Section 8 of this report). Water-extractable selenium includes selenite, water-extractable selenate, and minor amounts of organically associated selenium (Weres et al., 1989; Long et al., 1990).

Table 2.5.1. Summary of 1992 soil selenium concentrations in the top 15 cm of the soil profile based by habitat. Values represent geometric mean concentrations expressed in mg/kg-soil.

	Habitat	Geometric Mean*	95 % C.I.	Range
Total Se	Fill	.58	.34 - 1.0	.14 - 6.5
	Grassland	1.8	.89 - 3.5	.24 - 41
	Open	9.6	5.6 - 16	1.1 - 160
Total Wat Se	Fill	.05 A	.02 - .11	.01 - 1.6
	Grassland	.08 A,B	.05 - .15	.01 - .74
	Open	.17 B	.12 - .25	.05 - .65
Selenite	Fill	.01 A	.01 - .02	.01 - .03
	Grassland	.01 A	.01 - .02	.01 - .05
	Open	.01 A	.01 - .02	.01 - .13
Selenate	Fill	.04 A	.02 - .10	.01 - 1.6
	Grassland	.07 A	.03 - .12	.01 - .74
	Open	.16	.11 - .22	.05 - .61
Sulfate (arithmetic mean)	Fill	570 A	73 - 1060	11 - 3360
	Grassland	690 A	240 - 1150	18 - 2430
	Open	2110	1700 - 2520	750 - 3700
Chloride	Fill	120 A	58 -240	22 - 4020
	Grassland	60 A,B	35 - 110	15 - 430
	Open	45 B	20 - 90	5 - 490

* Geometric means *not* sharing the same letter are significantly different at a 95% confidence level.

2.5.3. Results and Interpretation

Analysis of Variance (ANOVA) was performed to determine if there were significant differences in soil selenium concentrations between years (1989, 1990, 1991, and 1992), trisections (T1, T2, T3), habitats (F, G, O), and depths (0-15 cm, 15-50 cm, and 50-100 cm).

Total selenium, water-extractable and phosphate-extractable selenium, water-extractable and phosphate-extractable selenite, and chloride data were determined to be log-normally distributed using the fractile method described in Warrick and Nielsen (1980). Sulfate concentrations were found to be normally distributed. The Fisher's protected least significant difference (PLSD) method was used to determine significant differences in concentrations within year, trisection, habitat, and depth ($P<.05$) (Mead, 1988). Tables 2.5.1 and 2.5.2 provide means, confidence intervals, and ranges for the 1992 data set by habitat and trisection delineation respectively. Mean values and confidence intervals for the entire data set based on year are summarized in Table 2.5.3. Mean values and confidence intervals for years 1989, 1990, 1991, and 1992 based on habitat, and trisection delineation are shown in Table 2.5.4. Table 2.5.5 provides mean values and confidence intervals for the 1992 data set based on the sampled depth intervals. All concentrations reported are in units of mg/kg on a dry weight basis.

Table 2.5.2. Summary of 1992 soil selenium concentrations in the top 15 cm of the soil profile based by trisection. Values represent geometric mean concentrations expressed in mg/kg-soil.

	Trisection	Geometric Mean*	95 % C.I.	Range
Total Se	Trisection 1	4.3 A	1.7 - 11	.18 - 160
	Trisection 2	1.3 B	.66 - 2.6	.24 - 14
	Trisection 3	1.9 A,B	.88 - 4.0	.14 - 23
Total Wat Se	Trisection 1	.15 A	.07 - .31	.01 - 1.6
	Trisection 2	.06 B	.03 - .09	.01 - .41
	Trisection 3	.09 A,B	.05 - .16	.01 - .31
Selenite	Trisection 1	.01 A	.01 - .02	.01 - .13
	Trisection 2	.01 A	.01 - .02	.01 - .03
	Trisection 3	.01 A	.01 - .02	.01 - .05
Selenate	Trisection 1	.13 A	.06 - .27	.01 - 1.6
	Trisection 2	.05 A	.03 - .08	.01 - .39
	Trisection 3	.07 A,B	.04 - .13	.01 - .29
Sulfate (arithmetic mean)	Trisection 1	1300 A	760 - 1850	32 - 3360
	Trisection 2	985 A	490 - 1480	20 - 2870
	Trisection 3	1090 A	420 - 1750	11 - 3700
Chloride	Trisection 1	130 A	60 - 265	14 - 4020
	Trisection 2	55 A,B	28 - 100	10 - 1400
	Trisection 3	50 B	28 - 89	5 - 295

* Geometric means *not* sharing the same letter are significantly different at a 95% confidence level.

The distribution and temporal changes provided in Tables 2.5.1-2.5.6 and Figures 2.5.2-2.5.14 can be categorized in terms of four main factors or trends: 1) spatial trends based on habitat and trisection delineation; 2) temporal trends due to the seasonal cycling of the soluble

selenium inventory; 3) temporal trends due to the oxidation of the selenium inventory and the decomposition of organic matter; and 4) depth trends. These are described in detail in the following sections.

Table 2.5.3. Summary of soil selenium concentrations in the top 15 cm of the soil profile over the four-year sampling period. Values represent geometric mean concentrations * expressed in mg/kg-soil. Confidence intervals within the ninety-five percentile are indicated below geometric mean concentrations.

	1989	1990	1991	1992	1993
Total Selenium	3.9 A (2.8 - 5.5)	2.7 A,B (1.9 - 3.8)	2.9 A,B (2.1 - 3.8)	2.3 B (1.5 - 3.5)	3.9 A (2.6-5.7)
Total Water-Extractable Se	.17 A,B,C (.11 - .25)	.12 A,B,C (.08 - .17)	.19 B,C (.12 - .30)	.09 (.07 - .13)	.11 (.08 - .16)
Ratio Water Ext./Total Se	.05 A (.04 - .06)	.04 A (.03 -.06)	.07 (.05 - .10)	.04 A (.03 - .05)	.03 B (.02 - .04)
Selenite	.02 A (.01 - .03)	.02 A (.01 - .03)	.02 A (.01 - .03)	.01 B (.005- .02)	.01 B (.007- .015)
Ratio Selenite/ Water- Ext. Se	.12 A,B (.08 - .17)	.16 A (.12 - .22)	.07 C (.05 - .20)	.10 B,C (.06 - .13)	.10 B,C (.07 - .13)
Sulfate (*Mean)	2120 A,B (1650 - 2600)	1800 B,C (1430 - 2170)	1380 C,D (1030 - 1730)	1125 D (815 - 1435)	2420 A (1820-3020)
Chloride	545 A (380 - 775)	220 B (140 - 350)	500 A (370 - 670)	70 C (50 - 100)	50 C (40-65)

* Geometric means *not* sharing the same letter are significantly different at a 95% confidence level.

2.5.4. Spatial Trends

Spatial trends are shown when 1989, 1990, 1991, and 1992 results are combined and grouped by habitat. The results indicate that selenium concentrations are greatest in the Open habitat and least in the Fill habitat as shown in Table 2.5.4. Significant differences between the three habitat types are detected in total selenium, total water-extractable selenium, total water-extractable selenite, sulfate, and chloride concentrations. This is consistent with the historical use of the Reservoir and the filling operations. Selenium concentrations in the sediments of Kesterson Reservoir are reflective of past depositional environments and the corresponding amount of soil organic matter associated with these sediments. The higher selenium values observed for the open habitat are associated with the high soil organic matter content of this habitat, its exposure to larger volumes of contaminated drainage water, and lower bulk density.

When 1989, 1990, 1991, and 1992 samples are combined and grouped by trisection, selenium concentrations are significantly greater in T1 than in either T2 or T3 as shown in Table

2.5.4. Significant differences between T1 and both T2 and T3 are detected in total selenium, total water-extractable selenium and chloride concentrations. As previously indicated, this is due to the historical use of the Reservoir as Ponds 1 and 2 of T1 were first to receive drainage water from the San Luis Drain.

Table 2.5.4. Habitat and Trisection Soil Selenium Concentrations. Summary of soil selenium concentrations in the top 15 cm of the soil profile over the initial three-year sampling period. Values represent geometric mean concentrations * expressed in mg/kg-soil. Confidence intervals within the ninety-five percentile are indicated below geometric mean concentrations.

	Total Selenium	Wat-Ext. Se	Ratio Wat-Ext./Tot Se	Selenite	Ratio Selenite/ Wat-Ext. Se	Sulfate (*Mean)	Chloride
Habitat							
Fill	1.1 (.82 - 1.4)	.06 (.04 - .08)	.06 A (.04 - .07)	.01 (.005- .015)	.11 A (.08 - .17)	965 A (580 - 1350)	230 A,B (145 - 380)
Grassland	2.6 (1.9 - 3.3)	.14 (.11 .19)	.06 A (.04 - .07)	.02 A (.01 - .03)	.15 A (.12 - .19)	1140 A (870 - 1410)	170 B (125 - 240)
Open	8.3 (6.7 - 10)	.30 (.23 - .37)	.03 (.02 - .04)	.02 A (.01 - .03)	.06 (.05 - .09)	2510 (2240 - 2280)	340 A (235 - 490)
Trisection							
T1	4.5 (3.3 - 6.2)	.24 (.17 - .35)	.06 A (.04 - .07)	.02 A (.01 - .03)	.07 A (.05 - .10)	1900 A (1550 - 2240)	395 (275 - 570)
T2	2.3 A (1.7 - 3.0)	.11 A (.08 - .15)	0.05 A (.04 - .06)	.01 A (.01 - .02)	.11 A,B (.08 - .15)	1450 A (1145 - 1750)	180 A (125 - 260)
T3	2.3 A (1.7 - 3.2)	.10 A (.07 - .13)	.04 A (.03 - .05)	.01 A (.01 - .02)	.14 B (.11 - .18)	1430 A (1050 - 1800)	200 A (130 - 295)

* Geometric means *not* sharing the same letter are significantly different at a 95% confidence level.

2.5.5. Temporal Trend due to Seasonal Cycles

In the analysis of the experimental data, it became evident that the sampling date relative to the seasonal cycle is an important variable. The significant year-to-year changes in sulfate and chloride concentrations, as well as in water-extractable selenium and in the ratio of water-extractable to total selenium detected in the data set are a reflection of seasonal leaching by infiltrating rainwater (Table 2.5.3, Figures 2.5.2-2.5.5). The decrease in both the ratio of water-extractable to total selenium and the chloride concentration between 1989 and 1990, followed by the increase between 1990 and 1991, followed by the significant decrease between 1991 and 1992, are representative of the seasonal cycling of the soluble inventory (Figures 2.5.3 and 2.5.5). Zawislanski et al. (1992) demonstrated that water-extractable selenium can be readily displaced vertically as a result of rainfall infiltration and evapotranspiration. It is therefore of

interest to consider the influence of seasonal transport of species and the potential impacts of seasonal cycling on long-term trends.

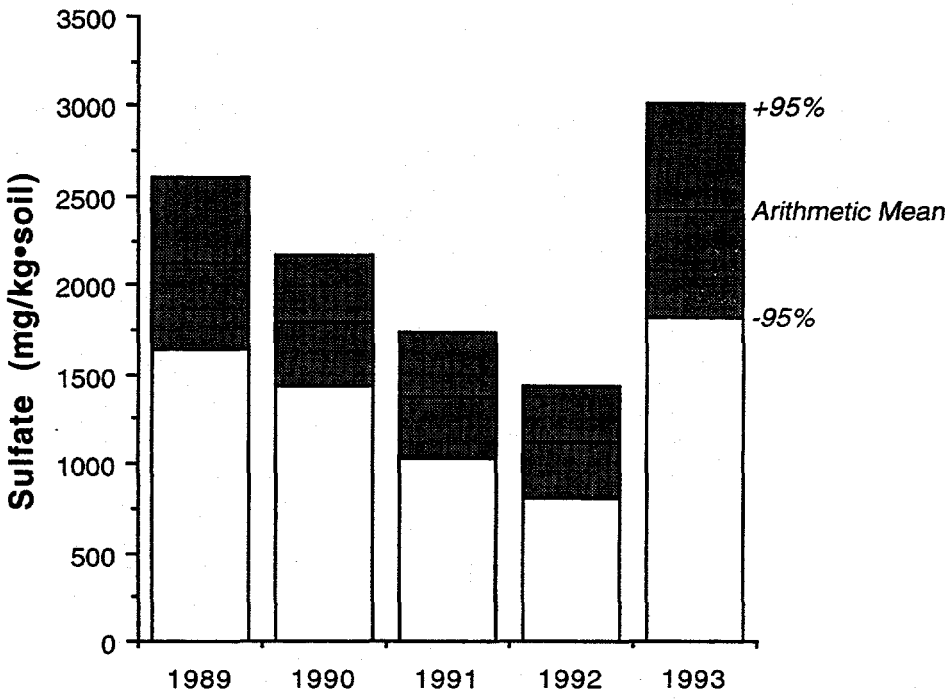

Figure 2.5.2. Sulfate concentrations in the top 15 cm of soil. Significant differences between 1989 and 1991, 1992; 1990 and 1992, 1993; 1991 and 1993; 1992 and 1993.

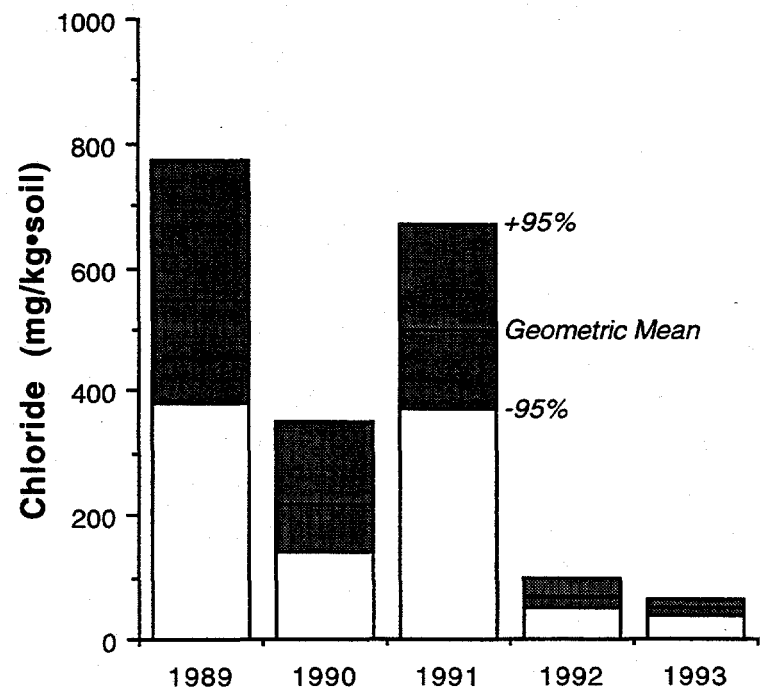

Figure 2.5.3. Chloride concentrations in the top 15 cm of soil. Significant differences between 1989 and 1990, 1992, 1993; 1990 and 1991, 1992, 1993; 1991 and 1992, 1993.

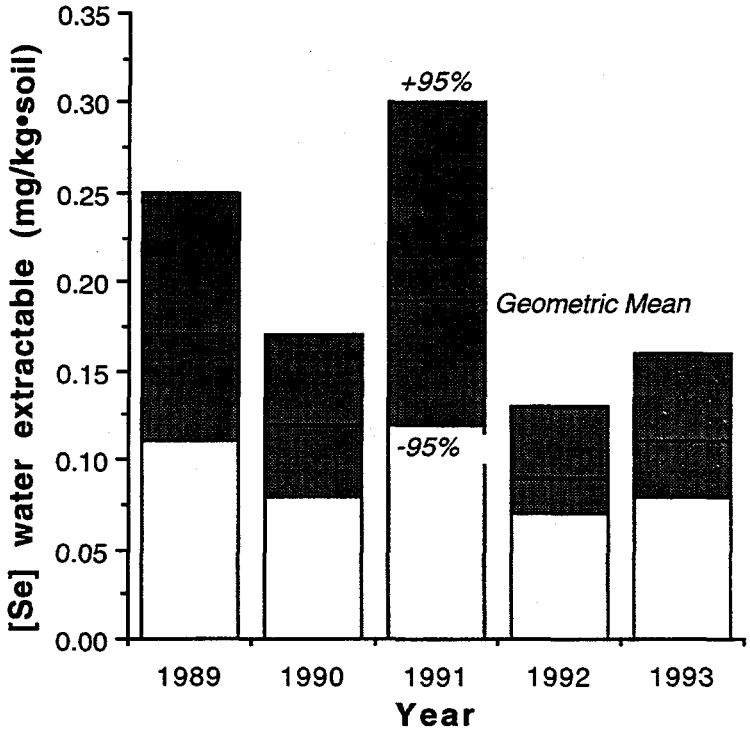

Figure 2.5.4. Water-extractable Se concentrations in the top 15 cm of soil. Significant differences between 1989 and 1992, 1989 and 1993, 1990 and 1991, 1991 and 1992, and 1991 and 1993.

As noted previously, samples were not taken at the same time of the year, with dates ranging from February to July. The heaviest precipitation period for each year as obtained from an on-site meteorological station were as follows: 1989-April; 1990-Jan., Feb.; 1991-March.; 1992-March. In March of 1992, as much as 26 mm of rainfall was measured immediately before the sampling event. In 1989, 1990, and 1992, soil samples were collected after the heavy winter rains for that season. As demonstrated in Zawislanski et al. (1992), it can be assumed that the rainfall leached the salts (sodium chloride and sulfate) and the more soluble water-extractable species which had accumulated at or near the soil surface. Under oxidized conditions, selenate (the dominant fraction of the water-extractable selenium inventory) and chloride would be transported deeper in the profile. In contrast, sulfate and selenite, the mobility of which is limited by precipitation and adsorption, respectively, are not driven further into the soil profile by the winter rains. (Figures 2.5.4 and 2.5.6) In addition, the lower redox potential created by saturating the soils with rain water would tend to favor reducing selenate to selenite and possibly, in reducing microsites to elemental selenium. Such conditions would also lead to the reduction of a certain percentage of the water-extractable selenium inventory, as indicated in the 1992 data

set where total water-extractable selenium shows a significant overall decrease of 50% over the four-year monitoring period.

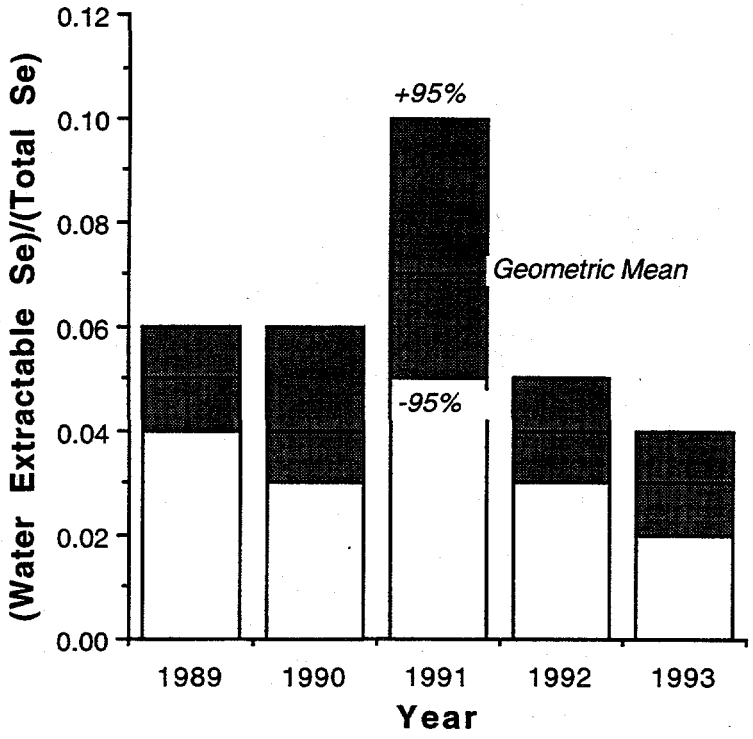

Figure 2.5.5. Ratio of water-extractable Se to total Se in the top 15 cm of soil. Significant differences between 1989 and 1991, 1989 and 1993, 1990 and 1991, 1991 and 1992, and 1991 and 1993.

In 1991, the samples were collected before the seasons heaviest rainfall and therefore compared to other years the soils were drier. Under these conditions, selenate will be the prevalent selenium species and chloride will not yet have leached from surface soils by the annual rainfall. This scenario explains both the increase in chloride concentrations from 1990 and 1991 and also the decrease in the ratio of water-extractable to total selenium (Figures 2.5.3 and 2.5.5).

As indicated above, the cycling of chloride and water-extractable selenium are driven by the processes of physical redistribution which are due to seasonal leaching by infiltrating rainwater and evaporative reconcentration. On the other hand, the sulfate inventory decreases over the four-year sampling period by 47%, but increases markedly between 1992 and 1993 (Figure 2.5.2). Differences in the overall behavior of sulfate and chloride can be explained by solubility limitations on sulfate (e.g., gypsum and thenardite solubilities). Once transported deeper in the profile, sulfate may precipitate due to the transpirative concentration of solutes in the root zone.

Chloride will remain mobile as a result of higher solubility limits and will at least in part be transported by evaporation back to the soil surface or to the root zone.

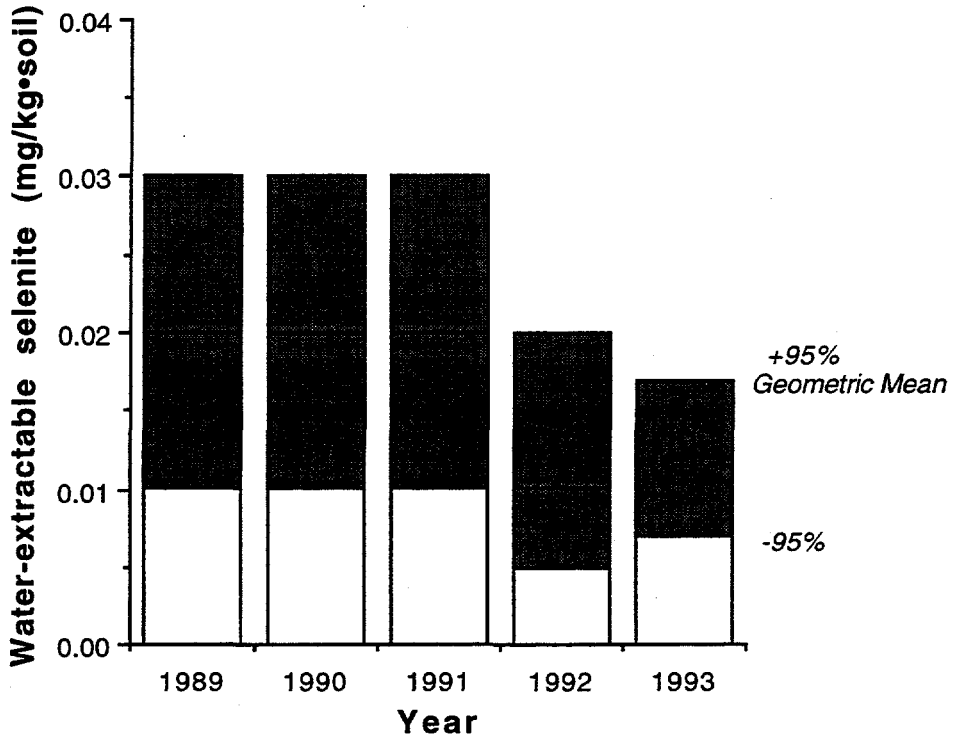

Figure 2.5.6. Selenite in the top 15 cm of soil. Significant differences between 1989 and 1992, 1989 and 1993, 1990 and 1992, 1990 and 1993, 1991 and 1992, and 1991 and 1993.

2.5.6. Temporal Trends due to the Oxidation of the Selenium Inventory

The termination of water deliveries to the Reservoir in 1986, and the prevalent drought conditions in the San Joaquin Valley over the past eight years, have dried out soil profiles and the vadose zone has become increasingly more oxidized. This change in redox conditions should result in the progressive oxidation and solubilization of the selenium inventory (Geering et al., 1968; Elrashidi et al., 1987). These trends have been observed in several soil profiles at Kesterson (Tokunaga et al., 1991). The Reservoir-wide sampling data has been reviewed to determine the extent to which this trend or others can be detected.

As indicated in Table 2.5.3, significant changes in the experimental data have not been detected in the total and water-extractable selenium inventories between 1989 and 1991. A 41% decrease in total selenium was detected between 1989 and 1992, followed by 41% increase in 1993 (Figure 2.5.7). Additionally, the water-extractable selenium value for 1992 (0.09 mg/kg) is significantly less than either 1989 (0.17 mg/kg), 1990 (0.12 mg/kg), and 1991 (0.19 mg/kg),

representing a 50% decrease in concentrations overall (Figure 2.5.4). However, there was a slight, though not significant increase in water-extractable Se in 1993 (0.11 mg/kg).

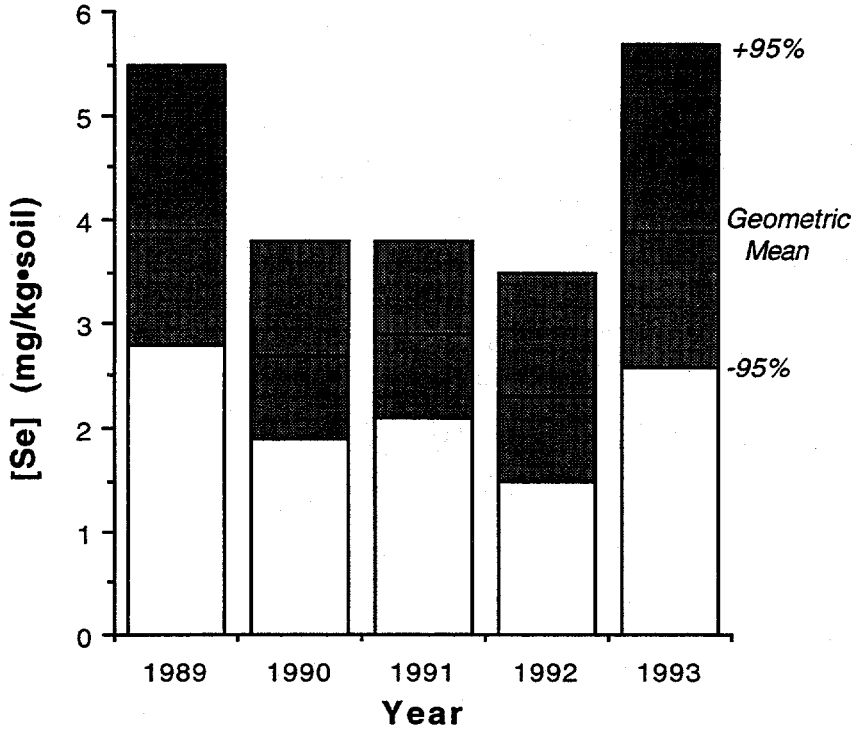

Figure 2.5.7. Total Se in the top 15 cm of soil. Significant differences between 1989 and 1992, and 1992 and 1993.

The fraction of the total selenium inventory that was water-extractable increased from 5% to 7% between 1989 and 1991, and then showed a significant decrease between 1991 and 1992 from 7% to 4%, and a further decline to 3% in 1993, as seen in Table 2.5.3. While this demonstrates that only a small fraction of the total selenium inventory is currently mobile and available for plant uptake, the trend observed between 1989 and 1991 may also support thermodynamic predictions that the inventory will oxidize to more soluble and mobile species given the right environmental conditions (i.e. drought). The increase in the water-extractable fraction between 1989 and 1991 is consistent with process-oriented monitoring described by Tokunaga et al. (1991), during which the San Joaquin Valley was under severe drought conditions. The subsequent decline in water-extractable Se percentage coincides with periods of increased rainfall and soil moisture.

Documenting long-term thermodynamic changes in the top 15 cm of the selenium inventory can be difficult as the speciation and distribution of selenium is greatly influenced by the

seasonal cycles of rainfall infiltration and evaporation. Approximately 26 mm of rainfall was measured at Kesterson Reservoir immediately before the 1992 sampling event. The measured concentrations for both total selenium and total water-extractable selenium were significantly less than the other years. A significant decrease is also detected in the ratio of water-extractable selenium to total selenium, therefore indicating the difficulty in predicting long-term trends during extremely variable drought/rainfall conditions.

As described in Section 2.5.4, there are very large differences amongst the three habitats in terms of Se concentrations. Therefore, a more perspicacious approach is to compare yearly changes in Se concentrations within habitats. The results of such comparisons are shown in Table 2.5.5 and Figures 2.5.8, 2.5.9, and 2.5.10.

Table 2.5.5. Soil Se concentrations in the top 15 cm of the soil profile over the five-year sampling period. Values represent geometric mean concentrations* expressed in mg/kg•soil. Confidence intervals within the 95%-ile are indicated below geometric mean concentrations.

Habitat	**1989**	**1990**	**1991**	**1992**	**1993**
Total Se					
Fill	1.51 A (0.82-2.76)	1.05 A (0.65-1.69)	1.39 A (0.83-2.34)	0.62 B (0.38-1.02)	1.23 A (0.75-2.02)
Grass	3.62 A (2.04-6.42)	2.85 A (1.70-4.80)	2.30 A,B (1.45-3.65)	1.81 B (0.92-3.54)	3.13 A (1.71-5.74)
Open	9.23 A,B (6.44-13.24)	7.42 A (4.80-11.48)	7.14 A (4.31-11.83)	9.58 A,B (5.69-16.15)	14.86 B (10.53-20.99)
Water extractable Se					
Fill	0.07 A,B (0.03-0.17)	0.04 A (0.02-0.08)	0.08 B (0.03-0.21)	0.05 A (0.02-0.11)	0.06 A,B (0.03-0.10)
Grass	0.22 A (0.12-0.40)	0.15 A (0.10-0.24)	0.15 A (0.07-0.33)	0.08 B (0.05-0.15)	0.10 B (0.06-0.17)
Open	0.30 A, B (0.19-2.07)	0.27 A, B (0.15-0.49)	0.53 A (0.34-0.82)	0.17 C (0.12-0.25)	0.26 B (0.19-0.36)

* Geometric means *not* sharing the same letter are significantly different at a 95% confidence level.

Although there are occasional significant changes in both total Se and water-extractable-Se concentrations, there are no consistent trends in these changes, with the exception of the Fill habitat in which both total Se and soluble Se concentration changes correlated well with changes in chloride concentrations (Figure 2.5.3). There was a significant increase in total Se in the Open habitat in 1993 relative to all previous years. There was an apparent decline in both total Se and soluble Se in the Grassland habitat from 1989 through 1992 but the 1993 values showed a marked increase, especially in total Se.

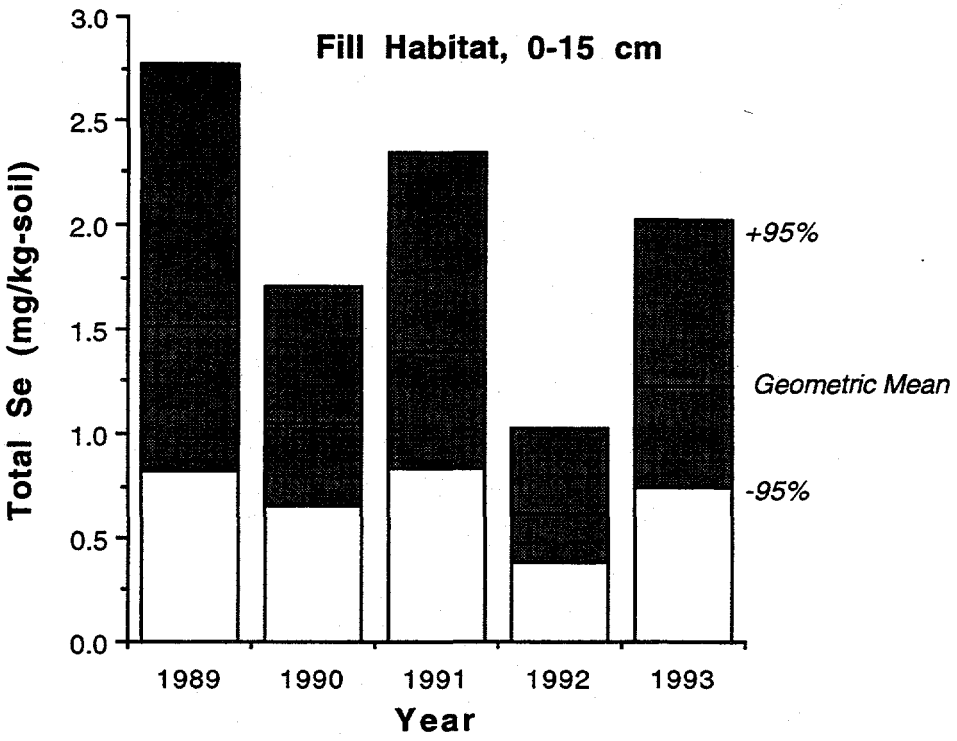

Figure 2.5.8. Total Se in the top 15 cm of soil in the Fill habitat.

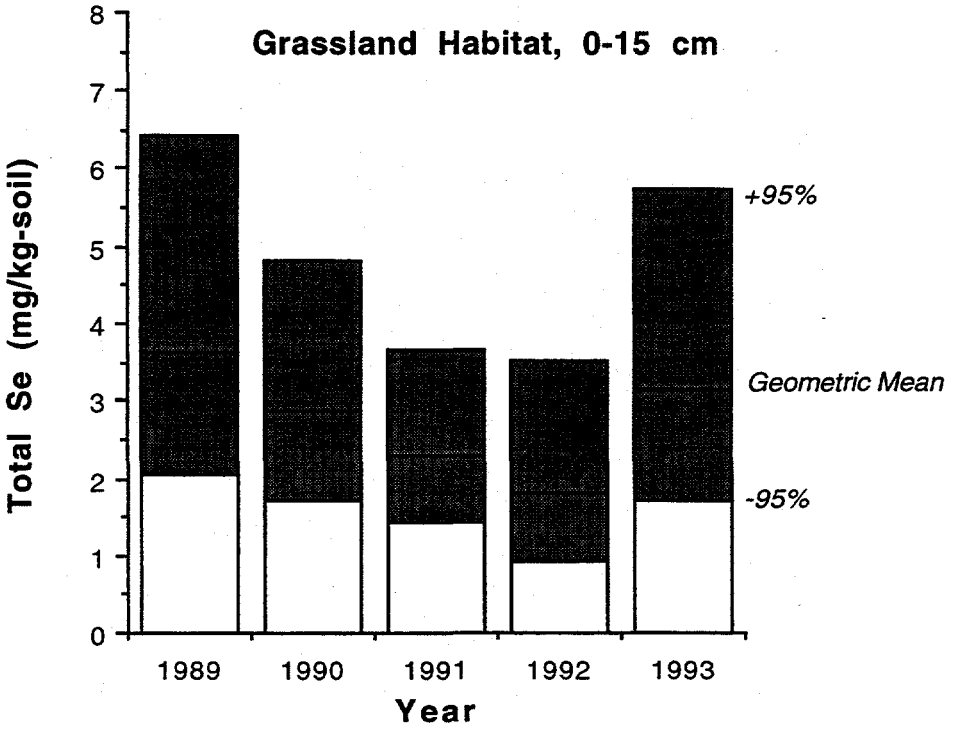

Figure 2.5.9. Total Se in the top 15 cm of soil in the Grassland habitat.

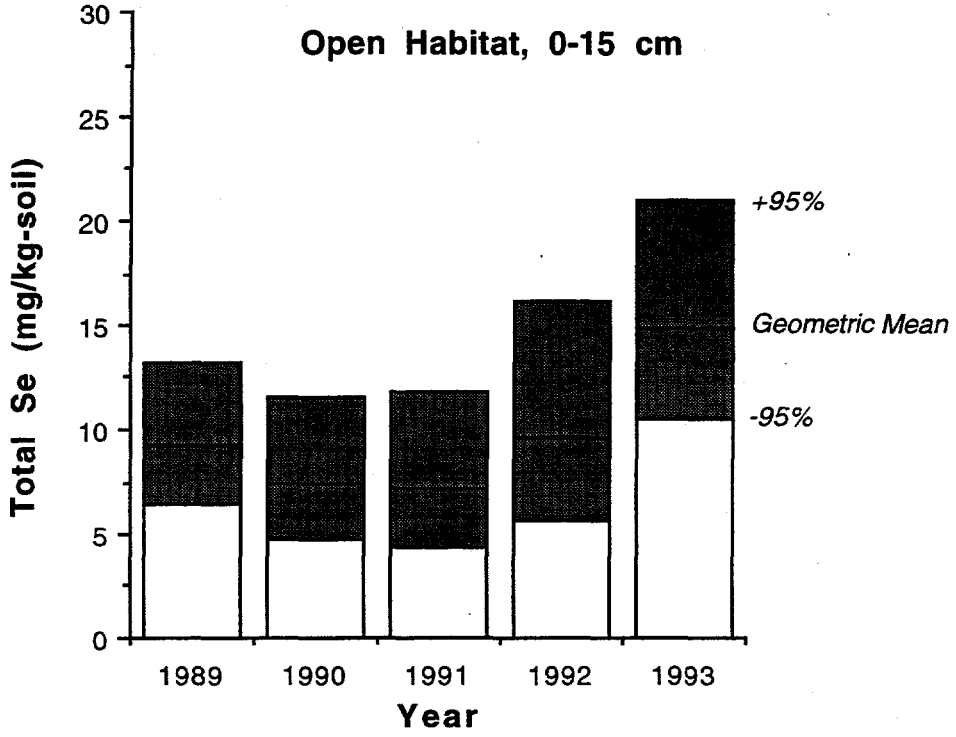

Figure 2.5.10. Total Se in the top 15 cm of soil in the Open habitat.

2.5.7. Depth Trends

As indicated in previous investigations (Weres et. al., 1989), total selenium concentrations decrease with depth. This pattern is observed in the 1992 data set where total selenium concentrations decrease by 81% between 0-15 cm and 50-100 cm and in the 1993 data set where the same difference is about 70% (Figures 2.5.11 and 2.5.12). There is a significant increase in total Se at all depths between 1992 and 1993, with the greatest relative difference (2.2-fold increase) at the 50-100 cm depth.

In 1992, the water-extractable fraction was greater by 41% at the 0-15 cm depth than at the 15-100 cm depth as shown in Table 2.5.6 and Figure 2.5.13. This increase is most likely a direct result of the 1992 rainfall event which may have leached the more soluble water-extractable component deeper into the soil profile. On the other hand, selenite, which is more resistant to leaching, is shown to be significantly higher in the 0-15 cm zone (Table 2.5.6). Sulfate concentrations show a significant increase with depth between the 0-15 cm and 15-100 cm depth. Sulfate concentrations between the 15-50 cm depth and the 50-100 cm depth are fairly constant (Table 2.5.6). As previously noted, once transported deeper in the profile, sulfate may precipitate and concentrate in the root zone. As indicated in Table 2.5.6, chloride concentrations significantly decrease with depth.

Table 2.5.6. Summary of selenium concentrations in the soil profile (0-100 cm) at Kesterson Reservoir. Values represent geometric mean concentrations * expressed in mg/kg-soil. Confidence intervals within the ninety-five percentile are indicated below geometric mean concentrations.

	0 - 15 cm	15 - 50 cm	50 - 100 cm
Total Selenium	2.3 (1.5 - 3.5)	.78 A (.50 - 1.2)	.50 A (.32 - .77)
Total Water-Extractable Se	.09 (.07 - .13)	.17 A (.13- .23)	.16 A (.12 - .22)
Selenite	.01 (.005 - .02)	.006 A (.004 - .009)	.004 A (.002 - .007)
Sulfate (*Mean)	1125 (815 - 1435)	325 A (280 - 375)	315 A (270- 360)
Chloride	70 (50 - 100)	385A (300 - 4950)	1135B (1026 -1260)

* Geometric means *not* sharing the same letter are significantly different at a 95% confidence level.

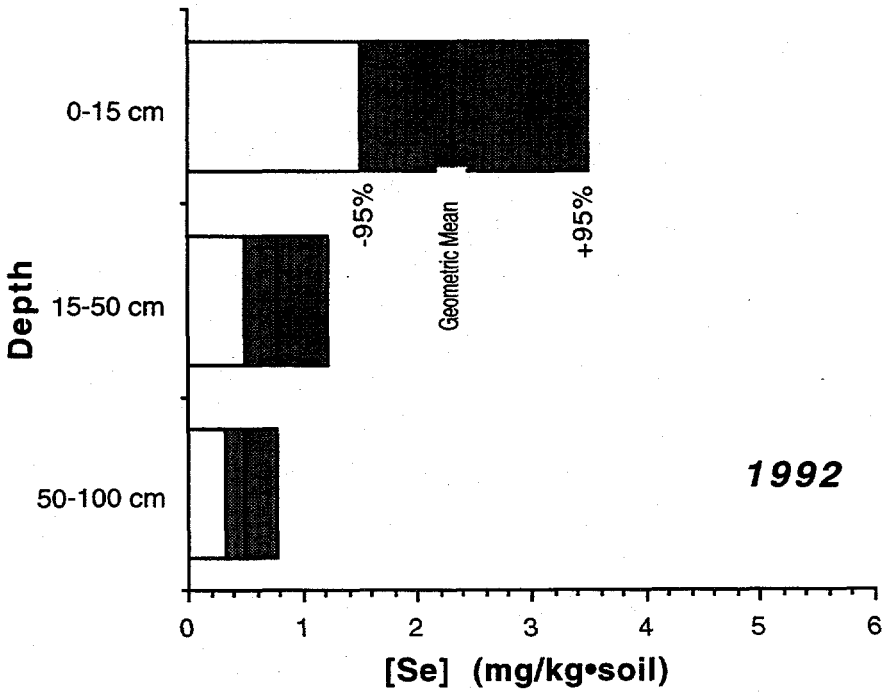

Figure 2.5.11. Total Se in the 0-100 cm soil profile, in 1992.

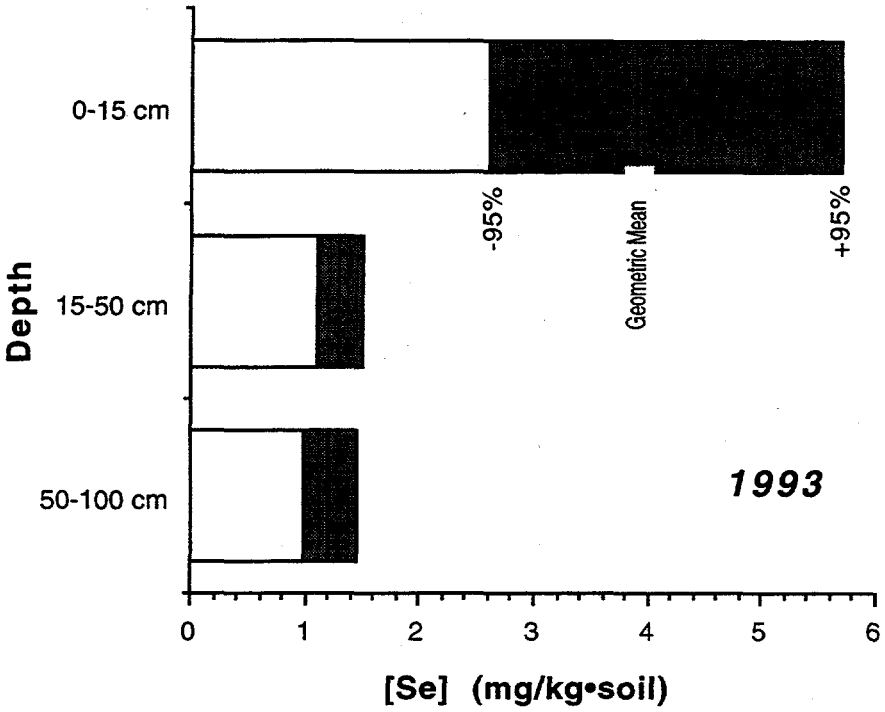

Figure 2.5.12. Total Se in the 0-100 cm soil profile, in 1993.

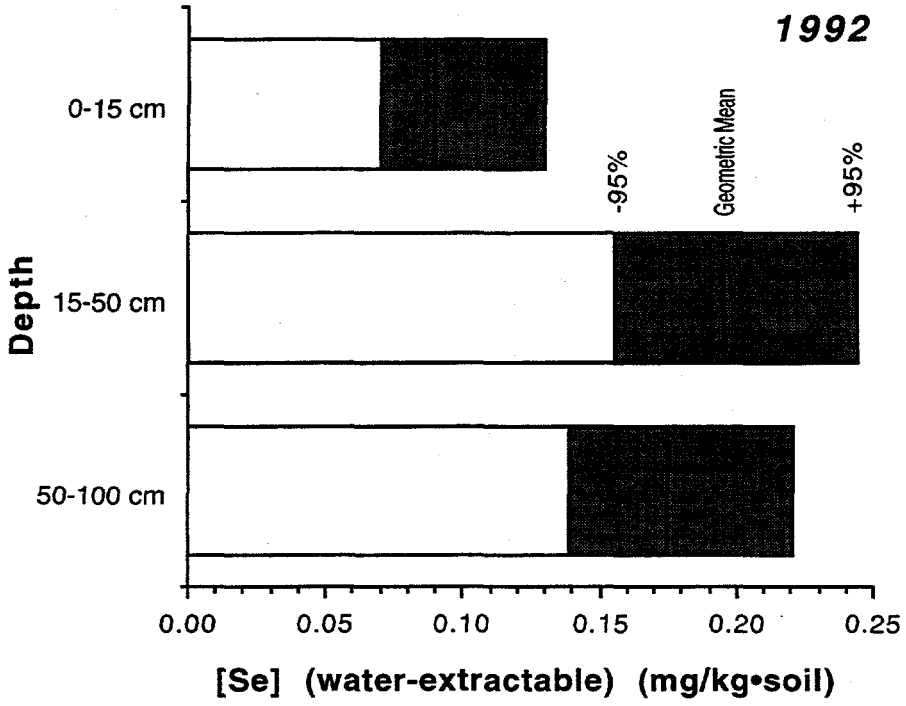

Figure 2.5.13. Water-extractable Se in the 0-100 cm soil profile, in 1992.

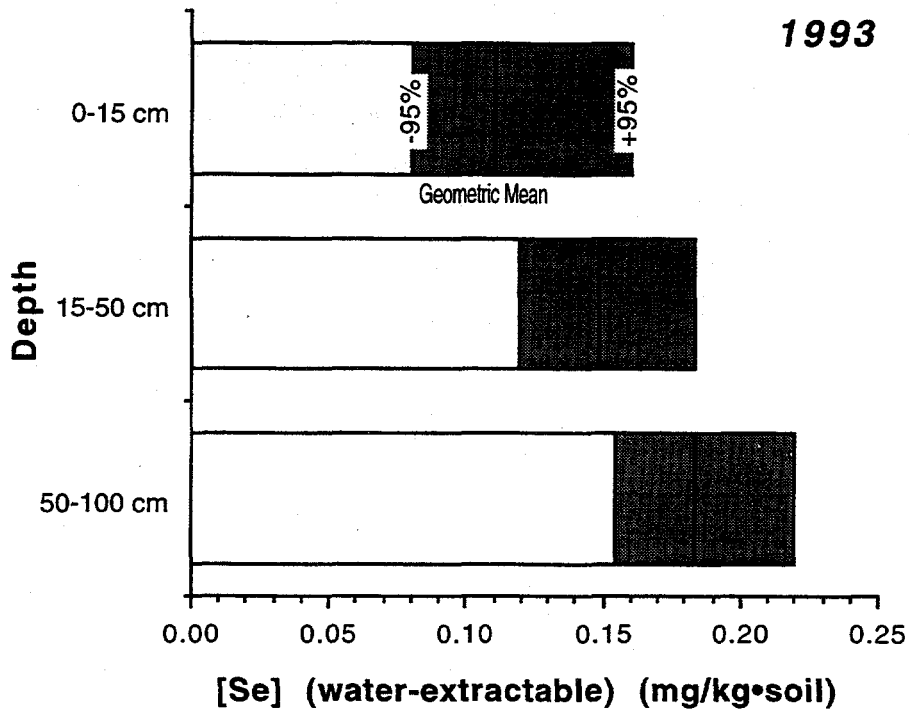

Figure 2.5.14. Water-extractable Se in the 0-100 cm soil profile, in 1993.

As seen in Figure 2.5.14, there is a shift of water-extractable Se from the 15-50 cm interval to the 0-15 cm interval, with the decrease in the 15-50 cm range being the only significant change.

2.5.8. Discussion and Summary

In analyzing the data, it became evident that the trends observed in the experimental data are analogs of processes described by more intensive sampling conducted by Tokunaga et al. (1991) and Zawislanski et al. (1992) on smaller sites within the Kesterson Reservoir soil environment.

In the top 15 cm of the soil profile, only 4 to 7% of the total selenium inventory is water-extractable, indicating that only a limited fraction of the total selenium inventory is mobile and available for plant uptake. However, as described in Tokunaga et al. (1991), bioavailable selenium is expected to increase slowly over time. The data collected here are consistent with these trends and confirm that increases are occurring slowly and seasonal events may obscure long-term trends. Processes contributing to this evolution may include microbial transformations of organic and inorganic forms of selenium, cyclic oxidation and reduction of selenium resulting from seasonal variation in soil moisture content and rainfall infiltration, oxidation of soil organic matter, and physical redistribution resulting from root uptake of soil moisture and/or selenium.

Both seasonal and spatial variability make it difficult to detect changes in chemical concentrations over time. For example, process-oriented studies have demonstrated that water-extractable selenium concentrations and conservative solutes such as chloride, are strongly influenced by the seasonal cycling of the inventory (Tokunaga et al., 1991; Zawislanski et al., 1992). This trend has also been observed in the experimental data set. These constituents are readily leached down into the soil profile with winter rains, and are transported back to the soil surface by evaporative processes as an oxidized environment is favored in the dry, summer months.

By using analysis of variance and considering the geometric means of sets of selenium concentration values, one can identify significant changes at a chosen level of confidence (95% in this case). However, most of the variability and even most of the "significant" changes, especially in total Se concentrations, cannot be explained through the application of a consistent model and most of the observed changes do not follow steady trends. This suggests that there are other factors which influence the measured concentration. One known factor is variability in sampling period relative to major rainfall events. This would have a particularly profound effect on water-extractable Se concentrations in the 0-15 cm interval. However, changes in total Se as observed, for example, in the Open habitat (Figure 2.5.14), cannot be explained as a result of vertical Se redistribution with soil water, as they would require water-extractable Se concentrations one order of magnitude greater than observed. Therefore, other factors may be responsible for such erratic fluctuations, such as inconsistencies in sampling technique, sample preparation, or sample analysis. Ultimately, the chosen method of statistical analysis may not be appropriate for the nature of spatial variability at Kesterson Reservoir. As pointed out by Wahl et. al. (1994), a much larger data set is required to look at the significance of changes given the very large spatial variability of Se concentrations at Kesterson.

All provisos aside, several conclusions may be drawn.

- Selenium concentrations are greatest in the Open habitat and lowest in the Fill habitat. This a result of the historical use of the Reservoir.

- Chloride and water-extractable selenium are subject to significant vertical redistribution due to the infiltration of rainwater and the evapotranspiration of soil water. This places special importance on the sampling schedule relative to rainfall events and the rainy season in general.

- Sulfate and selenite are much less affected by rainfall infiltration due to low solubility and strong sorption, respectively. The movement of selenate down to the root zone results in a net increase in selenite at that depth as some of the selenate will be reduced and immobilized. The rates and direction of these processes are strongly dependent on rainfall pattern and intensity.

- Changes in selenium concentrations in the Fill habitat can be qualitatively correlated with those in chloride, suggesting that fill material may be more oxidized and more permeable to water flow, allowing for more rapid flushing and re-oxidation of Se.

- Changes in selenium concentrations in the Open and Grassland habitats show no consistent trends.

- Total selenium concentrations are strongly skewed toward the soil surface. Total selenium below 15 cm is generally 3 to 4 times lower than between 0 and 15 cm depth.

- Water-extractable selenium concentrations are greater below the 15 cm depth than above, although the degree to which this is true depends strongly on rainfall pattern and intensity.

3.0 Mapping of Selenium Concentrations in Soil Aggregates with Synchrotron X-ray Fluorescence Microprobe

Tetsu Tokunaga
Earth Sciences Division
Lawrence Berkeley Laboratory

Stephen R. Sutton and Sasa Bajt
Department of Geophysical Sciences
The University of Chicago

The possible occurrence of reducing microsites in synthetic soil aggregates and their influences on the distribution of selenium species with redox-dependent mobilities was tested using the synchrotron x-ray fluorescence microprobe (SXRFM). Synthetic, effectively 2-dimensional soil aggregates of diameters ranging from 10 to 30 mm were constructed, with and without inclusion of sections of *Scirpus robustus* and *S. californicus* root sections. Each aggregate was uniformly wetted with a saline solution containing 240 g m^{-3} Se [98% as Se(VI), and 2% as Se(IV)]. Gas-phase porosities varied between individual aggregates from 0.00 to 0.40, and were maintained relatively constant during the incubation period of up to 17 days. Exchanges of soil gases with atmospheric air occurred only along the periphery of the aggregates. Scanning of the aggregates using SXRFM demonstrated that Se was essentially homogeneously distributed in soils without *Scirpus* root sections, suggesting that Se remained primarily as the soluble Se(VI) species. The SXRFM results revealed large accumulations of *total* Se in regions surrounding embedded sections of *Scirpus* roots. As much as 20-fold local enrichment with respect to total Se was measured in water-saturated soils within 1 to 4 mm of decomposing roots. These observations provide support for a model of localized reducing zones in which Se(VI) is reduced to less mobile Se(IV) and to insoluble Se(0), resulting in local accumulation of total Se. The measured Se accumulation in one microsite compared reasonably well with a simple transient Se(VI) diffusion model. It is postulated that such mechanisms may account for similar heterogeneities observable in some Se-contaminated soils at Kesterson Reservoir. Such heterogeneities in concentrations of Se and other constituents within individual soil aggregates have important implications with respect to reactivity, and need to be included in any detailed mechanistic modeling of chemical cycling within soils. This work also provides an example of the substantial capabilities of SXRFM in studies of soils.

3.1 Introduction

The potential importance of heterogeneous oxygen concentrations within soil aggregates has long been recognized. Within aggregates which physically may be essentially homogeneous, diffusion-limited transport of oxygen, coupled with sufficiently high microbial respiration rates may promote the generation of internal anaerobic regions. The anaerobic microsite model was developed to explain the observations of denitrification within macroscopically well-aerated soil profiles (e.g. Currie, 1961; Currie, 1965; Smith, 1977; Freney et al., 1979; Smith, 1980; and Leffelaar, 1986 and 1993). Although the anaerobic microsite studies cited above provide insight into the coexistence of oxidizing and reducing zones within soil aggregates, their simplicity with respect to uniform distributions of the controlling parameters may be unrealistic in many cases. For example, much higher denitrification rates in the immediate vicinity of particulate organic matter within soil aggregates were measured by Parkin (1987). Regardless of the specific geometry, the coexistence of oxidizing and reducing environments at the aggregate scale (typically in the range of 10 to 10^2 mm in effective diameter), can also have important consequences on the fate of many other elements susceptible to oxidation-reduction reactions in soils.

The importance of understanding redox conditions with respect to the behavior of selenium in soils also has a long history (Anderson et al., 1961; Rosenfeld and Beath, 1964; Sharma and Singh, 1983). Recently, attention has again been drawn to this problem with Se contamination of Kesterson Reservoir, California, as a result of wildlife deaths and deformities in a wetland supplied with seleniferous agricultural drain waters (Ohlendorf, 1989). Several previous studies have provided information on Se distributions within Kesterson Reservoir soils on the macroscopic scale of individual soil profiles (Weres et al., 1989; Long et al., 1990; Benson et al., 1991; Tokunaga et al., 1991; White et al., 1991; Zawislanski et al., 1992). These macroscopic analyses provide information on Se concentrations and speciation averaged over distances on the order of about 10 to 10^3 mm. A typical distribution of total Se in a Kesterson Reservoir soil profile during and after flooding with seleniferous drain waters is shown in Figure 3.1. Such profiles exhibited large accumulations of Se within the upper-most regions of ponded sediments, where transformation of ponded Se(VI) to both adsorbable and less-soluble reduced species occurred (Weres et al., 1989). In such approaches, the possibility of smaller-scale heterogeneities in Se concentrations were not addressed, and remained to be determined. The potential significance of such information stems from the need to understand the fate of Se in not only contaminated soils, but in natural soil environments as well. The occurrence of large concentration variations on a smaller-scale could imply significantly lower exposed surface areas

at which oxidation-reduction, precipitation-dissolution, and adsorption-desorption reactions take place relative to more uniformly distributed concentrations.

The redox- and pH-dependence of Se partitioning between aqueous, solid, and surface phases provides the basis for generating heterogeneous distributions of total Se within systems. When Se is introduced into a system in the soluble Se(VI) state, local enrichment with respect to Se occurs where reducing conditions occur. Under mildly reducing conditions, Se(VI) is transformed to Se(IV) (Elrashidi et al., 1987). Selenite is susceptible to pH-dependent adsorption and/or precipitation (Geering et al., 1968; Neal et al., 1987). Under more strongly reducing conditions, reduction to insoluble Se(0) occurs. Such microbially mediated reduction of Se(VI) operated during deposition of seleniferous drain waters in evaporation ponds at Kesterson Reservoir, resulting in substantially elevated concentrations of total Se within the upper 0.15 m of the soil profiles. Until recently, reduction to Se(0) could only be inferred from indirect evidence obtained through chemical extraction schemes. Recent x-ray absorption spectroscopy studies conducted at the Stanford Synchrotron Radiation Laboratory have provided the first direct evidence for Se(VI) reduction to both Se(IV) and Se(0) in sediments (Pickering et al., 1994).

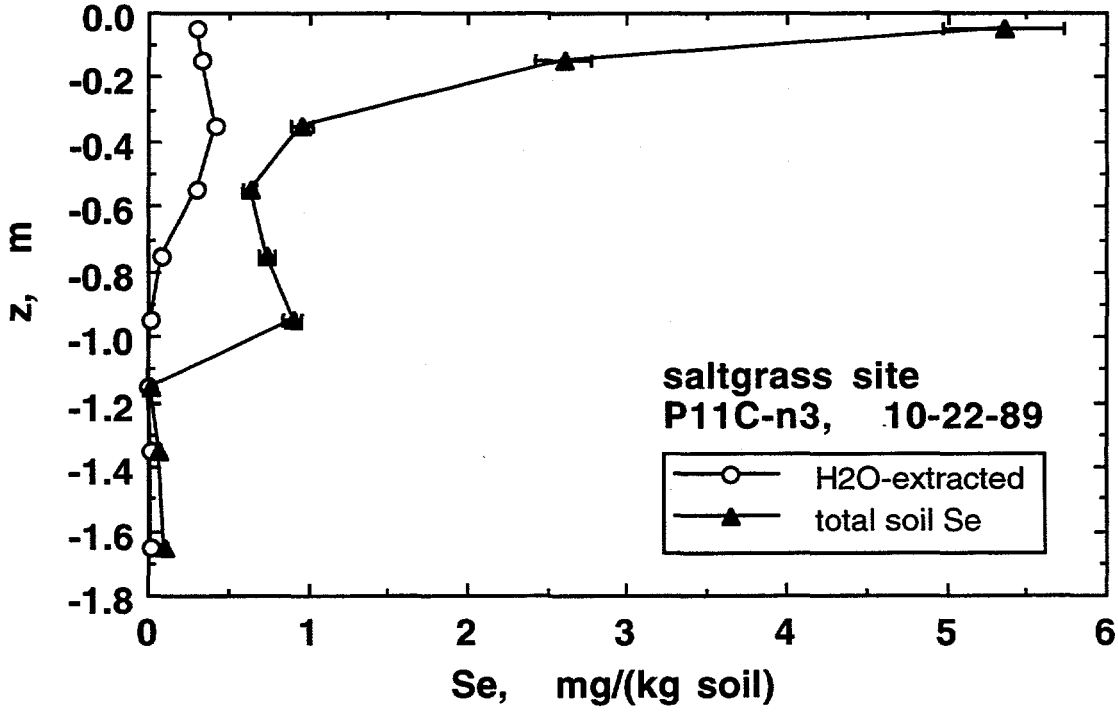

Figure 3.1. Profiles of total Se and Se(VI) in a Kesterson Reservoir soil, Pond 11 monitoring site P11C. (Data from Tokunaga et al., 1991).

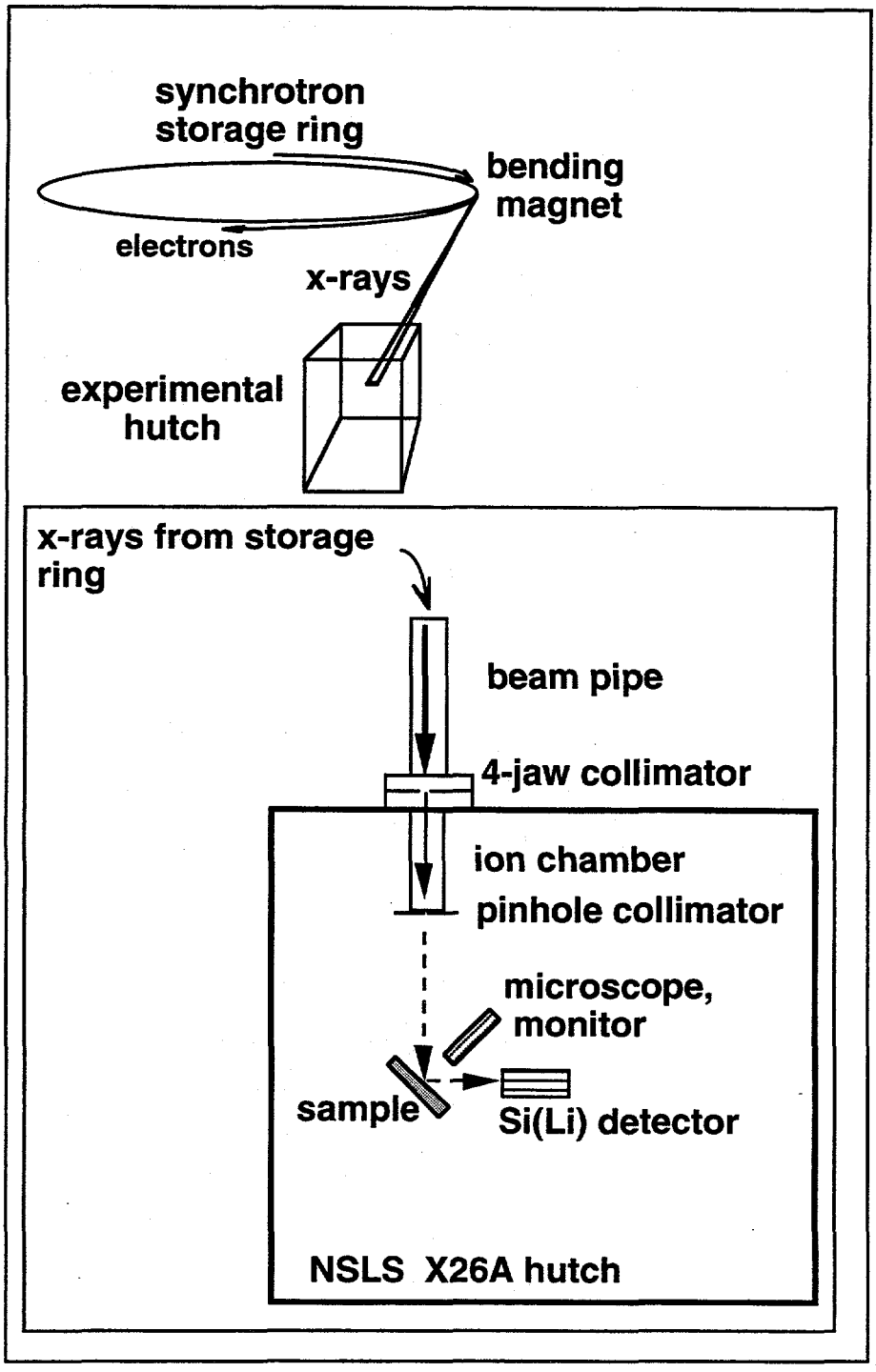

Figure 3.2. Basic components of the SXRFM at NSLS (beamline X26A).

It appears reasonable that such redox-dependent mobilities could also influence Se redistribution on the considerably smaller scale of individual soil aggregates. When regions with significantly lower redox potentials occur within portions of an aggregate, local reduction of Se(VI) would be expected to promote diffusion of Se(VI) towards the reduced zone from surrounding regions. Such redistribution might also apply for other redox-dependent elements such as Cr, Mn, Fe, Cu, and As, and their microscopic mapping may provide a supplemental approach to investigations of reducing microsite models.

The synchrotron x-ray fluorescence microprobe (SXRFM) provides the capability of mapping elemental distributions at a spatial resolution which, in some cases, approaches ≈1 μm, and has several important advantages with respect to studies on soils. The basic principles of the method are analogous to conventional x-ray fluorescence spectroscopy, applied on much smaller target areas. The highly focused, intense x-ray beams needed for such micro-scale analyses are emitted as synchrotron radiation from electrons accelerated around storage rings at facilities such as the National Synchrotron Light Source (NSLS, at Brookhaven National Laboratory) and the Advanced Light Source (at Lawrence Berkeley Laboratory). By exposing a sample to such an intense source of white radiation and measuring the resulting fluorescence spectrum emitted by the specimen, quantification of a range of elements is possible. Scanning a sample through the x-ray beam while simultaneously recording fluorescence spectra provides the opportunity to generate maps of elemental distributions. The basic features of the SXRFM are shown in Figure 3.2. Summary articles on the method are found in Jones and Gordon (1989), Wu et al. (1990), Rivers et al. (1991), and Sutton et al., (1993).

In the preliminary portion of this study, the SXRFM was used to map the distribution of Se in soil aggregates collected at Kesterson Reservoir. Results obtained in the preliminary stages of this study motivated the remainder of the laboratory aggregate experiments. These later experiments were designed to test the steady-state anaerobic microsite model, as well as a transient Se(VI) diffusion and reduction model as explanations for development of small-scale heterogeneities in total Se concentrations.

3.2 Theory

When the anaerobic microsite model is applied to a spherical aggregate of radius R, characterized by an effective oxygen diffusion coefficient D_{e,O_2}, the critical steady-state respiration rate needed to initiate anaerobiosis is obtainable from O_2 mass-balance considerations. The result,

$$S = \frac{6 D_{e,O_2} C_{o,O_2}}{R^2} \quad , \qquad [1]$$

where S is the respiration rate and C_{o,O_2} represents the O_2 concentration at the exterior surface of the aggregate follows from Currie (1961). In the case of steady-state radial diffusion in a cylindrical aggregate of radius R, the critical respiration rate is given by

$$S = \frac{4 D_{e,O_2} C_{o,O_2}}{R^2} \quad . \qquad [2]$$

Equation [2] is derived in the same manner as Eq.[1]. The analogous one-dimensional result gives a similar expression with a factor 2 in place of 4. Thus, a general N-dimensional expression which includes Eqs. [1] and [2] as special cases contains the factor 2N. The result presented in Eq. [2] will be considered later in the context of radial diffusion of O_2 in synthetic, homogeneous aggregates.

Naturally-formed soil aggregates may not exhibit the homogeneous features assumed in the simplest of models. Regions near decomposing plant roots may have higher probabilities of developing anaerobiosis, hence higher probabilities of exhibiting localized accumulations of Se when scanned with the SXRFM. A possible explanation for redox- and diffusion-controlled heterogeneities with respect to total Se concentrations in the vicinity of one particular Scirpus root cross-section will be considered in moderate detail. In this case, a root cross-section was embedded with its axis perpendicular to the plane of the 2-dimensional soil aggregate. The aggregate was water-saturated with a solution containing Se(VI). If Se(VI) reduction occurs at a specific radial distance in the vicinity of root-soil contact, this zone may be regarded as a cylindrical sink for Se accumulation as indicated in Figure 3.3a. This figure illustrates the possible diffusion of mobile Se(VI) to the cylindrically-symmetric reducing zone around a decomposing root. The initial condition is represented by a uniform concentration ($C_{o,Se(VI)}$) of Se(VI) in a saturated sediment in 2-dimensional space. After ≈1 day, which from our past experience represents a typical incubation time needed for reducing conditions to prevail, the reducing region is modeled as a cylindrical surface at which the Se(VI) concentration is zero. Thus, Se(VI) is induced to radially diffuse from the surrounding sediment towards the root zone. This model is mathematically analogous to the radial heat conduction problem solved by Smith (1937), and the problem of groundwater flow to an artesian well analyzed by Jacob and Lohman (1952). Qualitative representations of radial Se distributions at times $t0 < t1 < t2$ are depicted in Figure 3.3b. In regions outside of the reducing zone, only the hypothetical Se(VI) profiles are shown. The Se(IV) and Se(0) generated by Se(VI) reduction are uniformly distributed within the

reducing zone for purposes of this diagram. Following Smith (1937) and Jacob and Lohman (1952), the instantaneous rate at which Se(VI) diffuses into the reducing zone of radius R_e is given (per unit thickness in the axial direction) by

$$Q(t) = \left[2\pi D_{e,Se(VI)} C_{0,Se(VI)}\right] G\left(\frac{1}{4u(t)}\right) \qquad [3]$$

where $D_{e,Se(VI)}$ is the effective diffusivity of Se(VI) in the sediment, the time-dependent parameter u(t) is given by

$$u(t) = \frac{R_e^2}{4 D_{e,Se(VI)} t} \quad , \qquad [4]$$

and

$$G\left(\frac{1}{4u(t)}\right) = \frac{1}{\pi u} \int_0^\infty x e^{-x^2/(4u)} \left\{ \frac{\pi}{2} + \tan^{-1}\left[\frac{Y_0(x)}{J_0(x)}\right] \right\} dx \quad . \qquad [5]$$

In Eq.[5], x is an integration variable, and Y_0 and J_0 represent Bessel functions of order zero of the first and second kinds, respectively. The effective diffusivity of Se(VI) in water-saturated sediment may be approximated by

$$D_{e,Se(VI)} \approx \alpha f D_{o,SO_4} \qquad [6]$$

where f is the (water-saturated) porosity, the complexity parameter α includes porous media influences of tortuosity and mobility (Hillel, 1980), and D_{o,SO_4} $\approx 1.1 \times 10^{-3}$ mm^2 s^{-1} is the sulfate diffusivity in water at 27° C (Robinson and Stokes, 1959). This latter diffusivity was used because of physical-chemical similarities between sulfate and selenate, and because of confidence placed in D_{o,SO_4} values obtained from various independent sources. In addition, estimated vales of D_{e,SeO_4} may be compared with reported values of D_{e,SO_4}. We later integrate Eq.[3] to obtain predicted cumulative Se diffused into the reducing zone according to this simple model, and compare calculations with measurements obtained with the SXRFM.

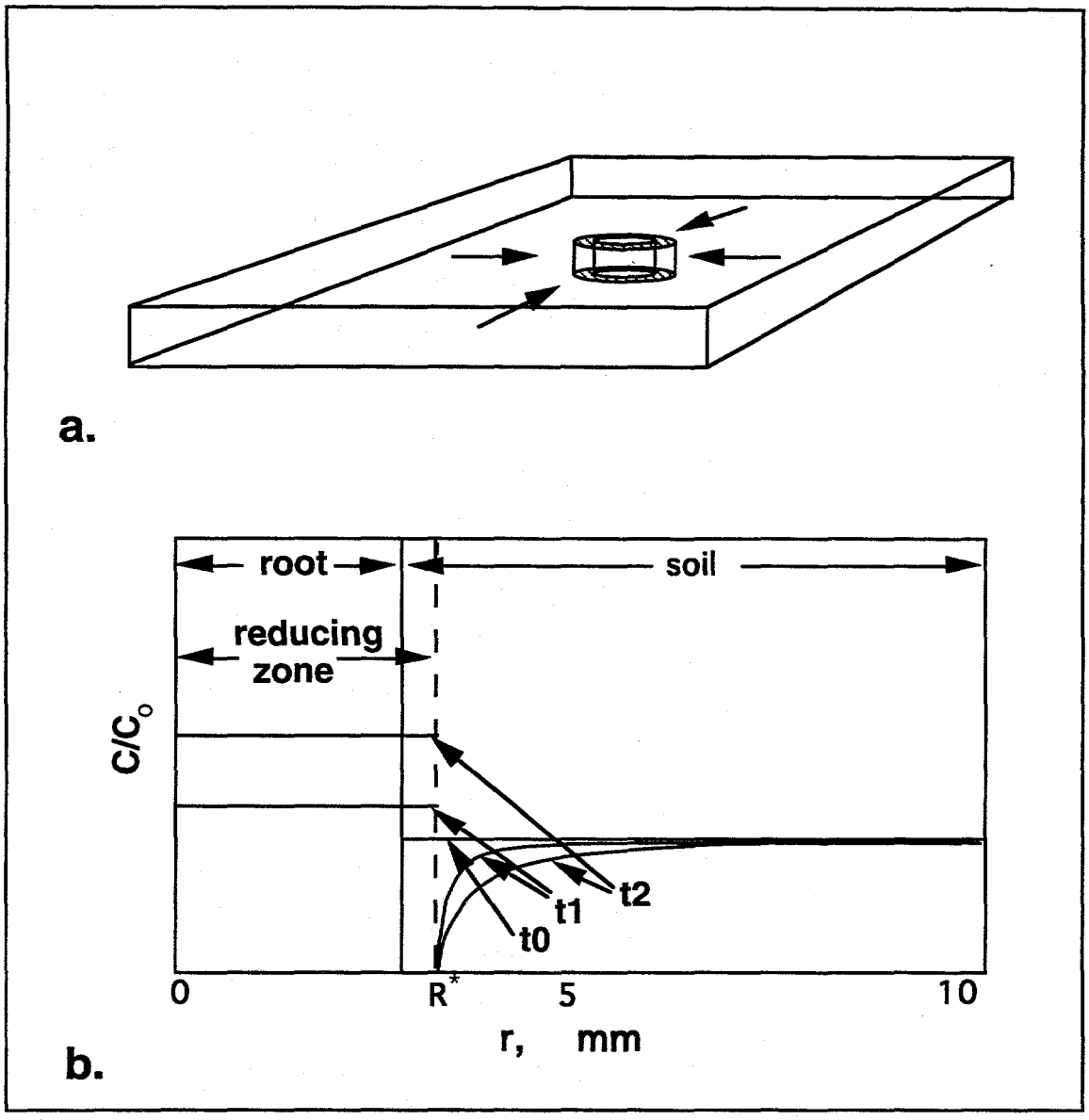

Figure 3.3. (a) Representation of a decomposing root cross-section embedded in water-saturated sediment. Both the root-soil interface and a hypothetical surface at which the concentration of Se(VI) becomes 0 due to reduction are shown. (b) Idealized radial distributions for Se(VI) prior to and following the development of reducing conditions outside the root at R^*. The hypothetical Se(VI) distribution is uniform throughout the system at time zero. At later times, the Se(VI) concentrations decrease towards zero as the reducing zone is approached from the soil zone. The Se(IV) and Se(0) hypothetically formed at R^* are uniformly distributed within $r \leq R^*$ for purposes of this illustration.

3.3 Materials and Methods

Four natural soil aggregate samples from Kesterson Reservoir were analyzed with the SXRFM. Since the sample preparation and results were similar for each of these, only one aggregate will be described in detail. This field soil aggregate sample was obtained on April 28, 1991, from a depth of about 0.07 m in the former Pond 4 region of Kesterson Reservoir. The soils of this area are mapped as Albic Natraqualfs (Turlock sandy loam, Nazar, 1990), although considerable variability of natural and anthropogenic origin is observable within the mapping unit. This site was ponded with seleniferous agricultural drain waters from 1981 to 1986, and primarily vegetated with *Typha latifolia*. The Se concentrations in these saline agricultural drain waters were typically in the range of 250 to 350 mg m^{-3} (250 to 350 ppb). Since 1986, no further disposal of agricultural drain waters occurred at Kesterson Reservoir, and the Pond 4 sampling site remained covered with a dense surface litter of *Typha* leaves and sparse annual forbs (dominated by *Lactuca serriola*). The ≈5.5 mm diameter, ≈1.2 mm thick sample was obtained from a larger (≈ 8 mm diameter) aggregate. The front (analyzed) surface of the sample was originally a cross-section through the aggregate interior. This surface was obtained by breaking open the original aggregate, without shearing, to expose a fresh surface. The sides and back of natural soil aggregates were trimmed with a razor blade, and mounted within a sample-holding cavity on a 50 mm by 50 mm plastic slide frame. The front surface of the sample was flattened by pressing it against the inside of the Mylar film window, rather than by slicing in order to avoid smearing of soil particles. This procedure minimized lateral translation of mineral grains to less than 0.3 mm along the newly exposed surface. Such precautions were necessary since the x-ray absorption and fluorescence are heavily weighted to the surface region (< 200 μm for Se). The front window through which synchrotron x-rays entered, and fluorescent x-rays exited, consisted of 25 μm thick Mylar. The absorption of Se fluorescence x-rays by this Mylar film was negligible.

The natural soil aggregate samples were prepared about 3 days prior to scanning with the SXRFM. Exposure of new surfaces to air during this interval was not expected to significantly alter Se distributions since measured Se re-oxidation rates in Kesterson Reservoir soils are relatively slow. For example, data from long-term (1987 to 1992) monitoring of Kesterson Reservoir soils indicates that re-oxidation to water-soluble Se(VI) under predominantly vadose conditions occurs at a rate of about 5% of the reduced soil Se pool per year (Tokunaga, et al., 1991; and Lawrence Berkeley Laboratory, Earth Sciences Division, unpublished data, 1987-1992). Conversely, rates of Se (VI) reduction in flooded surface soils are typically quite rapid (about 1 to 2 days, from Tokunaga, 1987 unpublished data).

The major portion of this study involves a set of laboratory-prepared soil aggregates in which Se was initially homogeneously distributed in the soluble Se(VI) state. The aggregates were constructed to provide a range of conditions with respect to aeration. Six of the disc-shaped aggregates were each effectively homogeneous, with exposure to atmospheric oxygen permitted only along the radial boundaries (i.e., impervious boundaries were imposed on both circular faces of each aggregate). If the steady-state approximation is adequate, Eq.[2] can be used to describe the necessary conditions for development of anaerobiosis within these 6 aggregates. In cases where central regions of aggregates became anaerobic, it was expected that Se(VI) reduction to adsorbable and less soluble Se(IV), and possibly to insoluble Se(0) within these zones would lower the local chemical potential of Se(VI). This in turn would initiate diffusion of Se(VI) towards reducing core regions from more aerated outer regions of the aggregates. Thus the total Se concentration would increase within reducing zones, and become depleted in aerated regions within the same aggregate. After a period of incubation, the synthetic aggregates were scanned with the SXRFM in order to determine the spatial distribution of Se in order to test for the development of such patterns.

Synthetic soil aggregates were prepared using soils collected from the Kesterson National Wildlife Refuge, in an area also mapped as Albic Natraqualf. These soils had no prior history of exposure to the seleniferous drain waters, and had a Se concentration of < 0.5 mg kg^{-1}. (Contaminated surface soils at Kesterson Reservoir commonly had total Se concentrations > 4 mg kg^{-1}.) The original field soil contained U.S.D.A. size fractions of clay, silt, and sand in 20%, 37%, and 43% portions respectively. In order to minimize noise in x-ray fluorescence arising from particle-size influences (Bertin, 1978), most of the >50 μm fraction of this field sample was removed via sedimentation. (Other experimental evidence from the original soil material showed that Se concentration gradients are easily resolvable, but that smoother spatial maps could be obtained with finer grain-size.) The final laboratory soil material contained clay, silt, and sand size fractions in 32%, 60%, and 8% portions respectively, and 1% organic matter. The laboratory soil aggregates were formed by mixing tap water into homogenized soil material to provide an initial water:soil mass ratio of 0.30 ±0.04. Laboratory-aggregated soil materials were formed into flat pellets of various sizes, and pressed onto sample holders (Fig. 3.4). The synthetic soil aggregates ranged in diameter from 10 mm to about 30 mm. Equivalent dry bulk densities of these pellets ranged from 1.1×10^3 kg m^{-3} to 1.2×10^{-3} kg m^{-3}. The square (50 mm sides), 6.35 mm thick, polycarbonate plastic sample holders provided a rigid backing through which gas diffusion was negligible. Aggregates were placed into the central portion of 2.6 ±0.2 mm deep cavities milled into the plastic. For most samples, large (3 to 10 mm diameter) gaps were provided between the perimeters of the aggregate and borders of the milled cavity. Syringe needles provided lateral ports through which external air equilibrated with the perimeter of the

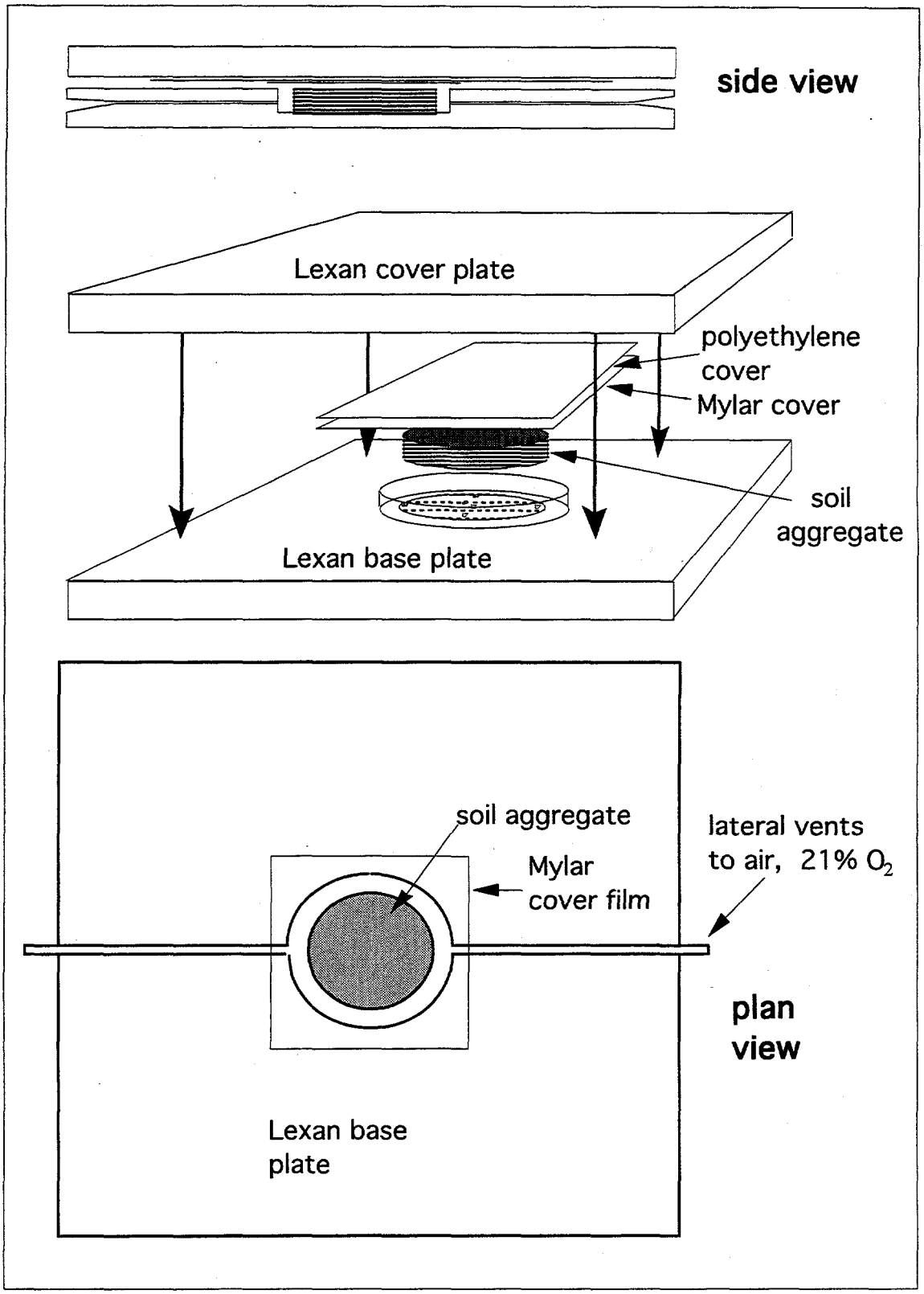

Figure 3.4. Synthetic soil aggregate mounting for SXRFM analysis. See text for construction details.

soil aggregates during incubation. In some of the water-saturated samples, the cavity was completely soil-filled.

About 80% of the originally added water was permitted to evaporate from these aggregates over a 2 day period. After this time, selenium was added to each of the samples in an aqueous solution with major ion composition similar to that of agricultural drainage waters. Selenium, was added in this solution at a total concentration of 240 g m^{-3}, primarily (98%) as Se(VI), with the remainder as Se(IV). It should be noted that this concentration is about 10^3 times higher than that of the seleniferous drain waters which contaminated Kesterson Reservoir. The high Se concentration was used to ensure that later microprobe analyses would be able to detect Se distributions with small relative uncertainties. Previous laboratory experiments on these soils indicated that these high Se concentrations did not significantly inhibit microbially mediated Se transformations (Pickering et al., 1994). A pre-weighed quantity of Se(VI) solution was distributed along the edge of each aggregate via syringe needle, with the source pressure kept within 50 Pa of local atmospheric pressure. The amount of seleniferous water added was varied between individual aggregates in order to obtain saturation ranging from 40% up to 100%. This resulted in initial soil Se concentrations ranging from 30 to 70 mg kg^{-1} (mass of Se per wet soil mass). The characteristic soil water sorptivities and Se(VI) diffusivities were large enough relative to the aggregate dimensions to permit practically uniform distributions of water and Se(VI) within several hours. In several aggregates, sections of roots cut from *Scirpus robustus* and *S. californicus*, two common wetland plants, were embedded into the upper surface.

Upon wetting with the seleniferous solution, the open face of the system was sealed with Mylar film (25 μm thickness). The Mylar film was covered with two layers of 70 μm polyethylene film, which in turn was covered with a 3.2 mm thick polycarbonate plastic top plate. Upon compressing the top plate and intermediate film layers onto the sample and sample holder, the upper surface was also made impervious to gas exchanges. Thus, gas exchange occurred only along the perimeters of aggregates. The various laboratory aggregate samples were incubated for 6 to 17 days, under fluctuating temperatures (27° ±5° C). Samples were stored in a humidified container (99% to 100% relative humidity) during the incubation period. Periodic weighing of the samples in their holders indicated no significant changes in water content during the incubation. Periodic extraction of small volumes of gas from the hypodermic needle ports, and injection into a polarographic oxygen analyzer (Beckman model 0260, with a custom-built low-volume sensor port) indicated that O_2 concentrations along the aggregate exteriors remained at atmospheric values.

The distributions of Se and several other elements were determined in seven synthetic soil aggregates. Two, 10 to 11 mm diameter, aggregates had air-filled porosities (denoted by f_a) of 0.30 and 0.10 (both ±0.03) respectively. Four, 25 to 30 mm diameter, soil aggregates were also

studied. These 4 aggregates had f_a values of 0.32, 0.20, 0.10, and 0.07 (all ±0.04). Sections of *Scirpus* roots were embedded in the 0.10 and in the 0.20 f_a sample. A final sample (≈30 mm diameter, f = 0.57±0.04) consisted of a completely water-saturated soil, in which sections of Scirpus tissue were embedded. These samples were only scanned with the SXRFM after prescribed incubation periods. Scanning of these samples at their time-zero conditions was not possible because of limited availability of experimental time at the NSLS, and because of potential adverse effects on soil microbes. Previous SXRFM experiments on Se(VI) introduced into soil aggregates exhibited essentially homogeneous initial Se distributions.

All SXRFM measurements were performed at the NSLS, beamline X26A. A plan view of the major components within the experimental hutch of the SXRFM was shown in Figure 3.2. The collimated incident x-ray beam strikes a sample mounted at a 45° angle. For these experiments, white x-rays emitted from the synchrotron ring were used without a monochrometer. A video monitor was used to position the sample relative to the incident x-ray beam. Fluorescence x-rays were monitored with a Si(Li) energy-dispersive detector (≈200 eV energy resolution at the Se Kα energy) mounted at 90° relative to the incident beam. The Kα energy denotes the photon energy released during L- to K-shell electron transitions. For Se, these photons are in the range of 11.2 keV. Fluorescent x-rays are emitted from all points on the beam path within the sample with approximately exponentially decreasing intensity. Since the incident beam and fluorescence detector are aligned on a common horizontal plane, the measured fluorescence originates from an asymmetric volume within the soil. More specifically, higher spatial resolution is retained along the vertical, and broader horizontal averaging occurs. For this reason, one-dimensional scans of samples were performed along the vertical direction. Scanning of a sample is performed by moving the sample with motorized drives relative to the essentially stationary incident x-ray beam.

For the natural soil aggregates, the SXRFM scans were performed by holding the sample in a fixed position on the beam during a counting interval, and moving the sample vertically across the beam path in discrete steps between counting periods. The samples were typically scanned over about 5 mm by 5 mm areas, with vertical and horizontal steps ranging from 50 to 250 μm. The nominally 10 μm beam spot averages over a larger region of the sample because of the substantial thickness. The effective x-ray absorption depth for Se in the soil matrix is about 200 μm, thus our samples are of effectively infinite thickness.

In the later studies of synthetic aggregates, the sample was slowly scanned while fluorescence data were collected. Using this approach, fluorescence spectra represented moving averages of 0.5 mm vertical traverses. This was done to smooth out small-scale heterogeneities in fluorescence spectra resulting from grain-size effects. For both the natural and synthetic soil aggregates, the background-corrected, beam current-normalized fluorescence count rates were

converted into total Se concentrations by equating their average values with independent measurements of bulk concentrations. These latter concentrations were obtained with conventional energy dispersive x-ray fluorescence spectrometry on the bulk samples (Giauque et al., 1977).

3.4 Results and Discussion

The SXRFM map of total Se concentrations within the field soil aggregate is shown in Figure 3.5. The local Se concentration was then taken to be linearly proportional to the background-subtracted Se Kα fluorescence count rate. Note that large variations in total Se concentrations were observed at the scale of about 1 mm. The persistence of high gradients in total Se concentrations suggest that insoluble Se(0) and Se(IV) species account for most of this element. More soluble Se(VI) is expected to uniformly distribute on the aggregate scale via diffusion. Note also that the spatial distribution of Se within this aggregate interior cross-section is neither radial nor apparently random. The sample preparation process could not have introduced more than about 0.3 mm displacements in mineral grain positions as noted previously. These results indicate that intra-aggregate heterogeneities may be important in initiating reduction in patterns contrary to that of the radially symmetric microsites expected in homogeneous aggregates. Also, within the aggregate, the total Se concentrations are approximated by a log-normal probability distribution as shown in Figure 3.6.

Previous experiences with wetting of synthetic soil aggregates with Se(VI) solutions have indicated that uniform short-term Se distributions are easily achieved. The homogeneity with respect to short-term (~ 1 day) Se distributions is expected based on uniformity of wetting over short distances characteristic of the aggregate scale and previously observed time lags associated with Se reduction. The possibility of Se redistribution in response to localized Se reduction is addressed in the remainder of this study.

The distribution of Se, expressed in terms of normalized Kα fluorescence count rates, along a central transect through the 11 mm diameter synthetic soil aggregate is show in Figure 3.7. Note that relatively homogeneous distributions of total Se were measured in this sample on day 17. Similar results were obtained in the 10 mm diameter synthetic soil aggregate, as well as in larger soil aggregates in regions which did not contain embedded plant tissue. Such observations are expected when Se(VI) remains essentially unreduced, and is free to diffusively distribute to minimize concentration gradients. Thus, the presence of reducing zones in these aggregates appear very unlikely. In the context of the 2-dimensional (cylindrical) anaerobic microsite model, these observations imply that

$$S < \frac{4 D_{e,O_2} C_{o,O_2}}{R^2} \quad . \qquad [7]$$

For these experiments, essentially no deviations from atmospheric concentrations of O_2 were measured at the aggregate exteriors. Therefore the $C_{o,O_2} \approx 270$ g m^{-3} for O_2 at the aggregate exteriors. D_{e,O_2} values may be estimated from various model functions which rely on calculations from f_a. The calculated D_{e,O_2} values will have large uncertainties, partly because of the ±0.03 absolute uncertainties in the f_a, and also because no single model for porous media diffusivity is sufficiently general to account for influences of pore-structure differences. For our present purpose, we used the regression relation of Sallam et al. (1984),

$$D_{e,O_2} = \frac{f_a^{3.1}}{f^2} D_{o,O_2} \qquad [8]$$

where f represents the total porosity, and D_{o,O_2} is the O_2 diffusivity in air, while recognizing

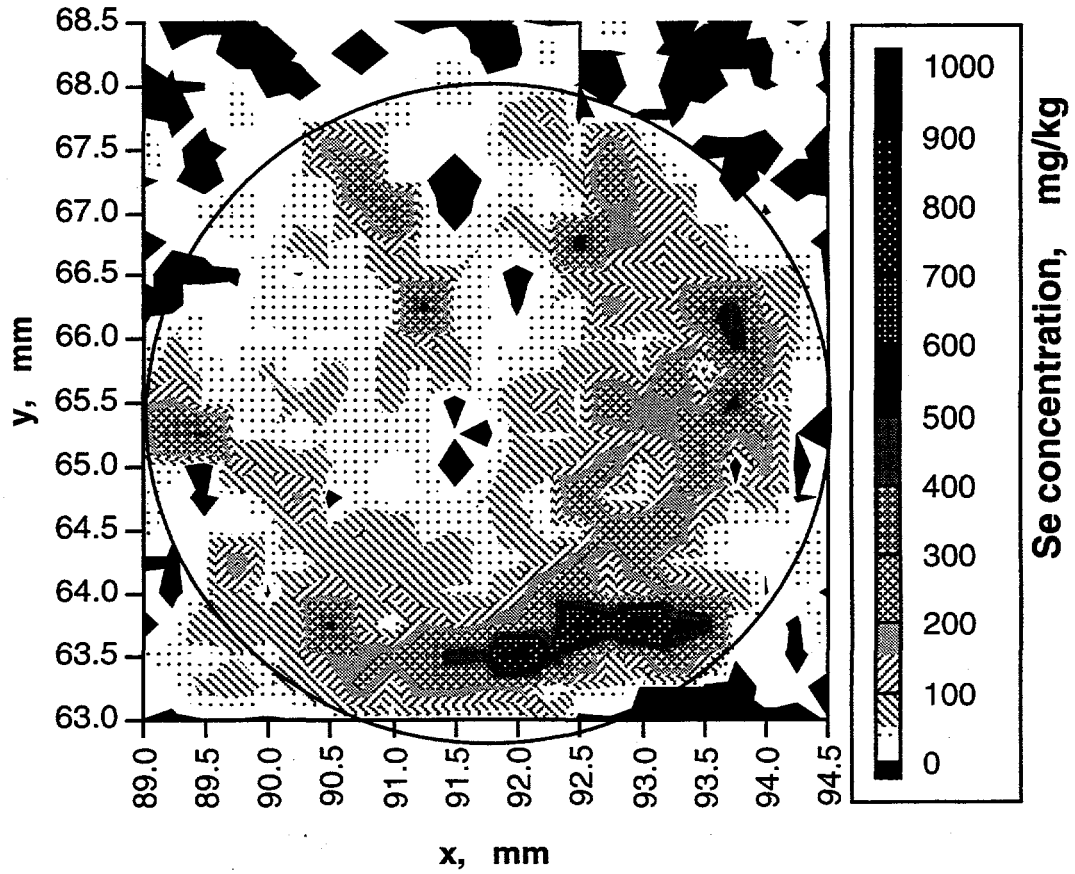

Figure 3.5. Spatial distribution of total Se in a natural soil aggregate sampled at Kesterson Reservoir.

that deviations from predicted D_{e,O_2} can be large (e.g. Xu et al., 1992). The D_{o,O_2} values ranged from 2.05×10^{-5} to 2.17×10^{-5} m^2 s^{-1} for the range of temperatures covered during incubation. For the case of f = 0.57±0.02 and f_a= 0.07±0.04, values of D_e from Eq.[8], range from 1.0×10^{-4} to 6.6×10^{-3} m^2 day^{-1}. Using parameters characteristic of the aggregates, along with Eqs. [7] and [8], we may estimate upper limits on O_2 consumption rates. Using the lowest estimated D_e in the largest, wettest aggregates (without added plant tissue) this analysis indicates that S < 500 g O_2 m^{-3} day^{-1}. This upper limit on S is still much higher than values typically reported for bulk soil respiration rates. For example, soil respiration rates from Black (1968), Smith (1980), and Buyanovsky et al. (1986) are in the range of 20 to 80 g O_2 m^{-3} day^{-1}. Estimates of S, based upon simplified models used to obtain Eqs. [2] and [7] can be difficult to apply because of the needed for approximately steady-state conditions and uncertainties in values of D_e. Direct measurements of S on individual aggregates would have provided a better understanding of these systems. An example of a such an experimental design is provided in Leffelaar (1986 and 1993).

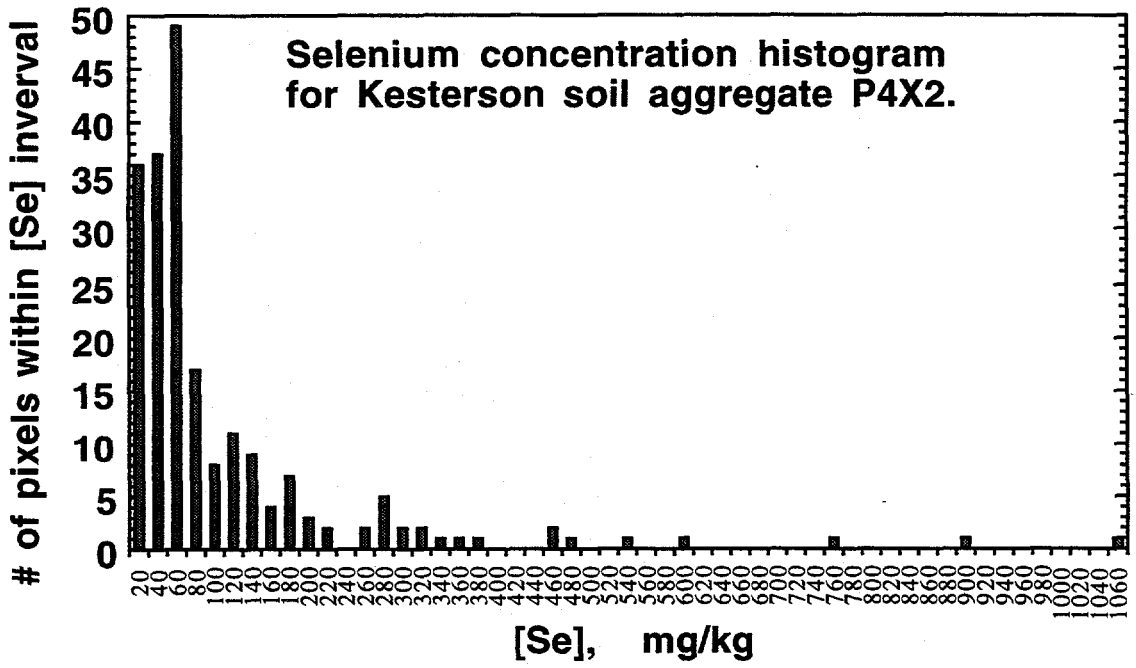

Figure 3.6. Histogram of total Se concentrations measured in the Kesterson Reservoir soil aggregate. The distribution function for total Se is approximately log-normal.

Also shown in Figure 3.7 are normalized fluorescence count rate transects for total Fe and total Sr in the aggregate. Note that these elements are also distributed relatively uniformly, and that the boundaries of the aggregate are easily recognized from the drop-offs in count rates of each of the constituents.

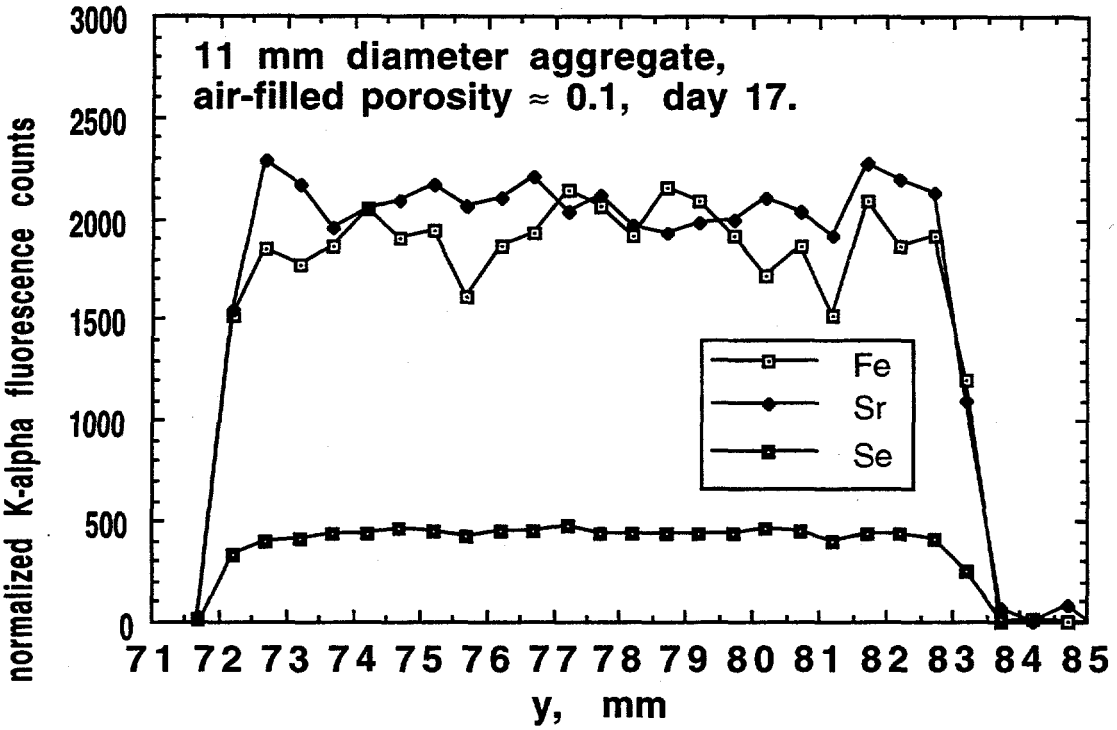

Figure 3.7. Spatial distributions of total Se, Fe, and Sr along a central transect through the 11 mm diameter synthetic soil aggregate after 17 days of incubation. Data are displayed as (background-subtracted) normalized Kα fluorescence count rates.

The total Se concentration along an aggregate transect which intercepted an embedded *Scirpus* root section is shown in Fig. 3.8. The SXRFM mapping was performed after 17 days of incubation. (Measurements on the initial Se distribution in this sample were not possible because scheduling conflicts. However, results of SXRFM mapping on very similar samples at and near time-zero displayed essentially homogeneous Se profiles similar to those shown in Fig. 3.7.) The *Scirpus* root-embedded aggregate had an $f_a = 0.10 \pm 0.03$. The location of the root section was determined directly from the Fe and Sr concentration profiles also obtained in the x-ray fluorescence spectra. The root position is clearly indicated by local minima in both Fe and Sr count rates. Note that only in regions adjacent to the decomposing root section is there evidence of Se accumulation, indicating that this region experienced reducing conditions during the incubation period. The relatively uniform concentrations of Se throughout the rest of the aggregate indicate that oxidizing conditions prevailed in all other areas of the aggregate. Although redox-induced transport of Fe may be possible, this element was highly correlated with Sr (which is largely associated with the solid phase and will not undergo redox transformations) in this and all other samples tested. Such correlations indicate that mobilization of Fe(II) did not occur to any significant extent during the course of these experiments.

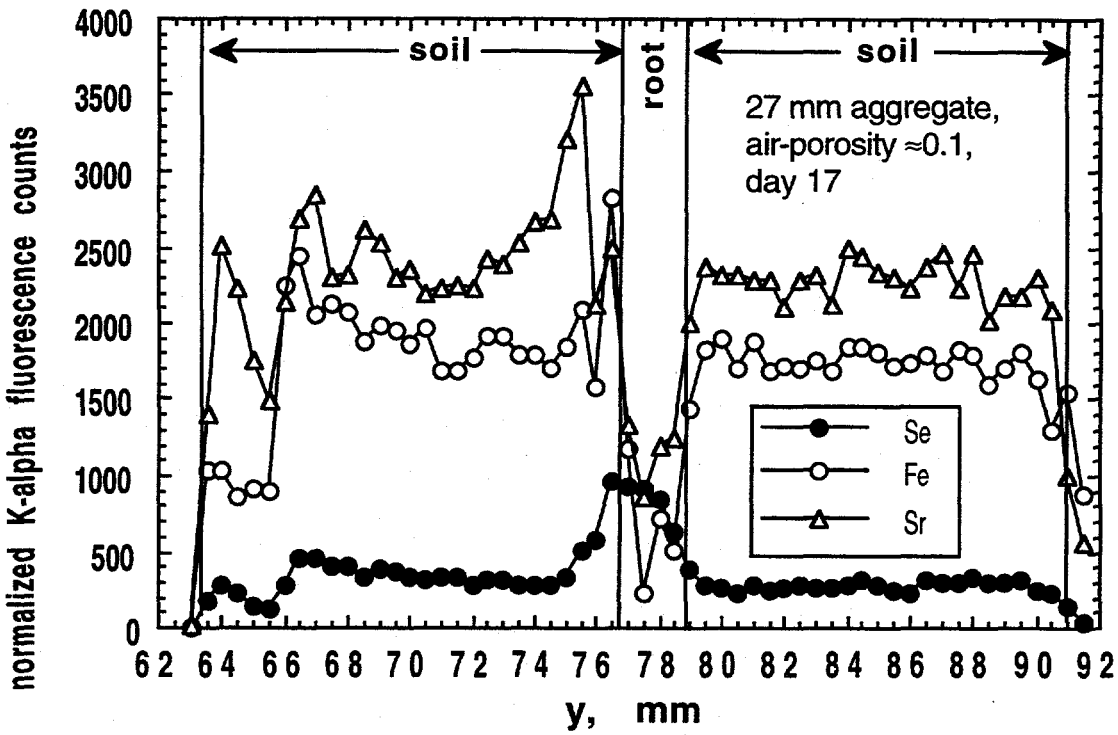

Figure 3.8. Spatial distributions of total Se, Fe, and Sr along a transect through a decomposing *Scirpus* root, laterally-embedded within a 27 mm diameter synthetic soil aggregate after 17 days of incubation. Data are displayed as (background-subtracted) normalized Kα fluorescence count rates.

Both one-dimensional transects and two-dimensional maps of total Se were generated on days 6 and 7 for the case of a *Scirpus* root cross section embedded within a water-saturated sediment ($f = 0.57$, $f_a = 0$). (Again, measurements on the initial Se distribution in this sample were not possible because scheduling conflicts.) The root-sediment boundary was determined from Fe and Sr concentration profiles. The 2-dimensional distribution of total Se concentrations in this case is shown in Figure 3.9. (The coordinates in this figure are those of the x-y stage on the SXRFM.) Note that very large accumulations of Se were observed within the 7 day incubation period. More than 20-fold increases in total Se were measured in sediments near the root interface. Although the distributions shown through the data in Figure 3.9 are for total Se, the evolution of the profile is hypothesized to result from reduction of Se(VI).

A qualitative set of radial distributions for Se(VI), Se(IV), and Se(0) which may be associated with the total Se distribution (Figure 3.9) is presented in Figure 3.10. The region in which total Se concentrations were measurably enriched must correspond to a zone dominated by essentially immobile species. Otherwise, the very steep concentration gradients would result in diffusive dissipation of the accumulated Se. Thus, Se(0) and possibly Se(IV) accumulated in this zone since these are the much less mobile species. The presence of these species indicates

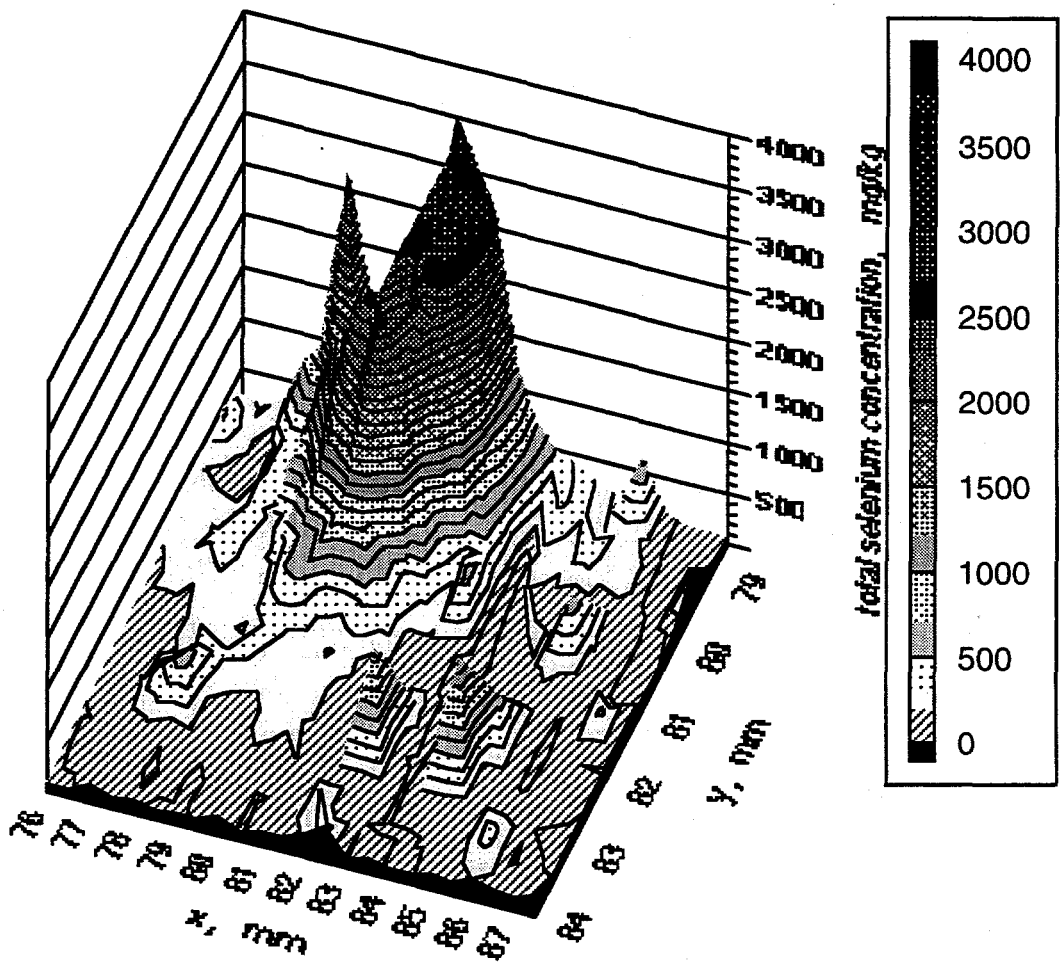

Figure 3.9. Two-dimensional SXRFM map of total Se concentration in the vicinity of the *Scirpus* root embedded in water-saturated soil after 7 days of incubation. The homogeneous initial Se concentration was 70 mg kg^{-1} in the soil.

Se reduction. The Se(VI) concentration is expected to approach zero in this region of total Se accumulation since this species is very unstable under reducing conditions. At each position, the sums of Se(0), Se(IV), and Se(VI) concentrations are constrained to add up to the total Se concentration.

Although the details of the Se(VI), Se(IV), and Se(0) concentration distributions remain unknown, the simplified model based on Eq. [3] may be used to determine whether or not Se(VI) diffusion to a reducing zone could account for the magnitude of the observed total Se accumulation. This calculation was performed by setting the radius of the Se(VI) zero-concentration boundary at $R^* = 3.3$ mm (Fig. 3), based on the mean radius at which the total Se concentration was 2 times elevated with respect to the initial concentration. For this model,

$D_{e,Se(VI)}$ was approximated by values calculated as 35 mm^2 d^{-1} using Eq.[6], assuming a reasonable value of $\alpha = 0.65$. This estimated value of $D_{e,Se(VI)}$ is in very good agreement with temperature-corrected values of D_{e,SO_4} reviewed by Iversen and Jorgensen (1993) for sediments having the same porosity. The time-dependence of the Se(VI) diffusion rate into the reducing zone at 3.3 mm was calculated from Eq.[3]. This result was then integrated with respect to time to obtain the modeled cumulative diffusive flux. The modeled cumulative diffusive flux of Se into the reducing zone is shown in Figure 3.11, along with the case in which $D_{e,Se(VI)}$ is half as large as the predicted magnitude. The measured average total Se concentration within the reducing zone on days 6 and 7 are plotted in Figure 3.11 for comparison. Discrepancies between measured and modeled results probably originate from uncertainties in (1) the spatial and temporal distribution of reduction activity, (2) the actual concentrations of Se(VI) in the reducing region, (3) $D_{e,Se(VI)}$, and (4) likely counter-diffusion of Se(IV). In view of these uncertainties, diffusive transport of Se(VI) to a reducing zone appears to adequately account for the accumulation of Se.

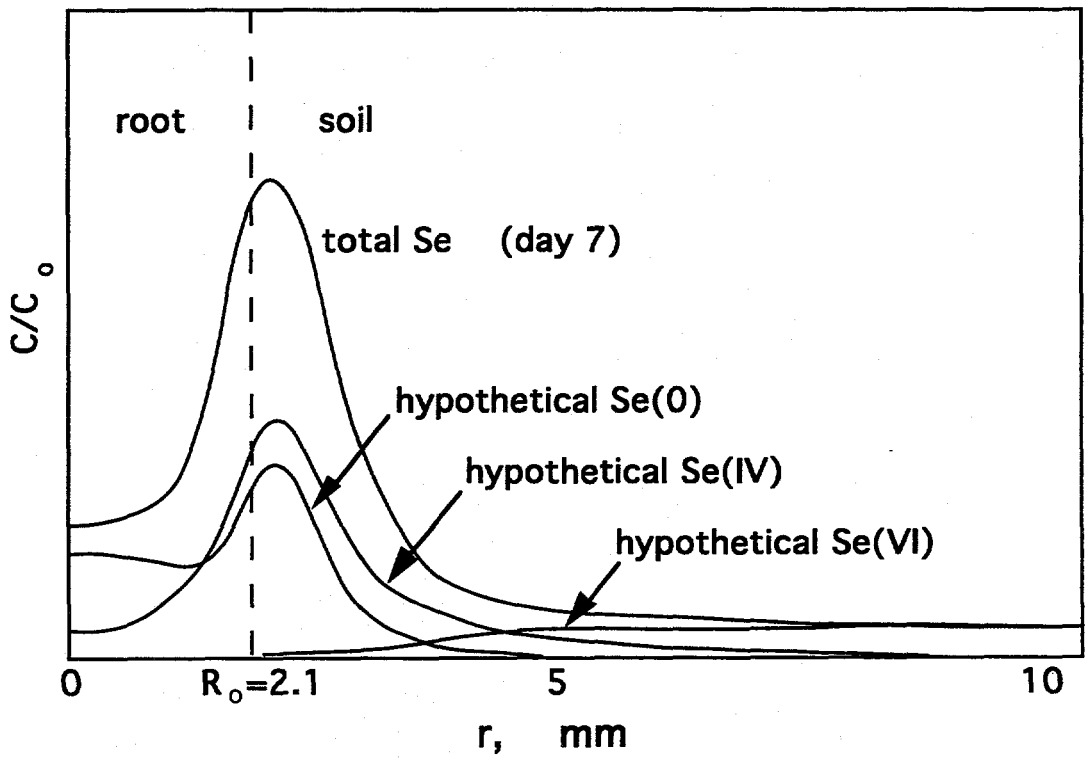

Figure 3.10. Hypothetical radial distributions of Se(VI), Se(IV), and Se(0) after 7 days of incubation in the vicinity of the decomposing *Scirpus* root embedded in sediment.

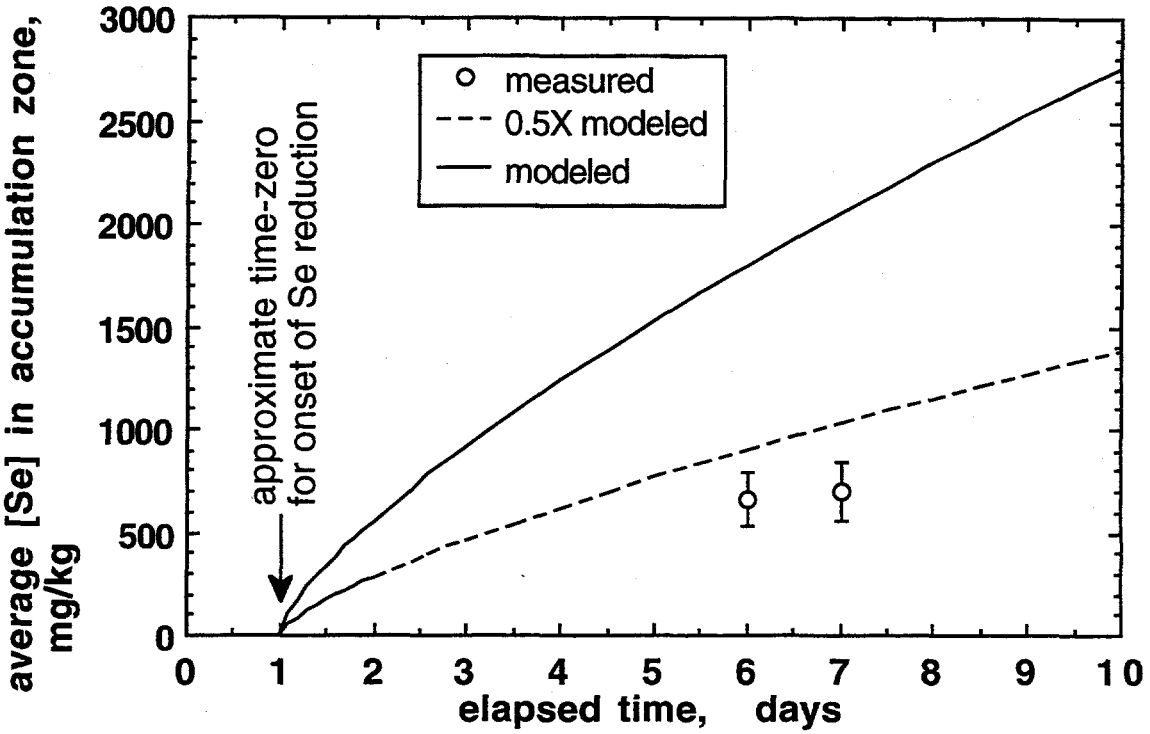

Figure 3.11. Model calculations of time-dependence of the average total Se concentration in reducing zone around the decomposing *Scirpus* root, assuming radial diffusion to a zero concentration boundary at r = 3.3 mm. The (day 6 and 7) SXRFM-measured average values of total Se concentration in this zone are also shown. The lower curve represents predictions based on an effective Se(VI) diffusivity which is one-half that of the estimated $D_{e,Se(VI)}$ (upper curve).

3.5 Concluding Remarks

Synchrotron x-ray fluorescence microprobe analyses of Se-contaminated soil aggregates obtained from Kesterson Reservoir indicated the presence of localized zones, typically with dimensions of ≈ 1 mm, in which significantly elevated concentrations of total Se occur. Such small-scale heterogeneities in Se concentrations can only persist when effective diffusivities of the dominant Se species are very low. Both Se(0) and various possible solid phase forms of Se(IV) may account for these localized Se-concentrated zones. If re-oxidation of Se(0) and Se(IV) in soils occurs primarily as reactions at solid phase surfaces, highly localized accumulations of reduced species may influence these reaction rates. Re-oxidation of Se(0) and Se(IV) in microsites may occur slowly relative to the case where these species are uniformly dispersed throughout aggregates. In the former case, re-oxidation may proceed by sequentially oxidizing layers of Se from a limited area. In the latter case, all reduced Se species may be

simultaneously exposed to oxidants. Thus, localization of reduced Se species may partially explain the slow re-oxidation rates observed for Se in Kesterson Reservoir soils (Tokunaga et al., 1991).

The present study of Se distributions in both natural and laboratory-constructed soil aggregates provides examples of how trace elements with redox-dependent solubility can be used to study variable redox environments in soils. The application of the SXRFM for trace element mapping within soil aggregates illustrates the potential usefulness of this tool in soil science. It is emphasized in this context that much higher spatial resolution (approaching 1 μm) is possible with this method, and that the ≈ 100 μm resolution associated with the present study was due to sample thickness effects.

The laboratory experiments demonstrated the potential importance of decomposing organic matter in generating localized reducing zones for Se accumulation. However, the simple model of Se(VI) diffusion to a cylindrical sink underestimated the measured amount of Se accumulation in the vicinity of a section of *Scirpus* root embedded in a water-saturated sediment. Improved understanding of the dynamics of such processes, hence improved modeling awaits experiments in which maps of individual Se species are obtained along with high-resolution measurements of spatial distributions of diffusivity and respiration rates.

Improved resolution with respect to chemical speciation in SXRFM is another current area of expanding research. Most SXRFM studies to date have provided maps of total elemental concentrations within samples. As our previous discussions indicated, direct mapping of individual oxidation states, i.e. Se(VI), Se(IV), and Se(0) mapping, is needed to better understand the complex dynamics of reactions and transport. Synchrotron-based x-ray absorption spectroscopy (XAS) permits direct determinations of valence in elements which undergo oxidation and reduction (Waychunas et al., 1983; Wong et al., 1984; Waychunas, 1987; Brown and Parks, 1989). Shifts in the position of the x-ray absorption edge, typically by about 2 to 4 eV per oxidation state, may be used to directly determine the valence composition of elements of interest. This feature of XAS has recently been utilized in research conducted at the Stanford Synchrotron Radiation Laboratory (I.J. Pickering et al., 1994) to demonstrate the occurrence of Se(0) in Kesterson Reservoir soils, and to track the reduction of Se(VI) to Se(IV), and ultimately to Se(0) in laboratory experiments. By inclusion of a monochrometer in the SXRFM, with which characteristic features of the Se x-ray absorption edge are obtained for each pixel, one could obtain individual maps for Se(VI), Se(IV), and Se(0) concentrations. Such micro-XAS studies with Se in sediments will be initiated in the near future. Recent examples of the value of this approach include studies of Cr by Sutton et al. (1993) and by Bajt et al. (1993), and U by Bertsch et al. (1994, *in press*). Synchrotron-based x-ray methods have tremendous future applications in studies of soils. The capabilities of direct, nondestructive measurements

with respect to elemental mapping, speciation, and elucidation of bonding structures of a wide range of elements make these methods highly attractive research tools.

4.0 Selenium Transport Between Ponded Waters and Shallow Sediments

Tetsu Tokunaga
Earth Sciences Division
Lawrence Berkeley Laboratory

Gordon E. Brown, Jr. and Ingrid J. Pickering
Stanford Synchrotron Radiation Laboratory
Stanford University

Stephen R. Sutton and Sasa Bajt
Department of Geophysical Sciences
The University of Chicago

The importance of selenium as an essential nutrient and as a potentially toxic trace element requires that its speciation and transport between various environmental compartments be understood. In this study, Se partitioning and transformations in hydrostatically ponded laboratory sediments are compared with a simple model, based on transport of Se(VI) and Se(IV) between well-mixed surface waters and shallow sediment pore waters. Two types of sediment columns were tested, one consisting of a homogeneous soil, and the other in which plant tissue (*Bromus mollis*) was incorporated as an organic matter amendment to the surface sediment. In both systems, seleniferous waters (primarily containing Se(VI)) were ponded over initially nonseleniferous sediment columns. Provisions for apparent first-order reduction of Se(VI) to Se(IV) within ponded waters were included. Measured concentrations of Se(VI) and Se(IV) in sediment pore waters collected from 25 mm below the pool-sediment interface were used as time-dependent boundary conditions to model concentrations of these species in overlying pool waters. Two adjustable parameters, the mass transfer coefficient and pool Se(VI) apparent reduction rate constant, were varied to provide best fits to data. Agreement between data and the model were obtained for the two types of ponded sediments. A more mechanistic approach, relying on diffusive transport of Se(VI) and Se(IV) through a boundary region was also considered. This approach could not adequately account for removal of Se from ponded waters since most of the accumulation of reduced Se occurred within the boundary zone, rather than below it. Therefore, the successful application of mass transfer coefficients to this process results from Se reduction rates within the boundary zone being proportional to Se concentration gradients acting across this zone. X-ray absorption spectroscopy provided direct evidence for Se reduction to Se(0) in these sediments. Synchrotron X-ray microprobe analyses showed large variations in Se concentrations within millimeters of the sediment surface, indicating that reduction of Se within this thin boundary region can be significant. The extremely large gradients in Se concentrations observed at the surfaces of these sediment columns indicate that

experimental methods with spatial resolution of about 1 mm are needed before mechanistic diffusion-redox analyses can be successfully applied to these types of systems.

4.1 Introduction

Transport across boundaries between surface waters and underlying sediments are important in cycling of many trace elements (Santschi et al., 1990). Selenium is both an essential nutrient and a potentially toxic trace element (Rosenfeld and Beath, 1964; Jacobs, 1989; Frankenberger and Benson, 1994). Its solubility and mobility in the environment are strongly dependent on its valence and specific chemical state. Common inorganic species include soluble selenate (Se(VI)), selenite (Se(IV)), insoluble elemental selenium (Se(0)), and various metal and organic selenides (Elrashidi et al., 1987; Masscheleyn et al., 1990). Selenite, which is stable under moderately reducing conditions, is soluble, but can strongly adsorb onto surfaces of common soil minerals and organic matter (Geering et al., 1968; Hingston et al., 1971; Hamdy et al., 1977; Balistrieri and Chao, 1987; Bar-Yosef and Meek, 1987; Neal et al., 1987; Christensen et al., 1989). Organo-selenium species include seleno-amino acids and volatile methylated Se compounds (Reamer and Zoller, 1980; Zieve and Peterson, 1981; Doran, 1982; Thompson-Eagle and Frankenberger, 1989). The essential role of microorganisms in catalyzing most Se transformations of environmental importance is now well-recognized (Doran, 1982; Zehr and Oremland, 1987; Jacobs, 1989; Macy et al., 1989; Oremland et al., 1989, 1990; Lortie et al., 1992; Frankenberger and Benson, 1994). Knowledge of Se speciation and partitioning within various environmental compartments is also important in evaluation of potential risks arising from deficiency or toxicity (Ohlendorf, 1989; Luoma et al., 1992). Wide variations in Se solubility and sorption characteristics among its different forms require that its speciation be understood in order to predict transport between compartments.

Portions of the Se cycle in wetlands, lakes, rivers, ocean bottoms, and agricultural drainage water evaporation ponds occur across interfaces between surface waters and sediments (Cutter and Bruland, 1984; Weres et al., 1989a). Selenium transport and transformations in such environments has received considerable attention over the past ten years since the implication of Se toxicity in wildlife deaths and deformities at Kesterson Reservoir, California (Presser and Barnes, 1985; Ohlendorf, 1989; Weres et al, 1989a; Gilliom, 1989; Long et al., 1990; Benson et al., 1991; White et al., 1991; Tokunaga et al., 1994a). Although transport of Se across surface water-sediment boundaries is recognized, quantitative comparisons of measurements with models are needed to test the relative importance of various mechanisms.

This study is concerned with accounting for Se transport and transformations in shallow, hydrostatically ponded laboratory sediments. Hydrostatic columns provide ideal experimental

conditions for evaluating the relative importance of diffusive exchanges of Se species between ponded waters and sediments, and Se reduction within ponded waters. They can also represent major features of natural vernal pools as well as ephemeral pools formed over selenium-contaminated soils of Kesterson Reservoir (Tokunaga and Benson, 1992; Poister and Tokunaga, 1992). In this study, a mass transfer model for the exchange of soluble selenate (Se(VI), as SeO_4^{2-}) and selenite (Se(IV), as SeO_3^{2-}) between well-mixed surface waters and shallow sediment pore waters is tested. Measured concentrations of Se(VI) and Se(IV) in sediment pore waters provided time-dependent boundary conditions with which these species exchanged with overlying pool waters. These exchanges are modeled with mass transfer coefficients. First-order reduction of Se(VI) to Se(IV) within ponded waters was included in the model. Mass transfer coefficients and pool Se(VI) reduction rate constants serve as adjustable parameters, optimized to provide best model fits to data. The mass transfer coefficients are later compared with reasonable values of diffusion coefficients and diffusion lengths for the purpose of testing a diffusion-based interpretation of Se transport between ponded waters and sediments.

Investigations of redox-dependent trace element transport require speciation with respect to valence states. Trace element speciation methods for sediments typically rely on selective extraction techniques (Chao and Sanzolone, 1989; Lipton, 1991; Tokunaga et al., 1991). Such techniques can introduce uncertainties arising from possible alteration of speciation during extraction procedures (Kheboian and Bauer, 1987; Gruebel et al., 1988; Beckett, 1989; Belize et al., 1989). X-ray absorption spectroscopy (XAS) has become established as an analytical method which permits direct speciation of a wide range of elements (Brown et al., 1988; Koningsberger and Prins, 1988; Brown and Parks, 1989). The method has been applied to in situ determinations of Se(IV) and Se(VI) adsorption at mineral surfaces (Hayes et al., 1987). The valence-sensitivity of x-ray absorption near edge spectroscopy (XANES) has been exploited in oxidation state studies of various elements (Waychunas et al., 1983; George and Gorbaty, 1989). More recently, XAS has been used to determine Se oxidation states in contaminated soils from Kesterson Reservoir, and to track Se reduction in sediments during flooding (Pickering et al., 1994; Pickering et al., submitted 1994; Tokunaga et al., submitted 1995). In the present paper, we return to parts of this recent research, with a focus on Se transport across the surface water-sediment boundary.

Concentrations of various chemical species at interfaces between surface waters and sediments often change abruptly over very short distances (Santschi et al., 1990; Davison et al., 1994). Information on chemical concentrations at appropriately high spatial resolution is essential when testing models of chemical transport and transformation in such environments. The synchrotron x-ray fluorescence microprobe (SXRFM) permits two-dimensional mapping of a wide variety of trace elements, with spatial resolution approaching 1 μm (Jones and Gordon,

1989; Sutton et al., 1993a). This tool has recently been used to study small-scale heterogeneity of Se concentrations in contaminated sediments from Kesterson Reservoir (Tokunaga et al., 1994b). The combined use of XANES and SXRFM, referred to as micro-XANES, is now being explored to obtain valence-specific maps of different oxidation states of particular trace elements (Bajt et al., 1993; Sutton et al. 1993b). In the present work, the SXRFM was used to obtain a high-resolution Se map within a region of a sediment column expected to exhibit large concentration gradients.

4.2 Materials and Methods

Laboratory soil columns were designed to study Se reduction within sediments following ponding with seleniferous waters. A portion of this study involved applications of XAS to determine changes in oxidation states of Se (Pickering et al., 1994; Pickering et al., submitted 1994; Tokunaga et al., submitted 1995). Soils for these columns were collected from Kesterson National Wildlife Refuge, in an area with no previous history of exposure to seleniferous waters. The total Se concentrations in the sampled soil was < 0.5 mg kg^{-1}. Homogenized soils were packed (while still at a field-moist water content of 0.178 kg kg^{-1}) to a depth of 100 mm in 4 PVC columns (76.5 mm diameter), and to an equivalent dry bulk density of 1.28 Mg m^{-3} (Fig. 4.1). The total porosity and initial water-filled porosity were 0.52 and 0.23 respectively. The column bottoms were sealed, and the walls were sufficiently tall to permit ponding above the soils. Two of the columns (denoted C1 and C3) were uniformly packed with soil. The other two columns (denoted C2 and C4) were amended with cuttings of *Bromus mollis* leaves and stems added to the uppermost 30 mm of soil, in order to observe possible influences of decomposing vegetation on Se reduction. The mass of organic matter added in this manner amounted to an air-dry equivalent of 0.2 kg m^{-2} (1.03 g per column), which corresponds to a typical quantity of annual grass biomass produced at the field site. Soil water samplers were embedded at 25 and 75 mm below the soil surface in one unamended (C3) and one organic matter-amended (C4) soil column. These samplers were similar in design to that described in Tokunaga (1992), with the exception of using a smaller ceramic tip (7 mm diameter, 10 mm length, 0.2 ml pore volume). The use of the calomel reference electrode and platinum wire electrodes (Fig. 4.1) along with associated redox measurement results are described in Tokunaga et al. (submitted 1995).

Waters with an initial Se concentration of 240 g m^{-3} (3.0 mM) were ponded over these previously uncontaminated soils. These initial aqueous Se concentrations are about 10^3 times higher than typical values observed in the agricultural drainage waters ponded at Kesterson Reservoir. Laboratory experiments were conducted with elevated Se concentrations in order to assure collection of high quality x-ray absorption spectra on sediments (Pickering et al., 1994;

Pickering et al., submitted 1994; Tokunaga et al., submitted 1995). Water and sediment sampling, and chemical analyses are discussed in greater detail in these studies on applications of x-ray absorption spectroscopy (XAS) in studies of Se in soils. Selenium was added to the laboratory solution as 98% Se(VI) (from Na_2SeO_4) and 2% Se(IV) (from $NaSeO_3$). This ratio of Se(VI) to Se(IV) was representative of typical agricultural drain waters which were drained into Kesterson Reservoir. Analysis of Se in ponded waters and soil waters were routinely performed by hydride-generation atomic absorption spectrometry (Weres et al., 1989b). Occasional total solution Se analyses were also performed by inductively coupled plasma spectrometry. Comparisons between these two spectrometric methods, along with XAS results showed that Se(VI) and Se(IV) were the only aqueous Se species occurring at significant concentrations in these experiments. The major ion composition of the laboratory solution was designed to resembled that of the agricultural drain waters as well, dominated by Na^+, SO_4^{2-}, and Cl^-, and was similar to that reported in Poister and Tokunaga (1992). Ponding with seleniferous water was established by dispensing 550 ml of solution over the soil surface over about a 1 minute interval. This volume corresponded to an equivalent water column 120 mm deep. Upon dispensing the solutions, each column contained an initial ponding depth of 90 ±3 mm, indicating that the soil profiles were near saturation (101 ±10 %). A small amount of trapped air was expected to persist at the bottoms of these soil columns because of the flooding procedure and the sealed bottom boundary.

Ponded waters in columns were disturbed as little as possible, in an attempt to discern the development of gradients in Se concentrations and speciation within the static water columns. Samples of ponded waters were collected at two depths; one at about 7 mm below the water-air interface, and a second sample at about 7 mm above the sediment-water interface, via 1 mm I.D. polyethylene tubing attached to a syringe. Solution sample masses were kept small, ranging from 50 to 200 mg, in order to minimize disturbances to columns. Pond water sampling intervals ranged from daily (initially), up to 14 days towards the end of the ponded phase. Sediment pore water samples were also collected during the 48 to 51 day ponding period. Under ponded conditions, the empty samplers were sealed with initial pressures at or slightly above ($\Delta P < +1.0$ kPa) local atmospheric pressure in order to keep sample volumes small. Collected pore water samples were in the range of 1 to 3 g. Dilutions of both the pond and pore water samples were performed gravimetrically (1 mg resolution) prior to analyses.

Methylated Se will not be considered in this study since the alkaline H_2O_2 traps for collection of gaseous Se (Weres et al., 1989b) included in this experiment (Fig. 4.1), showed that less than 0.5% of the total Se inventory was volatilized (Tokunaga et al., submitted 1995). The experiment was terminated after about 50 days of ponding. Depth profiles of total Se were measured by energy-dispersive x-ray fluorescence (Giauque et al., 1976). Surface soil Se was

analyzed by XAS at Stanford Synchrotron Radiation Laboratory at several times at the beginning of ponding (0 to 4 days), and at the end of the experiment (Pickering et al. 1994; Pickering et al. submitted 1994; Tokunaga, submitted 1995). A sample of surface sediment from the C4 column was also analyzed for Se with the SXRFM at the National Synchrotron Light Source in order to obtain depth profiles of total Se with high spatial resolution (0.25 mm vertical step sizes).

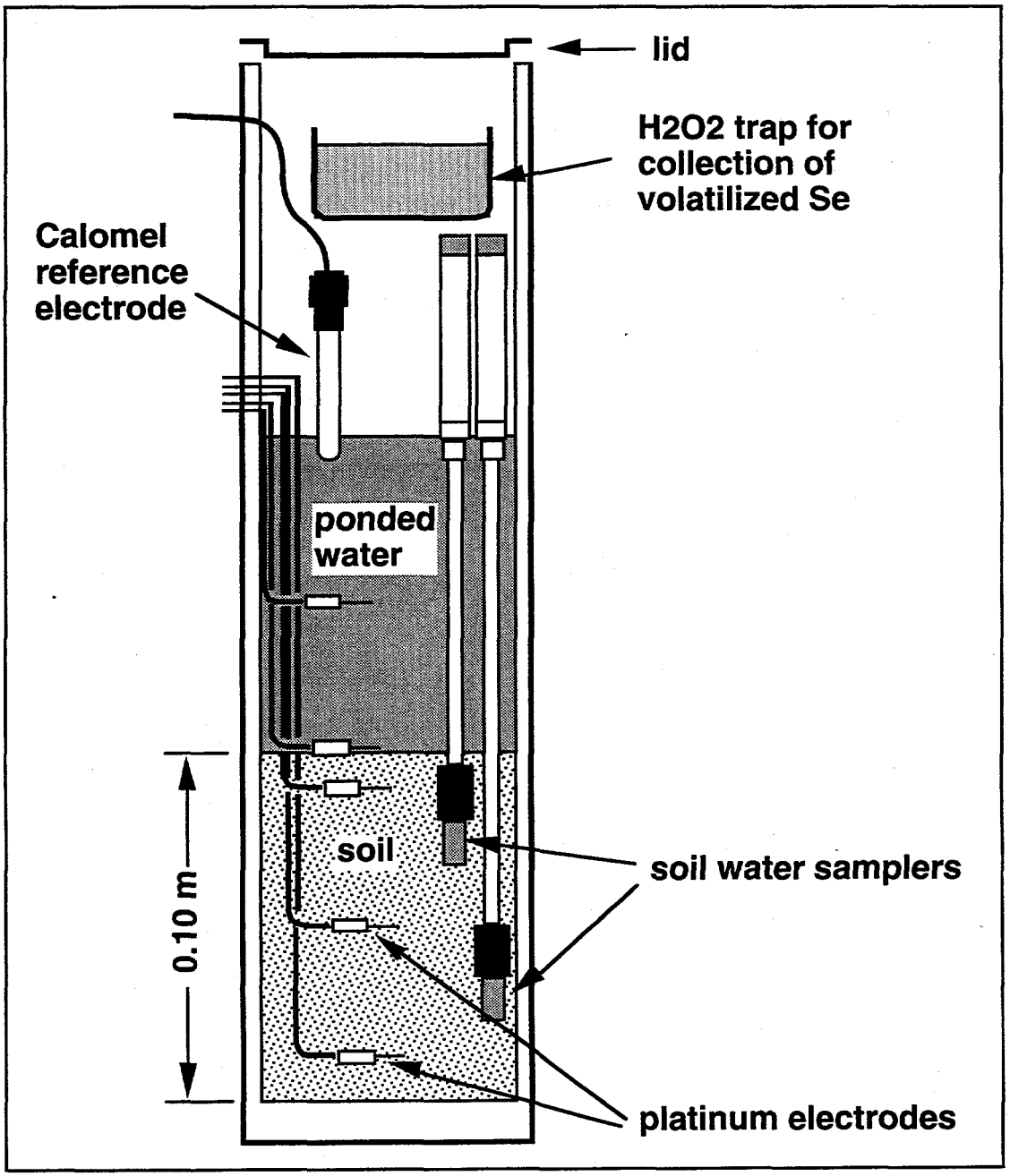

Figure 4.1. Experimental column design.

4.3 Results and Discussion

4.3.1 Experimental

Similar time trends in surface water Se composition were observed within the duplicate columns. Considerably different trends in surface water Se concentrations were observed between columns without and with surface soil organic matter additions. Since only one column from each of the two treatments was instrumented with pore water samplers, only these instrumented systems (C3 and C4) will be considered in detail. Depth profiles combining data on Se(VI) in ponded waters and in sediment pore waters for several different times are shown in Fig. 4.2a (unamended C3) and Fig. 4.3a (organic matter amended C4). Depth profiles for aqueous phase Se(IV) for these same times are presented in Figures 4.2b and 4.3b. In both systems, surface water Se(VI) concentrations declined over time, while Se(IV) concentrations increased for at least some portion of the ponded period. Net decreases in total dissolved Se occurred in surface waters of both systems, with more rapid declines in systems with organic matter added to surface soils. No significant gradients in concentrations of the Se species were detectable within the ponded water columns. This observation supports describing the ponded waters as well-mixed volumes. Furthermore, while the sampling tube was placed vertically downwards to about 7 mm above the pool-sediment interface during collections, it appears reasonable that the sampled volume extends 1 to 2 mm closer towards the sediment. Thus, the diffusion boundary layer above the sediment, over which significant gradients in Se concentrations could occur, is probably less than 7 mm in thickness.

More rapid rates of Se reduction occur within the sediments than in the ponded waters. The XAS study showed Se(VI) reduced sequentially from Se(IV) to Se(0) during ponding, with Se(0) occurring as early as 3.8 days after flooding in the amended sediments (Pickering et al., 1994; Pickering et al., submitted 1994; Tokunaga et al., submitted 1995). By the end of the experiment, 25% of the original Se in the surface waters was transported into unamended sediments. For systems amended with organic matter, 95% of the Se originally in ponded waters was transported into the sediments. Accumulations of Se within sediments were largely confined to the near-surface regions in each type of column (Figure 4.4a and 4.4b). The onset of reducing conditions is expected to occur earlier in surface sediments than in deeper sediments of both types of systems because of some soil air displacement and entrapment in the column bottoms. This process would provide a residual supply of O_2 in the deeper portions of the columns. In addition, columns with surface soils amended with readily reducible organic carbon would be expected to become anaerobic even more rapidly. Reducing conditions in surface sediment would promote Se(VI) reduction to Se(IV) and to Se(0), allowing a net accumulation of

insoluble Se species. The XAS study (Pickering et al., 1994; Pickering et al., submitted 1994; Tokunaga et

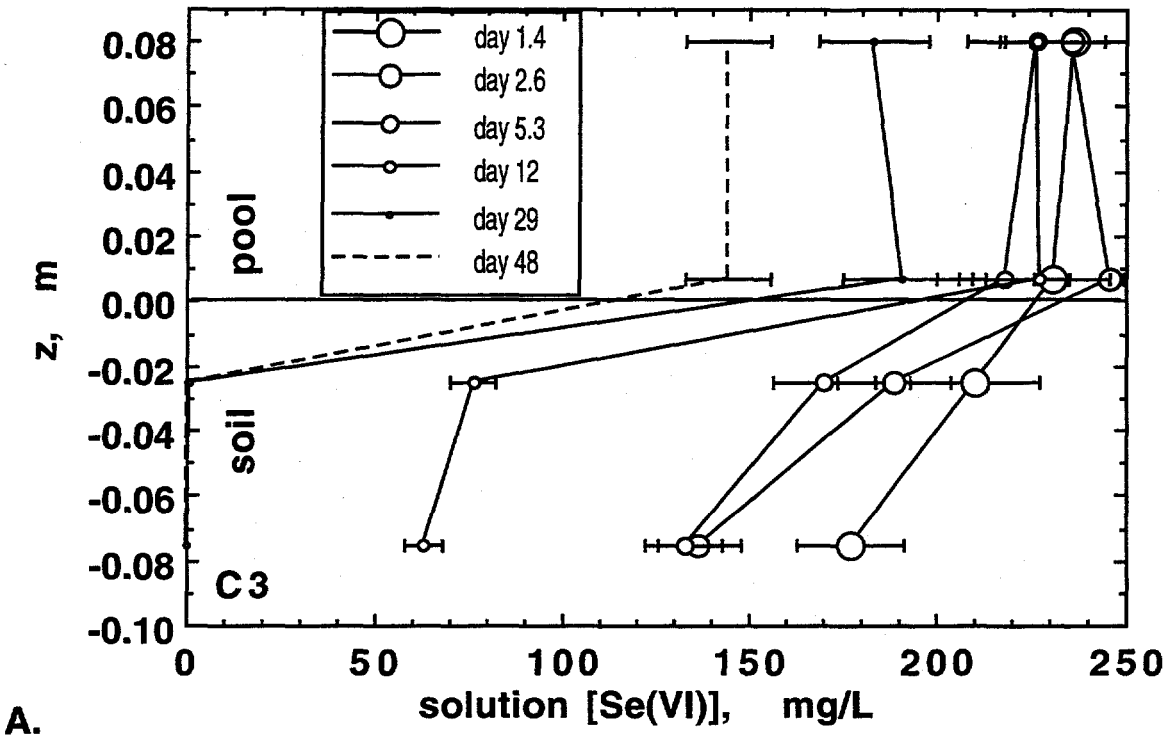

A.

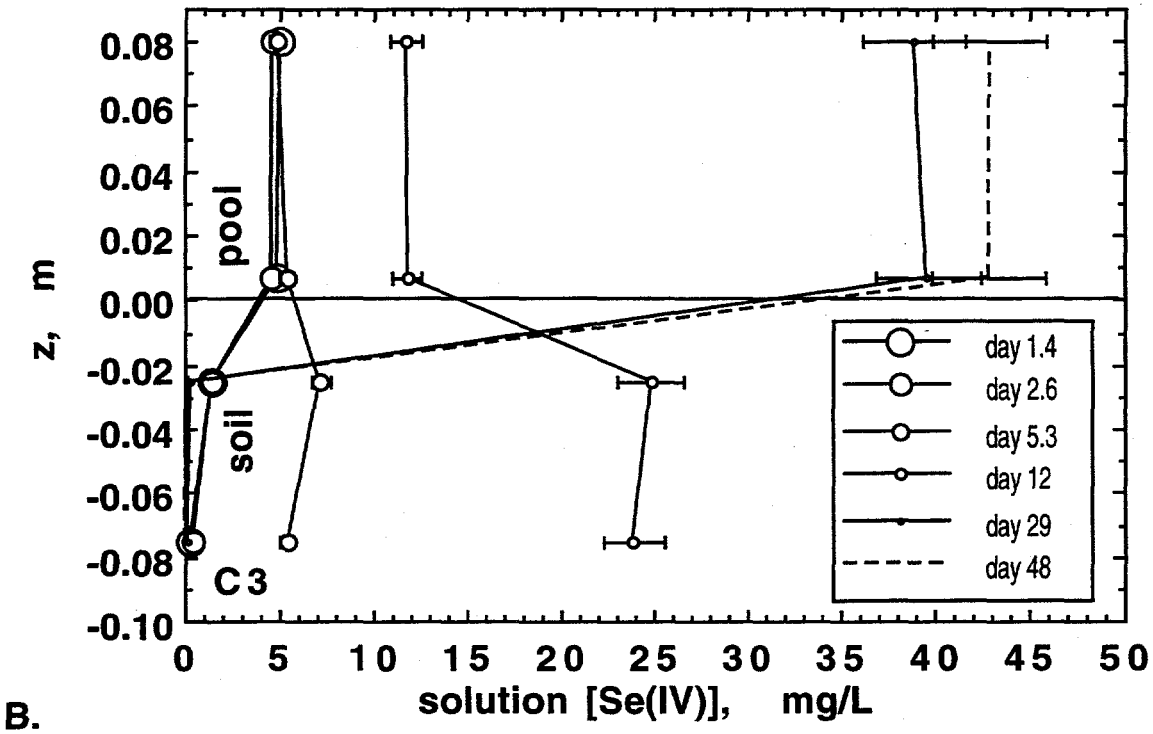

B.

Figure 4.2. Depth profiles of total dissolved Se(VI) (**A**), and Se(IV) (**B**) in unamended columns, combining ponded waters and sediment pore waters.

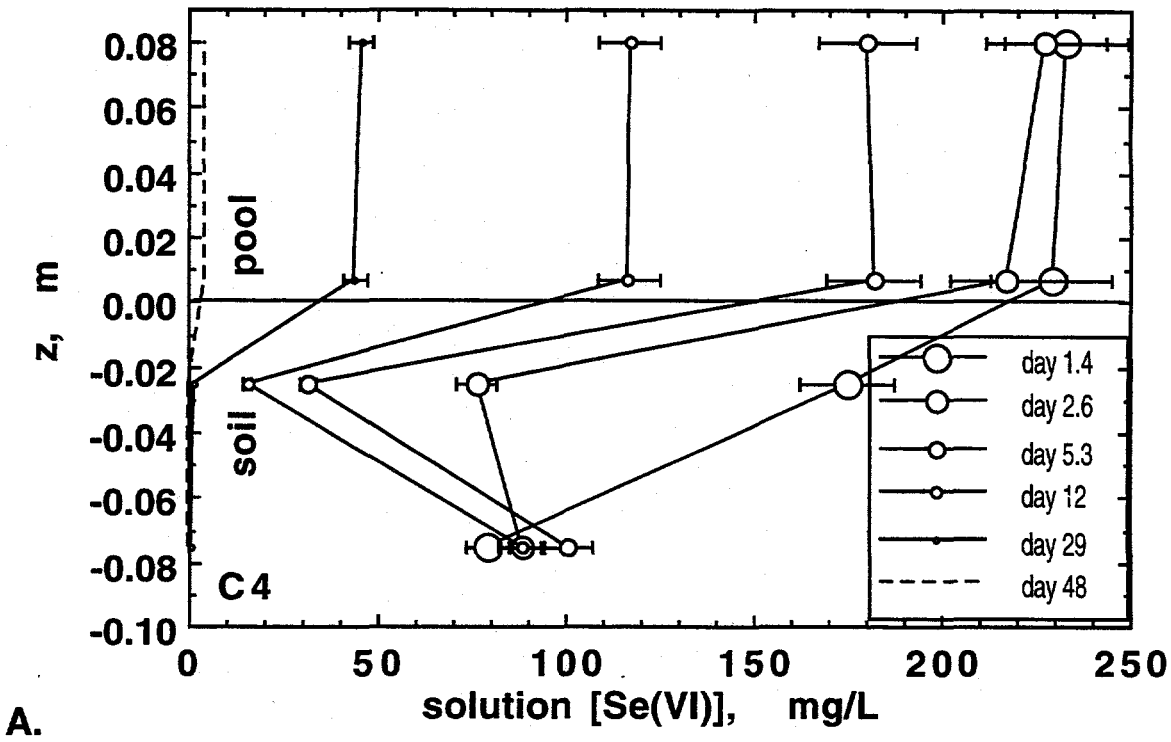

A.

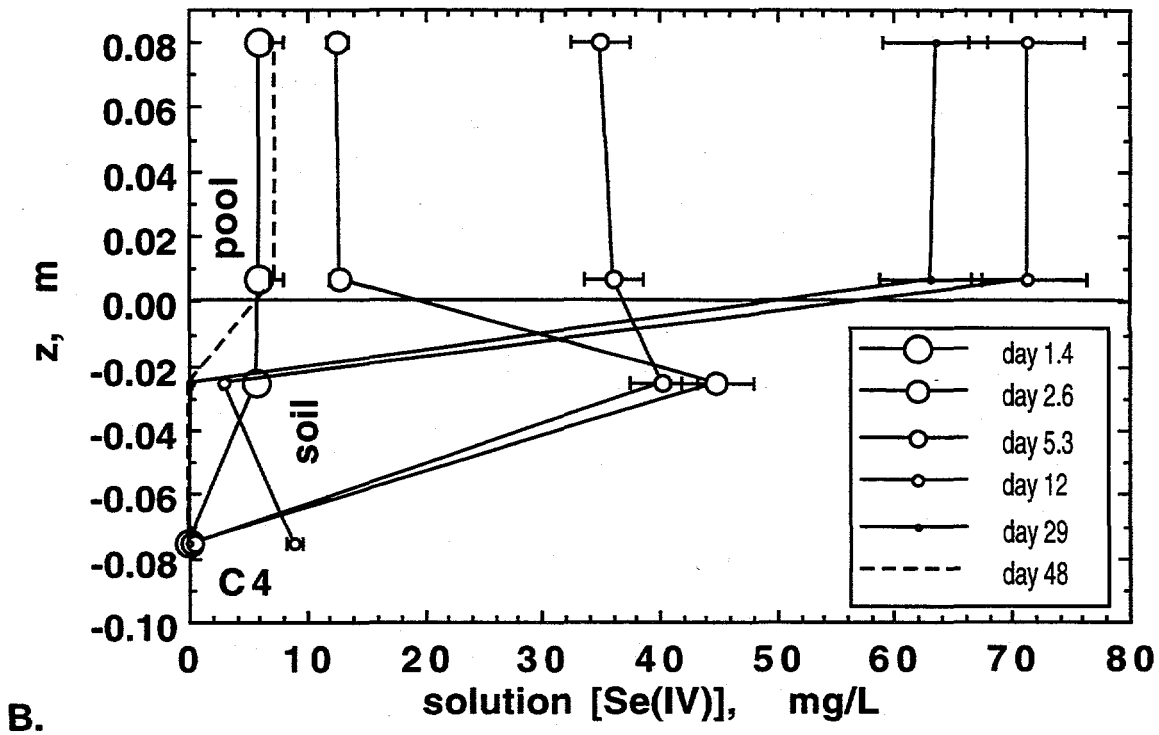

B.

Figure 4.3. Depth profiles of total dissolved Se(VI) (A), and Se(IV) (B) in columns amended with organic matter, combining ponded waters and sediment pore waters.

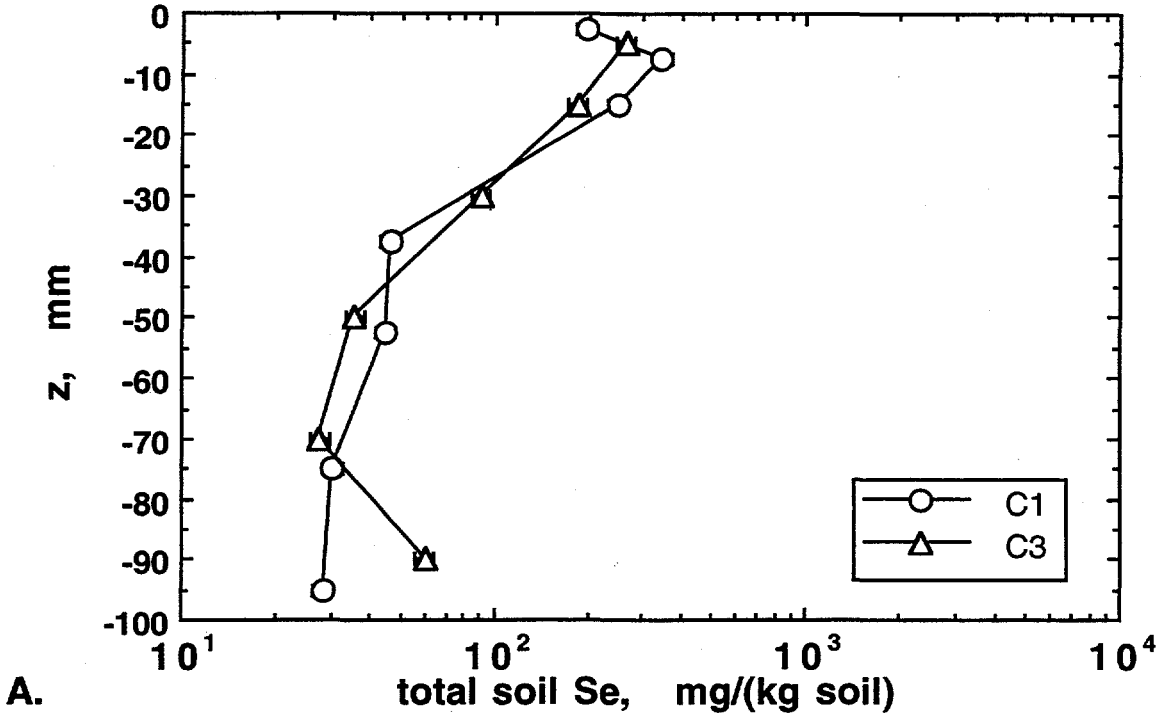

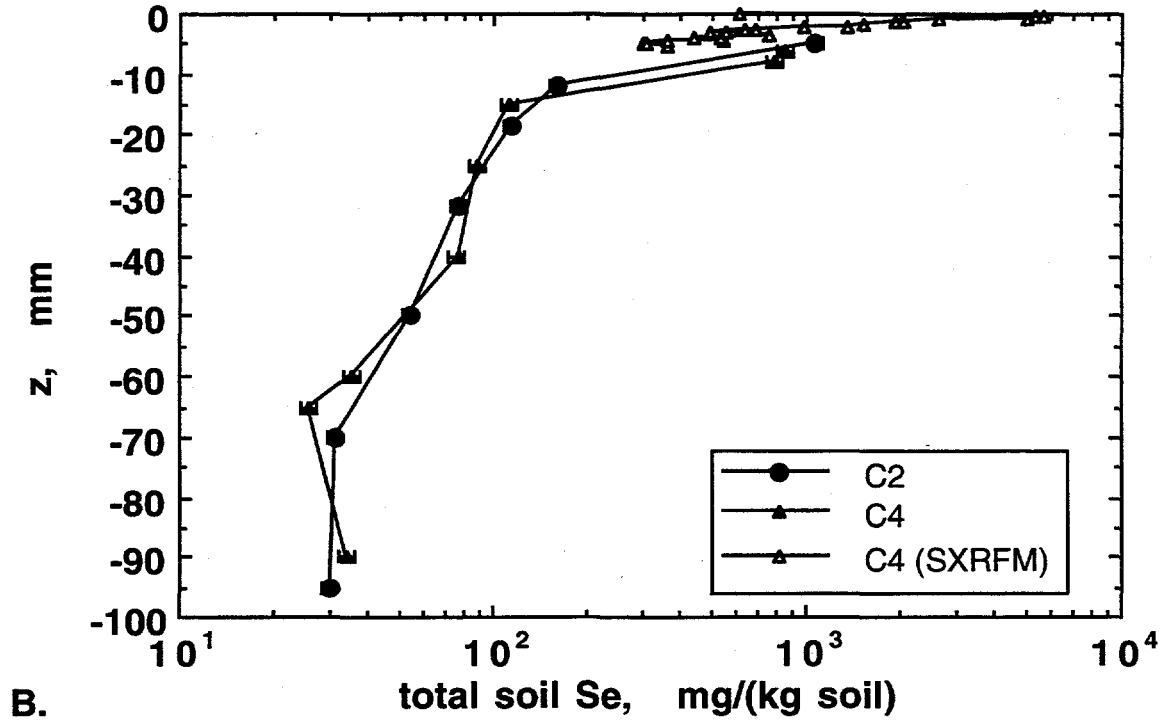

Figure 4.4. Total Se concentration profiles in sediment samples analyzed at the end of the ponding experiment: (a) unamended sediments, and (b) sediments amended with organic matter within the upper 30 mm region. Higher spatial resolution Se analyses in a surface sample from the amended soil (b) were obtained with SXRFM.

al., submitted 1995) provided direct evidence for transformations of Se(VI) to Se(IV), and finally to Se(0). From Figure 4.4b, it appears that the organic matter amended sediments become extremely reducing at the interface with ponded waters. The procedure used to sample the columns permitted only relatively coarse spatial resolution (5 to 10 mm along the vertical column) in the conventional XRF analyses for Se. In view of the highly skewed distribution of Se in the coarser-scale XRF analyses of the organic matter amended sediment, a higher resolution map of a surface subsample was obtained with SXRFM. The SXRFM map was performed over a 2 mm wide, 5 mm high vertical slice of the surface sediment. The vertical and horizontal steps were taken in 0.25 mm and 0.50 mm increments respectively. Horizontally averaged (over the 2 mm width) total Se profiles are included in Figure 4.4b. These data show that the highest accumulations of Se occur within the surface 1 mm of this column, suggestive of rapid reduction of Se to Se(0). The two-dimensional SXRFM map of Se concentrations in this surface sediment is shown in Figure 4.5. Heterogeneities in total Se concentrations along the horizontal direction are also evident in this representation, although these are not as varied as the vertical heterogeneities.

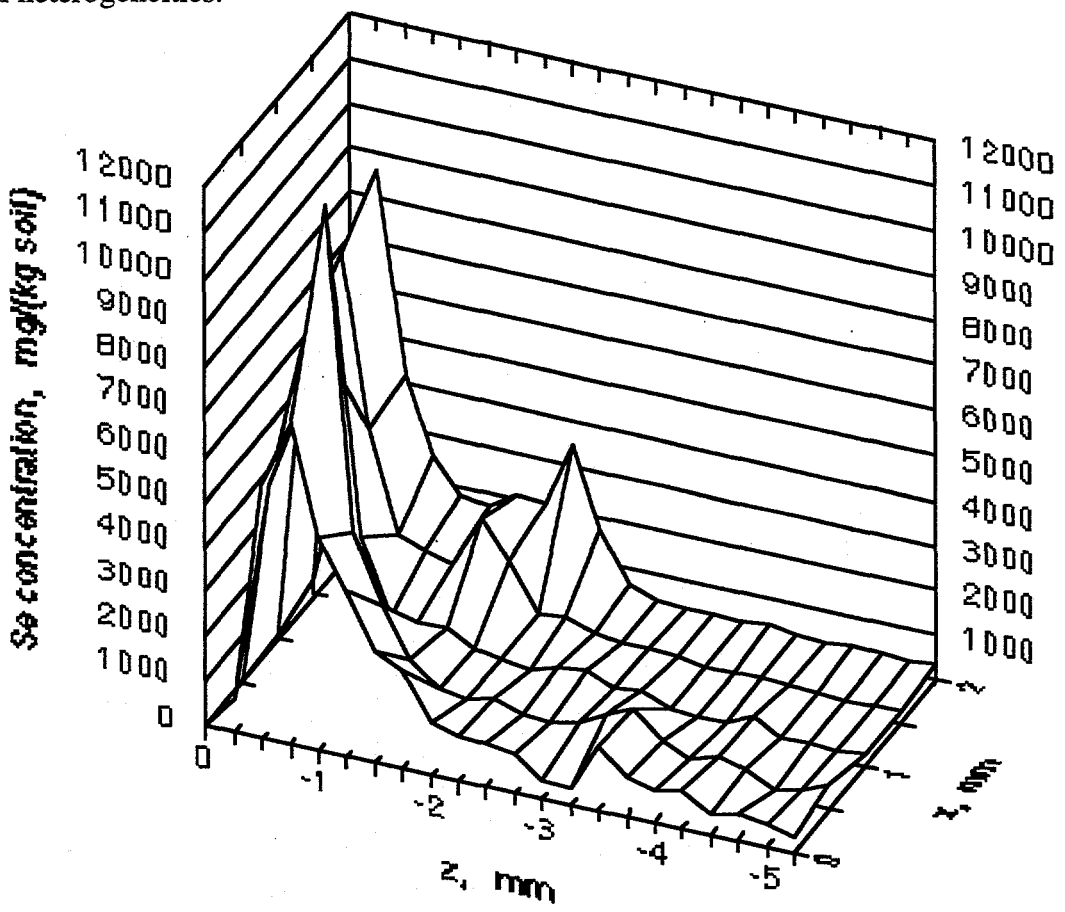

•Figure 4.5. SXRFM map of Se within a surface sediment sample from the amended column.

4.3.2 Transport Model

The conceptual model used to account for temporal variations in surface water Se concentrations is shown in Figure 4.6. Based upon previous XAS results, only Se(VI), Se(IV), and Se(0) are included in the systems under consideration. Measurements from the H_2O_2 traps indicated that volatile losses of Se accounted for less than 0.5% of the total Se inventory. Based on lack of measurable gradients in Se concentrations within water columns, the surface waters are approximated as a well-mixed compartments. This approximation is likely to be reasonable in shallow vernal pool environments.

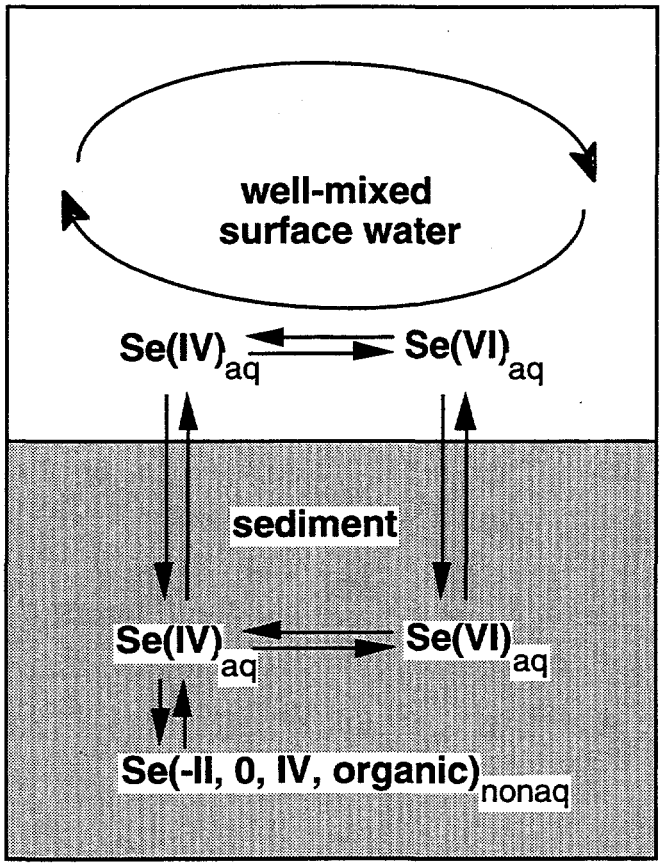

Figure 4.6. Conceptual model for Se cycling within the pond-sediment system.

Information on Se concentrations in sediment pore waters from the shallowest sampler (at the 25 mm depth) in each column was used to predict Se(VI) and Se(IV) exchanges between sediments and ponded waters. These exchanges were modeled with mass transfer coefficients (Cussler, 1984) rather than with diffusion coefficients because the former approach is not mechanism-specific. We later evaluate the adequacy of diffusive transport across a thin boundary layer in accounting for pool-sediment Se exchanges. In the present approach, the mass

transfer coefficient for valence state i (equal to VI or IV) is denoted by $k_{Se(i)}$ ($L\ T^{-1}$). For a pool of constant volume V_p, the mass transfer relation across a pool-sediment interface is given by

$$V_p \frac{\partial [Se(i)]_p}{\partial t} = -Ak_{Se(i)} \left\{ [Se(i)]_p - [Se(i)]_s \right\} \quad (1)$$

where A is the macroscopic surface area of the pond-sediment interface, and the subscripts p and s denote pond and sediment respectively. Concentrations in both pond waters and sediment pore waters are referenced to a unit volume of the aqueous phase. The above equation ignores changes in concentrations of Se(VI) and Se(IV) due to reactions. When reactions within ponded waters are dominated by Se(VI) reduction, and when they are treated as being apparent first-order with respect to Se(VI) concentration, then

$$\frac{\partial [Se(i)]_p}{\partial t} = -\frac{k_{Se(i)}}{L_p} \left\{ [Se(i)]_p - [Se(i)]_s \right\} \pm k_r [Se(VI)]_p \quad , \quad (2)$$

where L_p denotes the height of the ponded water column, and k_r is the apparent first order Se(VI) reduction rate constant. Given initial concentrations of Se(VI) and Se(IV) in the pool waters $[Se(i)]_{p,0}$, and time-dependent concentrations of these species in sediment waters, Eq. (2) was numerically integrated to model time-dependent Se(VI) and Se(IV) concentrations

$$[Se(i)]_{p,t} = [Se(i)]_{p,0} + \int_0^t \frac{-k_{Se(i)}}{L_p} \left\{ [Se(i)]_p - [Se(i)]_s \right\} \pm k_r [Se(VI)]_p dt \quad . \quad (3)$$

For this purpose, the sparse set of data on sediment pore water concentrations (collected at 1 to 11 day intervals) was enhanced via linear interpolation to provide more continuous sediment concentration versus time values (0.5 day intervals). Values of $k_{Se(i)}$ and k_r were taken as constant for a given simulation, and adjusted to provide the best overall fits to data. Although separate $k_{Se(i)}$ could be applied for Se(IV) and Se(VI) transfers within a given system, only one value was used in order to minimize the number of adjustable parameters. If the Se mass transfers could be accounted for solely by diffusion through a boundary layer, the above equations would have the same form. However, $k_{Se(i)}$ would be replaced by D_e/L_B, where D_e and L_B are the pond-sediment boundary region effective diffusivity and diffusion length respectively.

Before proceeding to the modeled results, it is warranted to consider some important limitations associated with this procedure. The approach taken amounts to curve-fitting with a

minimum number of parameters (2 per system, 3 if separate $k_{Se(i)}$ values were used for Se(IV) and Se(VI) mass transfers). While these parameters are assigned constant values within a given simulation, the factors which they attempt to represent are likely to be time-dependent. The $k_{Se(i)}$ depend fundamentally upon the effective thickness of the L_B, and on time-dependent reactions (both microbially mediated redox, and exchange at mineral surfaces) which take place within and beyond this boundary region. The k_r is also expected to be time-dependent, especially because of its dependence on microbial population dynamics. On the other hand, use of constant parameters allow for direct comparisons of the average behavior of different systems. In addition, direct comparisons between $k_{Se(i)}$ and D_e/L_B can be made.

In the diffusion-based approach to describing mass transfer between ponded waters and sediments, Se transport is assumed to occur through a diffusion-limited region, described by series resistance (water and water-saturated sediment) diffusivities. Diffusive exchanges are modeled without inclusion of Se reactions (reduction or adsorption) within the boundary layer because of insufficient supporting data. The diffusivities of both SeO_3^{-2} and SeO_4^{-2} in water-saturated sediments were equated with values predicted for SO_4^{-2} diffusivities in saturated porous media. Combining information on sediment porosity f (0.52 in this case) and the diffusivity of sulfate in water $D_{w,SO4}$ (1.0×10^{-9} m^2 s^{-1} = 86 mm^2 d^{-1} at 20° C) with the empirically-based expression for the diffusion coefficient in a sediment

$$D_s = \alpha f D_{w,SO_4} \tag{4}$$

gives D_S = 29 mm^2 d^{-1}, when a typical α value of 0.65 is used. Similar D_S values were reported in the reviewed by Iversen and Jorgensen (1993). The series resistance effective diffusivity through the water-sediment boundary layer, D_e, is

$$D_e = \left(L_w + L_s\right)\left(\frac{L_w}{D_w} + \frac{L_s}{D_s}\right)^{-1} , \tag{5}$$

where L_W and L_S represent diffusion lengths in the water and sediment segments, respectively. L_W is the vertical distance from the sediment-pond interface up to the lowest region of the ponded water which sustains well-mixed solute concentrations. L_S is taken as the distance from the sediment-pond interface downwards to the region in the sediment at which aqueous Se concentrations are equal to those obtained in the shallowest soil water sampler. The sum of these two lengths is defined as the boundary layer thickness, L_B. In the analyses to follow, modeling of time trends for solution Se concentrations in a given system will only permit direct evaluation

of the pond-sediment mass transfer coefficient equal to the quotient D_e/L_B. From Eqs. (4) and (5), we have

$$\frac{D_e}{L_B} = \frac{D_w}{L_w + \left(\frac{L_s}{\alpha f}\right)} \quad . \tag{6}$$

This result will be used later, when magnitudes of L_s are compared for two systems with very different rates of Se removal from ponded waters. As noted previously, (D_e/L_B) will be equated with optimized $k_{Se(i)}$ for this purpose.

The two adjustable parameters, the mass transfer coefficient $k_{Se(i)}$, and the rate constant k_r, were varied in order to determine optimum values for matching measured pool concentrations. Best-fit results for modeling Se(IV) and Se(VI) concentrations in pools over the two sediment types are shown in Figures 4.7a and 4.7b, along with several other trial curves. For these calculations, trial values of $k_{Se(i)}$ ranging from 1.06 to 1.16 mm d^{-1} were initially used. These initial choices were based on the diffusion boundary layer approach. The distance of the center of the shallow pore water sampler below the interface (L_s assigned equal to 25 mm), a range of reasonable lower pool diffusion boundary layer thicknesses (L_w ranging from 7 to 0 mm), and values of other parameters previously introduced through Eq.(4) were combined in Eq.(6) to obtain trial values of $k_{Se(i)}$. Values of $k_{Se(i)}$ were subsequently increased or decreased to obtain better fits with data. In the case of the unamended soil, the $k_{Se(i)}$ which yielded the best fits without using a reduction rate constant were in the range of 0.80 to 0.93 mm d^{-1}. While these fits matched the time-dependence of $[Se(VI)]_p$ quite well, the buildup in $[Se(IV)]_p$ with time was significantly underestimated (Figure 4.7a). Both time trends in $[Se(VI)]_p$ and $[Se(IV)]_p$ were well matched (r^2 equal to 0.957 and 0.960, for Se(IV) and Se(VI) respectively) by setting $k_{Se(i)}$ = 0.80 mm d^{-1}, and by assigning a value of 4 x10^{-3} d^{-1} to k_r. For the system amended with organic matter (Fig. 4.7b), the optimum matches were obtained with k_r = 3 x10^{-2} d^{-1}. Best matches (r^2 equal to 0.894 and 0.986, for Se(IV) and Se(VI) respectively) for both $[Se(VI)]_p$ and $[Se(IV)]_p$ time trends were obtained with $k_{Se(i)}$ = 4.0 mm d^{-1}. Thus, mass transfer of both Se species from ponded waters into sediments occurs 5 times more rapidly in the columns with organic matter amendments added to the sediment surface. The fact that optimum $k_{Se(i)}$ values differed significantly from initial estimates provides an indication that the diffusion boundary layer approach may be inadequate. Note also that Se(VI) reduction within ponded waters occur about 8 times faster in the amended system. The fact that a significantly large k_r was needed to match data in C4 than in C3 shows that other important factors in pool waters differed between these two systems. The plausible factors are higher concentrations of easily reducible organic carbon

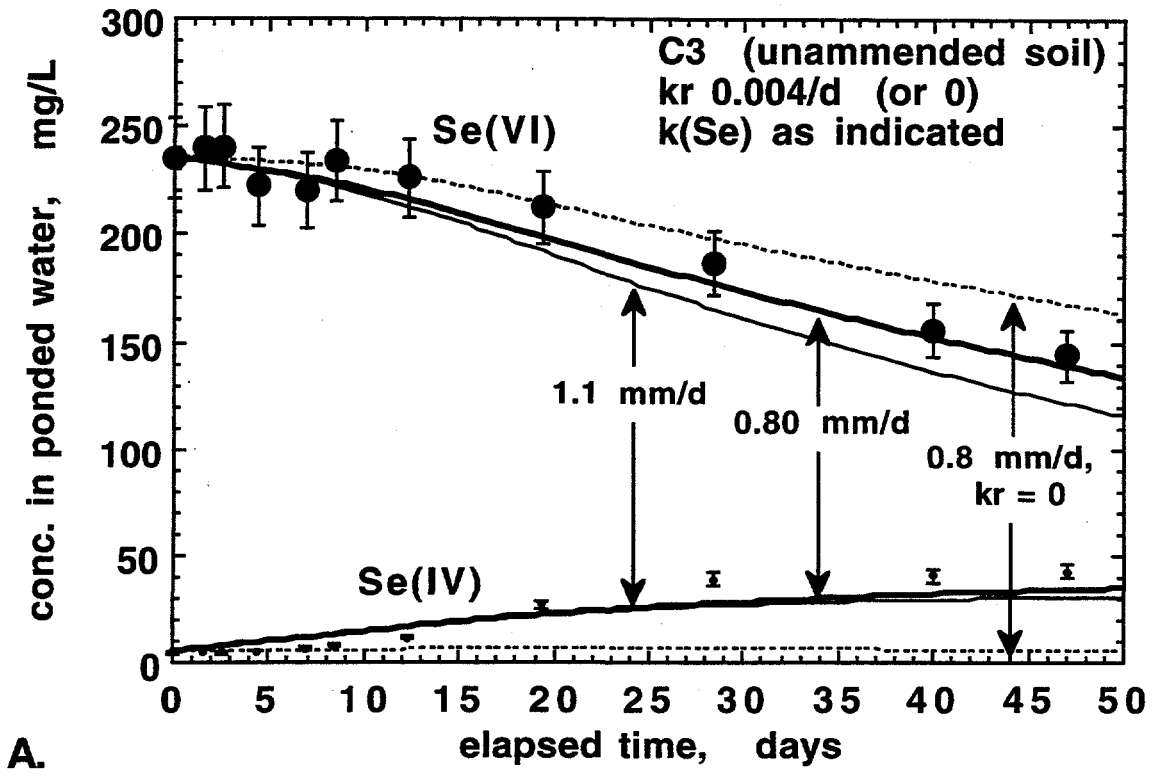

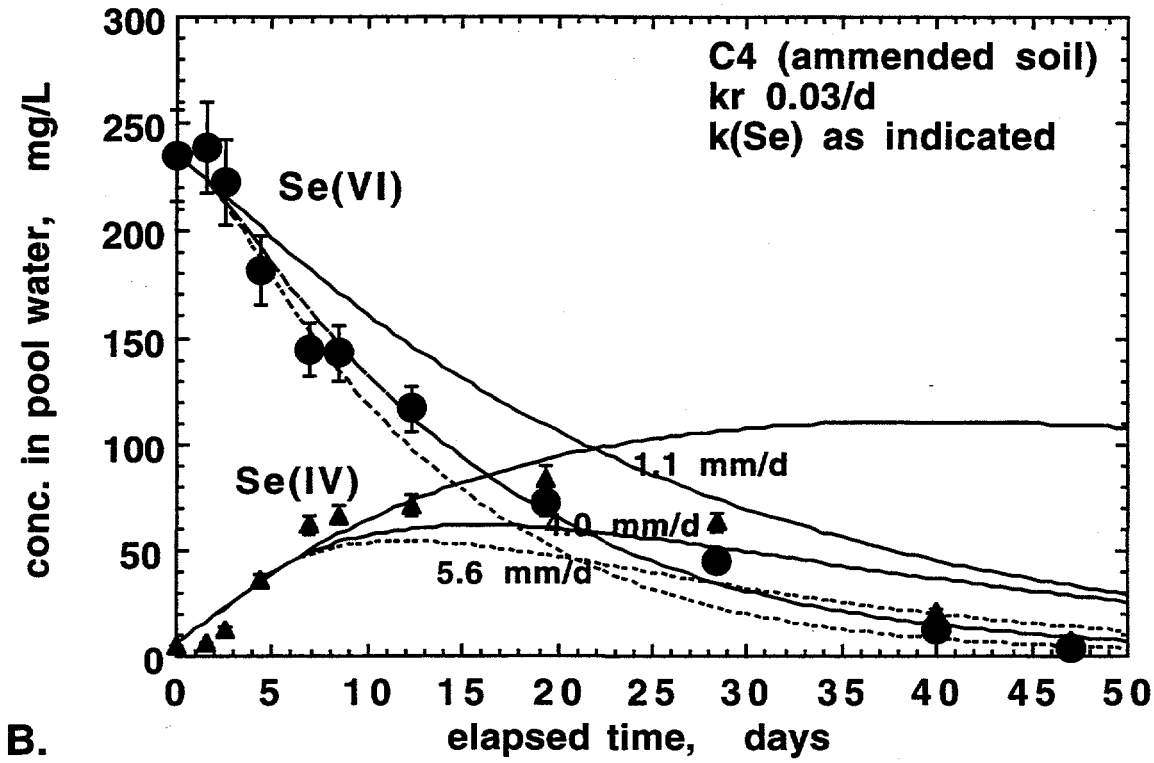

Figure 4.7. Time trends for measured pool water Se(VI) and Se(IV) concentrations (data points) and modeled results (curves) for (**A**) unamended sediments, and (**B**) sediments amended with organic matter.

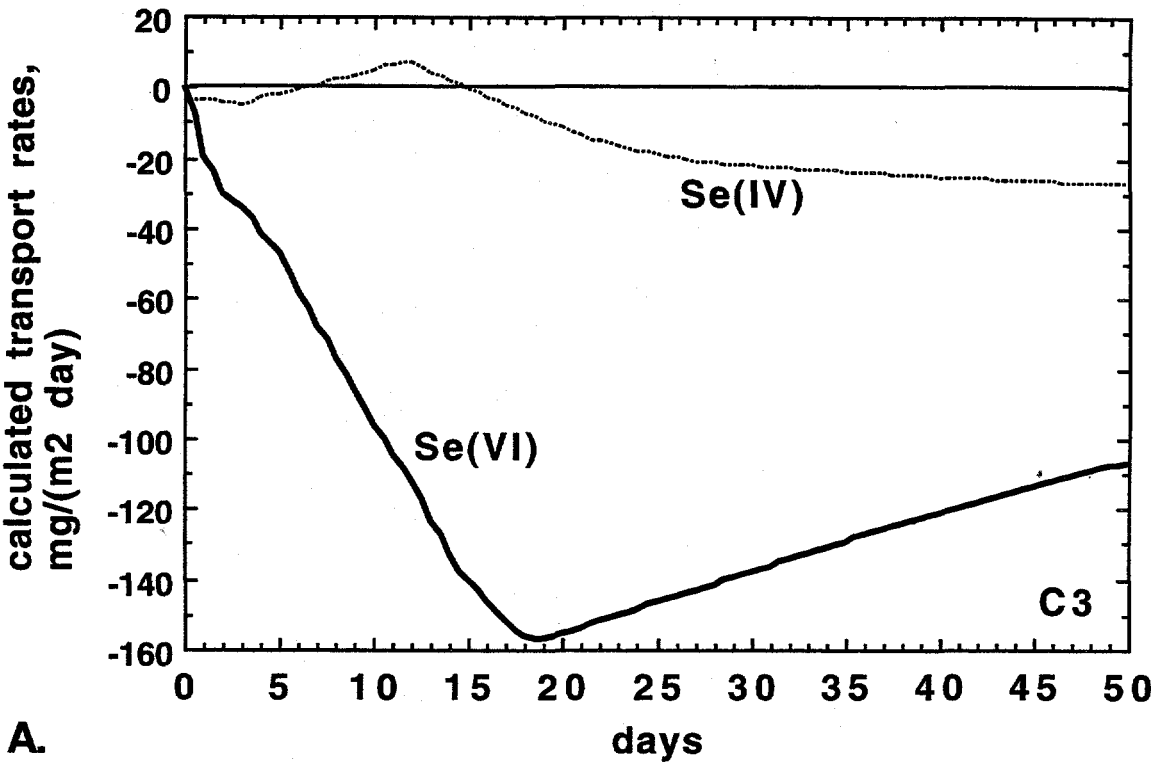

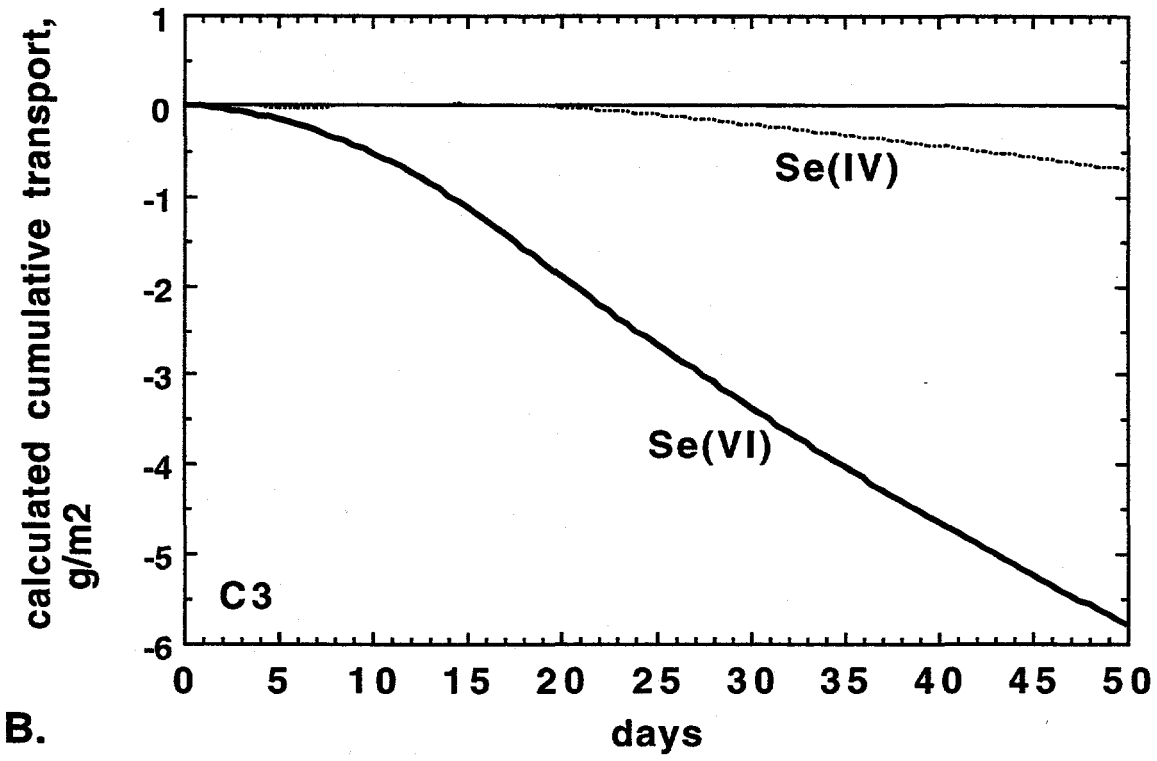

Figure 4.8. Calculated transport rates (A), and cumulative transport (B) of Se(IV) and Se(VI) between ponded waters and unamended sediment.

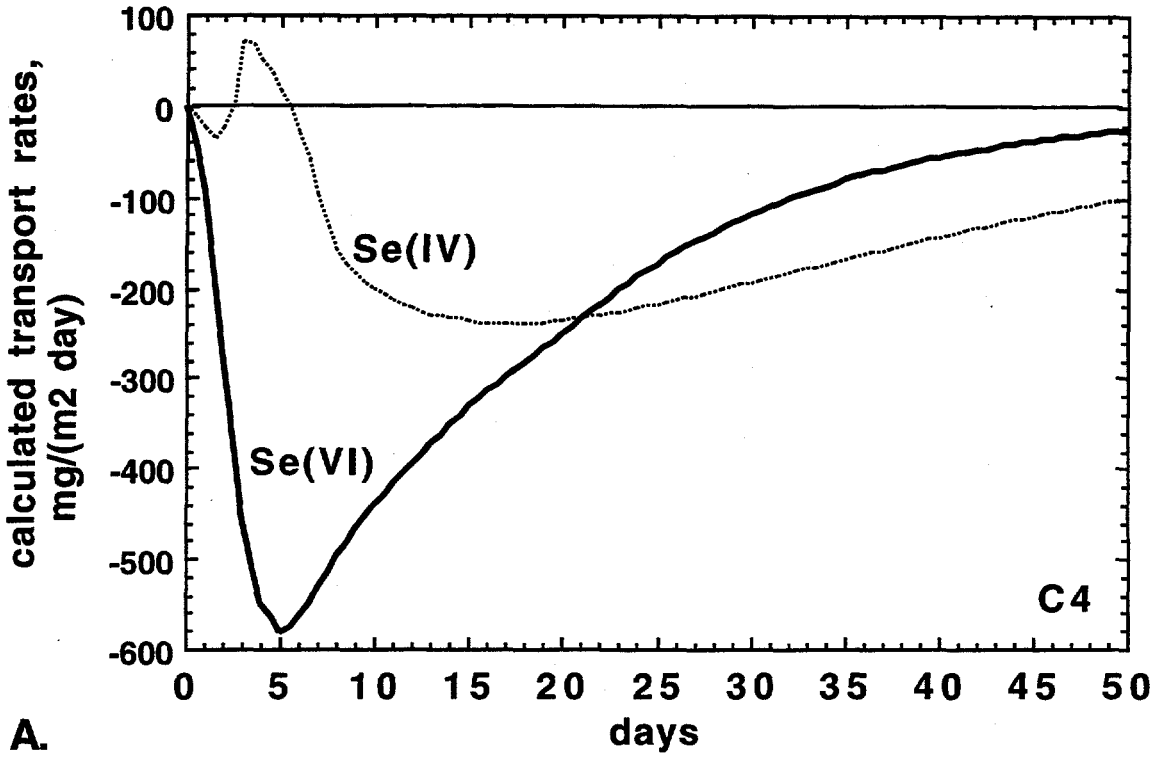

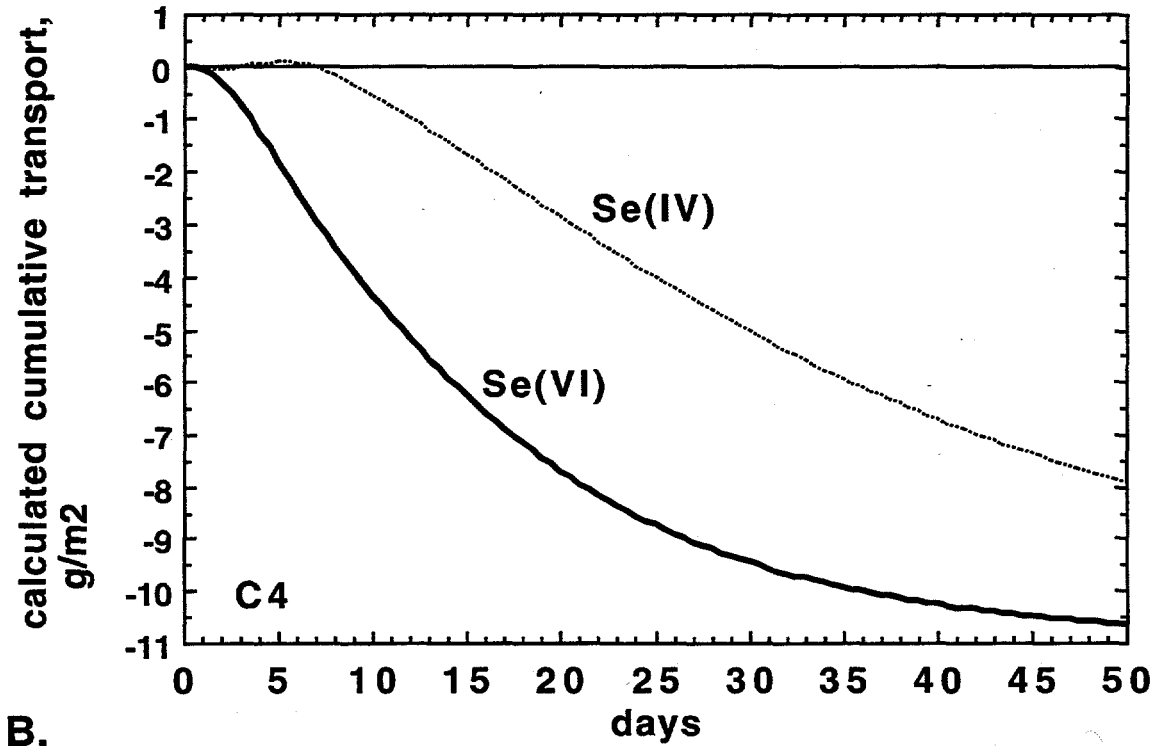

Figure 4.9. Calculated transport rates (**A**), and cumulative transport (**B**), of Se(IV) and Se(VI) between ponded waters and amended sediment.

and of selenium-reducing bacteria in the waters ponded over the amended C4 columns. Diffusive release of organic matter from soils into water columns, the dynamics of microbial growth, and biochemistry of Se reduction are beyond the scope of this study.

The optimized $k_{Se(i)}$ values can be combined with data on gradients of [Se(VI)] and [Se(IV)] at the pond-sediment boundaries to calculated fluxes of these species. Transport rates and cumulative mass transfers are obtained through Eq.(1) and its numerical integration respectively. Results of these calculations for the unamended system show transported dominated by Se(VI) at all times (Fig. 4.8a and 4.8b). In these graphs, values less than zero indicate transport from the surface water into sediment. By the end of the experiment, only 11% of the Se transport into the sediment occurred in the Se(IV) form. A short period of Se(IV) transport back from the unamended sediment pore waters into surface waters is suggested (Fig. 4.8a), but the magnitude of this flux is insignificant. Mass transfer calculations on the amended system show very different behavior (Figure 4.9a and 4.9b). The initial mass transfer rate for Se(VI) into sediments becomes very large within the first 5 days, then gradually diminishes over the remainder of the experiment. A significant transfer of Se(IV) from shallow sediment pore waters back into surface waters is also predicted between days 2 to 6, followed by a long period of Se(IV) transport from surface waters back into sediments (Fig. 4.9a). Transport from sediments back into ponded waters are predicted whenever concentrations of a particular species are higher in shallow pore waters than in the pond. The fact that such behavior is predicted only for Se(IV) results from more rapid Se(VI) reduction in sediments than in ponded waters. Calculations also indicate that about 43% of the Se mass transfer into the amended sediment occurred through Se(IV) transport (Figure 4.9b).

The feasibility of accounting for the pond-sediment mass transfer solely by diffusion through a boundary layer was tested by assigning the optimized values of $k_{Se(i)}$ to D_e/L_B for each system. Thus, the unamended and amended columns have D_e/L_B values of 0.80 and 4.0 mm d^{-1}, respectively. In order to test the reasonableness of a diffusion boundary model for exchanges between ponded waters and shallow sediments, it will be useful to determine the surface sediment diffusion length L_s. Although the shallowest soil water samplers are centered at 25 mm below the interface, it is conceivable that the sampled solution chemistry is representative of a different or wider depth range. Together with known or approximate values of D_w, α, and f, we have two equations (in the form of Eq.(6)) with four unknowns (the L_w and L_s for the two cases). It is reasonable to equate the L_w in the unamended system to that in the amended system. Using previously noted values, this leads to L_s(unamended) = L_s (amended) + 29 mm. The physical constraint that the diffusion boundary layer in the ponded waters must occur below the deepest point of pool sampling requires that $0 < L_w < 7$ mm. This in turn leads to the conclusion that L_s(unamended) = 35 ±1 mm, and L_s(amended) = 6 ±1 mm. The diffusion boundary layer model

thus leads to calculated values of L_S which are inconsistent with the location of the shallow pore water samplers.

In this simple diffusion boundary layer model the region within L_S (and for that matter, within L_B) serves only to transport mass from one region into another, and does not allow for appreciable mass accumulation. However, such a conceptualization is clearly inconsistent with data on the vertical distribution of Se within these columns (Fig. 4.4b and Fig. 4.5). The bulk soil analyses by conventional XRF showed that most of the Se was concentrated within the upper 30 mm of the C3 sediment, and within the upper 10 mm in the C4 sediment. Therefore, the successful fits achieved with the mass transfer coefficients do not result from diffusive transport across the region over which aqueous phase concentration gradients were measured. Instead, Se immobilization within this zone was proportional to these concentration gradients. XAS showed that insoluble Se(0) accounts for more than 90% of the Se in this zone (Pickering et al. 1994; Pickering et al. submitted 1994; Tokunaga et al., submitted 1995). Higher resolution analyses by SXRFM on a C4 sediment sample showed maximum Se reduction and accumulation within less than 1 mm of the interface with ponded waters. These data collectively show that the Se reduction and accumulation within the short distance (25 mm) between the sediment surfaces and the shallowest pore water samplers accounts for most of the Se removed from the ponded waters, and that large concentration gradients occur in this boundary region.

Comparisons of data and model results from these two types of columns show that the depths associated with Se reduction and diffusion-limited transport within sediments of shallow aquatic systems can strongly influence trends in surface water quality. These findings can be useful in understanding trends in ephemeral pool water quality in trace element-contaminated environments. The extremely large gradients in Se, and the reduction of Se within this short boundary region show that much higher spatial resolution in Se concentrations and speciation are required in order to support mechanistic transport models of these systems. When such high spatial resolution is necessary, the direct, nondestructive approach of micro-XANES becomes attractive. Recently, investigations have been initiated to apply micro-XANES to real-time tracking of redox-dependent transport and reactions of Se and Cr in sediment systems (Sutton et al., 1994; Tokunaga et al, 1994c). Encouraging results have been obtained in these feasibility studies, and current research plans include real-time micro-XANES applications to pond-sediment interfaces.

5.0 Pond 2 Pilot Scale Microbial Volatilization Study: Vadose Zone Monitoring

Peter Zawislanski
Earth Sciences Division
Lawrence Berkeley Laboratory

Microbial volatilization is a potential remedial measure to decrease the selenium inventory at Kesterson Reservoir. Past studies in both the field and the laboratory suggest that a significant percentage of the selenium inventory may be removed in this fashion. The objectives of this study include the quantification of selenium losses and a test of a pilot-scale design which in the future may be used in other parts of the Reservoir.

In 1989, the site for this study was chosen in the northern end of Pond 2, an area which was very frequently flooded during the operation of the Reservoir and supported primarily cattail vegetation. Preliminary soil sampling in this plot in November 1989 revealed some of the highest Se concentrations in the Reservoir: mean [Se] in the top 15 cm (5 samples) was 291 ppm; in the 15 to 30 cm interval it was 27.3 ppm. Furthermore, the same soil intervals were found to be less saline than average (1:10 soil:water extract electrical conductivity normalized to field water content ranged from 23 dS/m to 69 dS/m). In preparing this plot for the study, cattail remains on the soil surface were incorporated in 1990 into the top 20 cm or so of soil by repeated disking and rototilling. The plot was then divided into four subplots, each being reserved for a particular treatment: irrigation only (I), irrigation and disking (rototilling) (ID), disking (rototilling) only (D), and control or no treatment (C) (Fig. 5.1). An 11.6 meter buffer zone was set up between the irrigated and non-irrigated plots in order to prevent irrigation water from falling onto the disked plot. Losses of selenium in the soil are being monitored by annual sampling along selected transects and in randomly selected subplots as well as by direct measurement through charcoal trapping of dimethylselenide (UC Davis). Monitoring of the vadose zone for potential short-term and long-term leaching of selenium deeper into the profile is being conducted. In order to determine the amount of near-surface selenium lost to volatilization, selenium displaced by infiltrating water must be quantified. These efforts aid in constructing a selenium mass balance in the vadose zone and estimating selenium losses due to volatilization. This report describes the results of soil and soil-water sampling as well as monitoring of the moisture regime in the soil profile. An overview of plot management, sampling schemes, and groundwater table fluctuations can be found in LBL's December 1992 Annual Report (Benson et. al., 1992).

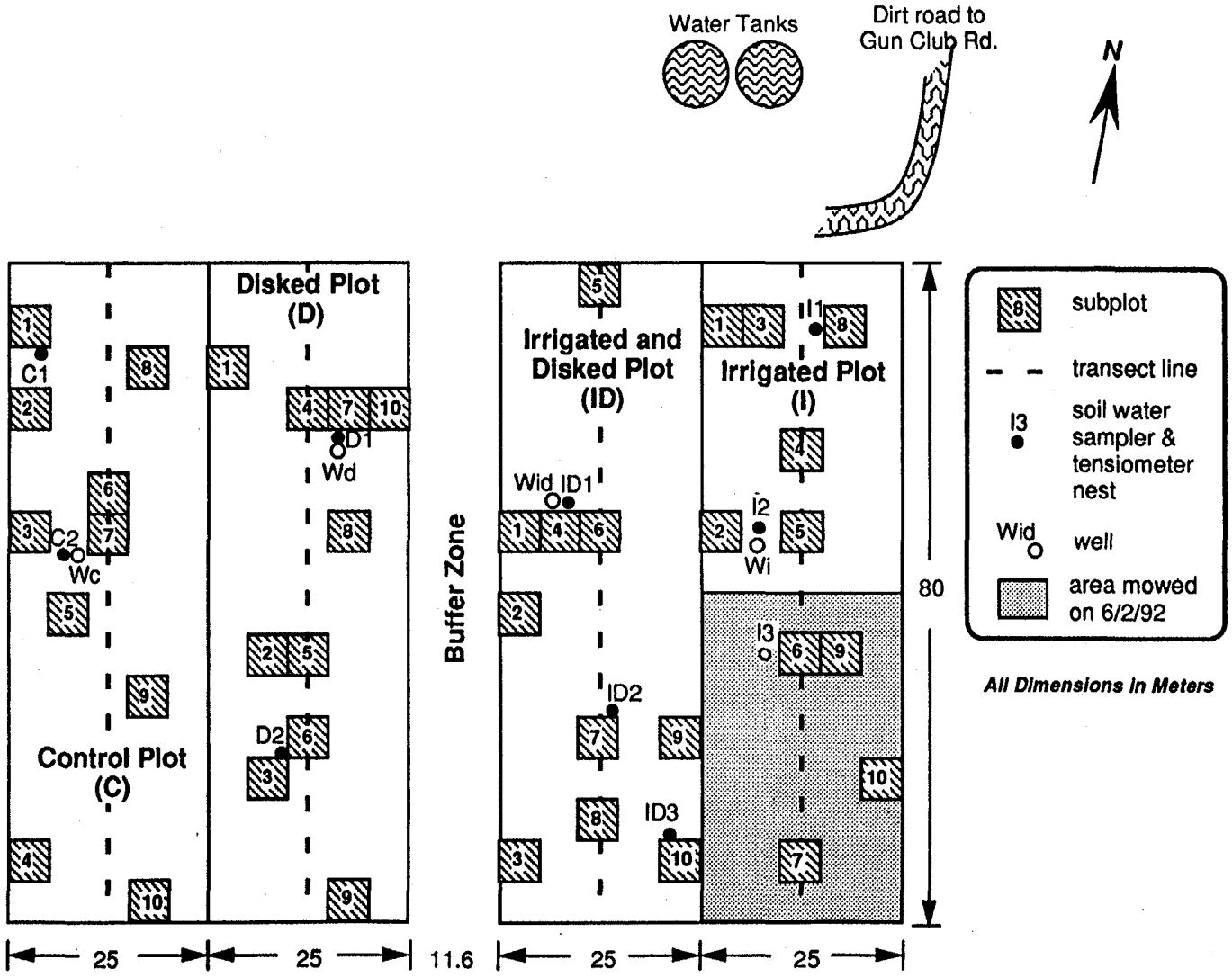

Fig. 5.1 Pond 2 (Pilot Scale) Volatilization Site (P2VS).

5.1 Moisture and Solute Monitoring

The design and operation of the vadose zone monitoring system are described in Benson et. al. (1992). General long-term trends in soil moisture content are shown in Fig. 5.2 and 5.3. These data are based on neutron probe readings obtained in PVC wells and integrated over a depth of 2.1 m. Moisture content is inversely proportional to the degree of vegetation within the plot. As there is no vegetation in the rototilled treatments (ID and D), and the soil is mulched through this process, evapotranspiration is minimized and the soil profile retains moisture throughout the year. Conversely, plants in the non-rototilled treatments remove water via transpiration, resulting in a very dry soil profile throughout most of the year. All treatments are affected by winter and spring rainfall, which in the case of treatment I can result in as much as a tripling of moisture content. The vast and rapid changes in moisture content following major rainfall events have great significance in terms of solute transport into the soil profile. Changes can occur over relatively short periods of time. For example, moisture content before and after the major storms of 1991 and 1992 is shown in Fig. 5.4 through 5.7. Clearly, the greatest changes occurred in treatment I (as represented by nest I2). Not only did the moisture content increase most significantly in this treatment, but rainwater infiltrated as deep as 1.6 m in March

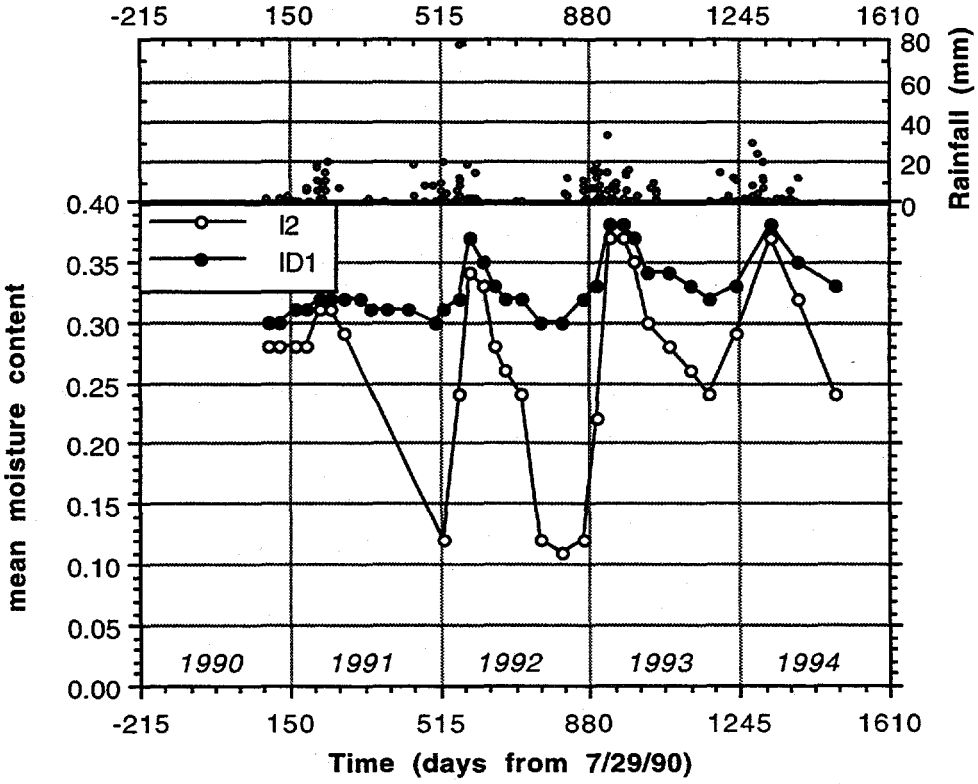

Figure 5.2. Changes in mean moisture content over the top 2.1 m of soil in treatments I and ID, as estimated from neutron probe readings.

of 1992. Conversely, increases in moisture content in treatment ID and D were much smaller and limited to the top 1 m or less in depth. Although moisture content increased significantly in treatment C in March of 1992, because of the relative high position of the water table (about 1 m below the surface), infiltration was limited to the top 1 m. The significance of these findings is that there is potential for transporting soluble Se below the depth to which the soil is sampled, especially in treatment I.

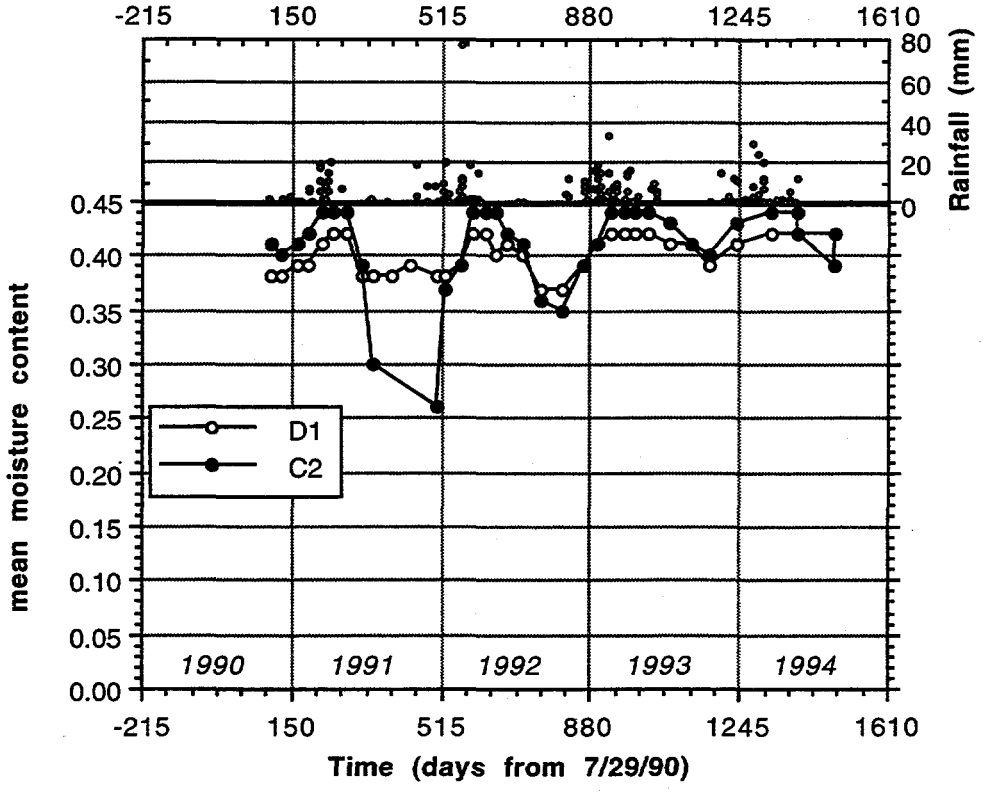

Figure 5.3. Changes in mean moisture content over the top 2.1 m of soil in treatments D and C, as estimated from neutron probe readings.

The degree to which solute movement is affected by rainfall infiltration is borne out by changes in soil-water Se and Cl concentrations. These data, which are depth-integrated between 0.425 and 1.00 m, are shown in Fig. 5.8 through 5.11 and are expressed as mass per m^2 in order to be comparable with soil Se data, presented in the following subsection. In response to rainfall-induced infiltration, pulses of Se equivalent to as much as 2 g m^{-2} and of Cl equivalent to as much as 1500 g m^{-2} have been observed, although generally Cl concentrations do not vary as much since the Cl depth-gradient in most cases is rather flat. The Se pulses are equivalent to as much as 25% of the Se in the top 0.60 m of the soil profile and could be evidence of major Se redistribution. Two caveats need to be placed on this argument. Firstly, soil water samplers are

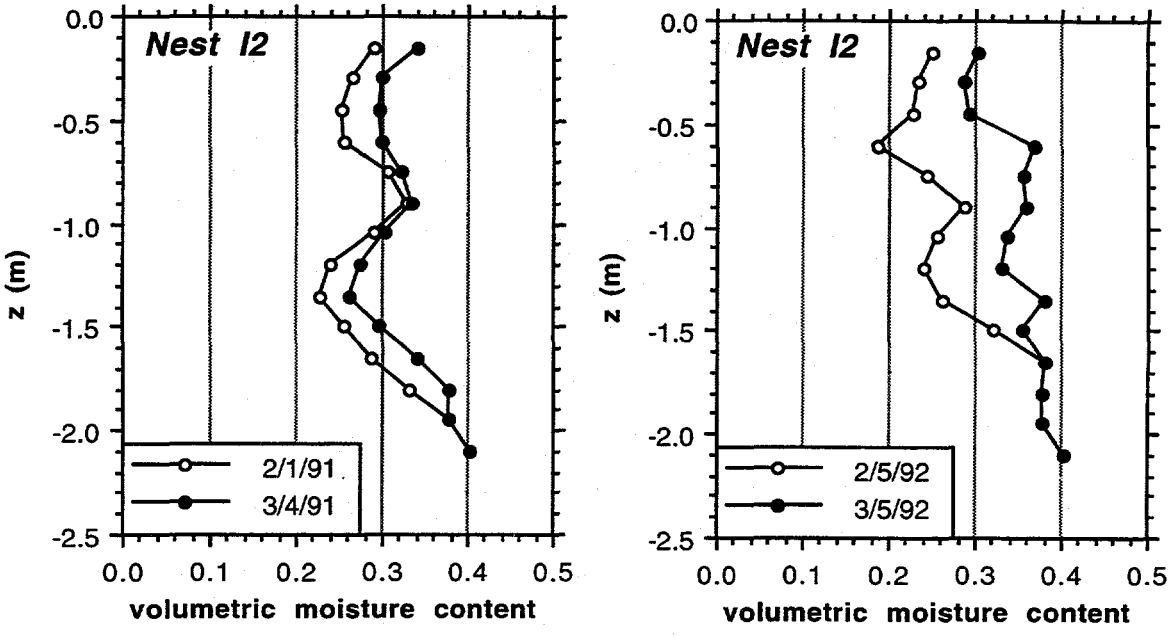

Figure 5.4. Changes in moisture content in treatment I, due to heavy rains over periods of roughly 1 month, as estimated from neutron probe readings.

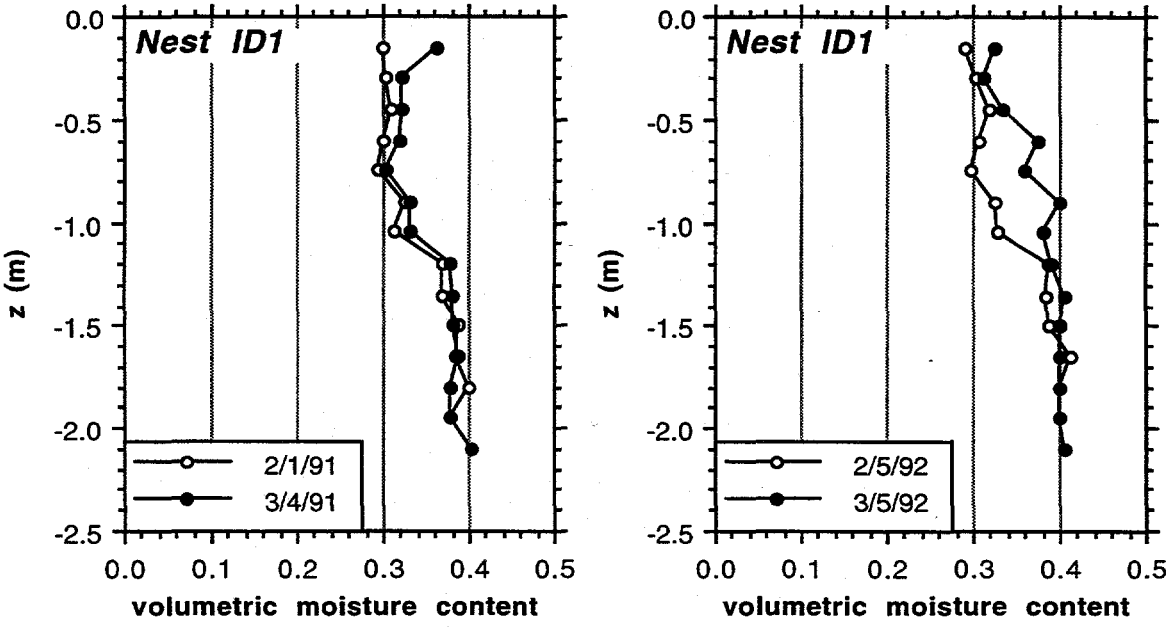

Figure 5.5. Changes in moisture content in treatment ID, due to heavy rains over periods of roughly 1 month, as estimated from neutron probe readings.

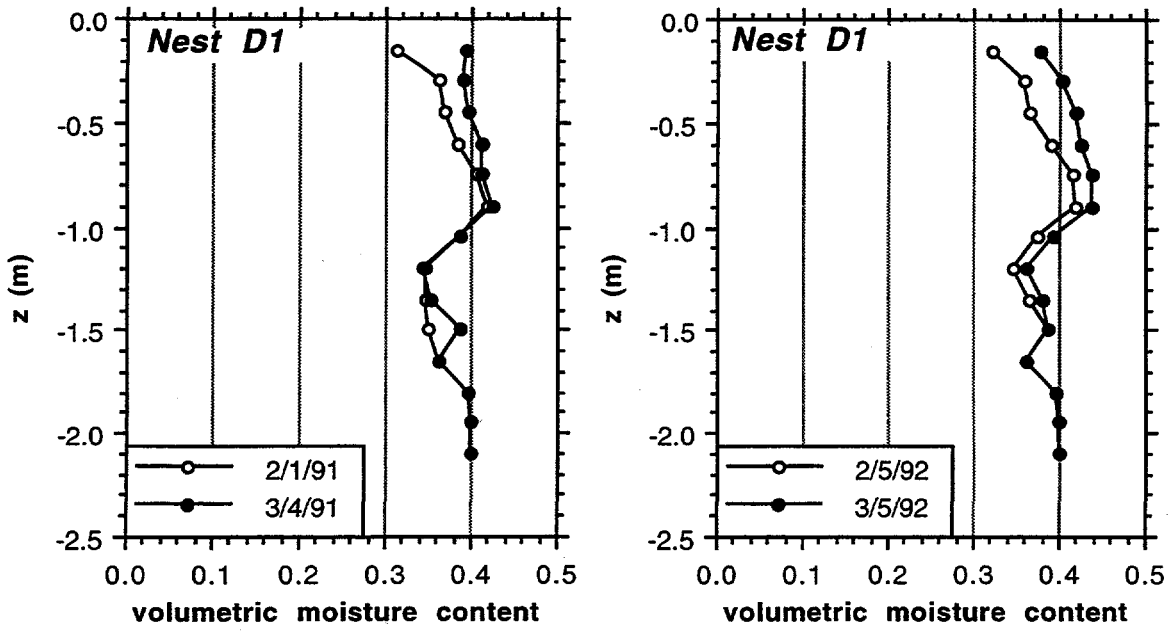

Figure 5.6. Changes in moisture content in treatment D, due to heavy rains over periods of roughly 1 month, as estimated from neutron probe readings.

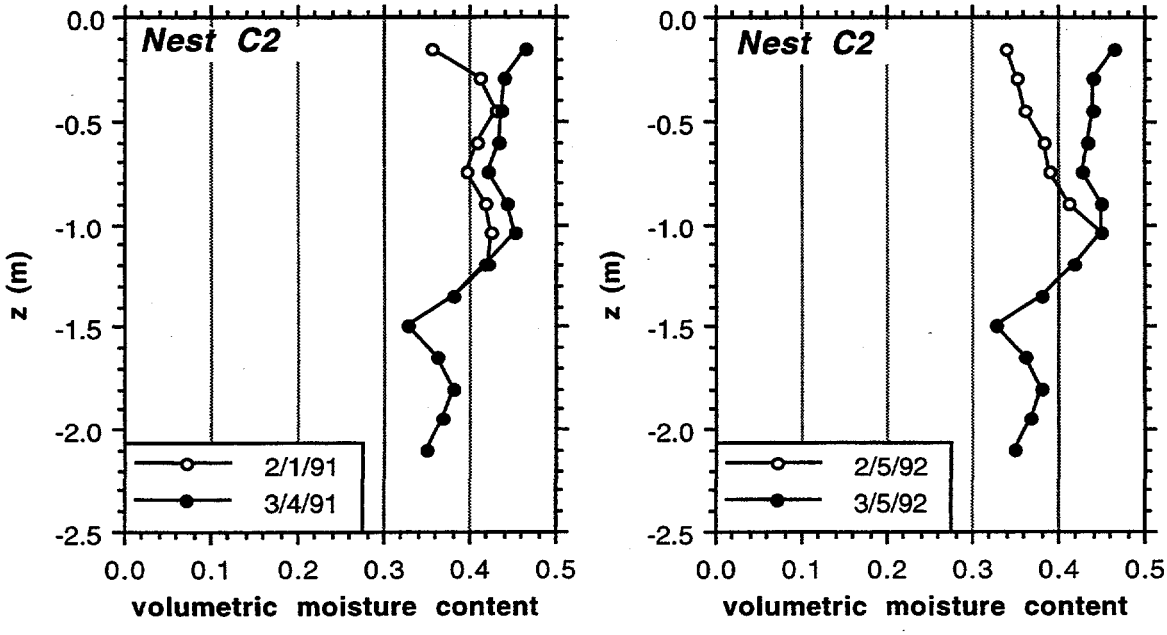

Figure 5.7. Changes in moisture content in treatment C, due to heavy rains over periods of roughly 1 month, as estimated from neutron probe readings.

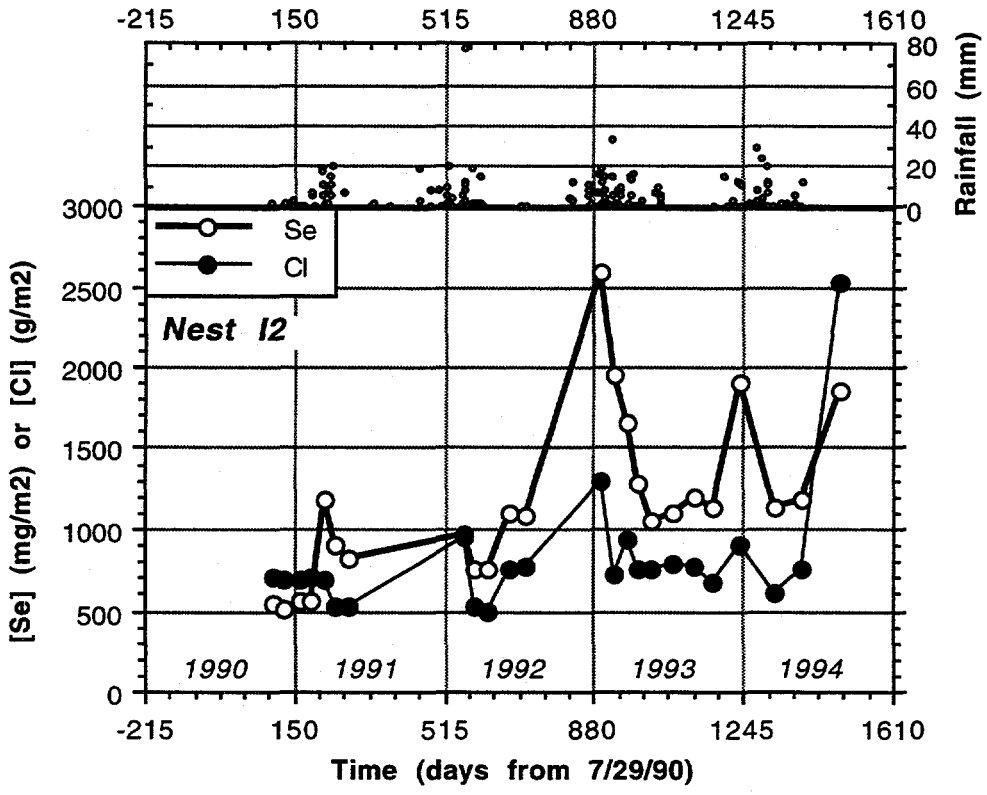

Figure 5.8. Mass of Se and Cl over the depth of 0.4 m to 1.00 m in treatment I, based on data from soil water samplers and neutron probe measurements at nest I2.

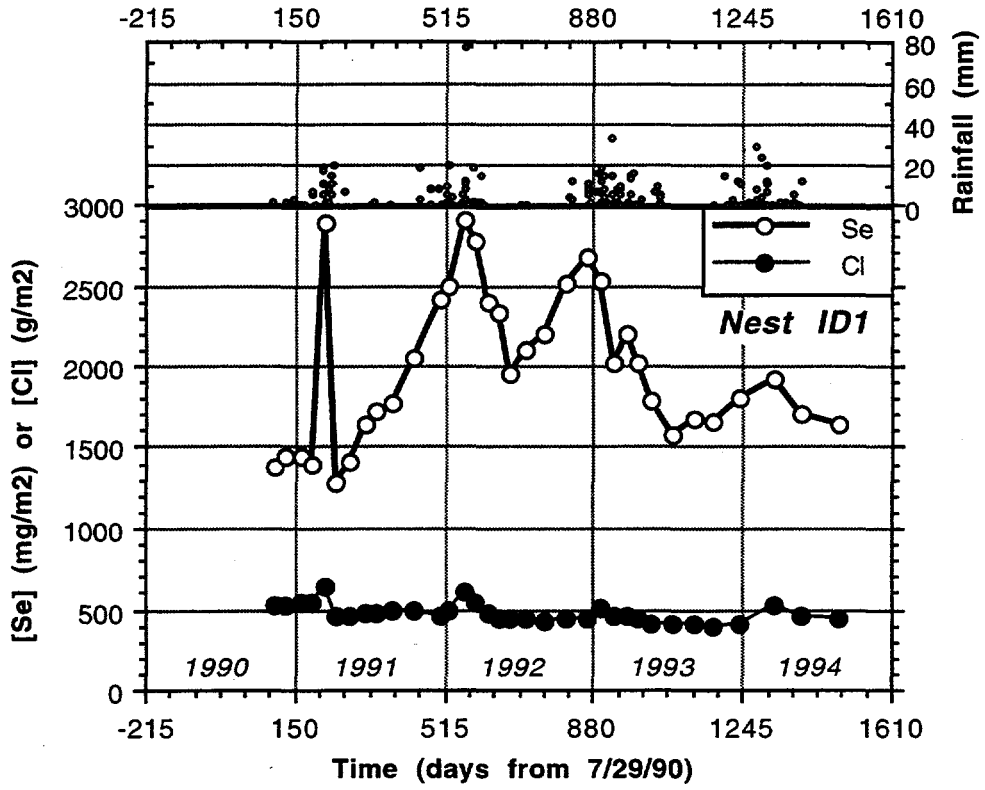

Figure 5.9. Mass of Se and Cl over the depth of 0.4 m to 1.00 m in treatment ID, based on data from soil water samplers and neutron probe measurements at nest ID1.

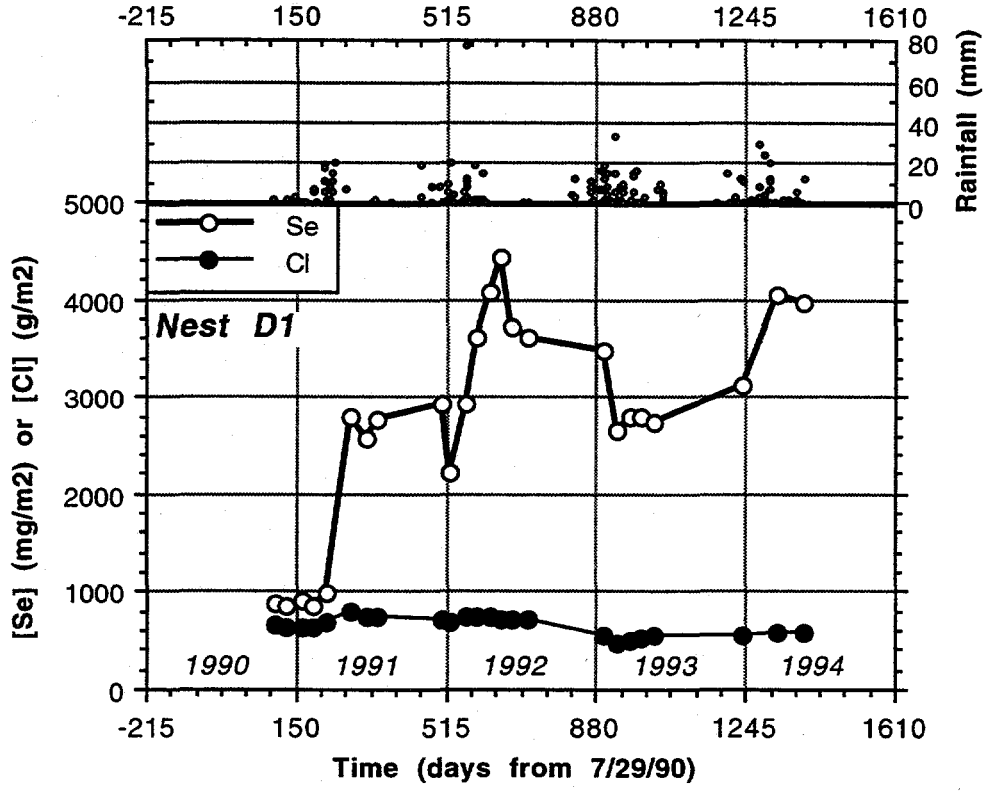

Figure 5.10. Mass of Se and Cl over the depth of 0.4 m to 1.00 m in treatment D, based on data from soil water samplers and neutron probe measurements at nest D1.

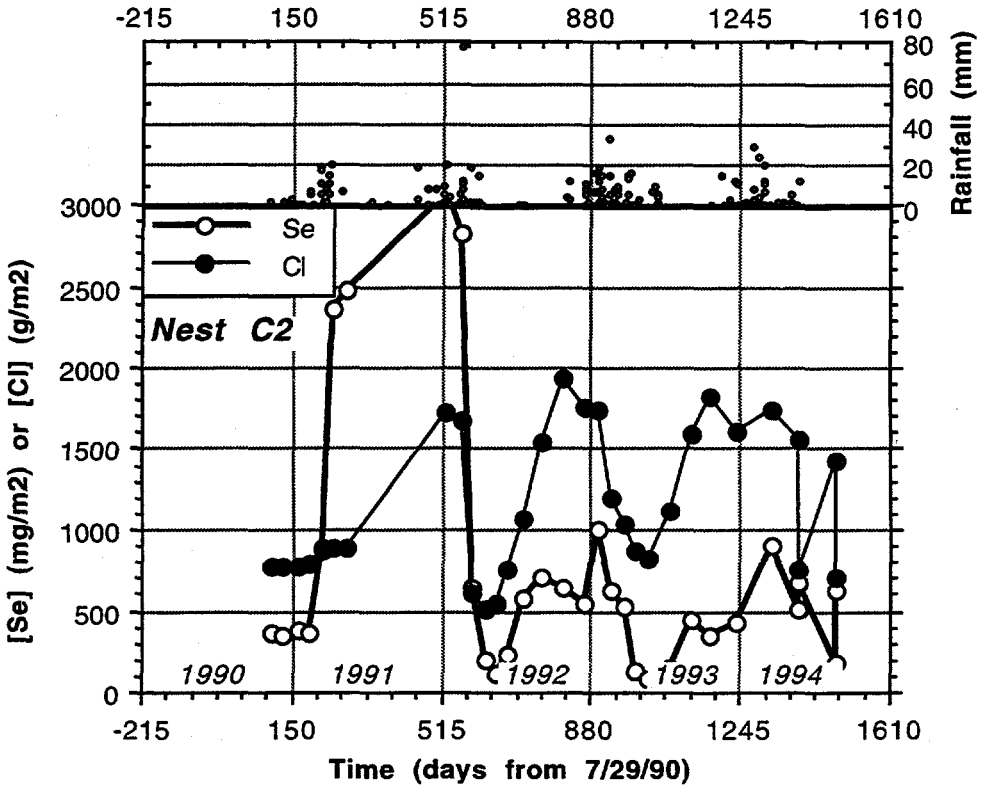

Figure 5.11. Mass of Se and Cl over the depth of 0.4 m to 1.00 m in treatment C, based on data from soil water samplers and neutron probe measurements at nest C2.

generally biased to collecting sample from macropores when macropores are water-saturated. As this is likely the case following rainstorms, solute concentrations observed in this manner may not be representative of the bulk solution and may lead to an overestimation of the net mass of solute being displaced. Secondly, some percentage of solute being displaced downward in the winter will be transported upward during the summer and fall due to evapotranspiration. Movement toward the root zone may be more important than toward the surface in vegetated plots, such as in treatment I. Nevertheless, the net loss of solutes from the top 0.60 m may be significant.

5.2 Soil Monitoring

Two types of soil samples are taken. An annual N-S transect is taken through the middle of each treatment in July. Samples are taken every 3 m along these lines and down to the depth of 0.60 m, in 0.15 m increments. Soil from the transects is extracted using a 1:5 soil:water extract and extracts are analyzed for total soluble selenium via HGAAS. Also, every October, 10 subplots within each treatment are sampled. Soil is cored to 0.60 m in 0.15 m increments, except

for 30% of the subplots in which an additional two increments, 0.60-0.90 m and 0.90-1.20 m, are taken. Five such cores are taken in each subplot and composited by depth. All soil samples are extracted for total Se via an acid digest and analyzed via HGAAS by the Engineering Research Institute, C.S.U. Fresno. See Figure 5.1 for sampling locations.

5.2.1 Soil-Se and Salinity Along N-S Transects

Data from the 1990, 1991, 1992, and 1993 transects are presented herein. Samples were also collected in 1994, but as of yet have not been analyzed. Total Se distributions along each transect in the 0-0.15 m interval are shown in Fig. 5.12-5.15. This is the depth interval of nominally the greatest interest because of the highest Se concentrations and the favorable conditions for fungal growth. Within this interval, the average plot-wide total Se concentration was 50 ppm, with transect soils from the I treatment being high above that average at 97.8 ppm in July 1990. Although it is clear that declines in total Se were observed in treatments I and ID and to a lesser extent D and C, they are difficult to quantify from these figures due to the large spatial variability. Mean transect Se concentrations, expressed as mass per area, are shown in Fig. 5.16-5.19. Here the year-to-year changes in Se concentrations are more readily discerned. The largest and most consistent declines in total Se were observed in the irrigated treatment (Fig. 5.16). An average of roughly 2 g m^{-2} of Se were lost from the top interval per year. However, as mentioned above, Se concentrations in this treatment were anomalously high in 1990. In fact, 1990 Se concentrations were distinctly higher in all intervals, whereas there were no significant changes subsequent to 1991 below 0.15 m. There were declines in Se in the top 0.15 m of treatments ID and D from 1990 to 1991 and from 1991 to 1992, but no changes were observed between 1992 and 1993. The observed declines are on the order of 1 g m^{-2} per year. In treatment D, only between 1991 and 1992 was there a significant decline observed in the top 0.15 m interval, a decrease on the order of 2 g m^{-2}. However, year to year decreases were observed in the 0.15 to 0.30 m interval. No significant changes in total Se concentrations in the top interval of treatment C were observed, but much like in treatment D, declines in the 0.15 to 0.30 m interval were observed, primarily between 1990 and 1991, and 1991 and 1992.

There are two mechanisms which can be invoked to explain the observed patterns: microbial volatilization and physical redistribution of Se with moisture fluxes. Generally, the first mechanism applies to the 0 to 0.15 m interval only, whereas transport of Se by infiltrating rainwater can affect the entire soil profile. As noted in a previous section, vertical displacement of Se on the order of 1 to 2 g m^{-2} has been commonly observed following rainstorms. Since these changes are on the order of the net changes observed in total Se decrease, potential losses of Se via volatilization are difficult to quantify, but appear to be on the order of 0.5 g m^{-2} yr^{-1} or

less. This rate by far exceeds Se methylation rates commonly measured at Kesterson Reservoir (Frankenberger and Karlson, 1988).

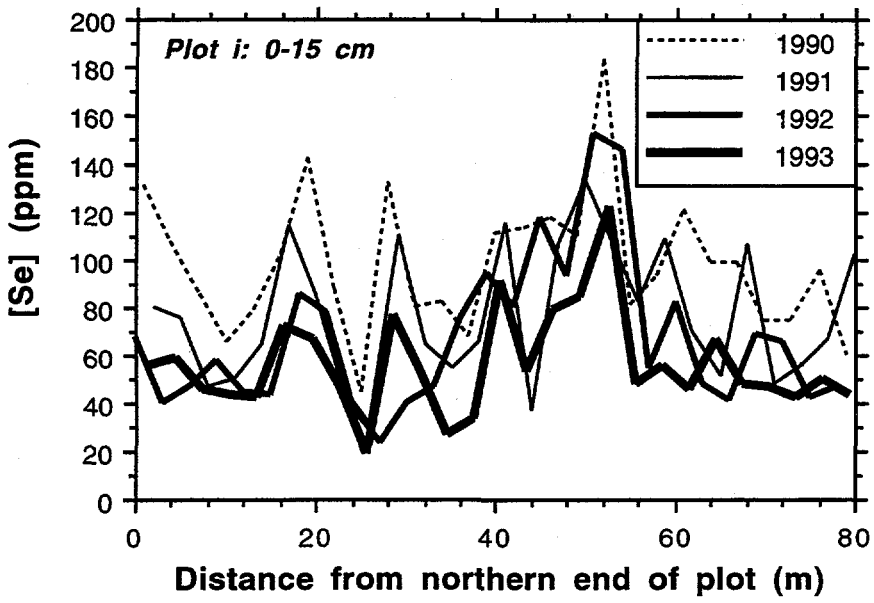

Figure 5.12. Total Se in the top 0.15 m of the soil profile along the N-S transect of treatment I.

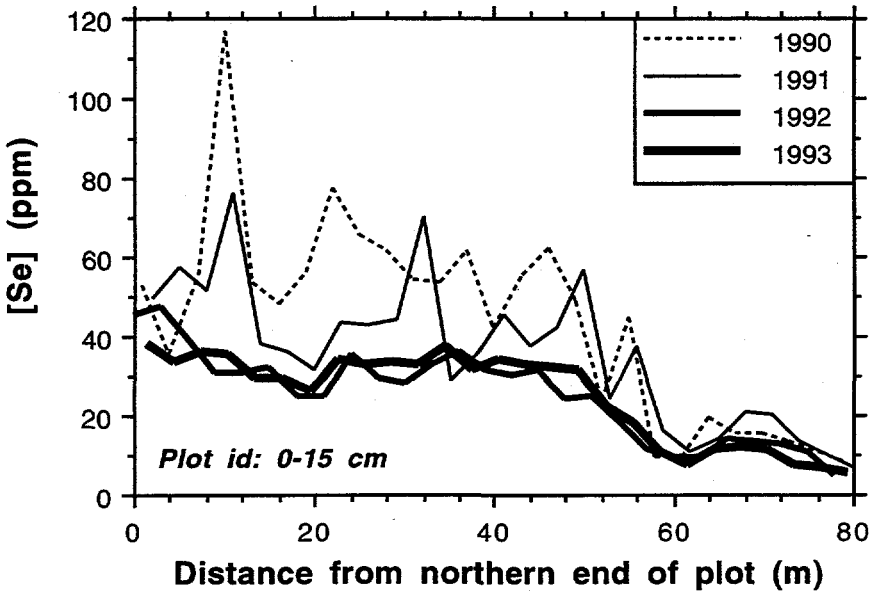

Figure 5.13. Total Se in the top 0.15 m of the soil profile along the N-S transect of treatment ID.

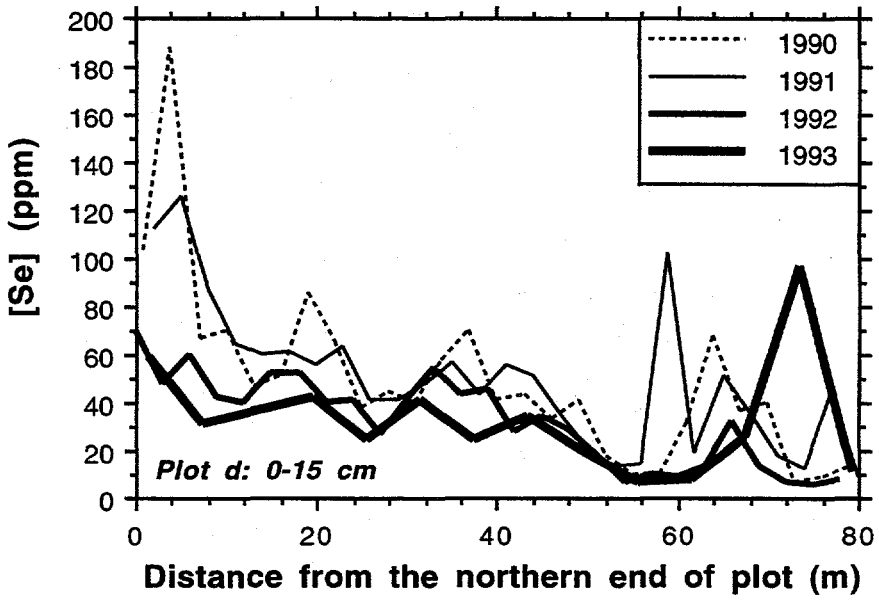

Figure 5.14. Total Se in the top 0.15 m of the soil profile along the N-S transect of treatment D.

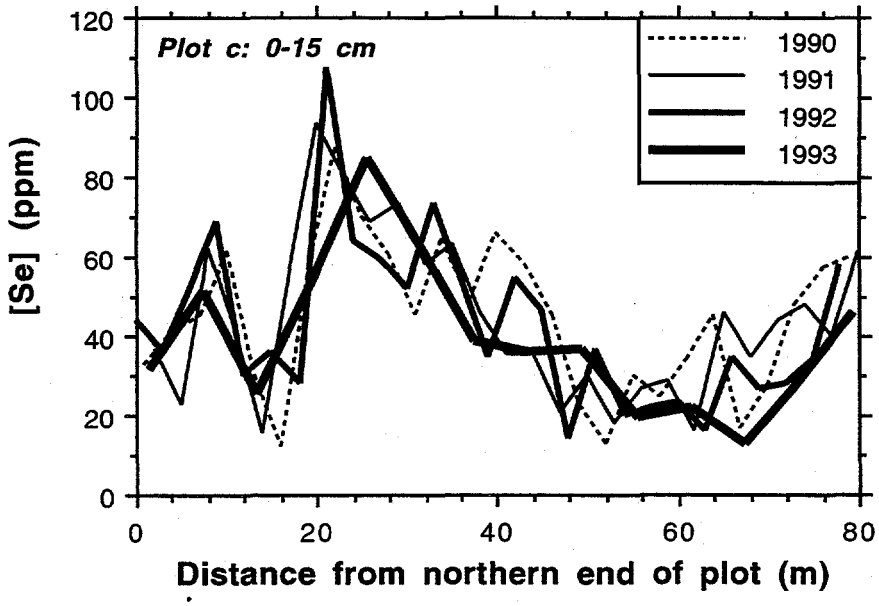

Figure 5.15. Total Se in the top 0.15 m of the soil profile along the N-S transect of treatment C.

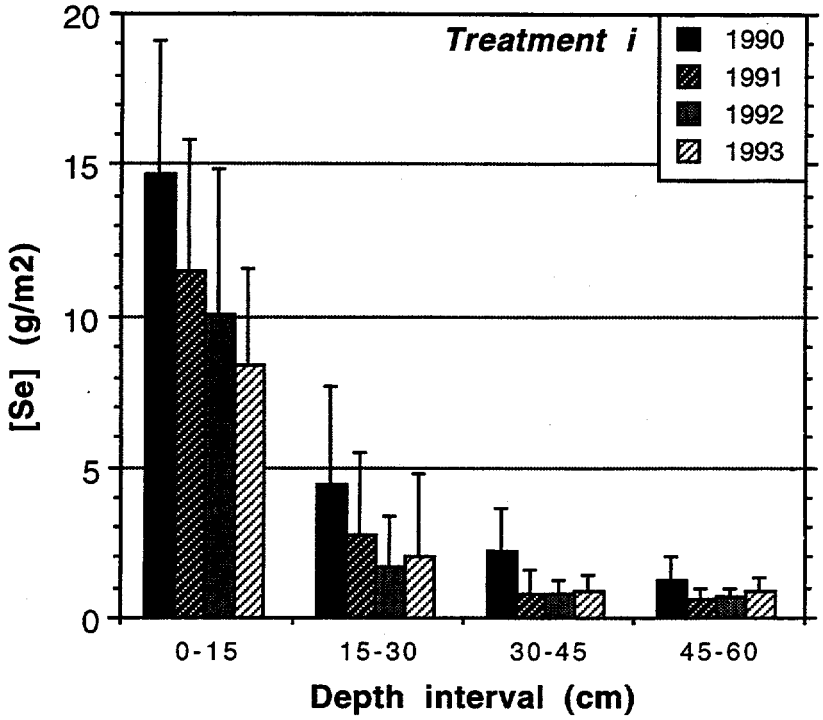

Figure 5.16. Total Se in the soil profile along the N-S transect of treatment I.

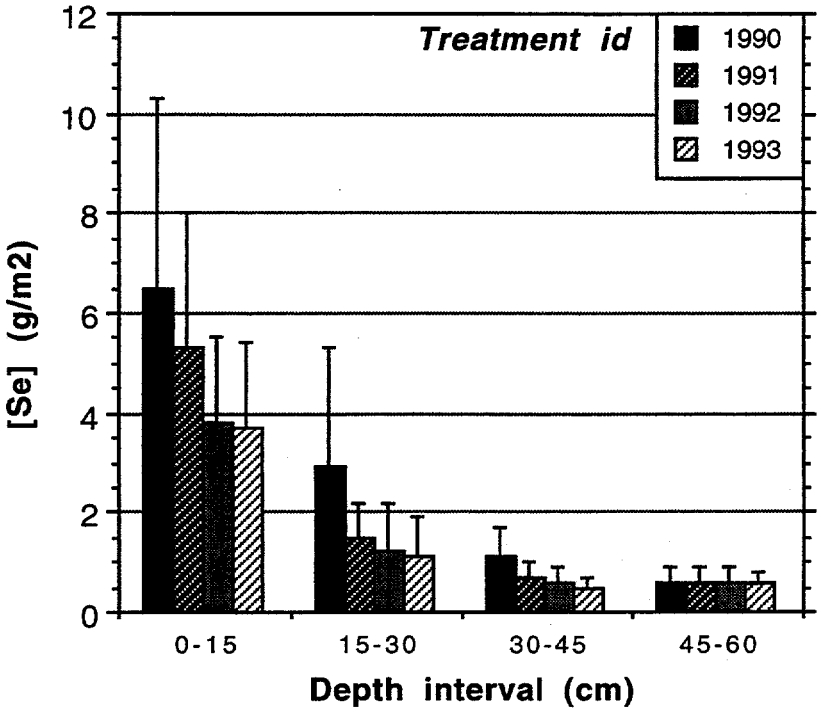

Figure 5.17. Total Se in the soil profile along the N-S transect of treatment ID.

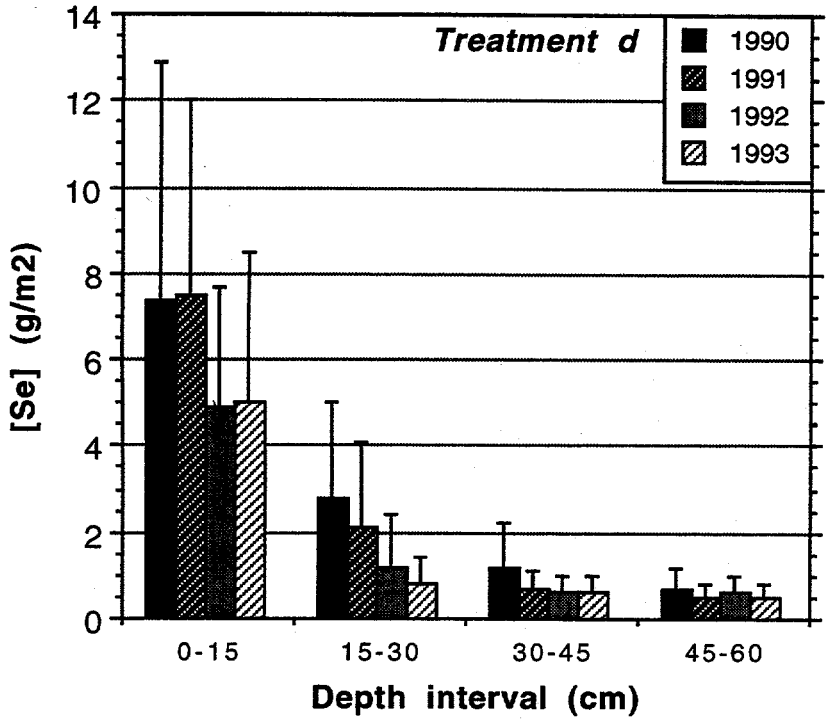

Figure 5.18. Total Se in the soil profile along the N-S transect of treatment D.

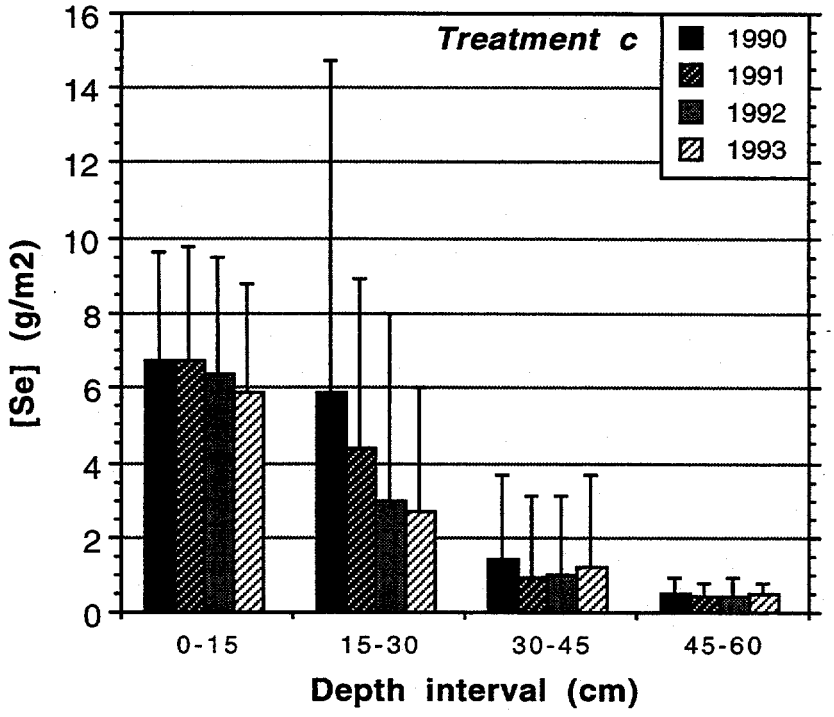

Figure 5.19. Total Se in the soil profile along the N-S transect of treatment C.

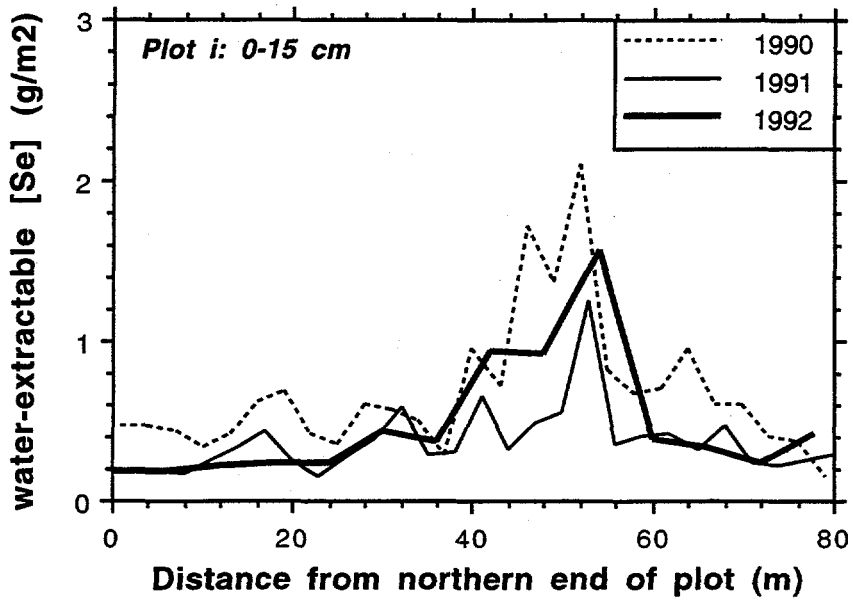

Figure 5.20. Water-extractable Se in the top 0.15 m of the soil profile along the N-S transect of treatment I (1993 data not available).

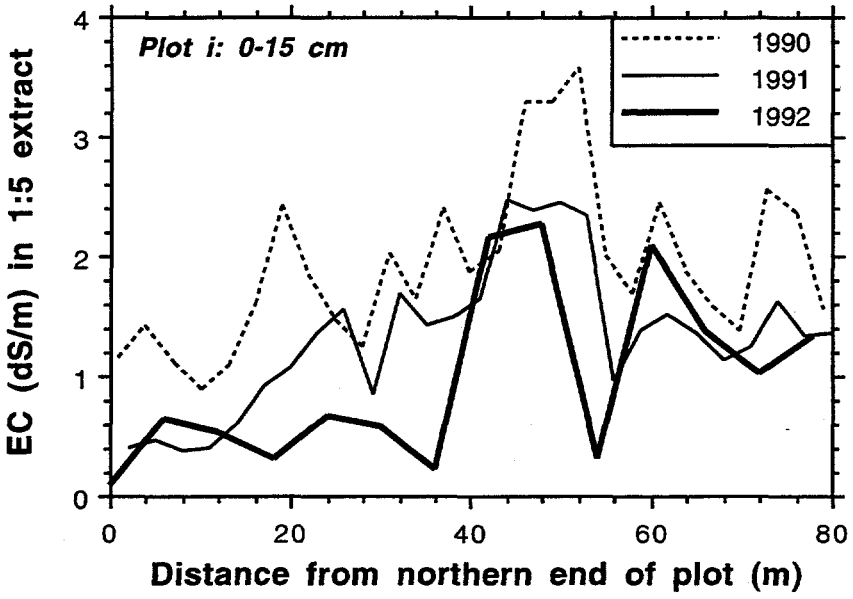

Figure 5.21. Electrical conductivity in a 1:5 water extract of the top 0.15 m of the soil profile along the N-S transect of treatment I.

The amount of Se which can be vertically displaced may be estimated from the water-extractable Se in the top 0.15 m of soil. This data for treatment I is shown in Fig. 5.20 and represents the results of analysis of 1:5 soil:water extracts, normalized to soil mass. Once again,

1 to 2 g m^{-2} of Se is in a water-soluble form and potentially available for downward transport. Furthermore, soluble Se concentrations do not vary significantly from year to year, suggesting a re-oxidation of elemental or organic Se over the summer period. Rates required to replenish such quantities of soluble Se are within the ranges observed in laboratory and other field experiments (see Section 6). Electrical conductivity (EC) measured in the same extracts is also an indicator of downward displacement of solutes. This data for treatment I is shown in Fig. 5.21 and is indicative of very significant net downward movement of solutes as salinity in this interval was reduced by as much as 75%.

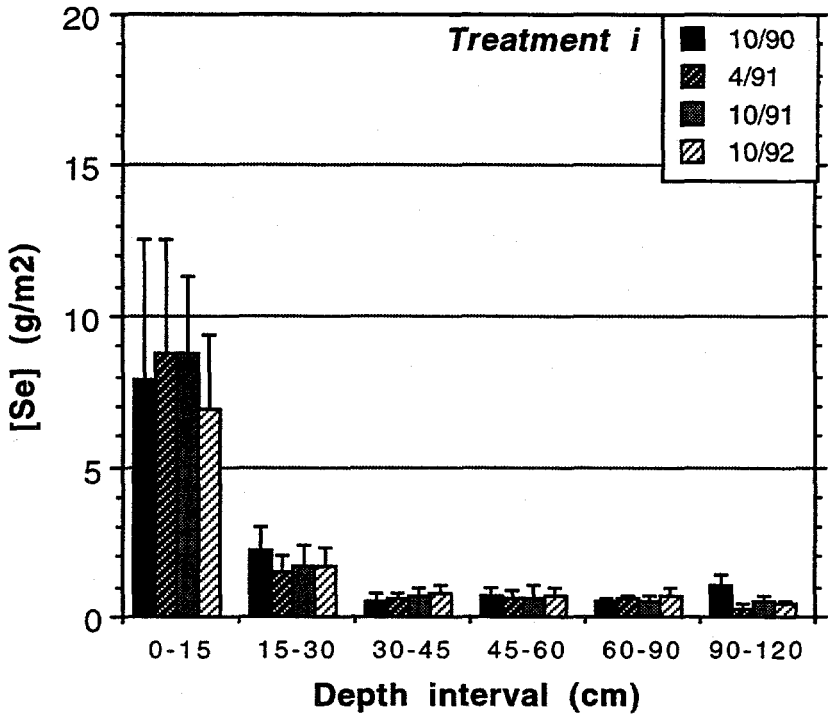

Figure 5.22. Total Se in soil from subplots from treatment I.

5.2.2 Soil-Se in 5 by 5 m Subplots

Soil samples were collected from 5 by 5 m subplots (see Fig. 5.1 for locations) in October 1990, 1991, 1992, 1993 and April 1991. Samples from October 1993 have not been processed to date. Total Se concentrations, expressed in terms of mass per m^2 are shown in Fig. 5.22 through 5.25. These data do not show the same trends as N-S transect data. Specifically, there appear to be no consistent declines in total Se concentrations, except in the 0-0.15 m interval of treatment D. There are no easy explanations for this disparity. One possibility is the re-distribution of Se over the period of July to October. Also, subplot data are derived from samples composited from five cores and therefore may better represent the sampled area. Data from 1993 may help

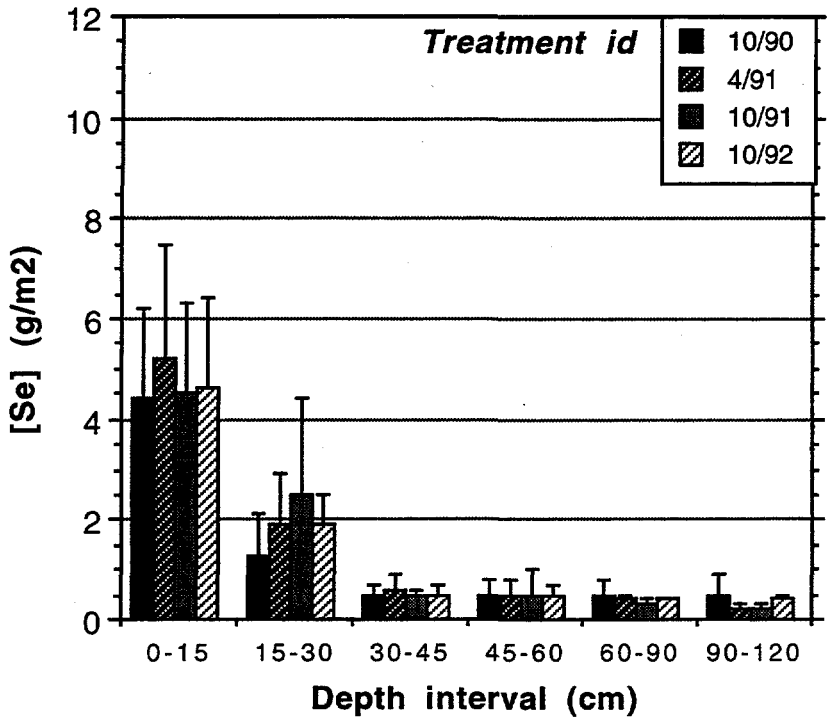

Figure 5.23. Total Se in soil from subplots from treatment ID.

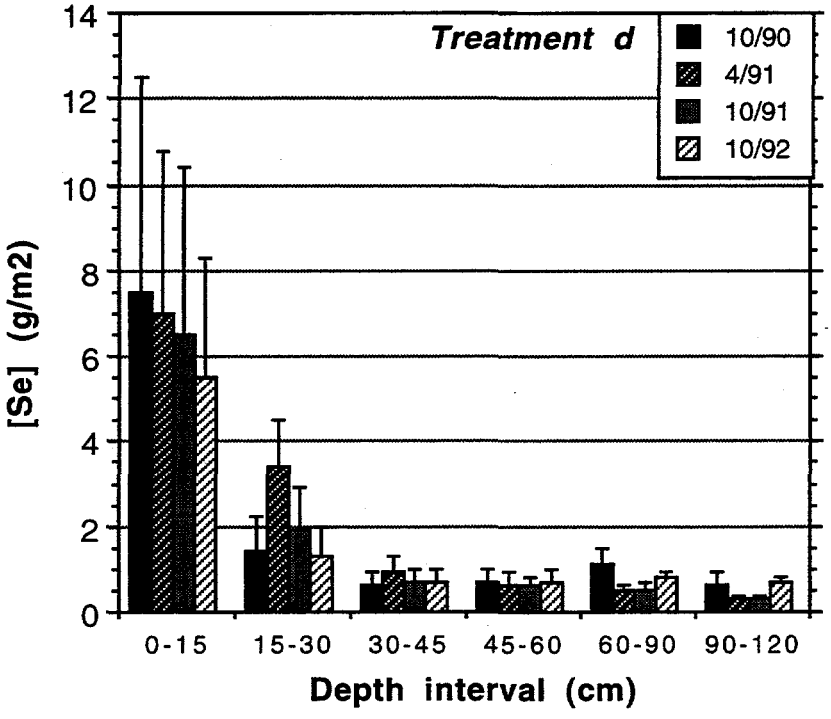

Figure 5.24. Total Se in soil from subplots from treatment D.

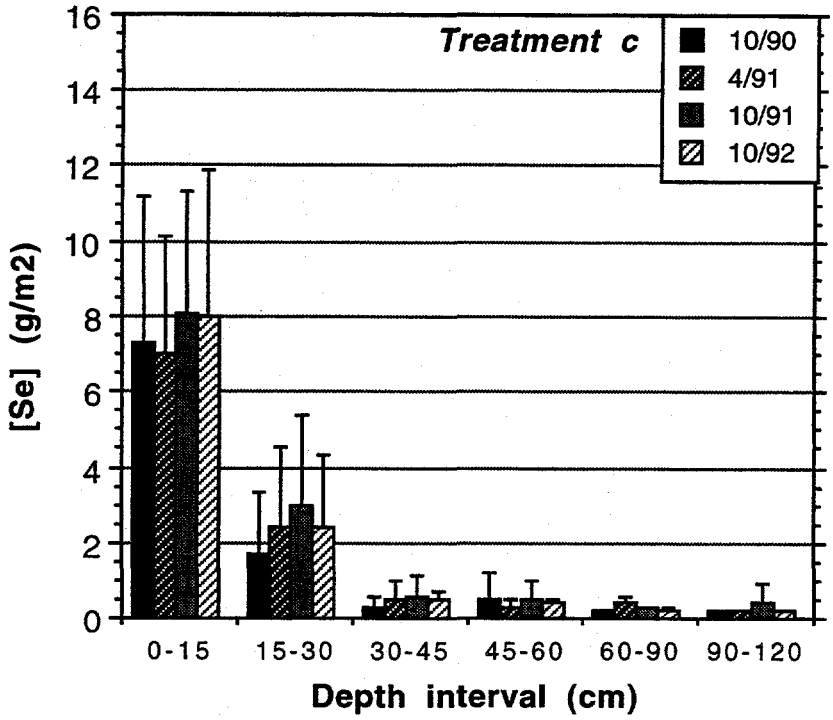

Figure 5.25. Total Se in soil from subplots from treatment C.

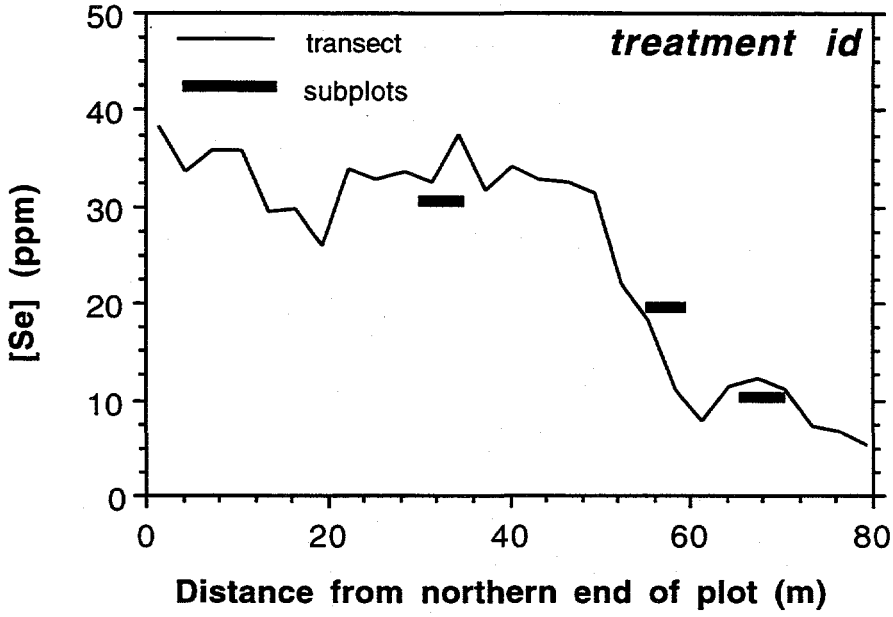

Figure 5.26. Total Se in the top 0.15 m of soil from the 1993 transect subplots from treatment ID as compared with data from concurrently sampled subplots.

resolve these uncertainties. During the July 1993 collection of transect soils, selected subplots (I4, 6; ID6, 7, 8; D4; and C6) were sampled for the purpose of comparison. As seen in Fig. 5.26, these results were fairly close to data from nearby transect samples, suggesting that the two sampling approaches are consistent with each other and that changes observed between transect data collected in July and subplots in October are not a function of sampling approach, but rather actual temporal changes and differences in spatial distribution of Se concentrations.

5.2.3 Synthesis of Soil Data

All currently available soil Se data from transect and subplot soils was integrated over the sampled depth of 0.0 to 0.60 m (Fig. 5.27 through 5.30). This representation accounts for Se which may have been flushed out of the top 0.15 m but was not displaced below 0.60 m. With the exception of the July 1990 sample in treatments I, ID, and C, and declines from 1991 to 1993 in treatment D, there are no consistent trends in total Se concentrations. One needs to note that the spatial variability of the July 1990 sample in treatment ID is significantly greater than in subsequent data sets, likely a result of soil homogenization with bi-weekly rototilling. Also, spatial variability is generally smaller in the subplot data sets than in transects, which is especially apparent in the I treatment. This is clearly a function of the composite nature of the subplot samples.

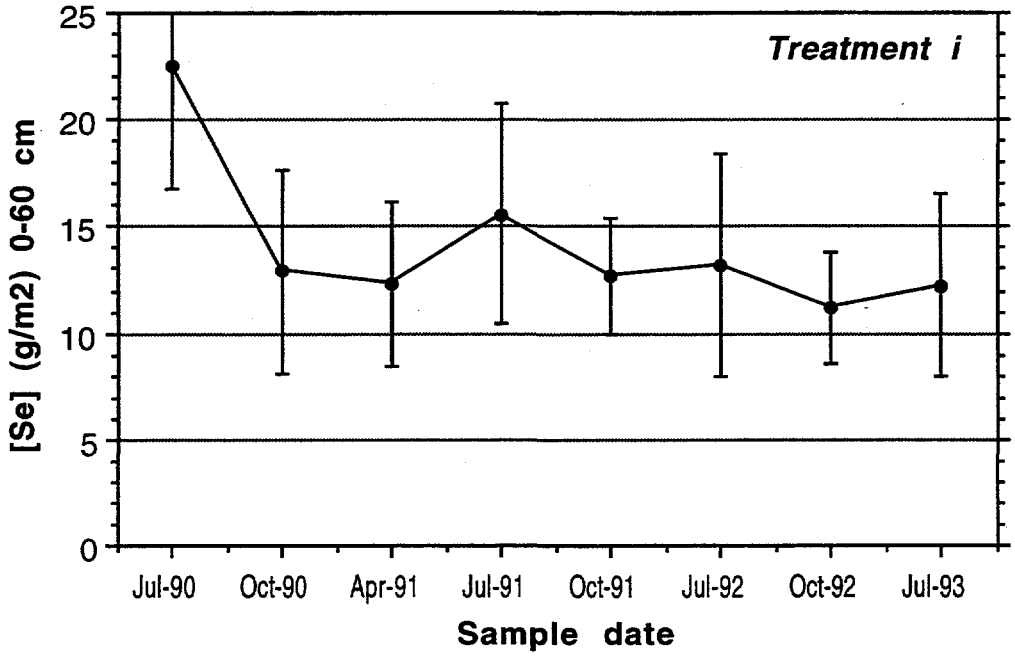

Figure 5.27. Cumulative total Se in soil from transects and subplots from treatment I.

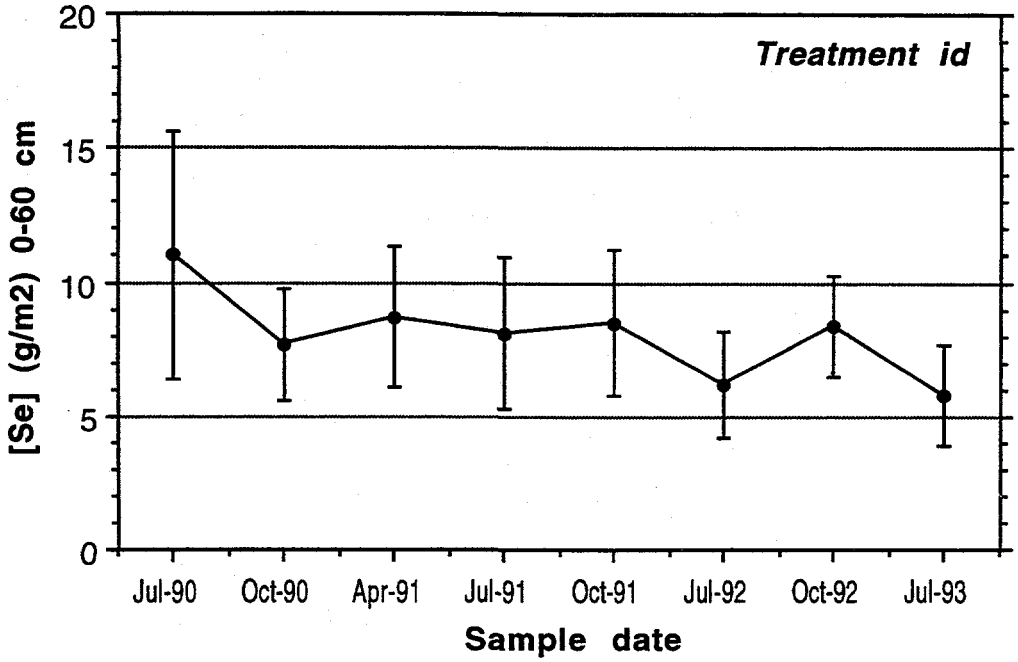

Figure 5.28. Cumulative total Se in soil from transects and subplots from treatment ID.

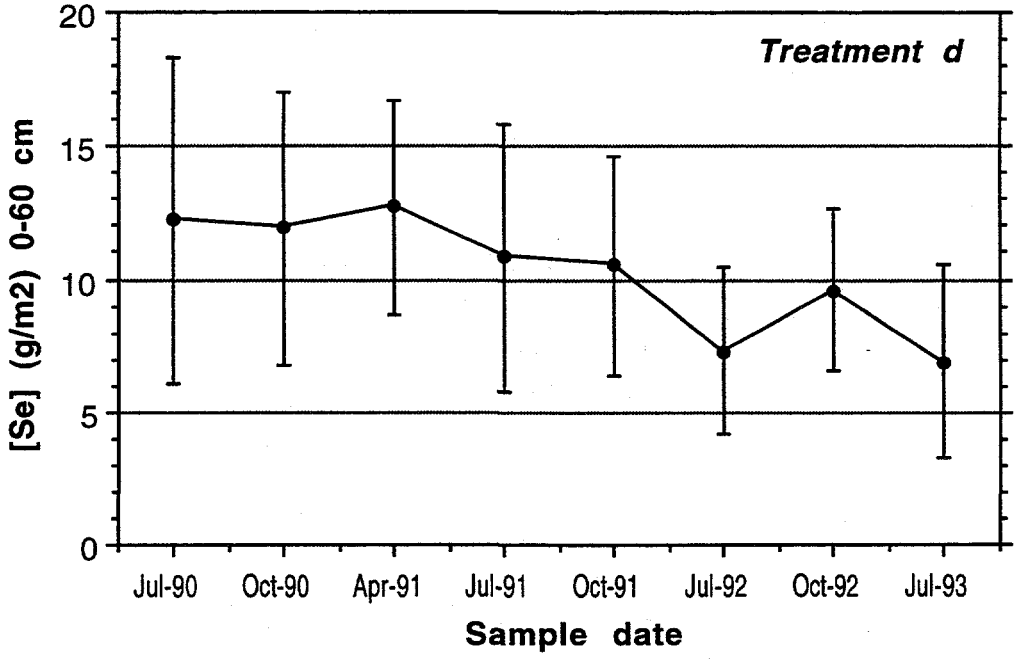

Figure 5.29. Cumulative total Se in soil from transects and subplots from treatment D.

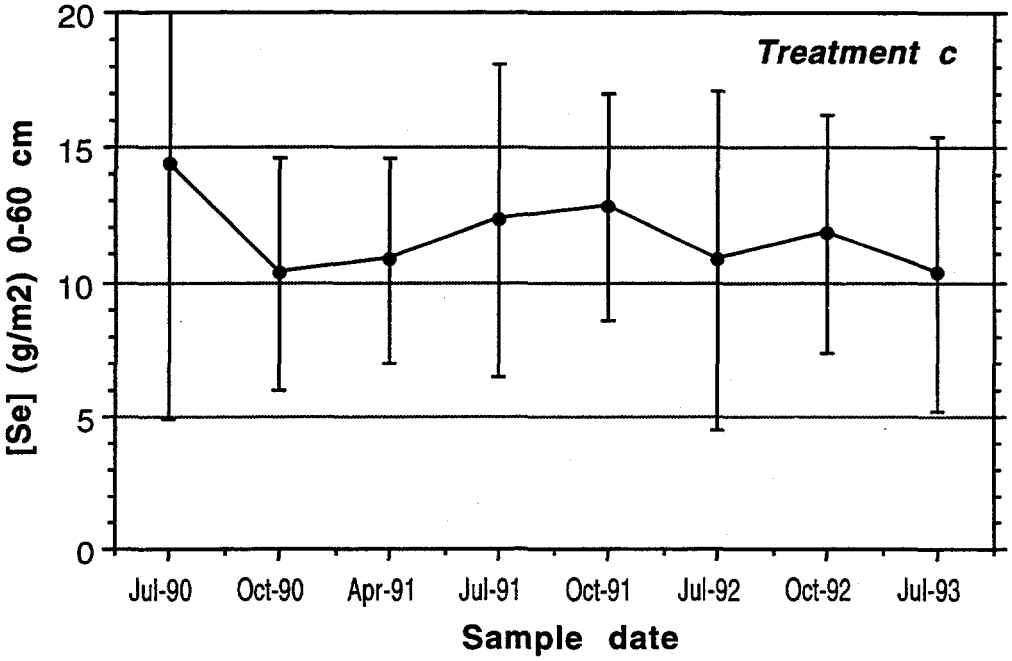

Figure 5.30. Cumulative total Se in soil from transects and subplots from treatment C.

5.3 Conclusions

Both soluble Se concentrations and EC generally display trends which are consistent over periods of weeks to months, suggesting that significant changes in soluble-Se of up to 5 to 10 ppm have occurred in the soil profile of most areas within this plot, especially treatments I and ID. These changes are the result of downward flushing of soil-water by infiltrating rain water and redistribution of solutes due to plant-root water extraction (the latter applies to treatments I and C only). When translated to bulk Se concentrations, these changes are on the order of 2 to 3 ppm per year and can account for much, but probably not all of the decline in total Se in soil intervals below 0.15 m.

6.0 Laboratory Accelerations of Soil Selenium Transformations

Peter Zawislanski and Mavrik Zavarin
Earth Sciences Division
Lawrence Berkeley Laboratory

Soils from sites in three ponds were incubated over a period of 2.5 years at temperatures of 15°C, 25°C, and 35°C, in order to accelerate Se oxidation and help identify the most readily oxidizable fractions. A range of soil moisture conditions was maintained. Six Se fractions: soluble Se(IV), soluble Se(VI), adsorbed-Se, organic-Se, carbonate-Se, and refractory Se, were monitored via periodic extraction. Oxidation rates were estimated based on changes in the relative proportions of these fractions with time Soils from a depth of 0.45 to 0.55 m appeared close to equilibrium with respect to Se fractionation, as no significant changes were noted. Transformations were observed in surface soils (0 to 0.10 m). The most prominent change was the oxidation of up to 50% of refractory-Se to soluble Se(VI). A smaller portion of the organic-Se pool was also oxidized. X-ray absorption spectroscopy confirmed the dominance of Se(0) in the refractory pool. First-order oxidation rates were between 0.058 yr^{-1} and 0.29 yr^{-1} for organic-Se , and between 0.11 yr^{-1} and 2.4 yr^{-1} for refractory-Se, with a strong positive correlation with temperature. No losses of total-Se were observed, indicating the relative insignificance of methylation. An apparent plateau in oxidation of the refractory pool suggests heterogeneity of this pool, with some components more readily oxidized than others. In soils incubated at or near saturation, Se was readily reduced. In soils which were exposed to varying moisture and temperature conditions, Se went through oxidation and reduction cycles, with a small but significant net oxidation trend. Over periods of years to decades, currently immobile and leach-resistant Se may become available to the biological system.

6.1 Introduction

The bio-availability of trace metals in soils is of great interest. Metals may be present in the soil environment in relatively high concentrations without necessarily having toxic effects. This depends in large measure on the oxidation state and physico-chemical association of the element in soil. Such associations have been studied repeatedly as related to the state of selenium in both

naturally-occurring (e.g. Chao and Sanzalone, 1989) and contaminated soils (e.g. Weres et. al., 1989; Tokunaga et. al., 1991). Although no single method for the assessment of Se toxicity in soil has been unequivocally accepted, some fractions are known to be more readily available than others (Mikkelsen et. al., 1989). Predicting future bioavailability of Se is of utmost importance in determining potentially harmful environments. Selenium which is found in reduced and less available forms is known to oxidize under favorable conditions and become water-soluble. The rates of these transformations have been observed in both the field (Tokunaga et. al., 1991) and the laboratory (Masscheleyn et. al., 1990). Each of these general approaches has drawbacks. Field studies of in-situ Se oxidation are difficult because of the spatial variability of Se concentrations and require many years to complete because of the very slow rates observed in the natural environment. Furthermore, vertical displacement of dissolved Se is observed due to rainfall infiltration and evaporation (Zawislanski, et. al., 1992), which complicates mass balance calculations. Although more reproducible and easier to conduct, laboratory batch studies do not represent field conditions and therefore measured rates are of questionable utility.

The purpose of this experiment was to measure oxidation rates of Se under laboratory conditions closely resembling those in the field. An additional objective was the identification of Se fractions which are most readily oxidized. By incubating soils at temperatures elevated relative to field conditions, transformations were accelerated in order to ascertain long-term oxidation rates and fractions involved.

Soils used in this experiment represent three environments: an originally cattail- (*Typha latifolia*) vegetated area with very high Se concentrations, a predominantly *Bassia hyssopifolia*-vegetated playa with moderately high Se concentrations, and a saltgrass- (*Distichlis spicata*) covered upland area with relatively low Se concentrations.

6.2 Theory

In order to understand Se transformations, fractionation of the element must be known. This presents difficulties as Se is found in a number of forms in soil which have in general been characterized based solely on operationally-defined extraction procedures (e.g., Fujii et. al., 1988; Chao and Sanzalone, 1989; Lipton, 1991). Recently, x-ray absorption spectroscopy of soils (Brown and Parks, 1989) has shed some light on in-situ Se speciation (Pickering et. al., 1994), but its current applicability is limited to samples with concentrations greater than 10 ppm and can only be performed at synchrotron facilities. Therefore, extractions are currently the practical approach to Se fractionation and can provide meaningful results when carefully interpreted.

Aqueous Se chemistry has been thoroughly described (Geering et. al., 1968; Elrashidi et. al., 1987). Not surprisingly, the application of thermodynamic equilibrium in soils leads to vast errors in the prediction of speciation. For example, under strongly oxidizing conditions, Se is expected to occur as Se(VI). However, Se(VI) is generally a small fraction of the inventory in near-surface soils (Chao and Sanzalone, 1989; Weres et. al., 1989; Tokunaga et. al., 1991). Significant amounts of Se(IV), primarily as an adsorbed form, and even greater amounts of organically-associated Se and refractory Se are found. The refractory pool has been characterized differently by various workers, but can be generally described as encompassing highly leach-resistant Se, intimately associated with the solid matrix, with a large fraction as elemental Se (Weres et. al., 1989). Again, because of the operationally-defined extractions, which generally alter Se speciation, a conclusive statement about the nature of the refractory pool cannot be made.

Similar uncertainties apply to the definition of an "adsorbed" phase (Tokunaga et. al., 1994), and the "organic" phase (Gruebel et. al., 1988; Tu et. al., 1994). The determination of an adsorbed Se phase is based on ligand exchange between adsorbed selenite and an excess concentration of phosphate. Strong theoretical arguments can be made in favor of this procedure, since the phosphate oxyanion is known to replace Se(IV) on, for example, goethite surfaces (Balistrieri and Chao, 1987). Equally strong arguments may be made stating that the procedure can, and probably does result in some liberation of Se from other phases, and is dependent on phosphate concentration (Tokunaga, et. al., 1994). A problem in defining an "organic" Se phase is the likely presence of a variety of such molecular forms (Abrams et. al., 1990). Furthermore, some of the Se may be associated with organic matter in only a physical sense, i.e. occluded or adsorbed. The predominant organo-Se forms found in soil organic matter (SOM) include selenomethionine, selenocystine, and methaneseleninate (Doran and Alexander, 1977). Selenomethionine is most common and is associated with hydrophobic fulvates (Abrams et. al., 1990). The predominance of reduced species in an oxidized environment, such as the generally unsaturated near-surface soils of Kesterson Reservoir, is indicative of very slow re-oxidation of species which were reduced during periods of prolonged ponding. For the purpose of this experiment, total Se is divided into six operationally-defined fractions: soluble Se(IV), soluble Se(VI), adsorbed Se, organic-Se, carbonate-Se, and refractory Se. Based on previous studies of Kesterson soils and sediments, these are the major Se associations (e.g. Lipton, 1991; Tokunaga et. al., 1991).

Increasing temperature generally results in an increase in reaction rate (Sparks, 1989). This dependence is modeled by the Arrhenius Equation:

$$k = Ae^{-E/RT} \qquad [1]$$

where k is the rate constant, A is a constant proportional to the frequency of favorable molecule collisions, E is the activation energy, R the ideal gas constant, and T is absolute temperature. Laboratory experiments have shown the dependence can in many cases be characterized by a Q_{10}, a factor ranging between 2 and 3, by which a reaction rate increases due to a temperature increase of 10°C. Such a dependence has been observed in a variety of reactions in soils, from mineral dissolution (Huang, et. al., 1968), nitrogen and sulfur mineralization (Marion and Black, 1987; Ellert and Bettany, 1992), CO_2 evolution (Blet-Charaudeau et. al., 1990), to ion exchange (Ogwada and Sparks, 1986). Not all reactions conform to this model in that there may be intermediate steps, which may have different reaction rates. Also, the magnitude of E is critical, but cannot be predicted for complex reactions in soil. When reactions are biologically-mediated, rates may drop off dramatically above certain temperatures, due to the sensitivity of the microbial community. Therefore, care must be taken not to expose samples to temperatures beyond this tolerance level. Microorganisms from warm environments, or mesophiles, are intolerant of temperatures in excess of 45°C (Brock, 1970). Temperatures chosen for this experiment, 15°C, 25°C, and 35°C, are above the mean annual field temperature (15.4°C) by approximately 0°C, 10°C, and 20°C, respectively. Thus, should the oxidation reactions conform to the Q_{10} model, the 15°C incubation would be roughly equivalent to field conditions, the 25°C incubation would accelerate reaction rates by 2 to 3 fold, and the 35°C incubation would cause a rate acceleration of 4 to 9 fold. This assumption cannot be used indiscriminately to interpret the data, as there may be a number of complicated steps involved in the liberation of Se from each fraction.

6.3 Materials and Methods

6.3.1 Sampling and Preparation

Soils were collected from three sites, two depths at each site: 0 - 0.10 m (referred to as "A" soils) and 0.45 - 0.55 m (referred to as "B" soils). In Pond 2, soil was collected from an area heavily used for agricultural drainage water ponding, an area which, before the draining of the Reservoir, was dominated by cattails (*Typha latifolia*). Since then, the cattails had been incorporated into the soil via disking and rototilling, but at the time of sampling, cattail fragments up to 0.10 m were still recognizable in the samples. Soils collected from Pond 9 represent an area which received moderate amounts of drainage water. Subsequent to the draining of the Reservoir, the area progressed from being a salt-laden playa, to a playa vegetated primarily with *Bassia hyssopifolia*, a salt-tolerant shrub. Soils from Pond 11 were collected in an

area which was used sporadically for drainage water ponding. The area is dominated by saltgrass (*Distichlis spicata*). The soil texture and organic carbon content are shown in Table 6.1.

Table 6.1. Soil texture and initial organic carbon content.

	Soil					
Components	P2A	P2B	P9A	P9B	P11A	P11B
% sand	38.7	40.8	41.6	5.5	53.0	54.7
% silt	38.3	44.8	33.9	51.1	28.7	22.8
% clay	22.9	14.5	24.5	43.4	17.4	22.4
% organic C	6.3	0.16	1.2	0.16	10.1	0.34

A total of roughly 20 liters of each soil was collected. Samples did not include above ground plant material, but did include roots. Samples were homogenized to pass a 4.75-mm mesh. Field moisture contents were measured and moisture release curves were determined for each soil at a bulk density of 1000 kg m^{-3} using a pressure plate apparatus (Klute, 1986).

6.3.2 Incubation Conditions

Subsamples of each soil (400 g of dry soil in a 600 ml glass beaker), in duplicate, were incubated at various combinations of temperature and moisture content. The bulk of the experiment ("Part I"), entailed the incubation of soils at constant moisture content and at three temperatures: 15°C, 25°C, and 35°C. Moisture contents corresponding to matric potentials of -0.03 MPa ($\theta 1$) and -0.50 MPa ($\theta 2$) for each soil were used (Table 6.2.). In Part II of the experiment, "A" soils were incubated at varying temperature and moisture conditions, as to simulate seasonal changes observed in the field (Table 6.3.). In Part III, "A" soils were kept at constant temperature (either 25°C or 35°C), but moisture content was varied (Table 6.4.). Soils were brought to the desired moisture content, homogenized, and packed to a bulk density of 1.0 g cm^{-3}. Soils were re-wetted with distilled water at a frequency adequate to maintain moisture content within ± 5% of the desired value. Prior to each sampling for the purpose of extraction, soils were homogenized within their beaker, and a small (approximately 40 g) sample was removed. The remaining soil was then re-packed to a bulk density of approximately 1.0 g cm^{-3}. Soils were removed from incubators for as short a period as possible to minimize changes in moisture and temperature conditions. Air was circulated using small fans inside each incubator. Incubators were vented to allow for air exchange. No-light conditions were maintained. Humidity was maintained with evaporation pans.

Table 6.2. Gravimetric moisture contents of soils as collected and at selected matric potentials. Moisture content at matric potentials of 0, -0.03, and -0.5 MPa, was measured at a bulk density of 1000 kg m^{-3}, and is equivalent to volumetric moisture content, θ. θ1 and θ2 refer to moisture contents at associated matric potentials, as imposed during incubation.

	Soil moisture content					
Matric potential	P2A	P2B	P9A	P9B	P11A	P11B
field conditions	0.122	0.210	0.051	0.220	0.074	0.110
0 MPa	0.65	0.55	0.48	0.82	0.63	0.60
-0.03 MPa ("θ1")	0.365	0.217	0.210	0.491	0.312	0.202
-0.50 MPa ("θ2")	0.206	0.149	0.123	0.354	0.167	0.138
air-dry	0.100	--	0.050	--	0.100	--

Table 6.3. Temperature and moisture conditions imposed on soils in Part II of the incubation. Moisture content is expressed as the corresponding matric potential, Ψ_m. An incubation "season" was five weeks long.

Season	$T_{mean, field}$	$T_{mean, lab}$	$\Psi_{m\ init}$	$\Psi_{m\ final}$	Wetting sequence
Summer	23.4°C	35.0°C	-0.50 MPa	air-dry	Not watered for 5 weeks, after initial moistening
Fall	15.3°C	25.0°C	air dry	-0.50 MPa	5 bar reached after 3 weeks and maintained
Winter	6.0°C	15.0°C	-0.50 MPa	-0.03 MPa	Held at 5 bar until 3rd day; brought to 0 bar on 8th day, allowed to dry to 0.3 bar and maintained
Spring	16.0°C	25.0°C	-0.03 MPa	-0.50 MPa	Brought to 0 bar on 7th day; allowed to dry to 0.3 bar over 2 weeks; maintained at 5 bar for remaining two weeks

Table 6.4. Range of moisture conditions imposed on samples in Part III. Each drying cycle was approximately two weeks long.

Treatment	Range of moisture conditions
α	0 to -0.50 MPa
β	0 MPa to air-dry
γ	-0.03 MPa to -0.50 MPa

6.3.3 Extraction and Analysis

Each sample was split into three subsamples: one for moisture content determination and acid digest, one for water extraction, and one for sodium phosphate/sodium hydroxide/sodium

acetate sequential extraction. Moisture content was determined by oven-drying at 105°C for 24 hours. The dried soil was then ground to pass a 425 μm mesh and saved for the acid digest procedure.

The acid digest procedure, designed to liberate all forms of Se in the sample, is a modification of a method suggested by Bakhtar et. al. (1989). The sample is digested using hot, concentrated HNO_3 and 30% H_2O_2 for 24 hours. The residue is then dissolved using hot 6M HCl and washed several times with HCl.

The water extraction is meant to liberate the water-soluble fraction of Se, assumed to represent Se which is dissolved or could be dissolved in the soil solution. Field-moist soil, or in this case, un-dried soil, is shaken with distilled water at a soil/water ratio of 1:5 for 1 h at room temperature, then centrifuged. Soluble fraction extractions often call for the use of a KCl solution rather than distilled water (e.g., Fujii et. al., 1988), but Kesterson soils are already salt-enriched, making the use of KCl superfluous.

The sodium phosphate extraction aims at removing both the soluble and the adsorbed fractions of Se from the sample. A 1:20 ratio of sample to 0.001 M Na_2HPO_4 is shaken for 24 h at room temperature. (Na_2HPO_4, rather than the commonly used K_2HPO_4 is employed because of the sodic nature of the soils.) The sample is centrifuged and the supernatant solution preserved for analysis. The residue is used for the sodium hydroxide extraction, which is designed to liberate Se associated with SOM. Soil and 0.02 M NaOH at a ratio of 1:10, are placed in an 85°C bath for 2 h, during which the solution is periodically shaken. The sample is then centrifuged and the supernatant solution preserved for analysis. This is a standard digestion for SOM (Schnitzer, 1982). SOM is not further fractionated into humic/fulvic components. The NaOH extraction is sequential after the phosphate extraction because of the potential for adsorbed phase liberation during the sodium hydroxide extraction.

A few selected soil samples were further extracted for carbonate-associated species using Na-acetate adjusted to pH 5 with acetic acid (Lipton, 1991). This procedure includes two Na-acetate extractions followed by a sodium phosphate wash to liberate any Se which would have been released from carbonates and subsequently adsorbed.

All supernatant solutions were passed through a 0.45 μm filter prior to analysis. Selenium analysis of all solutions was performed using hydride-generation atomic absorption spectrometry, HGAAS (Weres, et. al., 1989).

Soluble species were determined directly from the water extract. Adsorbed Se was calculated as the difference between the phosphate-extracted Se and the water-extracted Se since the phosphate procedure also liberates soluble Se. Organic-Se was determined directly from the NaOH extract. Carbonate-associated Se was determined directly from the Na-acetate extract.

Refractory Se was calculated as the difference between acid-digest-extracted Se and the sum of Se from all other extracts.

Organic carbon (OC) content was estimated using the Walkley-Black dichromate procedure (Nelson and Sommers, 1982).

Two samples were analyzed for Se speciation using x-ray absorption spectroscopy at the Stanford Synchrotron Radiation Laboratory. This method can be used to directly and non-intrusively determine Se speciation on a solid sample (Hayes et. al., 1987; Brown and Parks, 1989).

6.4 Results

6.4.1 Initial Fractionation

Initial fractionation of the six soils revealed several patterns (Fig. 6.1). Firstly, refractory Se dominates in surface soils (between 50% and 72% of total Se), while soluble Se was predominant in the "B" soils (45% to 62% of total Se). Although at first this may appear counterintuitive, since surface soils are generally more aerobic than deeper soils, it is explained by the history of Se deposition at Kesterson. The large percentage of water-insoluble Se (95.4% to 97.8%) in the "A" soils is due to strongly reducing conditions during ponding (White et. al., 1991). While most of the Se was immobilized in the top 15 cm of soil, Se which did subsequently penetrate to greater depths, evidently did so in a soluble form. The second most common pool of Se is the organic fraction, with the exception of P9A and P9B soils, in which carbonate-Se and refractory-Se, respectively, are more dominant. Total Se concentrations are one to two orders of magnitude higher in "A" soils than in "B" soils, once more in agreement with depositional history.

Carbonate-Se was measured only in selected samples over the course of the experiment, for two reasons. First, the carbonate pool was not expected to be affected by the incubation, as pH remained between 6.9 and 8, and second, the procedure is labor-intensive. Furthermore, with the exception of soil P9A, carbonate-Se is a minor fraction. Extractions of samples at the beginning and end of the incubation showed no significant changes in carbonate-Se concentrations.

6.4.2 Se Transformations: Time Trends

6.4.2.1 Part I: Constant Temperature and Moisture Content

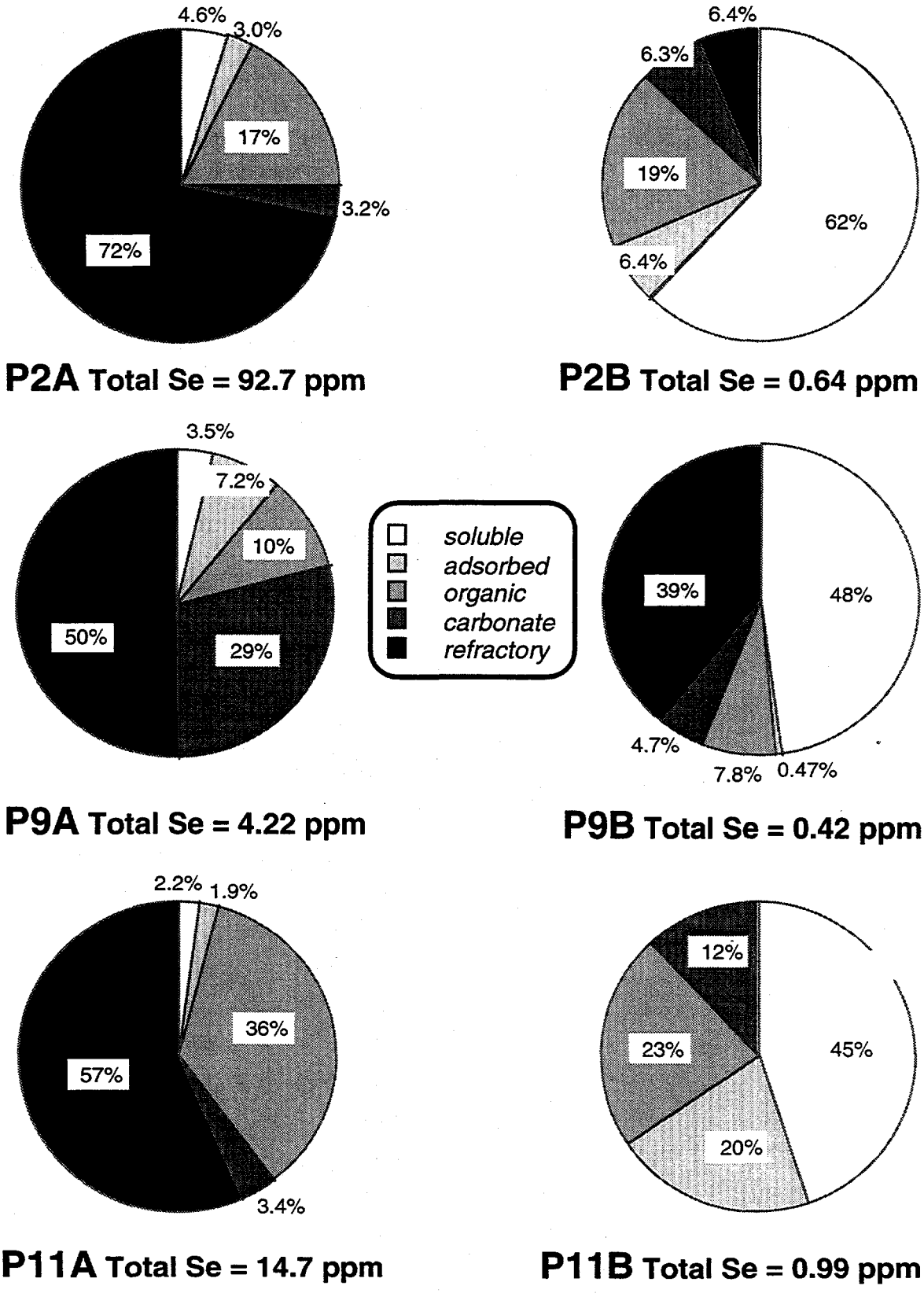

Figure 6.1. Initial Se fractionation of incubated soils.

Time trends in Se transformations are shown in Fig. 6.2 through 6.11. Total-Se for selected representative samples is shown in Fig. 6.2. The absence of decreasing trends with time suggests that volatilization of Se was not significant in this experiment. Se methylation likely did occur, but at rates too small to affect total-Se concentrations beyond the level of uncertainty associated with sample variability and analytical error. For example, should losses of Se due to volatilization be on the order of 1 $\mu g\ m^{-2}\ h^{-1}$, a rate measured at Kesterson Reservoir (Frankenberger and Karlson, 1988), then the concentration of total-Se in soil P2A would be reduced by 2.4 ppm over the 926-day period of the incubation. This is clearly within the range of uncertainty.

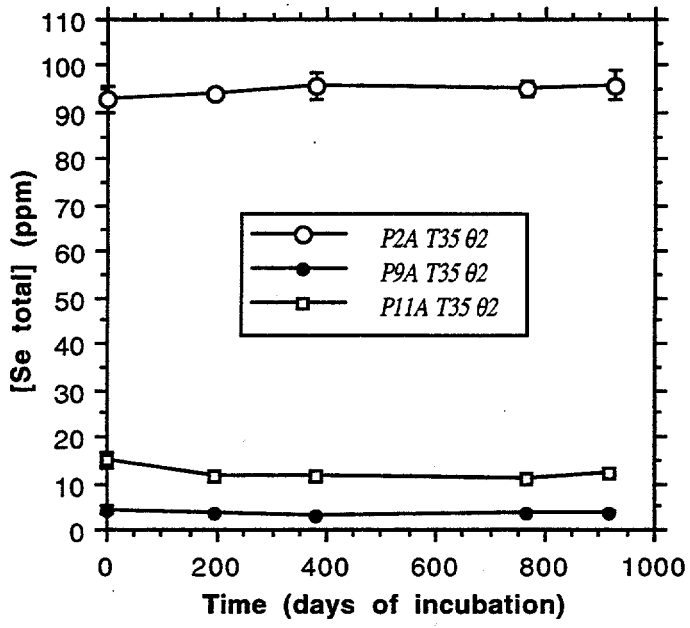

Figure 6.2. Total Se concentrations over the course of the experiment in selected soils.

As illustrated by data from soil P2B, which is representative of "B" soils, no significant changes in the fractionation of "B" soils were observed (Fig. 6.3). The trend is indicative of a system at quasi-equilibrium with respect to oxidation state. Selenium re-oxidation at depth has been documented by, among others, Tokunaga et. al. (1994). The oxidation state of Se in these samples at the time of collection reflects the result of this oxidizing trend which dominated the soil profile for four to five years after the Reservoir was drained.

Significant transformations were observed in the "A" soils (Fig. 6.4 through 6.7). With the exception of soil P2A, specifically at 35°C (Fig. 6.4 and 6.5), meaningful differences between fractionation at the two moisture conditions were not observed. As seen most clearly in Fig. 6.5, the dominant transformations were of refractory-Se and organic-Se conversion to the soluble

form. Adsorbed-Se concentrations did not change significantly. The degree to which transformations occurred was proportional to the concentration of total-Se. This is suggestive of a first, or higher, order kinetic rate dependence, which will be explored further in this paper. As seen in Fig. 6.8 through 6.11, there is a positive correlation between transformation rates and temperature, with very slow changes at 15°C and most rapid changes at 35°C. Based on data at 35°C from P2A and P11A soils, there appears to be a plateau in the refractory-Se levels, implying that the refractory-Se pool is not homogeneous with respect to its availability for oxidation: approximately 50% of this pool oxidized relatively rapidly, while the remainder did so slowly or not at all. This has important implications for estimating the long-term bioavailability of Se.

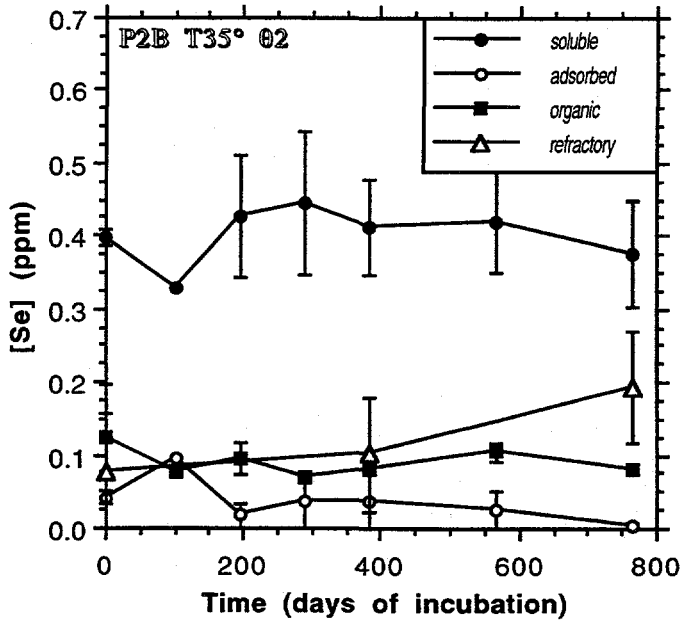

Figure 6.3. Changes in Se fractionation with time as measured in soil P2B, incubated at 35°C and moisture content θ2.

A reversal in the oxidation of refractory and organic Se took place in soil P2A incubated at 35°C at the high moisture content (θ1, Fig. 6.4 and 6.8). Following an increase in soluble-Se during the first 300 days, reduction took place through the remainder of the incubation. This probably is due to soil structure changes resulting from plant material decay over time. Visual observation of such decay over a period of about 1 yr agrees with rates of carbon turnover in plant fragments as observed by Buyanovsky et. al. (1994). This likely altered the shape of the saturation curve and resulted in θ1 being close to a saturation moisture content. θ1 is a significantly higher moisture content than what is observed in the field during most of the year (see Table 6.2) and is more likely to promote anaerobic site formation.

A decline in organic carbon content was expected, as there was no input of organic matter into the system. These losses were very minor in the "B" soils. In "A" soils, organic carbon

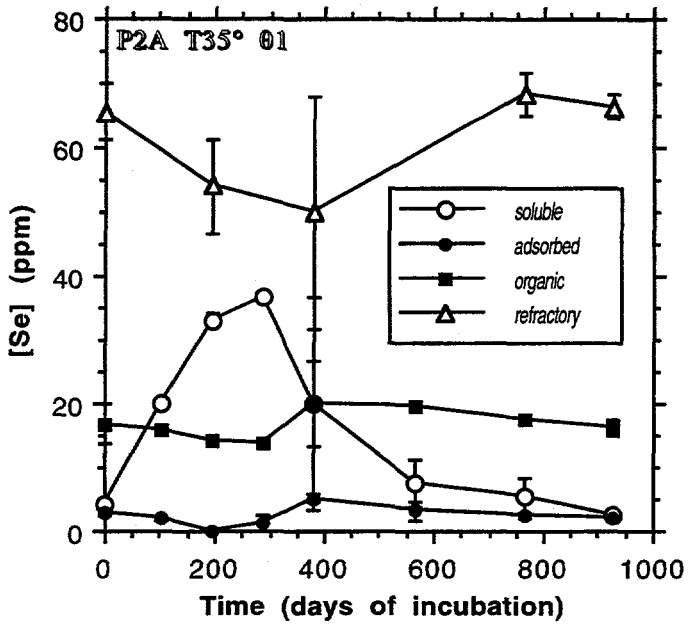

Figure 6.4. Changes in Se fractionation with time as measured in soil P2A, incubated at 35°C and moisture content θ1.

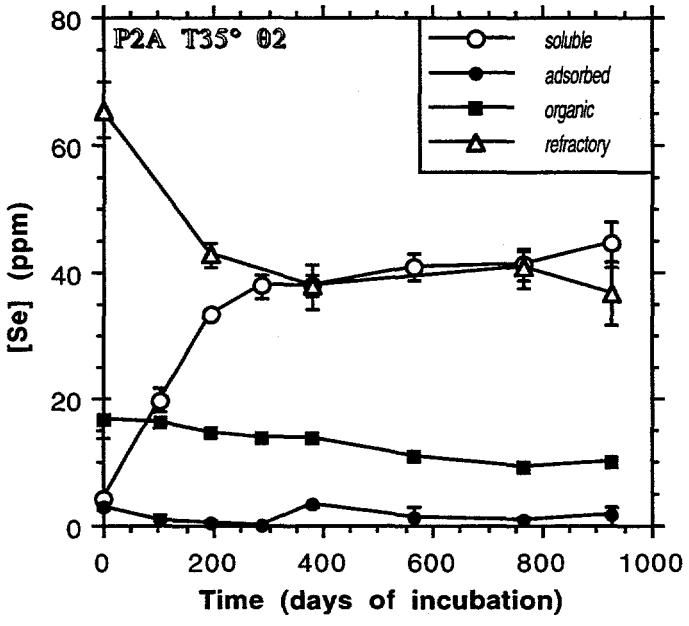

Figure 6.5. Changes in Se fractionation with time as measured in soil P2A, incubated at 35°C and moisture content θ2.

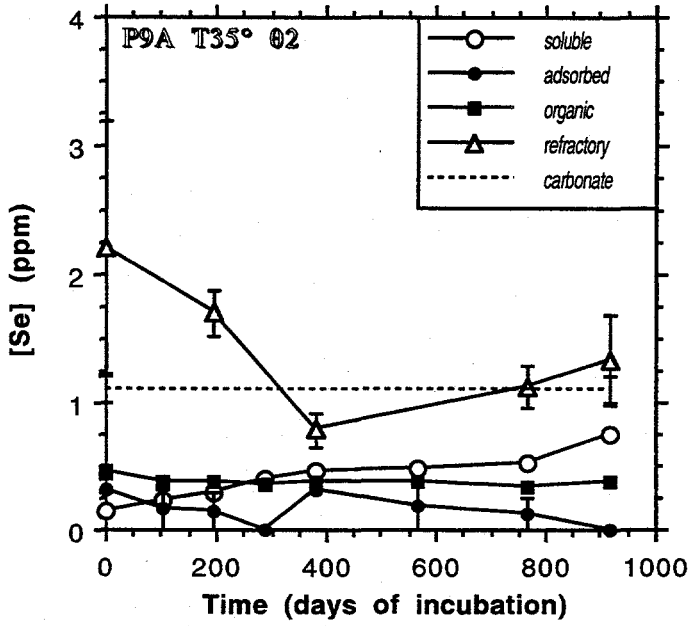

Figure 6.6. Changes in Se fractionation with time as measured in soil P9A, incubated at 35°C and moisture content θ2. The carbonate-Se concentration is based on an initial and final analysis only.

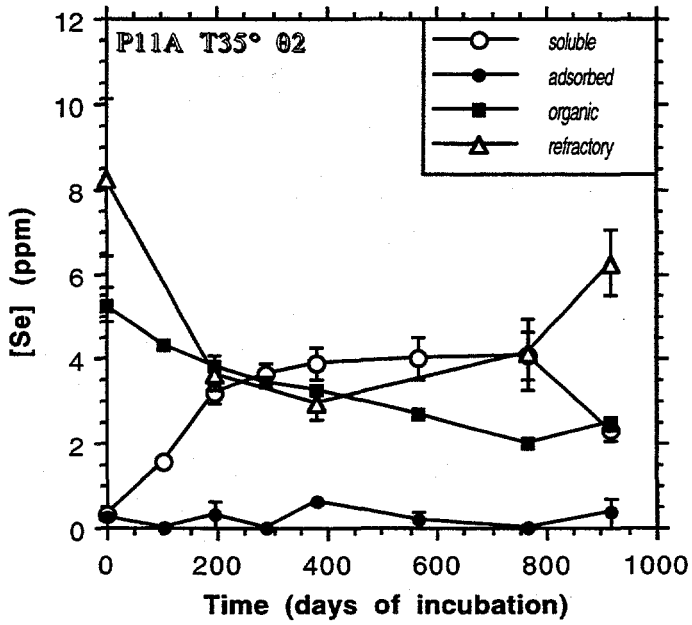

Figure 6.7. Changes in Se fractionation with time as measured in soil P11A, incubated at 35°C and moisture content θ2.

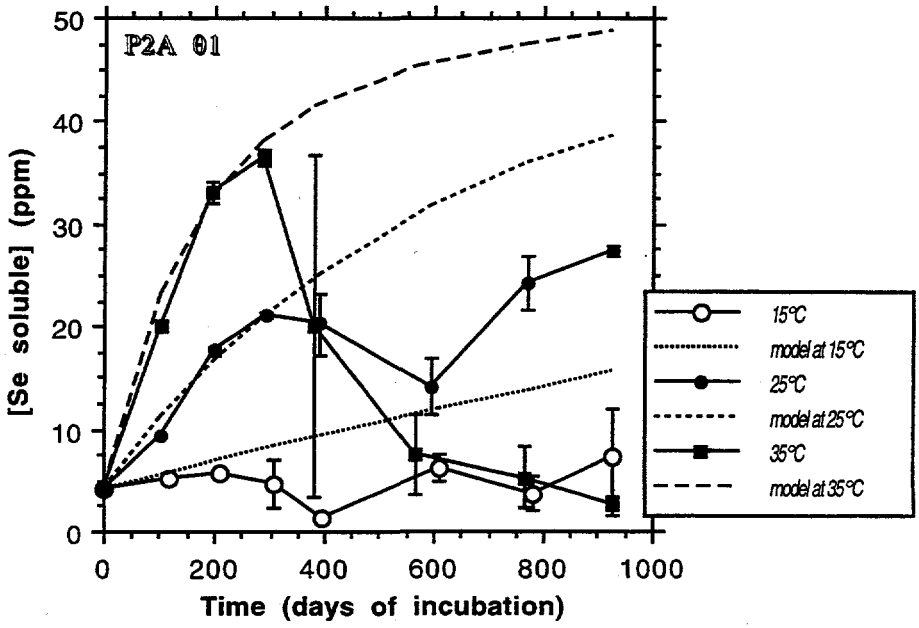

Figure 6.8. Changes in soluble-Se in soil P2A, as a result of incubation at 15°C, 25°C, and 35°C and moisture content θ1. Dashed lines correspond to results of modeling as discussed in text.

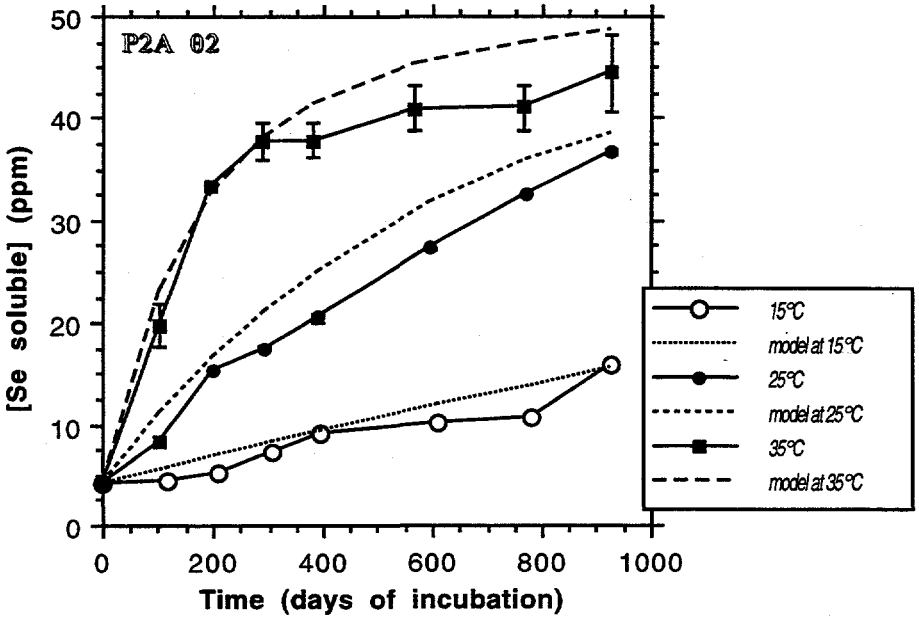

Figure 6.9. Changes in soluble-Se in soil P2A, as a result of incubation at 15°C, 25°C, and 35°C and moisture content θ2. Dashed lines correspond to results of modeling as discussed in text.

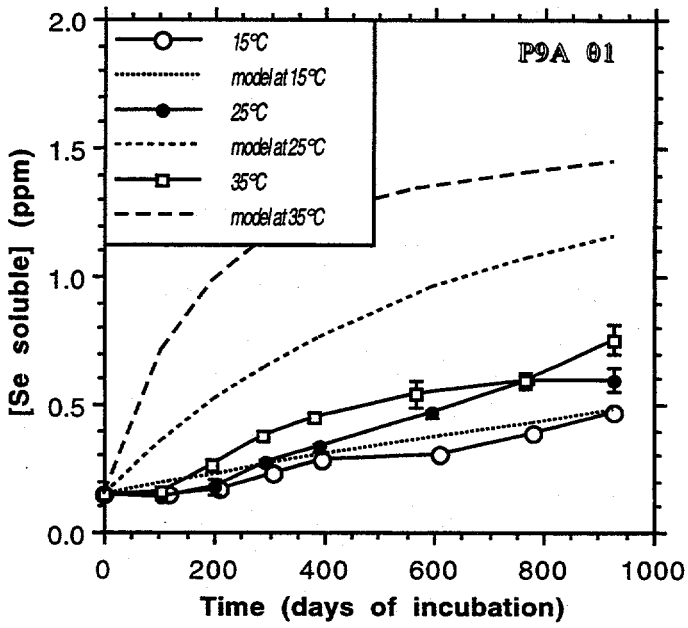

Figure 6.10. Changes in soluble-Se in soil P9A, as a result of incubation at 15°C, 25°C, and 35°C and moisture content θ1. Dashed lines correspond to results of modeling as discussed in text.

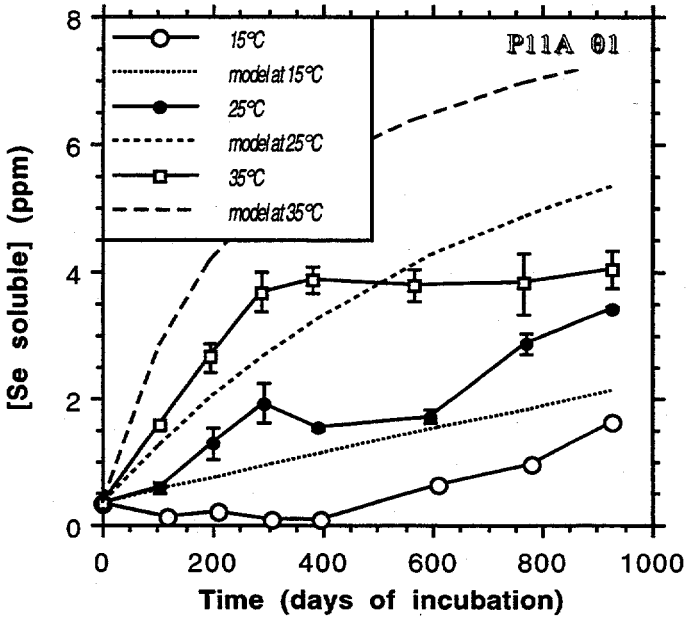

Figure 6.11. Changes in soluble-Se in soil P11A, as a result of incubation at 15°C, 25°C, and 35°C and moisture content θ1. Dashed lines correspond to results of modeling as discussed in text.

levels declined by 25% to 50%, with losses roughly proportional to incubation temperature (Fig. 6.12). Surprisingly, organic carbon declines were similar in both P2A soils incubated at 35°C, regardless of moisture content and the fact that the oxidation process was reversed in the soil incubated at high moisture content (P2A T35°C θ1). As there was a plateau in soluble-Se observed in soils P2A and P11A (see Fig. 6.5, 6.7, 6.9, and 6.11) after about 300 days, a question arises as to the effect of organic carbon depletion on oxidation. Therefore, in order to bring the organic carbon to its original level (Fig. 6.12), on day 835, glucose was incorporated into "A" soils incubated at high temperature (35°C) and low moisture content (θ2) conditions under which the most organic carbon had been consumed. Because of its simple form, the glucose was almost completely consumed over the subsequent three months. Only very minor increases of soluble-Se in P2A and P9A soils were observed over that period (cf. Fig. 6.5). An unexplained decline in soluble-Se occurred in soil P11A (Fig. 6.7). Although the results are somewhat ambiguous, it does not appear that the plateau in soluble-Se was a result of organic carbon depletion, but rather the depletion of a pool of more readily oxidizable Se.

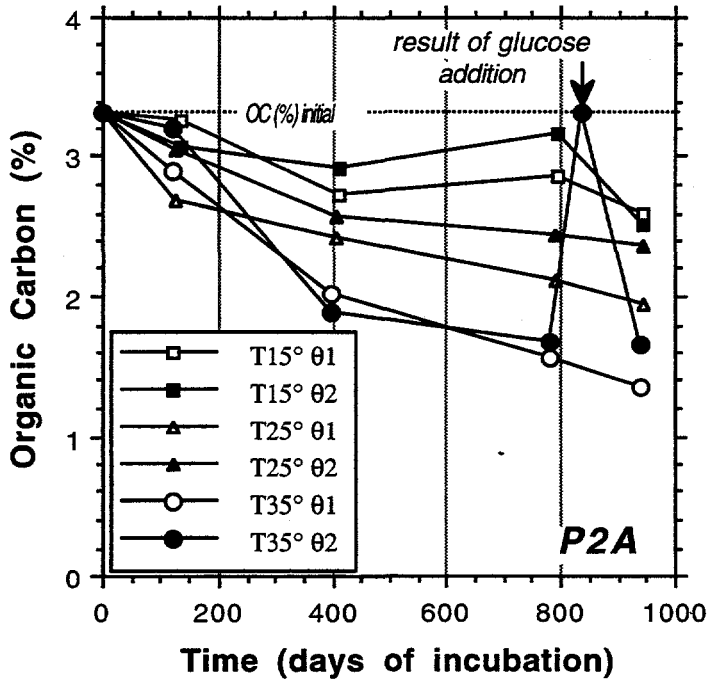

Figure 6.12. Changes in organic carbon content in soil P2A, as a result of incubation at 15°C, 25°C, and 35°C and moisture contents θ1 and θ2.

X-ray absorption analysis was performed on two samples: the initial P2A soil and P2A soil incubated at 35°C and low moisture content for 748 days. Selenium concentrations in the other soils were too low for this method. Results of the speciation of the original soil showed that the

operationally-defined refractory Se is indeed mostly Se(0) and that most of the remaining Se is Se(IV) (compare Fig. 6.13 with Fig. 6.1). The latter finding is somewhat surprising and suggests that most, if not all of the organic-Se pool is in fact in the Se(IV) form. No Se(-II) was detected. The day 748 sample speciation was in close accord with the notion of dominant oxidation of Se(0) to Se(VI). The relative percentages of species agrees moderately well with extracted fractions: on day 764, soluble-Se was 45% of total and refractory-Se was 43% of total. The decline in Se(IV) from 19% to 14% of total agrees qualitatively with the decline in the organic-Se fraction, but since the uncertainty in the x-ray absorption results is approximately 5%, the decline in Se(IV) is not significant.

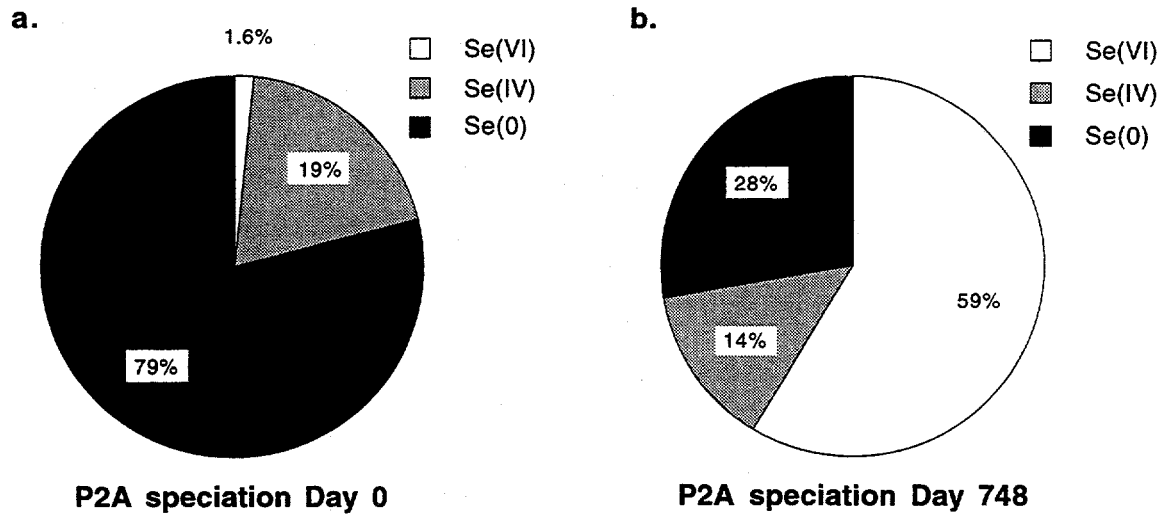

Figure 6.13. Selenium speciation results of x-ray spectroscopy of soil P2A, (a) before incubation and (b) after 748 days at 35°C and moisture content θ2.

6.4.2.2 Part II: Variable Temperature and Moisture Content

As seen in Table 6.3, each simulated "season" was five weeks long, or roughly 2.5 times shorter than a real season. Soluble-Se concentrations did not change nearly as rapidly as observed in Part I of the experiment. This is clearly due to the reduction/oxidation cycles caused by "flooding" the sample in the winter and spring parts of the cycle. Indeed, most of the rainfall observed at Kesterson Reservoir occurs in the spring (see Section 7.0). Also, following particularly intense rainfall, surface ponding is observed and results in reduction of soluble selenium (see Section 2.3). As seen in Fig. 6.14 through 6.16, selenium fractionation is very sensitive to moisture conditions. This effect is most pronounced in soils P2A and P11A. The period between Day 420 and 580, which encompassed the fourth simulated year, was closely

monitored. In soil P2A, Se oxidation resulted in an increase of soluble-Se from 2 ppm at the beginning of the summer to 8 ppm at the beginning of fall and to 11 ppm at the beginning of winter. Over the period of winter and especially spring, soluble-Se concentrations dropped back to around 2.5 ppm. Although fluctuations were observed, the net trend over the seven simulated years was that of oxidation, with soluble-Se measured at the end of the seventh fall season at over 13 ppm. In soil P11A, soluble-Se increased from an initial 0.32 ppm to a final 1.2 ppm. Soluble-Se in soil P9A was less affected by seasonal variations. Soluble-Se increased from an initial 0.15 ppm to a final 0.35 ppm. There is a suggestion of a dependence of reaction rate on Se concentration, which agrees qualitatively with findings from Part I.

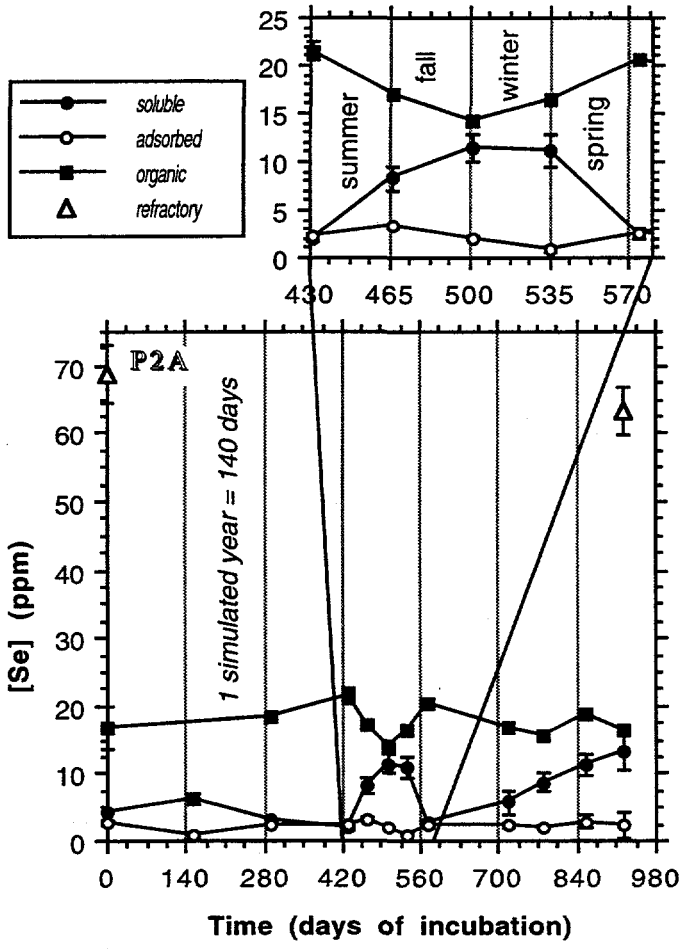

Figure 6.14. Changes in Se fractionation in soil P2A, as a result of incubation at varying moisture content and temperature. See Table 6.3 for incubation conditions.

It appears that when exposed to short term changes in moisture conditions, oxidation of organic-Se and reduction of soluble-Se back to organic-Se are the most prominent processes, in

contrast to long term oxidation, which is the result of refractory (or elemental) Se oxidation (Fig. 6.14 and 6.16). Based on x-ray absorption results, most of the organic-Se fraction has a valence of (+4). Selenite is more likely to be largely adsorbed onto organic matter rather than covalently bonded within the SOM structure. This would explain the ease with which Se is released from SOM upon oxidation as observed between Days 420 and 500.

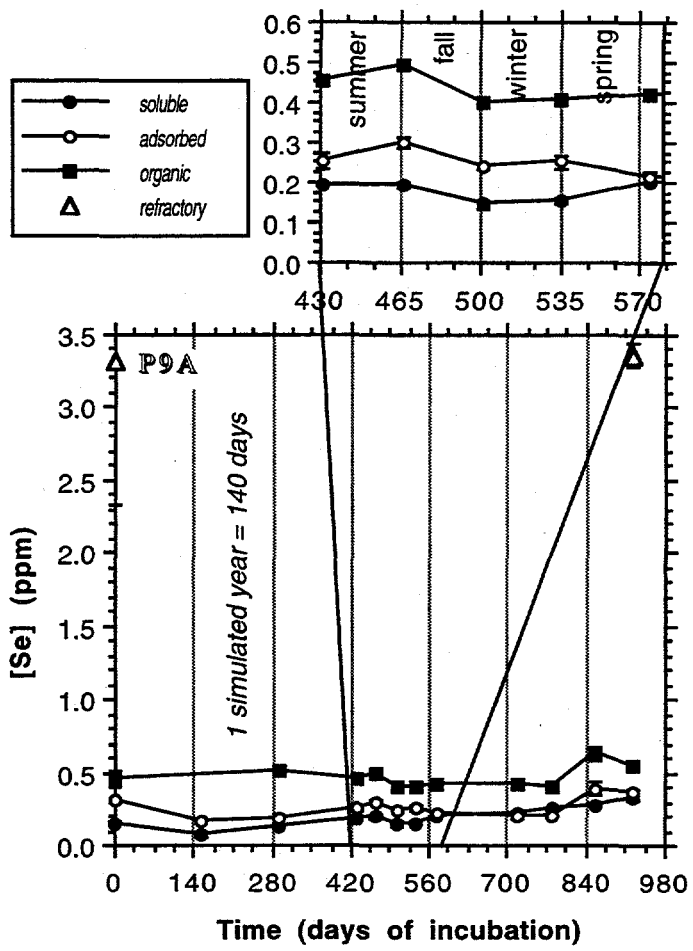

Figure 6.15. Changes in Se fractionation in soil P9A, as a result of incubation at varying moisture content and temperature. See Table 6.3 for incubation conditions.

There were no net significant changes observed in adsorbed-Se. This agrees with field observations. Even during periods of relatively rapid Se reduction, such as between Days 535 and 580, adsorbed-Se did not increase substantially, while the increase in organic-Se was roughly equivalent to the decrease in soluble-Se, once more suggesting association with SOM rather than adsorption onto inorganic solids.

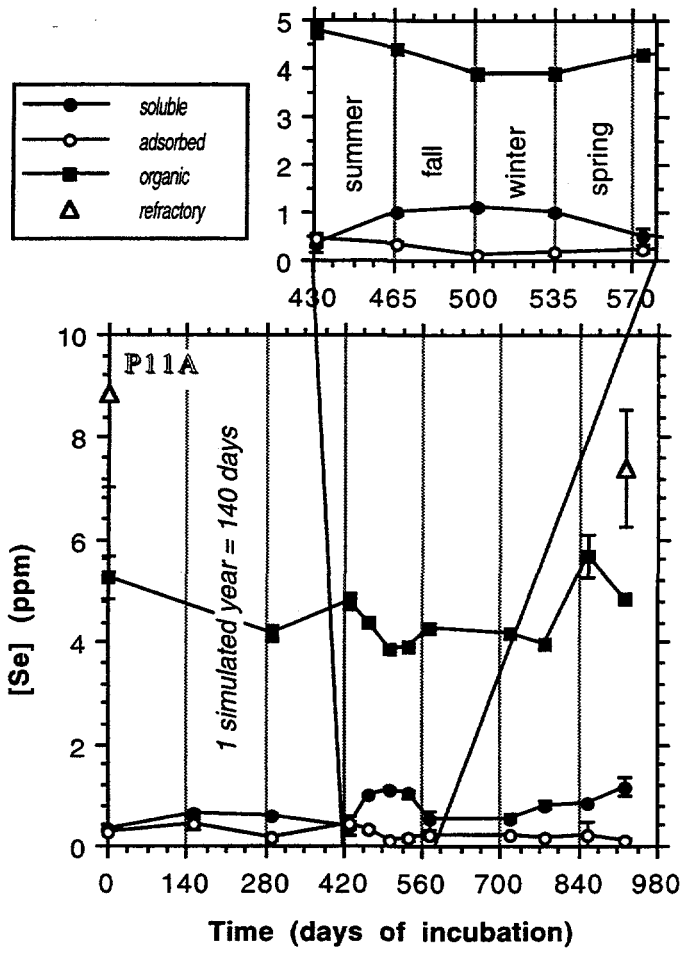

Figure 6.16. Changes in Se fractionation in soil P11A, as a result of incubation at varying moisture content and temperature. See Table 6.3 for incubation conditions.

6.4.2.3 Part III: Constant Temperature and Varying Moisture Content

The results of this part of the experiment are representative of what may happen in the field under conditions of fluctuating moisture conditions, here varied with a two-week periodicity. Incubation conditions α and β were similar in that in both cases samples were brought to full saturation and allowed to dry, although in treatment α, only to a moisture content equivalent to a matric potential of -0.5 MPa, whereas in treatment β, the soils were allowed to dry out to an "air-dry" condition. Surprisingly, the results of fractionation were very similar for both cases.

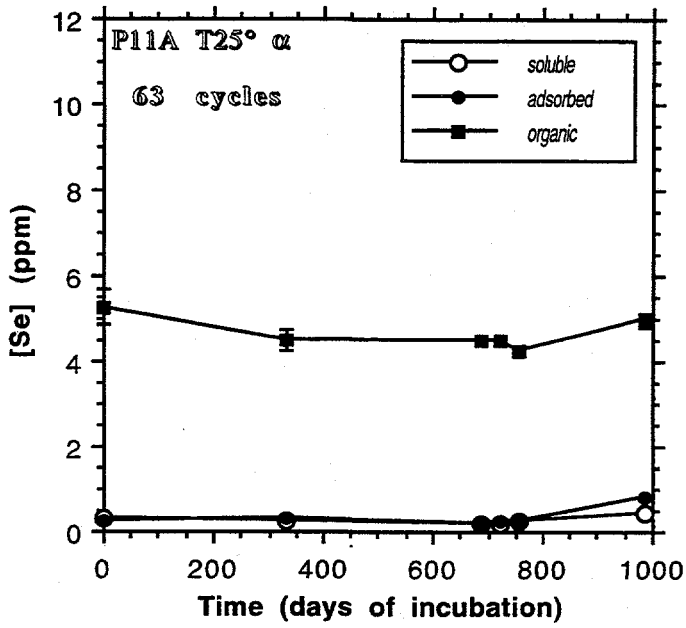

Figure 6.17. Changes in Se fractionation in soil P11A, as a result of incubation at 25°C and varying moisture content α. See Table 6.4 for incubation conditions.

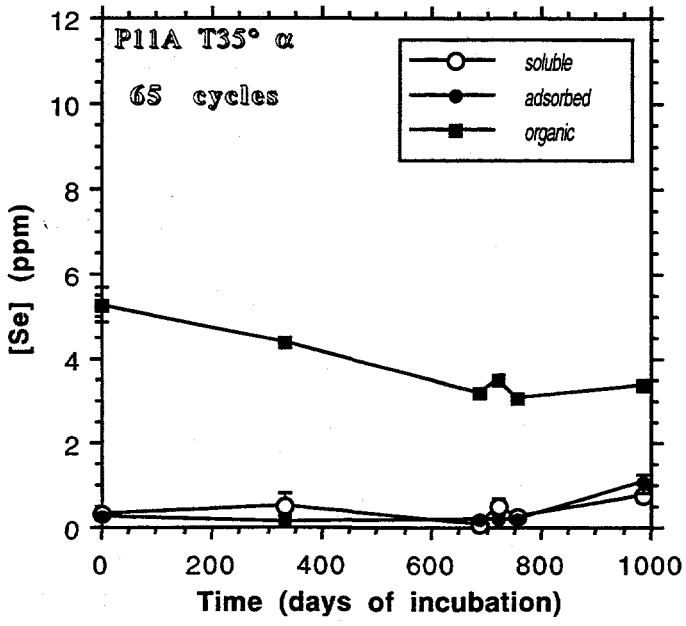

Figure 6.18. Changes in Se fractionation in soil P11A, as a result of incubation at 35°C and varying moisture content α. See Table 6.4 for incubation conditions.

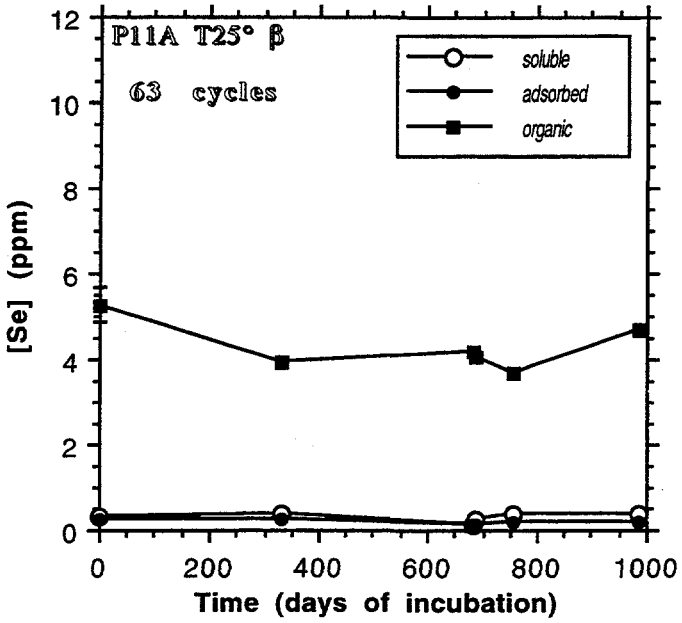

Figure 6.19. Changes in Se fractionation in soil P11A, as a result of incubation at 25°C and varying moisture content β. See Table 6.4 for incubation conditions.

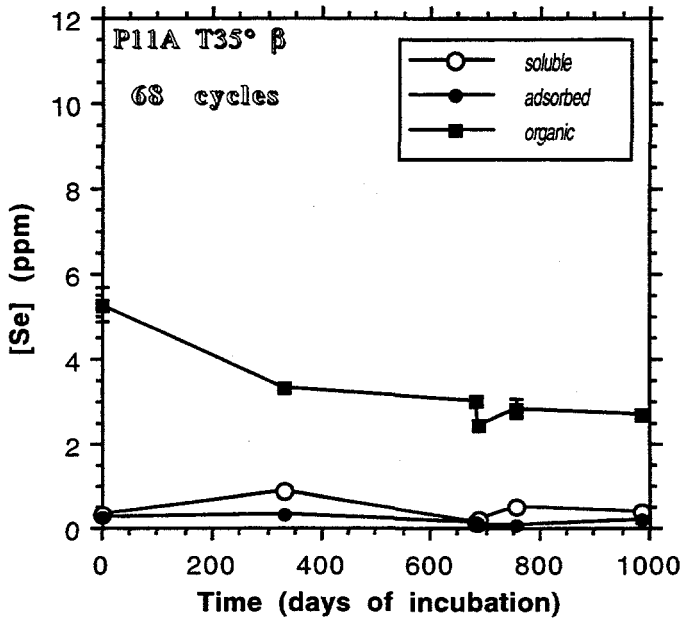

Figure 6.20. Changes in Se fractionation in soil P11A, as a result of incubation at 35°C and varying moisture content β. See Table 6.4 for incubation conditions.

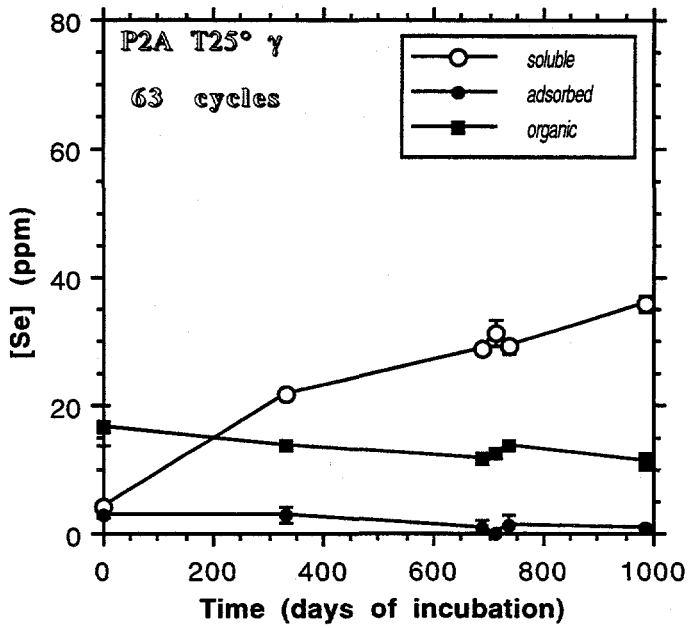

Figure 6.21. Changes in Se fractionation in soil P2A, as a result of incubation at 25°C and varying moisture content γ. See Table 6.4 for incubation conditions.

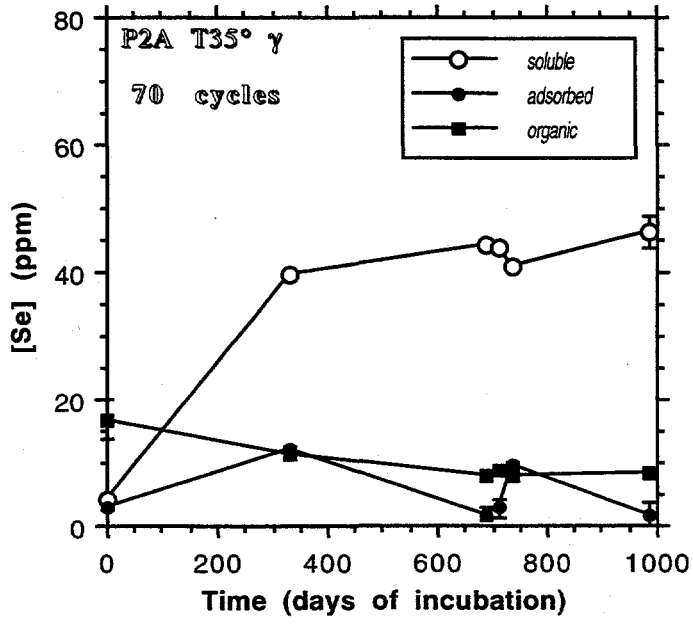

Figure 6.22. Changes in Se fractionation in soil P2A, as a result of incubation at 35°C and varying moisture content γ. See Table 6.4 for incubation conditions.

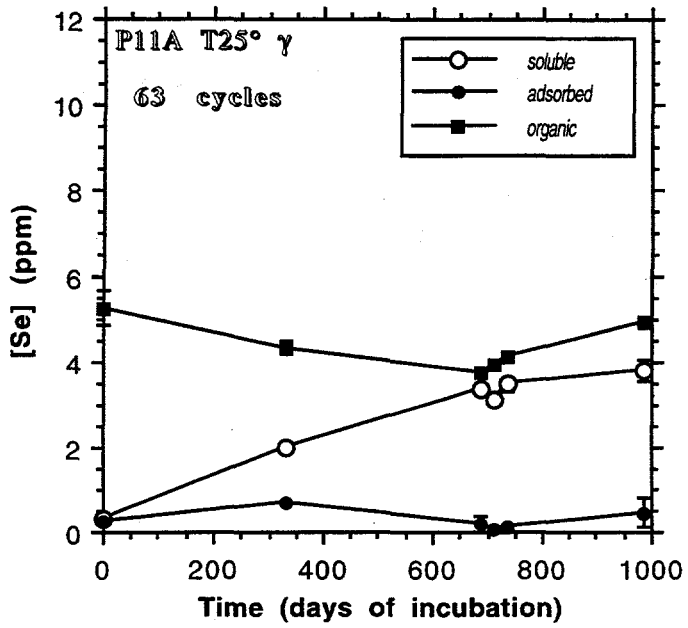

Figure 6.23. Changes in Se fractionation in soil P11A, as a result of incubation at 25°C and varying moisture content γ. See Table 6.4 for incubation conditions.

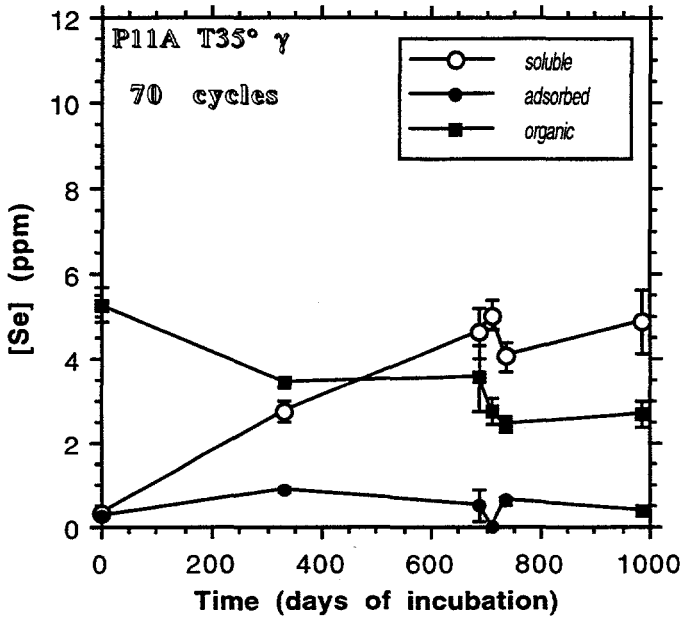

Figure 6.24. Changes in Se fractionation in soil P11A, as a result of incubation at 35°C and varying moisture content γ. See Table 6.4 for incubation conditions.

Generally, at 25°C, few long-term changes were observed, though there were fluctuations in both the organic-Se and the soluble-Se fraction within a wetting/drying cycle (Fig. 6.17 through

6.20; here soil P11A is shown as a representative example). These intra-cycle trends were somewhat more pronounced in the β treatment, which is on average drier than α.. The only long-term trend observed was the decline in organic-Se at 35°C (Fig. 6.18, 6.20). Since the corresponding soluble-Se concentrations were either smaller or nonexistent, it appears that organic-Se was being reduced to elemental Se, or at least moved into the refractory pool. These trends are indicative of a much faster reduction than oxidation of Se, which has been consistently observed in the field (Long et. al., 1992; Tokunaga et. al., 1994).

Treatment γ was different in that the range of moisture contents was within equivalent matric potentials of -0.03 MPa and -0.50 MPa. Thus, even though the -0.03 MPa-equivalent moisture content was relatively close to saturation and the -0.50 MPa dry limit was the same as in case α, the soil was never saturated. This produced vast differences in fractionation over the course of the incubation (Fig. 6.21 through 6.24). In fact, the moisture fluctuation seemed to have very little effect on Se transformations as compared with Part I where moisture content was maintained constant. For example, comparing Fig. 6.22 with Fig. 6.5, the trend of fractionation with time is more or less the same. There are vast increases in soluble-Se, at the expense of refractory-Se and to a lesser extent organic-Se. There also appears to be a plateau in soluble-Se at around 45 ppm. This result is indicative of the fact that as long as the soil is not saturated but kept within a range of likely field moisture conditions, Se transformation rates are not affected profoundly.

6.4.3 Quantification of Oxidation Rates

Given the observation of temporal changes in Se fractionation in Part I of this experiment, one can attempt to quantify rates of Se oxidation. Because of the frequent variation of incubation conditions in Parts II and III, such quantification would be ambiguous. The difficulty which arises is that unlike commonly conducted two-component kinetic experiments, the definition of species involved in these transformations is problematic. Although the main product of the reaction is clearly Se(VI), the reactants are poorly defined. As discussed earlier, organic-Se is an operationally-defined pool which likely includes a number of Se forms, though Se(IV) appears to dominate. Therefore, there are likely several rate constants which apply to components of this fraction. Although primarily consisting of elemental Se, similar provisos apply to the refractory-Se pool.

While understanding the uncertainties associated with this approach, rate constants for the oxidation of organic-Se and refractory-Se to soluble-Se were calculated. Given the apparent dependence of transformation rates on total Se concentrations, first-order reactions were assumed. Numerous studies have shown that the assumption of first-order kinetics may not best

represent the system (e.g. Onken and Matheson, 1982). Among other models, the fitting of data to a polynomial equation are often found to give best results (Marion and Black, 1987). However, in this case, it was felt that such a treatment would not improve the understanding of the processes in question. Furthermore, the application of a more complex model, given the limitations of what are largely operationally-defined results, would be inordinate.

As pointed out earlier, approximately 50% of the refractory-Se pool was readily oxidizable. For the purpose of rate determination, only this sub-fraction of refractory-Se, which will be called refractory-A, was considered. If one considers all refractory-Se, the data do not fit any of the commonly-used kinetic models. The two reactions to be considered are:

$$Se^{0}_{refA} \xrightarrow{k_{refA}} Se^{6+}_{sol} \qquad [2]$$

and,

$$Se^{4+}_{org} \xrightarrow{k_{org}} Se^{6+}_{sol}. \qquad [3]$$

Assuming first-order kinetics,

$$\frac{dSe^{6+}_{sol}}{dt} \approx -\left[\frac{dSe^{4+}_{org}}{dt}\right] - \left[\frac{dSe^{0}_{refA}}{dt}\right] \qquad [4]$$

where,

$$-\frac{dSe^{0}_{refA}}{dt} = k_{refA} Se^{0}_{refA} \qquad [5]$$

$$-\frac{dSe^{4+}_{org}}{dt} = k_{org} Se^{4+}_{org} \qquad [6]$$

After integration,

$$-\ln\left(Se^{0}_{refA}\right) + \ln\left(Se^{0}_{refA,init}\right) = k_{refA} t \qquad [7]$$

$$-\ln\left(Se^{4+}_{org}\right) + \ln\left(Se^{4+}_{org,init}\right) = k_{org} t \qquad [8]$$

Note that the valence states in the equations above are supported by limited information. Based on Equations [7] and [8], a plot of the negative natural log of the reactant versus time should be linear if first-order kinetics apply. Such plots for soil P2A are shown in Fig. 6.25. Generally, the

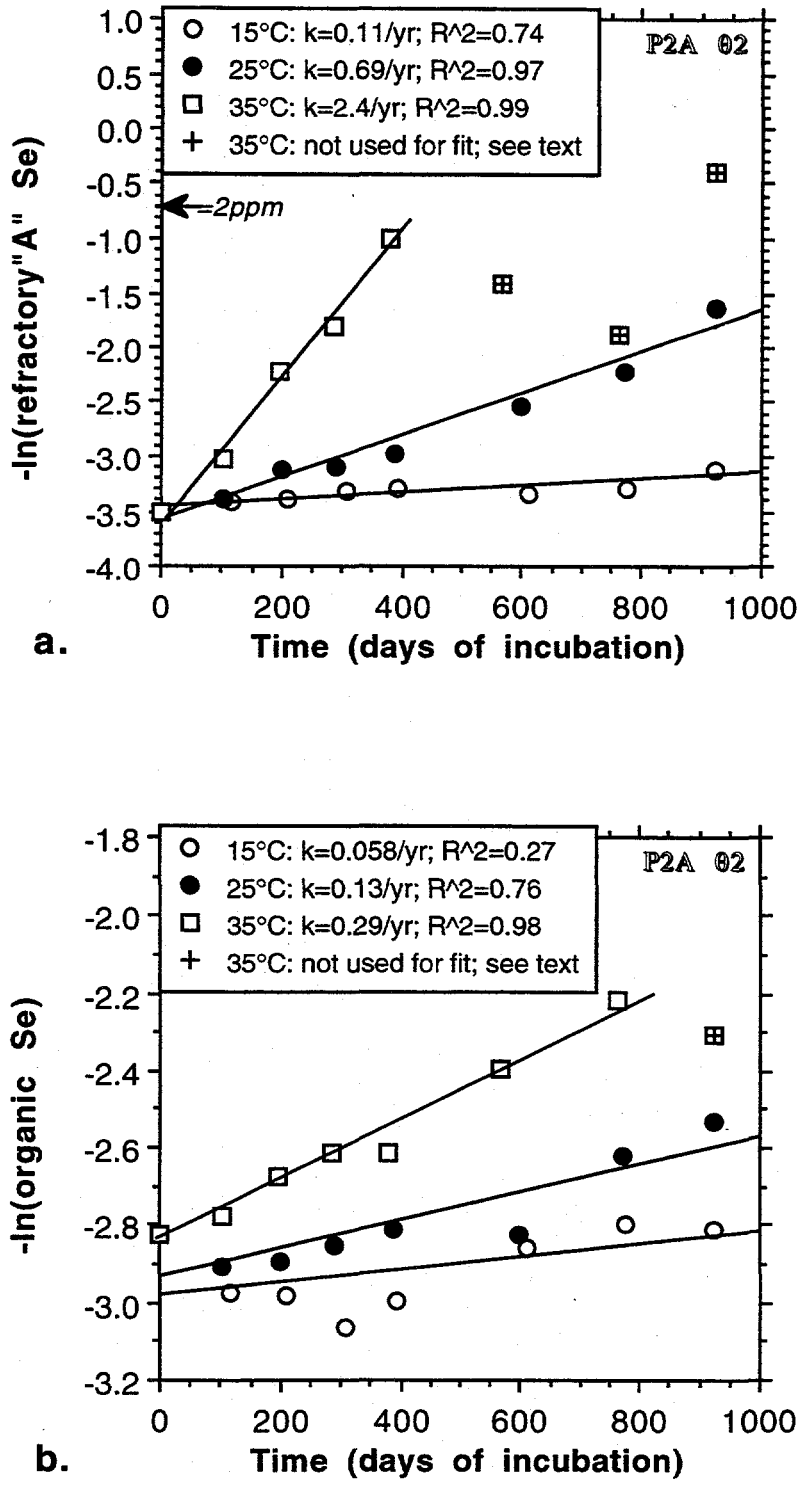

Figure 6.25. First-order fits to the decline in (a) refractory-A-Se and (b) organic-Se, in soil P2A, incubated at 35°C and moisture content θ2.

data conform to the model. The last three data points at 35°C were not used in Fig. 6.25a due to the large cumulative error in calculating the refractory pool and because they are very close to the aforementioned refractory-Se plateau (cf. Fig. 6.5). The last data point at 35°C was used in neither plot as it was measured after the addition of glucose to the system.

k_{refA} values fall between 0.11 yr^{-1} at 15°C and 2.4 yr^{-1} at 35°C, while k_{org} values fall between 0.058 yr^{-1} at 15°C and 0.29 yr^{-1} at 35°C. k_{org} increases with temperature at a consistent Q_{10} of approximately 2.2, while k_{refA} increases at a Q_{10} of 6.1 between 15°C and 25°C and 3.5 between 25°C and 35°C. Thus, the temperature dependence of k_{org} appears to fall in line with the Q_{10} concept, while that of k_{refA} does not. Overall, transformation rates in soil P2A were accelerated 20-fold at 35°C compared to 15°C.

A major assumptions in this analysis is the independence of each oxidation reaction. This is a very bold supposition, as there is no evidence that Se which is "released" from one reduced fraction does not cycle through another before becoming fully oxidized in the Se^{6+} state. What is evident is that Se is far more susceptible to net release from the refractory (?elemental) pool than from the organic pool. The rate constants presented in Fig. 6.25 were used to predict the formation of soluble-Se in the three soils (Fig. 6.8 through 6.11). In each case, only 50% of the refractory-Se was assumed to be oxidizable. As expected, the fit is very good for soil P2A θ2, since data from the incubation of this soil was used to derive the reaction rate constants. The model also fits the early time data for soil P2A θ1 very well, but subsequently fails as the aforementioned reduction took place after day 300. Oxidation of Se in soil P9A was modeled adequately at 15°C but was grossly overestimated at higher temperatures. Oxidation in soil P11A was also overestimated, but model results were within a factor of 2 for all temperatures.

The overall mediocre fit of the model to soils P9A and P11A suggests that the rates may be more strongly dependent on Se concentrations, organic carbon content, or a combination of both. A regression-based model of these variables may produce a superior fit.

6.5 Discussion

Several site-specific as well as broader conclusions may be drawn from the data presented herein. The absence of Se transformations in the "B" soils suggests that Se is more or less chemically stable in the deeper soils and sediments of Kesterson Reservoir. On the other hand, the relatively high percentage of soluble-Se allows for significant physical redistribution. Carbonate-Se in deeper soils may become a source of soluble-Se under lower pH conditions which are commonly generated as a result of root acidification (McBride, 1994, Ch.5). However, long-term oxidation of Se at depth will not critically affect the total inventory of soluble-Se.

Transformations observed in "A" soils help define readily oxidizable vs. stable pools of Se. Both the refractory-Se and organic-Se fractions were oxidizable under lab conditions. The precise nature of refractory-A-Se is not known, though all evidence suggests that it is primarily Se(0). The more stable sub-fraction of the refractory pool also appears to be Se(0), but may be more intimately associated with the solid matrix or some portion of SOM which was not extracted with the sodium hydroxide procedure. Oxidation rates are relatively low at mean field temperature (15°C). However, soil surface temperatures often reach 35°C during summer and early fall. Therefore, measured rates could be applied to modeling Se oxidation over a range of temperatures and unsaturated conditions.

Parts II and III, in which soils were incubated at varying moisture and temperature conditions were designed to mimic natural conditions but still accelerate transformation rates. Data from these incubations show a very strong tendency for reduction during periods of saturation. This agrees well with the much slower net oxidation of Se observed under field conditions (Tokunaga et. al., 1994). When wetting/drying cycles are of a two-week frequency, long-term Se oxidation rates are very slow and there appears to be an exchange of Se between the organic and refractory pool.

Quite clearly, Se oxidation rates need to be applied with great care to the field setting. They certainly apply to conditions observed during summer and fall months and provide an upper boundary on long-term transformation rates. Rates measured herein agree qualitatively with long-term rates observed in the field (Benson et. al., 1994). Summertime re-oxidation of Se near the soil surface contributes to the redistribution of Se deeper into the soil profile with infiltrating rainwater in the winter. The weak dependence on moisture variations in the unsaturated range, suggests that the oxidation cycle of Se at depth, while much slower, will be subject to fewer fluctuations in rate and direction.

The satisfactory correlation between results of wet chemistry extractions and x-ray absorption spectroscopy of P2A soil supports the use of extractions as a means for fractionation, provided that limitations are well understood. Probably the single most pressing question arising from this work is the nature of the oxidizable refractory-Se vs. the more resistant fraction. Further work with x-ray absorption in conjunction with wet extraction procedures may shed light on this issue.

7.0 Ephemeral Pools: Summary of 1992 to 1994 Water Quality

Tetsu Tokunaga
Earth Sciences Division
Lawrence Berkeley Laboratory

Concerns for selenium concentrations in ephemeral pools formed during the wet seasons at Kesterson Reservoir were first identified in the winter of 1986-87. Ephemeral pools were found in many areas which were not intentionally managed as ponded environments. Selenium concentrations in the ephemeral pools sampled in March 1987 ranged from 38 to 2550 ppb, with a geometric mean of 197 ppb (Figure 7.1). These early uncontrolled occurrences of surface waters resulted primarily from a combination of seepage from adjacent intentionally ponded areas of Kesterson Reservoir, and from the seasonal rise of the shallow water table. Rainfall provided a minor additional source for surface waters during that drought year. Thus, the process of formation of these earlier ephemeral pools differed from that commonly associated with vernal pools found in many other areas in the San Joaquin and Sacramento Valleys. Vernal pool formation is generally associated with rainfall ponding over low permeability soils. The seasonal rise of surface waters was identified as a mechanism for the formation of highly seleniferous pools in topographic depressions (LBL annual report, 1987). The rise of the shallow water table under Kesterson Reservoir soils in response to seasonal flooding of surrounding wetlands provides the possibility for displacing seleniferous soil waters (Se concentrations in the 100s to 1000s of ppb) upwards to pond at the surface. This phenomenon was expected to be even more common in the event that remediation activities involved excavation of the surface soils, leaving larger areas at lower elevations. Monitoring of an experimental test plot in Pond 6, in which the surface 1 ft of soil was removed, was performed to determine whether or not the anticipated high Se concentrations would surface. The water table intercepted the excavated surface from November 1987 through March 1988, resulting in ponding of waters with selenium concentrations ranging from 900 up to 6,000 ppb (Figure 2; from Tokunaga and Benson, 1992). Draining and filling of Kesterson Reservoir ponds was completed by the late summer of 1988 in order to prevent reoccurrence of ephemeral pools formed by water table rise. This action, along with below-average rainfall from 1988 through the end of 1991, resulted in three years without significant ponding. The only site which regularly re-ponded was a small monitoring area in Pond 10, left unfilled for purposes of observing this phenomenon.

7.1 Background

Ephemeral pools formed at Kesterson Reservoir since soil-filling have resulted almost exclusively from rainfall ponding rather than from shallow water table rise. These two different causes of ponding result in generally very different surface water composition. Rainfall ponding, typical of vernal pools, tends to be preceded by an interval during which salts (including soluble Se species) are leached from the soil surface downwards into the soil profile. This leaching process is generally more effective at Kesterson Reservoir than at more typical vernal pool areas which have clayey, low permeability surface soils (Barbour and Major, 1988). An additional factor contributing to rainfall ponding at Kesterson Reservoir is soil compaction from vehicle tracks. Both filled and unfilled areas subject to vehicle traffic can experience decreases in surface soil permeability as well as slight decreases in elevation. Some of the smaller but persistently ponded areas are associated with vehicle tracks. The resulting ephemeral pool waters can be initially relatively low in salinity and Se concentrations. As noted earlier, ponding from water table rise will displace soil salts and soluble Se into the resulting surface waters. Regardless of the mechanism for ephemeral pool formation, evaporation of surface waters and diffusive-advective exchanges of solutes between surface waters and surface sediment pore waters will determine time trends in surface water quality. In the case of Se, additional oxidation-reduction transformations in surface waters and surface sediments are also very important in determining time trends in surface water quality.

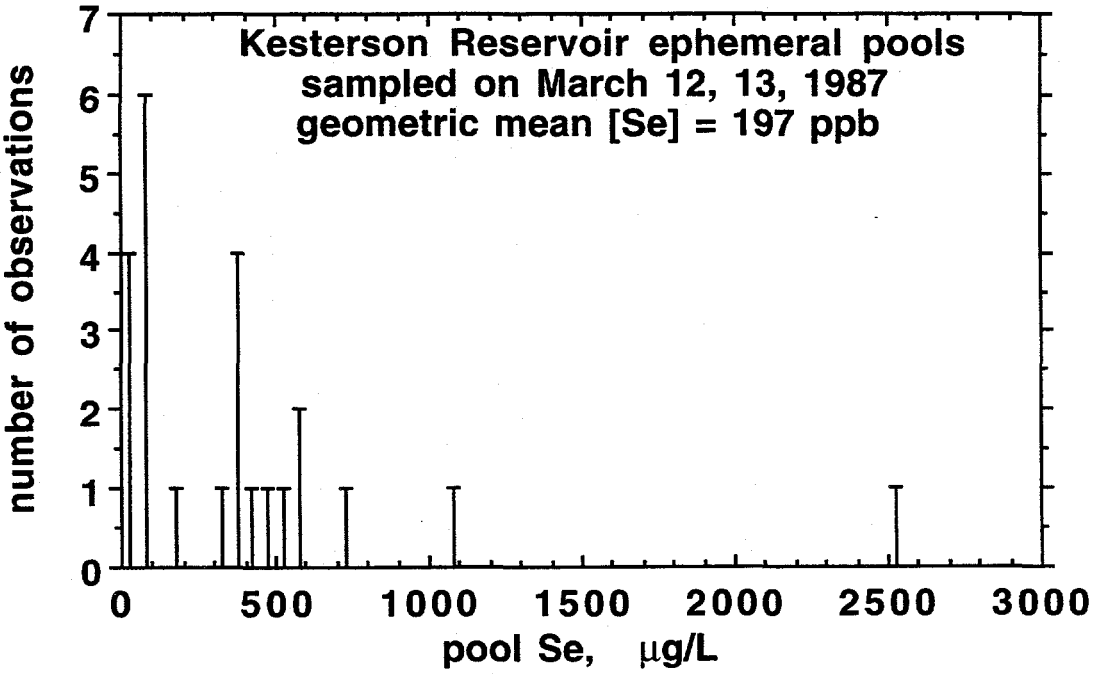

Figure 7.1. Histogram of selenium concentrations in March 1987 ephemeral pools.

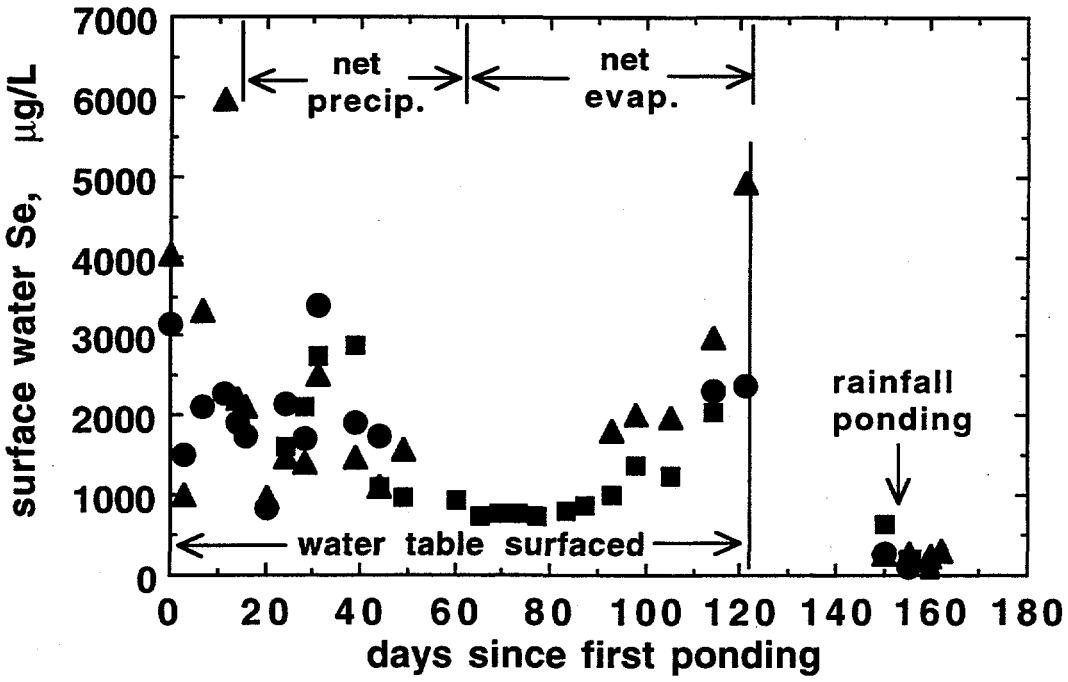

Figure 7.2. Selenium concentrations in an ephemeral pool generated by water table rise (Pond 6, site P6S12, 1987-1988 wet season).

7.2 Field Monitoring

During the wet seasons of 1991-92 and 1992-93, above-average rainfall was received, resulting in significant areal coverage with ephemeral pools (estimated to cover as much as 10 to 30% of Kesterson Reservoir). The large majority of these areas (more than 95%) formed from rainfall ponding rather than by shallow water table rise. Rainfall totals of 320 mm and 420 mm, respectively, were received in those two years. The latest wet season (1993-1994) brought an about average amount of rainfall (280 mm). Rainfall records at Kesterson Reservoir are summarized in Figures 3A and 3B. During each of these past three wet seasons, periodic monitoring of a set of ephemeral pools was performed by LBL, supplementing sampling by the USBR. During these years, LBL sampling of ephemeral pool waters at locations within Ponds 1, 3, 4, 5, 6, 9, 10, and 11 (Figure 4) was frequent enough to describe site-specific characteristics of ephemeral pool selenium concentrations. This chapter updates information provided in the LBL Dec. 1992 report, which was compiled following the first non-drought year since closure and (soil) filling of Kesterson Reservoir, and supplements data provided in USBR annual reports. Pools formed during the 1991-92 wet season lasted for up to about 60 days. Pools formed during the 1992-93 wet season were in many cases much more persistent, lasting for up to about 120

days. Pools formed during the 1993-1994 wet season were generally of short duration, typically lasting less than 30 days. Because of extensive vegetation coverage, estimating the area covered by shallow pools is generally difficult. Visual inspection indicates that Ponds 3 and 5 appear to experience the most extensive rainfall ponding. Perhaps as much as 30% of each pond was flooded during parts of 1992 and 1993. Ponds 4 and 6 also experience significant ponding during these wet seasons (perhaps as much as 15% coverage). All other areas of Kesterson Reservoir were less vulnerable to ephemeral pool formation.

In many cases, distinctions in surface water quality can be made between pools formed on fill soil versus pools formed on original Kesterson Reservoir soils Additional distinctions can be made between sites covered primarily with imported (initially nonseleniferous) fill soil versus sites covered with variable amounts of original (seleniferous) Kesterson Reservoir soil. Unfilled sites may be divided into areas which do or do not experience surfacing of the shallow water table. It should be noted that the few locations in which ponding has resulted from water table rise during the past three years are all in research sites where filling to meet target surface elevations has been postponed for the sake of obtaining monitoring results on long-term selenium behavior. Within individual pools, sampling was usually sufficient to obtain time trends in selenium concentrations and salinity within each wet season. The duration of ponding was very season- and site-specific. It is apparent from the data that selenium concentrations within a given pool can vary tremendously over time. Smaller variations in concentrations are typically observed in pools with low average selenium concentrations. Pools with high initial Se concentrations typically exhibit large declines in selenium during the ponded period.

Examples of ephemeral pool water quality from (1) sites covered primarily with imported fill soil, (2) sites filled with a mixture of original Kesterson soil and imported soil, (3) upland, unfilled sites experiencing rainfall ponding, and (4) unfilled sites experiencing water table rise will be presented in separate sections. Assignment of rainfall ponding versus water table rise to origins of individual pools is based on relative elevations of local soils surfaces and of shallow water tables. At most, only a few characteristic sites will be described in each of these four categories. Data to be presented in the following sections consist of time trends for selenium concentrations, salinities (EC), and ratios of selenium concentrations to EC measurements for pool waters. The [Se]/EC ratio provides an indicator for changes in surface water selenium concentrations relative to other common ions (primarily Na^+, Cl^-, and SO_4^{2-}). This ratio can help distinguish influences of either rainfall dilution or simple evaporative concentration, both of which would influence EC values in direct proportion to changes in Se concentrations. EC values are expressed in units of dS/m, which is equivalent to mmho/cm (also equal to 1,000 µmho/cm). Following these four descriptive sections, a short section on laboratory studies

concerning exchanges of Se between ponded waters and surface sediments is presented. Recommendations are included in the final section of this chapter.

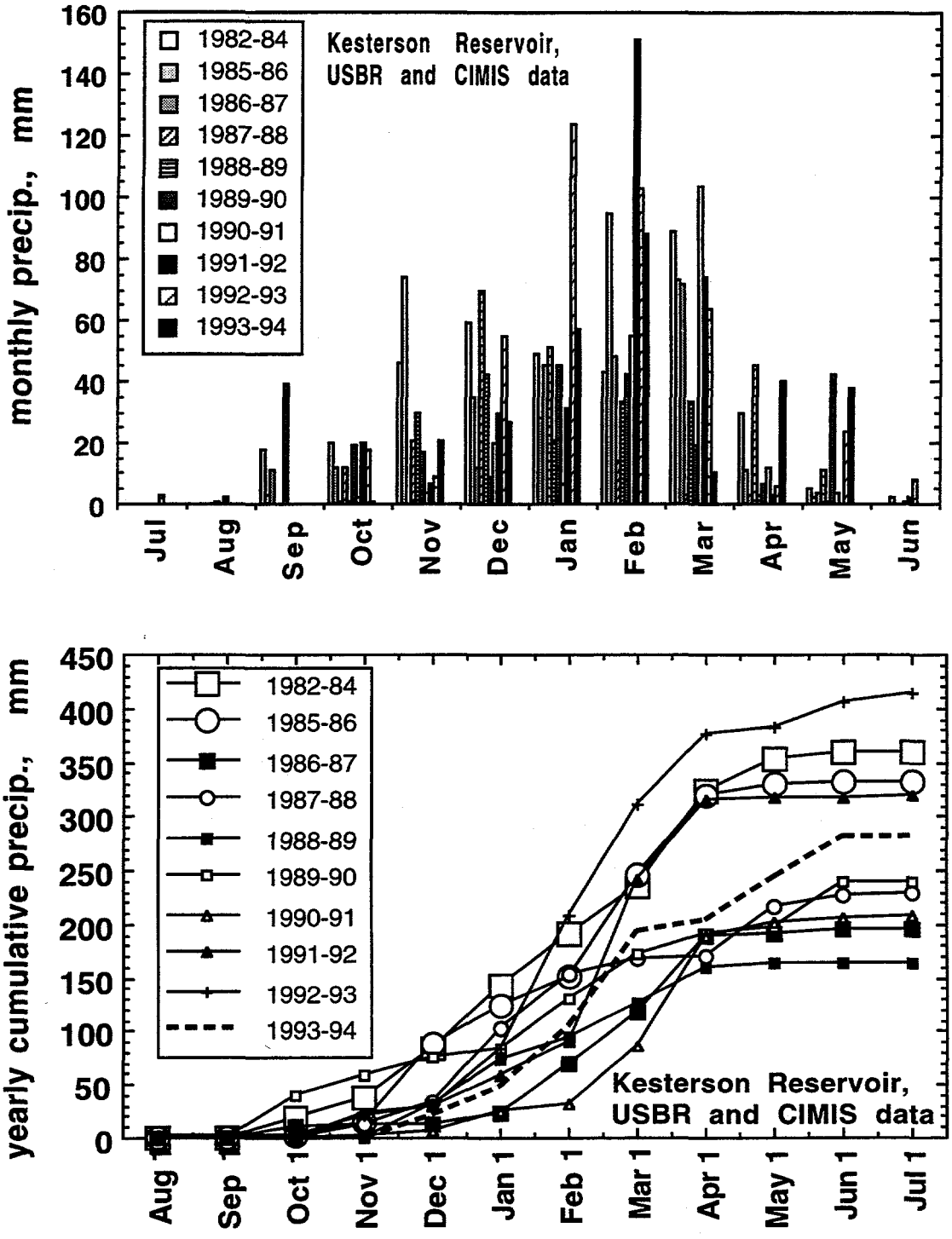

Figure 7.3. **A.** Monthly total rainfalls at Kesterson Reservoir. **B.** Cumulative yearly rainfall.

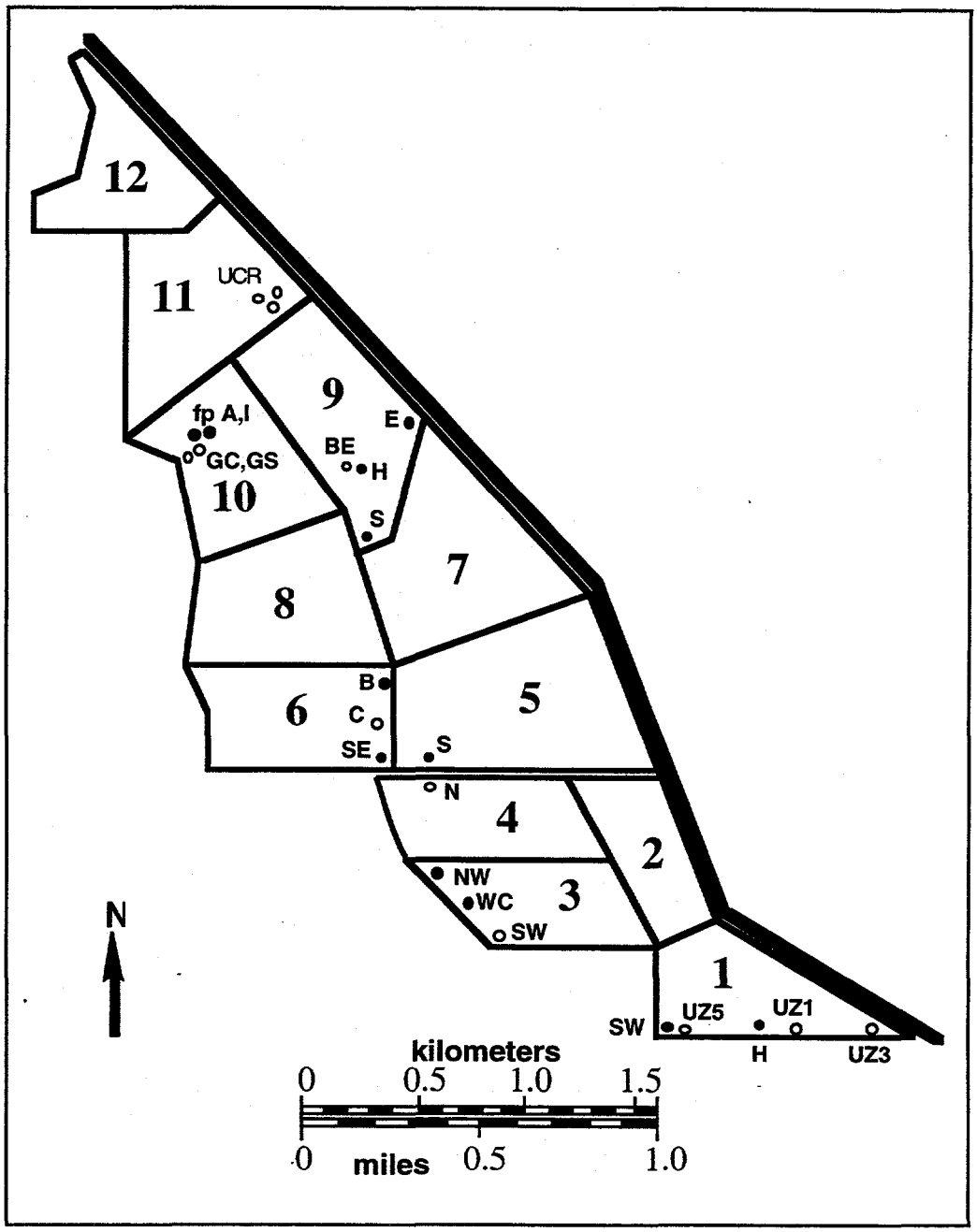

Figure 7.4. Locations of LBL ephemeral pool sampling sites.

7.2.1 Ephemeral pools in sites filled with imported soil

To date, no evidence for surfacing of the water table above fill soils has been encountered. Ponding still will occur when rainfall rates exceed infiltration and evaporation rates. Ephemeral pools formed by rainfall ponding on imported fill soil tend to be low in Se concentrations and in

salinity. The favorable surface water quality reflects less seleniferous and less saline imported surface soils, and leaching of soluble Se and salts below the near-surface zone. Filled sites at which ephemeral pool monitoring was conducted are denoted by the solid symbols in Figure 4. Pond 1 pool waters from site P1 fp H, and site P1 fp SW are typical of these environments. Significant ponding occurred at these sites in early 1992 and early 1993 only. Maximum pool depths at these sites were about 150 mm (6 inches). Time trends of pool water Se, EC, and the [Se]/EC ratio for these sites are shown in Figures 5A-5C. Selenium concentrations in these waters are low, typically remaining below the 5 ppb surface water quality goal. Fluctuations in absolute Se concentrations are small, and probably reflect a combination of analytical uncertainties and complex spatial and temporal heterogeneities within pool-sediment systems (Fig. 5A). Salinities in these waters are also typically low (EC < 1 dS/m), although general time trends show increases in EC indicating evaporative accumulation of salts (Figure 5B). The [Se]/EC ratios in these sites are typically noisy, reflecting uncertainties and variability in the low Se concentrations (Fig. 5C).

7.2.2 Ephemeral pools in sites filled with mixtures of Kesterson and imported soils

Some filled sites contain appreciable amounts of the original Kesterson Reservoir surface soils. Areas along the western portion of Pond 3 fall into this category based on field observations of soil characteristics. Rainfall ponding over these sites can result more seleniferous pools, reflecting exchanges with seleniferous surface soils (Figure 6A). The 5 ppb surface water quality goal is indicated by the horizontal line in this figure, and also in similar figures for the two pool categories to be described later. In sites containing appreciable amounts of the original Kesterson Reservoir soils, Se concentrations in pools can be very high during early stages of ponding. Sites with restricted infiltration are especially susceptible to high initial Se concentrations since leaching of soluble Se to depths significantly below the surface is limited. Soluble Se within the near-surface region may still diffuse up into ephemeral pool waters if reduction to adsorbed selenite or precipitation in selenite or elemental Se forms does not proceed at a sufficient rate. Selenium concentrations in these pools typically decline with time, although water quality goals are not necessarily met, even at long times (Fig. 6A). About half of the monitored sites in mixed-fill environments had Se concentrations exceeding the 5 ppb goal throughout the ponding period. Recent laboratory experiments have shown that changes in selenium concentrations in hydrostatically ponded waters may be attributed primarily to diffusive exchanges with surface sediments. When Se reduction rates within sediments are low, diffusion rates for Se transfer from pools back into sediments will also be low. Rates of selenate and selenite reduction are expected to be lower during the winter months, since temperatures in surface sediments will be at their lowest. Salinities in ephemeral pool waters in these

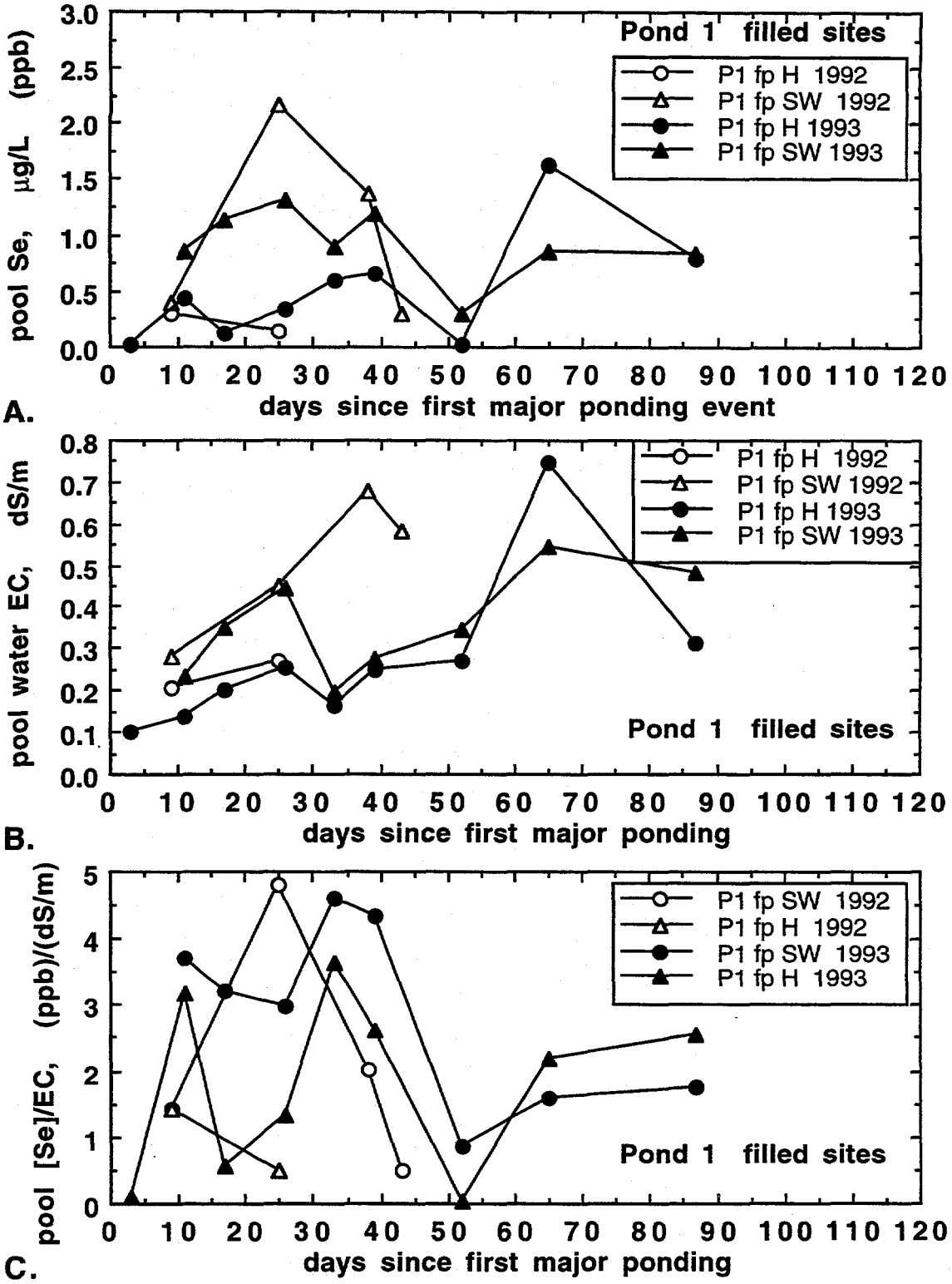

Figure 7.5. Examples of surface water quality in ephemeral pools formed over imported fill soil. Time trends for (**A**) selenium concentrations, (**B**) salinity (EC), and (**C**) [Se]/EC ratios.

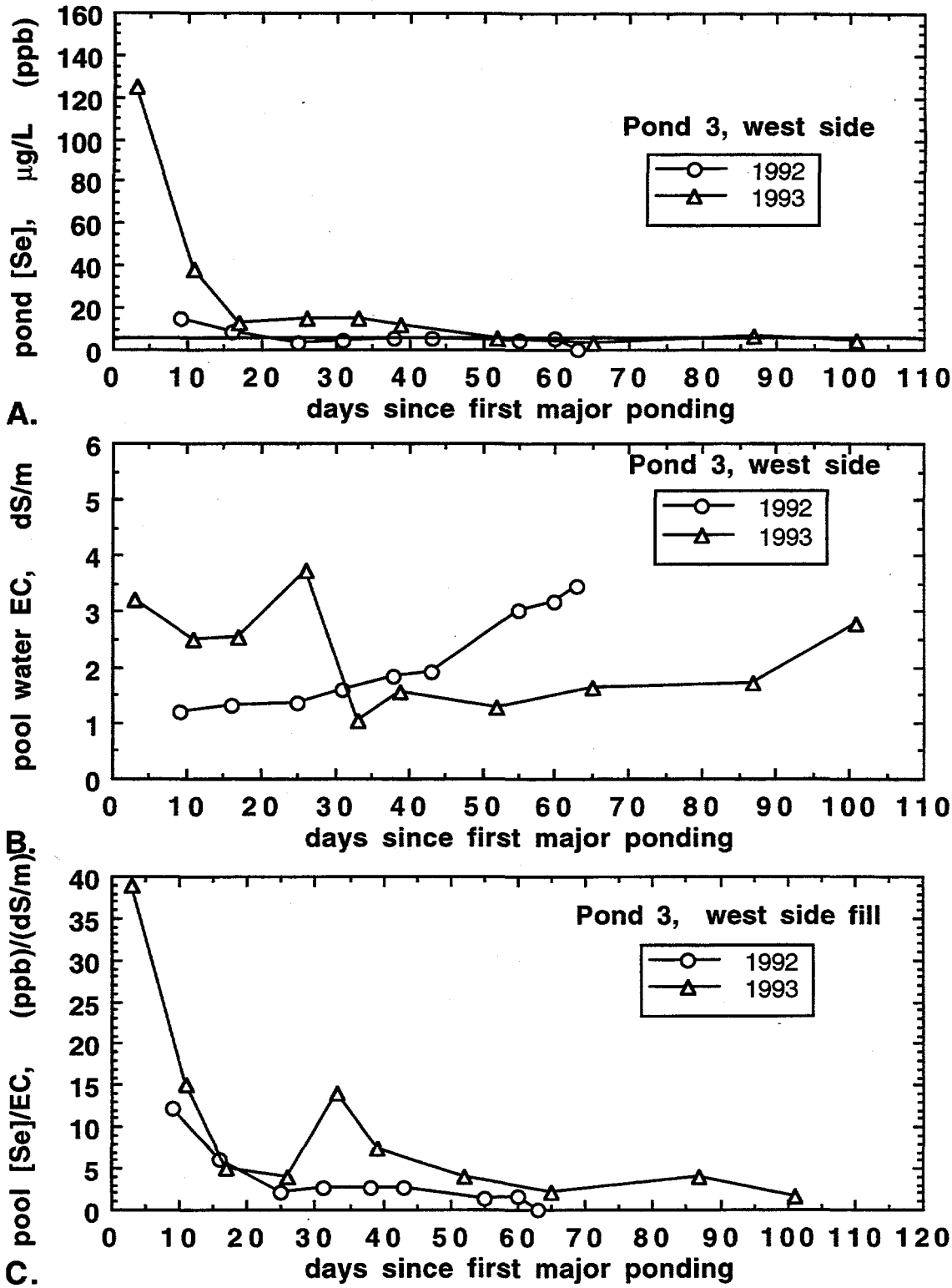

Figure 7.6. Examples of surface water quality in ephemeral pools formed over mixtures of imported fill and original Kesterson Reservoir soils. Time trends for (**A**) selenium concentrations (with surface water quality goal of 5 ppb indicated by the horizontal line), (**B**) salinity (EC), and (**C**) [Se]/EC ratios.

environments are variable, but still typically have low initial values trending to higher salinities due to net evaporative salt concentration during the ponding period (Fig. 6B). Ratios of [Se]/EC in these waters typically show significant declines during the ponding period, indicating net removal of Se relative to freely soluble major ions (Fig. 6C).

7.2.3 Ephemeral pools in unfilled, upland soils

Some sites where ponding commonly occurred consisted of upland surface depressions. These included some experimental and monitoring areas which were left unfilled (despite possibly being below the target fill elevation) for continuation of research activities. Sites which fit this description, and which were monitored for surface water quality are shown in the open circle symbols in Figure 4. Unfilled sites which represented rainfall ponding in upland areas included site SW in Pond 3, site C in Pond 6, and site UCR in Pond 11. During some years, this latter site may fit better in the unfilled, lowland category. These upland sites are hydrologically identical to local natural vernal pools. They are chemically distinct from local natural vernal pools because of formation on Se-contaminated soils. Since these ephemeral pools form directly on original Kesterson Reservoir soils, surface water quality will reflect this association. The Pond 11 UCR pools are the largest, and most persistent examples in this category. Time trends for pool water Se, salinity, and [Se]/EC ratios at the Pond 11 UCR pools are presented in Figures 7A-C. Pools formed from rainfall ponding on upland soils are initially fairly dilute with respect to solutes since ponding is preceded by leaching. Here, pool water Se concentrations are initially at about the limit of surface water goals, but steadily increase with time (Fig. 7A). Similar increasing concentration trends for major ions are reflected in the EC data (Fig. 7B). When normalized to salinities, the 1992 data show a decrease in the [Se]/EC followed by an increase, while the 1993 data indicate decreases followed by constant values (Fig. 7C). Increases and decreases in the [Se]/EC ratios with time probably reflect pool-soil exchanges resulting from net Se oxidation and net Se reduction, respectively, in the near-surface soil. Experimental work supporting this hypothesis is briefly described later.

7.2.4 Ephemeral pools in unfilled sites experiencing surfacing of the water table

Other experimental and monitoring areas which were left unfilled (despite being below the target fill elevation) were influences by a combination of shallow water table rise and rainfall ponding. Sites which fit this description (again, shown in the open circle symbols in Figure 4) include the UZ sites in Pond 1, site BE in Pond 9, and sites GC and GS in Pond 10. These are current or former LBL soil monitoring areas. Whether or not site N in Pond 4 falls into this category or the previous one was not clear. The temporal distribution of rainfall relative to water table rise can be an important influence on pool water quality in these systems. Lack of sufficient early season rains provides greater opportunities for upwards displacement of

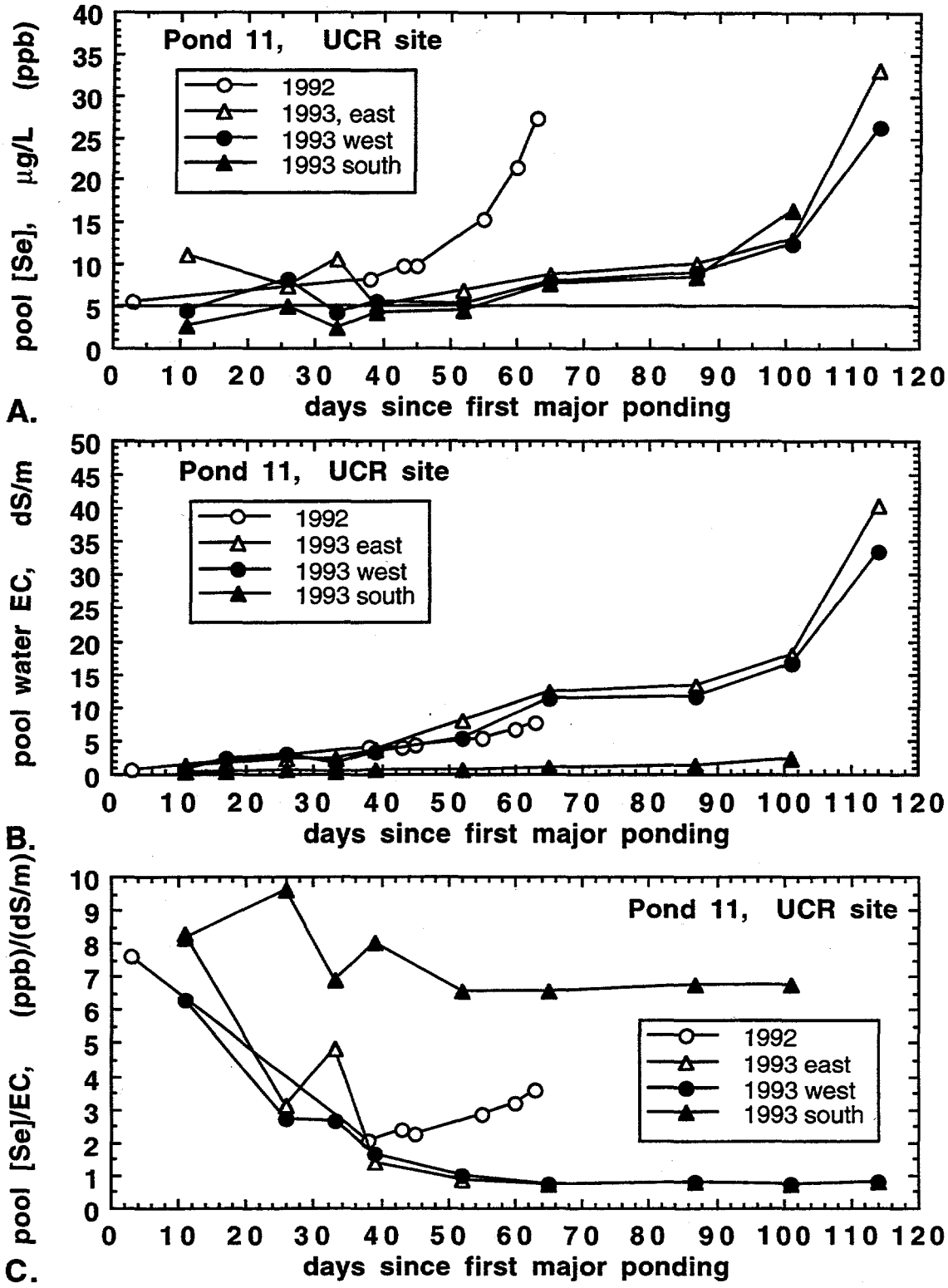

Figure 7.7. Examples of surface water quality in ephemeral pools formed over upland Kesterson Reservoir soils at site P11-UCR. Time trends for (**A**) selenium concentrations (with surface water quality goal of 5 ppb indicated by the horizontal line), (**B**) salinity (EC), and (**C**) [Se]/EC ratios.

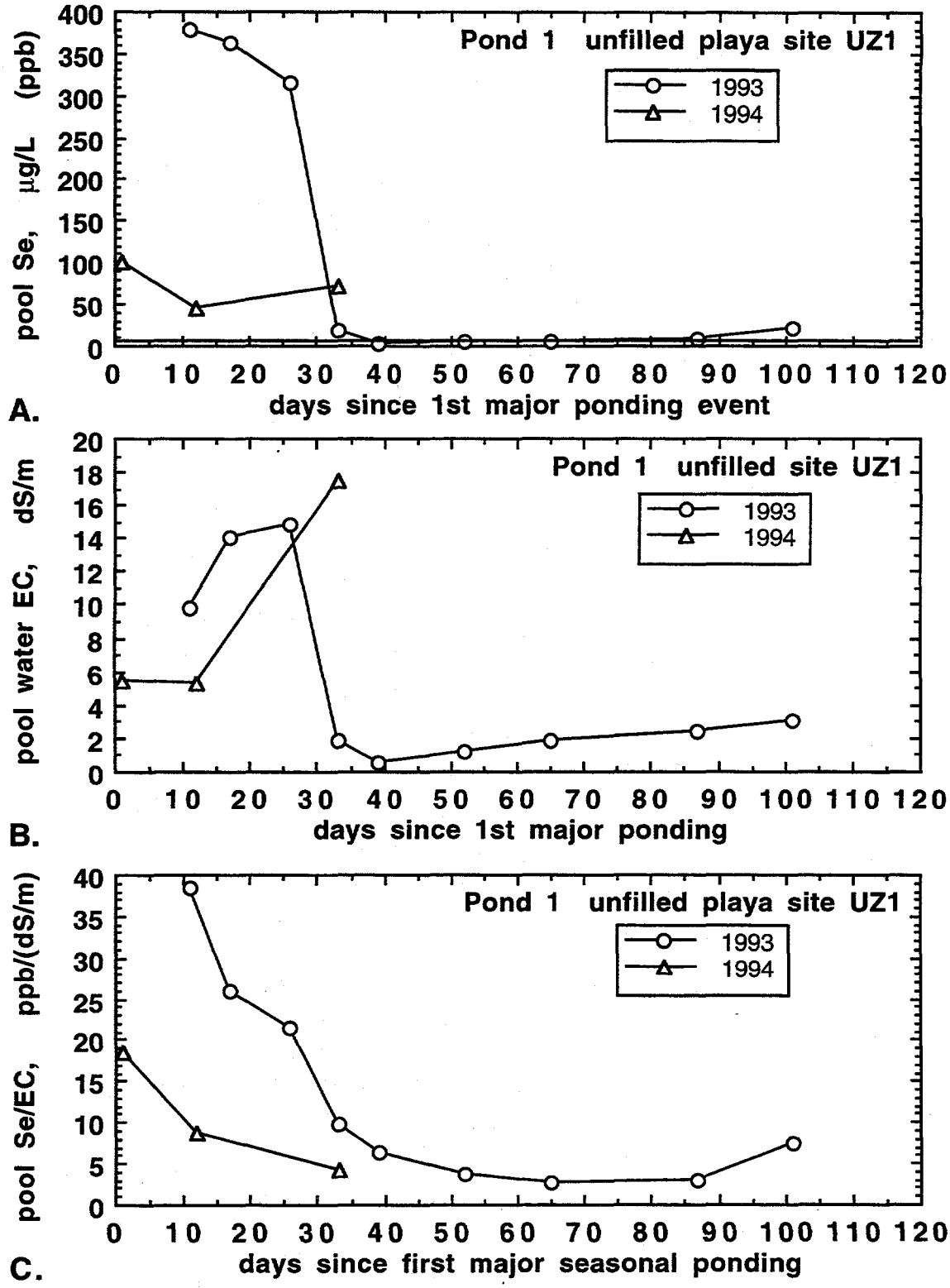

Figure 7.8. Examples of surface water quality in ephemeral pools formed over lowland Kesterson Reservoir soils subject to water table rise (site P1-UZ1). Time trends for (**A**) selenium concentrations (with surface water quality goal of 5 ppb indicated by the horizontal line), (**B**) salinity (EC), and (**C**) [Se]/EC ratios.

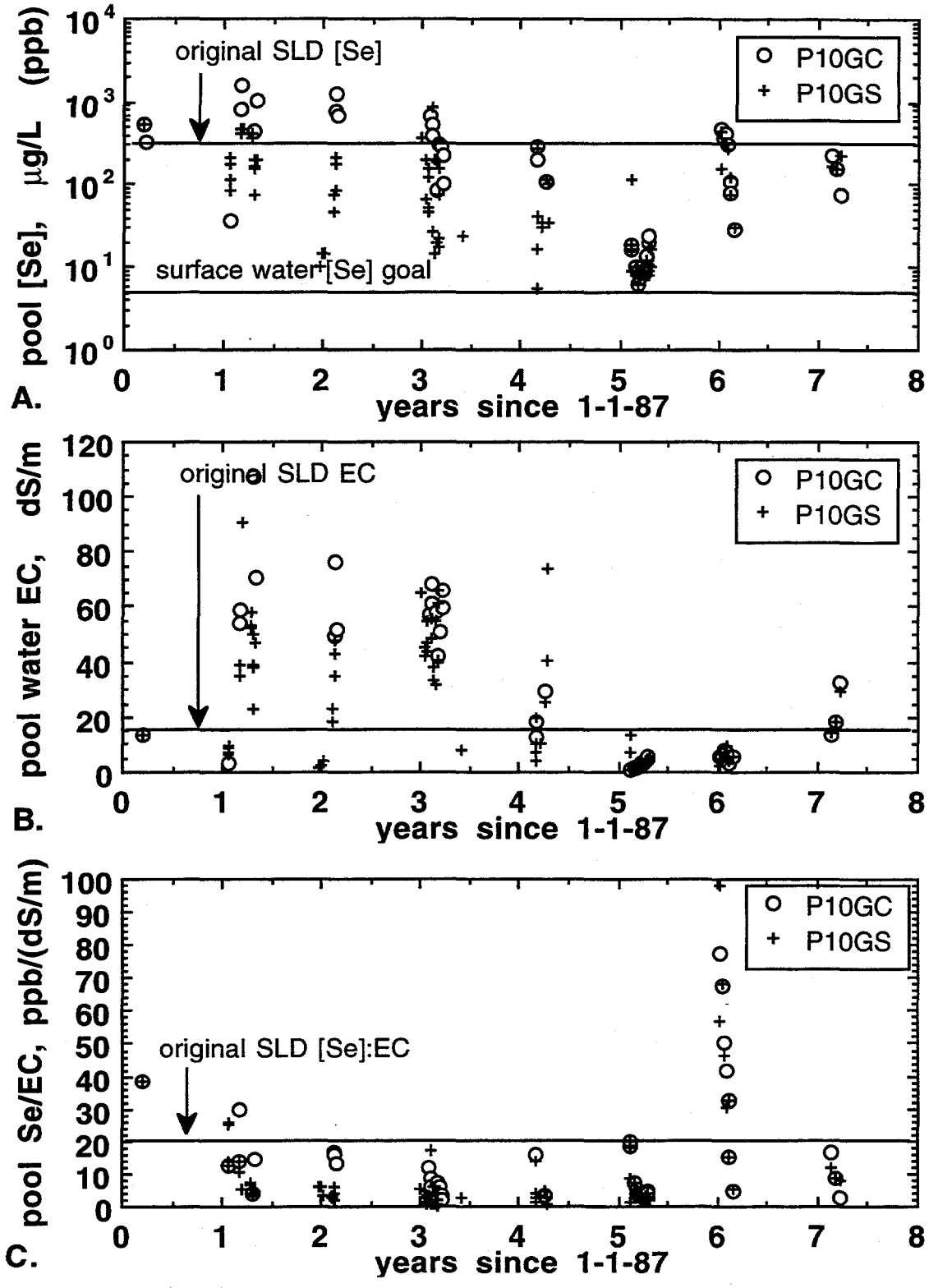

Figure 7.9. Surface water quality in ephemeral pools formed over lowland Kesterson Reservoir soils subject to water table rise (sites P10GC,GS). Time trends for (A) selenium concentrations, (B) salinity (EC), and (C) [Se]/EC ratios.

seleniferous soil pore waters into ephemeral pools (recall Figure 2). On the other hand, larger amounts of early season rainfall will probably not only pre-leach the soil surface, but also result in Se reduction to insoluble species deeper in the soil profile. This latter effect will diminish the soluble Se inventory available for displacement back up to the surface with the rising water table. Influences from the previous seasons ponding, evaporation, redox history, and solute distributions within soil profiles further complicate predictions of water quality in these ephemeral pools. Data from the Pond 1 UZ1 site are presented in Figures 7.8A-C. Note that initial Se concentrations can be very high (Figure 7.8A). This is expectable when soil pore waters contribute significantly to the ponding waters. Declines in Se concentrations over time primarily reflect rainfall dilution, and transfers of pool Se back into reducing sediments. Pool water salinities can also begin at high values characteristic of soil pore waters, followed by rainfall dilution and evaporative concentration (Figure 7.8B). The [Se]/EC ratio in these pool waters typically exhibits a declining time trend indicative of net Se removal relative to salts (Figure 7.8C). Ephemeral pool data from site P10GC and P10GS have been collected yearly, since 1987. Pool water Se concentrations have gradually decreased up through the 1992 wet season, but the more recent two years have shown reversals in this trend (Fig. 7.9A). The distinctly lower concentrations of Se in these waters during 1992 resulted from greater influences of rainfall dilution, which is also prominently expressed through lower salinities (Fig. 7.9B). Although above-average rainfall in both 1992 and 1993 are reflected in these EC data, note that Se concentrations are disproportionately high in 1993 (Figures 7.9A and 7.9C), suggesting significant soil Se re-oxidation during the preceding dry season. Cycles of Se reduction during each year's ponding are evident upon close inspection of Fig. 7.9C. Within each year's ponding period, the [Se]/EC ratio generally trends downwards.

7.3 Related Laboratory Research

In a previous laboratory experiment, selenium concentrations in waters ponded over Kesterson Reservoir soils decreased rapidly when organic carbon amendments were added (LBL annual report, 1987). Addition of available carbon stimulates microbially mediated Se reduction, resulting in removal of Se from the aqueous phase. More recent laboratory experiments suggest that selenium concentrations in relatively hydrostatic surface waters may be predicted based on exchanges of selenate and selenite at the pool-soil boundary, supplemented with minor selenate to selenite reduction within the ponded waters, and with evaporative concentration (Tokunaga et al., in preparation 1995b). In the absence of advective displacement of seleniferous pore waters by water table rise, soluble Se within the near-surface region can diffuse up into ephemeral pool waters if reduction to adsorbed selenite or precipitation in selenite and/or elemental Se forms

does not proceed at a sufficient rate. The depth-distribution of decomposable organic matter within the near-surface soil was also shown to strongly influence pool water Se concentrations. Fairly successful predictions of surface water selenate and selenite concentrations based on exchanges with sediments in laboratory columns indicate the importance of sediment-pool interactions. Details of this work are presented in Chapter 4.

7.4 Summary of Observations

Formation of ephemeral pools at Kesterson Reservoir can be expected during average and above-average rainfall years. During average rainfall years, pools will be sparse, small, and short-lived. During above-average rainfall years, a significant area (>10%) of Kesterson Reservoir can experience pool formation. Some of these pools will persist for at least two months. Selenium concentrations in filled sites are usually lower than in unfilled areas. Exceptions to this can be found in sites which were filled with a mixture of imported and native Kesterson Reservoir soils. The most seleniferous pool sites occur in lowlands where the water table intercepts the soil surface. These few sites consist of research/monitoring areas intentionally left unfilled for further study.

7.5 Recommendations

1. Fill-in the remaining open areas which are susceptible to ponding by water table rise. Research conducted at these sites has largely been completed. Only a relatively small area will need to be filled, and this will eliminate the most seleniferous pool environments. The LBL UZ sites in Pond 1, site EP in Pond 8, site BE in Pond 9, and sites GC and GS in Pond 10 will need to be included. Fill-in the Pond 11 UCR site since it now represents the largest persistently ponded area (during wet years) on original Kesterson soils.

2. Provide regular monitoring of a standard set of ephemeral pools during wet seasons. Approximately weekly surface water sampling and brief site descriptions would be obtained at about 20 locations. These locations should include the LBL pool sampling sites (those which still remain after additional filling), and USBR sites. This could be performed by USBR Kesterson field staff. Coordination with CH2M Hill biologists is needed to insure that relevant parameters are measured for determination of impacts on wildlife. Occasional consulting with LBL will also be useful.

3. Look into the availability of an efficient remote-sensing method for determining the spatial extend of ephemeral pools. Current estimates of ponding coverage are very rough, because of vegetation cover.

Table 7.1. Recommendations for ephemeral pool monitoring strategies.

pool type	approximate % of total pool areas	approx. [Se], ppb	salinity	recommendation
imported fill	40	<1 to 10	low	monitor
mixed fill	40	<1 to 50	low	monitor
Kesterson uplands	15	<1 to 50	low	monitor
Kesterson lowlands	5	<1 to 500	high	fill

8.0 Analytical Quality Control

Leon Tsao
Earth Sciences Division
Lawrence Berkeley Laboratory

The Geochemistry Group has had a quality assurance program in operation for eight years, covering chemical analysis for selenium in samples collected from the Kesterson Reservoir. The performance of the analytical program as monitored via quality assurance is presented herein.

8.1 Measurement Statistics

Analytical chemistry has a number of means to judge the quality of the measurements made. Here we are considering the entire measurement process which includes the performance of the analyst and preparation of samples prior to measurement. This means that blind quality control samples must be placed in the sample preparation process. We use standard solutions to gauge accuracy and precision, duplicates to gauge precision with the natural matrix, blanks to gauge contamination and spiked samples or known addition to gauge interference.

8.2 Operations

Selenium analysis is performed by hydride generator atomic absorption spectroscopy (HGAAS). Samples are fed untreated into the instrument to read selenite (SeO_3^{-2}) concentration. Total selenium is here defined as the sum of selenite and selenate (SeO_4^{-2}). It is analyzed by treating a 5.0 ml sample with 0.2 ml of a 2% w/v solution of ammonium persulfate and 5.0 ml of concentrated HCl. Our studies indicate that the concentration of organic forms of selenium in water samples is usually not significant. For selenium analyses it is often necessary, after an initial reading, to dilute samples to bring them into the linear range of reading.

The analyst prepares and runs operational control samples consisting of a continuing calibration standard each 10th analytical sample. There is one operational duplicate, a blank, and one or two spiked samples for each 20 analytical samples. In addition, 15% of the sample load consists of blind quality control samples prepared by the Quality Assurance Manager in containers intended to be indistinguishable from the others. These consist of standards, spiked samples, duplicates, and blanks placed in empty labeled containers provided by the investigators.

Prior to June 9th, 1994, calibration standard solutions of 5, 10, 20, and 40 ppb selenium were prepared fresh daily from a 1000 ppm selenium reference standard obtained from EM Science.

After that date our new hydride generator became operational and the shorter linear range forced us to substitute the 40 ppb calibration standard with one of 30 ppb. Blind standards containing both selenite and selenate are prepared from a stock solution which is prepared from a high concentration or "super" stock solution, which is itself prepared from dry sodium selenite and sodium selenate. The standard solutions used for blind standards are also used for spiking samples.

8.3 Blanks

We distinguish between the instrument limit of detection (ILD) and the method limit of detection (MLD). The ILD is determined by analyzing a series of standards prepared to contain known amounts of the analyte. This has been determined to be 0.25 ppb for selenium. The MLD is determined by analyzing blanks prepared blind in the same manner as any research sample. This year we have considered using the geometric mean rather than the arithmetic mean, when calculating MLDs. This is because the geometric mean makes the rejection of out-of range measurements easier. The MLDs for selenite and total selenium are 0.25 ppb and 0.67 ppb respectively. The method limits of quantification (MLQ) for selenite and total selenium are 1.01 ppb and 3.37 ppb respectively. Since we are now using log-normal statistics for blanks, these values are not strictly comparable to those reported in previous years. Re-calculating limits of detection and quantification for previously reported blank statistics and use of very dilute standards gives values very close to current ones. The limits reported this year are somewhat higher than previously and this is probably due to operator and instrument changes.

8.4 Selenium Standards

We have established standards with both selenite and selenate because speciation of selenium has been important in many of the studies we have performed. Because selenite solutions with concentrations in the range of 40 ppb or less oxidize rapidly we make up each standard from a concentrated stock. We report statistics on total selenium rather than selenate because total selenium is a direct analytical measurement and not a calculated quantity. Selenate concentrations may be calculated from selenite and selenate but this should incorporate the error of both direct measurements. The ratio of selenite to total selenium is useful for control. If the ratio of suspect coupled selenite-total selenium measurements is near the average, error in making up the standard is more likely than otherwise.

Table 8.1 gives the relative deviations of series of repeat measurements of sets of standard solutions run from March 1994 to September 1994. They were run blind to the analyst and subject to all sample preparation procedures. They represent a subset of an entire series, with values measured prior to March 1994 deleted to eliminate the effects of personnel changes.

Table 8.1. Selenium Standard Statistics 2/17/94 - 9/30/94

	Se +4			Σ Se		
Label	Conc. (ppb)	R.D. %	# of analyses	Conc. (ppb)	R.D. %	# of analyses
Se XXI	1.13	19.6	8	2.79	22.3	11
Se XXI B	4.51	12.1	9	11.24	14.1	12
Se XXI C	9.60	4.3	16	23.22	15.3	19
Se XXI D	18.05	4.9	10	46.20	13.3	13
Se XXII A	55.28	3.5	13	128.1	11.0	15
Se XXII B	107.0	7.4	6	222.9	4.4	6

Table 8.2. contains statistics for a similar set of standards run starting in March 1994 and continuing to the present.

Table 8.2. Selenium Standard Statistics 3/16/94 - 9/30/94

	Se+4			Σ Se		
Label	Conc. (ppb)	R.D. %	# of analyses	Conc. (ppb)	R. D. %	# of analyses
Se XXIII A	1.19	13.0	18	2.58	10.3	21
Se XXIII B	4.83	4.5	25	10.00	5.8	27
Se XXIII C	9.86	4.2	25	19.34	6.8	26
Se XXIII D	19.19	4.5	26	39.15	5.5	28
Se XXIV A	56.88	4.0	26	110.8	5.9	30
Se XXIV B	114.9	4.0	25	223.4	5.0	28

The smaller number of analyses of selenite is the result of researchers request for analyses of total selenium only and not due to rejection of more points. The greater relative deviations of total selenium measurements in all standards, in spite of more analyses being performed, is most likely due to divergence generated by sample preparation. The preparation for total selenium analysis involves the transfer of sample solution and addition of reagents which can all introduce volume error. There is also the possibility that the reactions converting selenium to a readable form are incomplete.

8.5 Spike Recoveries

An ongoing drawback in our spike recovery measurements has been the difficulty in knowing *a priori* what the selenium concentrations of many samples are. Ideally the spike of analyte added is equal to the amount of the original analyte. Spikes less than 1/4 or more than 4

times the concentration of the original analyses are not statistically meaningful. Spiked sample analyses which prove to be out of this range are rejected and not used to determine if an analysis is in control. In the year under consideration, 64 selenite analyses and 111 total selenium analyses were in a statistically meaningful range. The difference in the number of analyses performed results from some requests for total selenium analyses only. Our average recovery for a selenite spike was 90.7% and for a total selenium spike it was 99.5%.

Analysis of variance of spiked sample recoveries in earlier time periods has revealed that there are no statistically significant differences in spike recoveries for samples from different sources. Although analysis of variance was not performed on spike sample recoveries for the period reported here, we believe this continues to be the case.

8.6 Duplicates

Duplicates provide a measure of our analytical precision which includes factors such as foaming, which repeated measurements of standards do not reflect. Duplicates with at least one of the values less than the MLQ were discarded, giving 99 selenite and 153 total selenium duplicates used to calculate the averages given below. The difference in the number of analyses performed results from some requests for total selenium analyses only, as well as highly oxidized samples. The average relative difference in for duplicate selenite analyses in the period covered by this report was 8.2 % for selenite and 6.2 % for duplicate total selenium analyses.

8.7 Completion

In the year just ended, the analytical chemistry laboratory experienced personnel and instrument difficulties which resulted in some degradation of analytical quality. Our quality assurance program allowed us to detect and reject all problematic analyses. However, in a few cases it proved impossible to recover the data. In FY 1994 we received 2987 samples for selenite analysis and analyzed all of them for a completion rate of 100%. In the same period we received 3977 samples for total selenium analysis and analyzed 3973 for a completion rate of 99.9%.

9.0 References

Abrams, M.M., R.G. Burau, and R.J. Zasoski. 1990. Organic selenium distribution in selected California soils. Soil Sci. Soc. Am. J. 54:979-982.

Anderson, M.S., H.W. Lakin, K.C. Beeson, F.F. Smith, and E. Thacker. 1961. Selenium in agriculture. Agricultural Handbook No. 200. Agric. Res. Service, U.S. Dept. Agric. Government Printing Office, Washington, D.C.

Bajt, S., S.B. Clark, S.R. Sutton, M.L. Rivers, and J.V. Smith. 1993. Synchrotron x-ray microprobe determination of chromate content using x-ray absorption near-edge structure. Anal. Chem. 65:1800-1804.

Balistrieri, L.S., and T.T. Chao. 1987. Selenium adsorption by goethite. Soil Sci. Soc. Am. J. 51:1145-1151.

Bar-Yosef, B., and D. Meek. 1987. Selenium sorption by kaolinite and montmorillonite. Soil Sci. 144:11-19.

Barbour, M.G., and J. Major, editors. 1988. Terrestrial Vegetation of California, New expanded edition. California Native Plant Society, Special Publication No. 9. Sacramento, CA.

Beckett, P.H.T. 1989. The use of extractants in studies on trace metals in soils, sewage sludges, and sludge-treated soils. Adv. Soil Sci. 9:143-176.

Belzile, N., P. Lacomte, and A. Tessier. 1989. Testing readsorption of trace elements during partial chemical extractions of bottom sediments. Environ. Sci. Tech. 23:1015-1020.

Benson, S.M., T.K. Tokunaga, P.T. Zawislanski, and C. Wahl. 1994. Mechanisms and rates of selenium remobilization and transport in selenium contaminated soils. Submitted to American Chemical Society.

Benson, S.M., A.F. White, S. Halfman, S. Flexser, and M. Alavi. 1991. Groundwater contamination at Kesterson Reservoir, California 1. Hydrogeologic setting and conservative solute transport. Water Resour. Res. 27:1071-1084.

Benson, S.M., M. Delamore, and S. Hoffman. 1990. Kesterson Crisis: Sorting out the facts. In S.C. Harris (ed.) Irrigation and Drainage Proceedings of the 1990 National Conference. American Society of Civil Engineers. New York.

Bertin, E.P. 1978. Introduction to X-Ray Spectrometric Analysis. 485 p. Plenum Press, New York.

Bertsch, P.M., D.B. Hunter, S.R. Sutton, S. Bajt, and M.L. Rivers. 1994. In-situ chemical speciation of uranium in soils and sediments by micro x-ray absorption spectroscopy. Envir. Sci. Tech. : .

Black, C.A. 1968. Soil-Plant Relationships. 2nd ed. J. Wiley and Sons, Inc., New York.

Brock, T.D. 1974. Biology of Microorganisms. Prentice-Hall, Inc., Englewood Cliffs, New Jersey.

Brown, G.E., Jr., G. Calas, G.A. Waychunas, and J. Petiau. 1988. X-ray absorption spectroscopy and its applications in mineralogy and geochemistry. Rev. Mineral. 18:431-512.

Brown, G.E., Jr. and G.A. Parks. 1989. Synchrotron-based x-ray absorption studies of cation environments in earth materials. Rev. Geophys. 27:519-533.

Blet-Charaudeau, C., J. Muller, and H. Laudelout. 1990. Kinetics of carbon dioxide evolution in relation to microbial biomass and temperature. Soil Sci. Soc. Am. J. 54:1324-1328.

Buyanovsky, G.A., M. Aslam, and G.H. Wagner. 1994. Carbon turnover in soil physical fractions. Soil Sci. Soc. Am. J. 58:1167-1173.

Buyanovsky, G.A., G.H. Wagner, and C.J. Gantzer. 1986. Soil respiration in a winter wheat ecosystem. Soil Sci. Soc. Am. J. 50:338-344.

Chao, T.T., and R.F. Sanzalone. 1989. Fractionation of soil selenium by sequential partial dissolution. Soil Sci. Soc. Am. J. 53:385-392.

Christensen, B.T., F. Bertelsen, and G. Gissel-Nielsen. 1989. Selenite fixation by soil particle-size separates. J. Soil Sci. 40:641-647.

CH2M Hill. 1991. Kesterson Reservoir Biological Report (Draft). U.S. Bureau of Reclamation Mid Pacific Region.

Currie, J.A. 1961. Gaseous diffusion in the aeration of aggregated soils. Soil Sci. 92:40-45.

Currie, J.A. 1965. Diffusion within soil microstructure. A structural parameter for soils. J. Soil Sci. 16:279-289.

Cussler, E.L. 1984. Duffusion: Mass Transfer in Fluid Systems. Cambridge Univ. Press, Cambridge.

Cutter, G.A., and K.W. Bruland. 1984. The marine biogeochemistry of selenium: A re-evaluation. Limnol. Oceanogr. 29:1179-1192.

Davison, W., H. Zhang, and G.W. Grime. 1994. Performance characteristics of gel probes used for measuring the chemistry of pore waters. Environ. Sci. Technol. 28:1623-1632.

Doran, J.W. 1982. Microorganisms and the biological cycling of selenium. Adv. Microbial Ecology 6:1-32.
Doran, J.W. and M. Alexander. 1977. Microbial transformations of selenium. Appl. Env. Microbiol. 33:31-37.
Ellert, B.H. and J.R. Bettany. 1992. Temperature dependence of net nitrogen and sulfur mineralization. Soil Sci. Soc. Am. J. 56:1133-1141.
Elrashidi, M.A., D.C. Adriano, S.M. Workman, and W.L. Lindsay. 1987. Chemical equilibria of selenium in soils: A theoretical development. Soil Science 144:141-152.
Flaschka, H.A., Barnard, A.J., and P.E. Storrock. 1969. Quantitative Analytical Chemistry Vol. 1, Barnes and Noble. New York.
Frankenberger, W.T., Jr., and S.M. Benson, (eds.). 1994. Selenium in the Environment. Marcel Dekker, Inc. New York.
Frankenberger, W.T. and U. Karlson. 1988. Dissipation of soil selenium by microbial volatilization at Kesterson Reservoir. Final report to the U.S. Bureau of Reclamation.
Freney, J.R., O.T. Denmead, and J.R. Simpson. 1979. Nitrous oxide emission from soils at low moisture contents. Soil Biol. Biochem. 11:167-173.
Fujii, R., S.J. Deverel, and D.B. Hatfield. 1988. Distribution of selenium in soil in agricultural fields, western San Joaquin Valley, California. Soil Sci. Soc. Am. J. 52:1274-1283.
Geering, H.R., E.E. Cary, L.H. Jones, and W.H. Allaway. 1968. Solubility and redox criteria for the possible forms of selenium in soils. Soil Sci. Soc. Am. Proc. 32:35-40.
George, G.N., and M.L. Gorbaty. 1989. Sulfur K-edge absorption spectroscopy of petroleum asphaltenes and model compounds. J. Am. Chem. Soc. 111:3182-3186.
Giauque, R.D., R.B. Garrett, and L.Y. Goda. 1977. Determination of forty elements in geochemical samples and coal fly ash by x-ray fluorescence spectrometry. Anal. Chem. 49:1012-1017.
Gilliom, R.J. 1989. Preliminary assessment of sources, distribution, and mobility of selenium in the San Joaquin Valley, California. Water-Resources Investigations Report 88-4186. U.S. Geological Survey, Sacramento, CA.
Gruebel, K.A., J.A. Davis, and J.O. Leckie. 1988. The feasibility of using sequential extraction techniques for arsenic and selenium in soils and sediments. Soil Sci. Soc. Am. J. 52:390-397.
Hamdy, A.A., and G. Gissel-Nielsen. 1977. Fixation of selenium by clay minerals and iron oxides. Z. Pflanzenernaehr. Bodenkd. 140:63-70.
Hayes, K.F., A.L. Roe, G.E. Brown, Jr., K.O. Hodgsen, J.O. Leckie, and G.A. Parks. 1987. In-situ x-ray absorption study of surface complexes: Selenium oxyanions on a-FeOOH. Science 238:783-786.
Hillel, D. 1980. Fundamentals of Soil Physics. Academic Press, New York.
Hingston, F.J., A.M. Posner, and J.P. Quirk. 1971. Competitive adsorption of negatively charged ligands on oxide surfaces. Faraday Soc. Disc. 52:334-342.
Huang, P.M., L.S. Crossan, and D.A. Rennie. 1968. Chemical dynamics of K release from potassium minerals common in soils. Trans. Int. Congr. Soil Sci., 9th. 2:705-712.
Iversen, N., and B.B. Jorgensen. 1993. Diffusion coefficients of sulfate and methane in marine sediments: Influence of porosity. Geochim. Cosmochim. Acta 57:571-578.
Jacob, C.E., and S.W. Lohman. 1952. Nonsteady flow to a well of constant drawdown in an extensive aquifer. Trans. Am. Geophys. Union 33:559-569.
Jacobs, L.W. (ed.). 1989. Selenium in Agriculture and the Environment. SSSAJ Special Publ. No. 23. Am. Soc. Agron. Madison, WI.
Jones, K.W., and B.M. Gordon. 1989. Trace element determinations with synchrotron-induced x-ray emission. Anal. Chem. 61:341A-358A.
Kheboian, C, and C.F. Bauer. 1987. Accuracy of selective extraction procedures for metal speciation in model aquatic sediments. Anal. Chem. 59:1417-1423.
Klute, A. 1986. Water retention: Laboratory methods. *In*: Methods of Soil Analysis, Part 1 - Physical and Mineralogical Methods. A. Klute, ed. 2nd ed. Agronomy, 9, pp. 635-662.
Koningsberger, D.C., and R. Prins. 1988. X-ray Absorption: Principles, Applications, Techniques of EXAFS, SEXAFS and XANES. John Wiley and Sons, New York.
Lawrence Berkeley Laboratory. 1987. Kesterson Reservoir Annual Report. LBL-24250. Berkeley, CA.
Lawrence Berkeley Laboratory. 1988. Hydrological, Geochemical, and Ecological Characterization of Kesterson Reservoir. Annual Report. LBL-26438. Berkeley, CA.
Lawrence Berkeley Laboratory. 1990a. Hydrological, Geochemical, and Ecological Characterization of Kesterson Reservoir. Annual Report. October 1, 1988-September 30th, 1989. LBL-27993. Berkeley, CA.
Lawrence Berkeley Laboratory. 1990b. Hydrological and Geochemical Investigations of Selenium Behavior at Kesterson Reservoir. Annual Report. October 1, 1989-September 30th, 1990. LBL-29689. Berkeley, CA.
Lawrence Berkeley Laboratory. 1992. Hydrological and Geochemical Investigations of Selenium Behavior at Kesterson Reservoir. Annual Report. October 1, 1990-September 30th, 1992. LBL-33532. Berkeley, CA.

Leffelaar, P.A. 1986. Dynamics of partial anaerobiosis, denitrification, and water in a soil aggregate: experimental. Soil Sci. 142:352-366.

Leffelaar, P.A. 1993. Water movement, oxygen supply and biological processes on the aggregate scale. Geoderma 57:143-165.

Lindberg, R.D. and D.D. Runnells. 1984. Groundwater redox reactions: An analysis of equilibrium state applied to Eh measurements and geochemical modeling. Science 225:925-927.

Lipton, D.S. 1991. Associations of selenium in inorganic and organic constituents of soils from a semi-arid region. Ph.D. Thesis. University of California, Berkeley.

Long, R.H.B., S.M. Benson, T.K. Tokunaga, and A. Yee. 1990. Selenium immobilization in a pond sediment at Kesterson Reservoir. J. Environ. Qual. 19:302-311.

Long, R.H.: 1988. Analysis of selenium and chloride movement through a shallow pond sediment at Kesterson Reservoir. M.S. Thesis. University of California, Berkeley, CA.

Lortie, L., W.D. Gould, S. Rajan, R.G.L. McCready, and K.-J. Cheng. 1992. Reduction of selenate and selenite to elemental selenium by a *Pseudomonas stutzeri* isolate. Appl. Environ. Microbiol. 58:4042-4044.

Luoma, S.N., C. Johns, N.S. Fisher, N.A. Steinberg, R.S. Oremland, and J.R. Reinfelder. 1992. Determination of selenium bioavailability to a benthic bivalve from particulate and solute pathways. Environ. Sci. Technol. 26:485-491.

Macy, J.M., T.A. Michel, and D.G. Kirsch. 1989. Selenate reduction by a *Pseudomonas* species: a new mode of anaerobic respiration. Fed. Euro. Microbio. Soc. (FEMS) Microbiol. Lett. 61:195-198.

Marion, G.M. and C.H. Black. 1987. The effect of time and temperature on nitrogen mineralization in arctic tundra soils. Soil Sci. Soc. Am. J. 51:1501-1508.

Masscheleyn, P.H., R.D. Delaune, and W.H. Patrick. 1990. Transformations of selenium as affected by sediment oxidation-reduction potential and pH. Environ. Sci. Technol. 24:91-96.

McBride, M.B. 1994. Environmental Chemistry of Soils. Oxford University Press. New York.

Mead, R. 1988. The Design of Experiments: Statistical Principles for Practical Applications. Cambridge University Press. New York.

Mikkelsen, R.L., D.S. Mikkelsen, and A Abshahi. 1989. Effects of soil flooding on selenium transformations and accumulation by rice. Soil Sci. Soc. Am. J. 53:122-127.

Nazar, P.G. 1990. Soil Survey of Merced County, California, Western Part. U.S. Dept. Agriculture, Soil Conservation Service. U.S. Government Printing Office.

Neal, R.H., G. Sposito, K.M. Holtzclaw, and S.J. Traina. 1987. Selenite adsorption on alluvial soils: I. Soil composition and pH effects. Soil Sci. Soc. Am. J. 51:1161-1165.

Nelson, D.W. and L.E. Sommers. 1982. Total carbon, organic carbon, and organic matter. *In*: Methods of Soil Analysis, Part 2 - Chemical and Microbiological Properties. A.L. Page, R.H. Miller, and D.R. Keeney, eds. 2nd ed. Agronomy, 9, pp. 539-579.

Ogwada, R.A., and D.L. Sparks. 1986. A critical evaluation on the use of kinetics for determining thermodynamics of ion exchange in soils. Soil Sci. Soc. Am. J. 50:300-305.

Ohlendorf, H.M. 1989. Bioaccumumation and effects of selenium in wildlife. In Selenium in Agriculture and the Environment, Soil Sci. Soc. Am. Special Pub. 23.

Onken, A.B. and R.L. Matheson. 1982. Dissolution rate of EDTA-extractable phosphate from soils. Soil Sci. Soc. Am. J. 46:276-279.

Oremland, R.S., J.T. Hollibaugh, A.S. Maest, T.S. Presser, L.G. Miller, and C.W. Culbertson. 1989. Selenate reduction to elemental selenium by anaerobic bacteria in sediments and culture: Biogeochemical significance of a novel sulfate-independent respiration. Appl. Environ. Microbiol. 55:2333-2343.

Oremland, R.S., N.A. Steinberg, A.S. Maest, L.G. Miller, and J.T. Hollibaugh. 1990. Measurement of in situ rates of selenate removal by dissimilatory bacterial reduction in sediments. Environ. Sci. Technol. 24:1157-1164.

Parkin, T.B. 1987. Soil microsites as a source of denitrification variability. Soil Sci. Soc. Am. J. 51:1194-1199.

Pickering, I.J., G.E. Brown, Jr., and T.K. Tokunaga. 1994. X-ray absorption spectroscopy of selenium-contaminated soils. Stanford Synchrotron Radiation Laboratory 1993 Activity Report. Stanford University, Stanford, CA.

Poister, D., and T.K. Tokunaga. 1992. Selenium in Kesterson Reservoir ephemeral pools formed by groundwater rise: II. Laboratory experiments. J. Environ. Qual. 21:252-258.

Presser, T.S., and I. Barnes. 1985. Selenium concentrations in waters tributary to and in the vicinity of the Kesterson National Wildlife Refuge, Fresno and Merced counties, California. Water-Resources Investigations Report 84-4220. U.S. Geological Survey, Menlo Park, CA.

Reamer, D.C., and W.H. Zoller. 1980. Selenium biomethylation products from soil and sewage sludge. Science (Washington, D.C.) 208:500-502.

Rivers, M.L., S.R. Sutton, K.W. Jones. 1991. Synchrotron x-ray fluorescence microscopy. Synchrotron Radiation News 4:23-26.

Robinson, R.A., and R.H. Stokes. 1959. Electrolytic Solutions. Butterworths, London.
Rosenfeld, I., and O.A. Beath. 1964. Selenium geobotany, biochemistry, toxicity, and nutrition. Academic Press, New York.
Runnells and Lindberg (1990) Selenium in aqueaous solutions: The impossibility of obtaining meaningful Eh using a platinum electrode, with implications for modeling natural waters. Geology 18:212-215.
Santschi, P., P. Hohener, G. Benoit, and M. Bucholtz-ten-Brink. 1990. Chemical processes at the sediment-water interface. Mar. Chem. 30:269-315.
Sallam, A., W.A. Jury, and J. Letey. 1984. Measurement of gas diffusion coefficient under relatively low air-filled porosity. Soil Sci. Soc. Am. J. 37:189-193.
Schnitzer, M. 1982. Organic matter characterization. *In*: Methods of Soil Analysis, Part 2 - Chemical and Microbiological Properties. A.L. Page, R.H. Miller, and D.R. Keeney, eds. 2nd ed. Agronomy, 9, pp. 581-594.
Sharma, S., and R. Singh. 1983. Selenium in soil, plant, and animal systems. CRC Crit. Rev. Environ. Control 13:23-50.
Smith, K.A. 1977. Soil aeration. Soil Sci. 123:284-291.
Smith, K.A. 1980. A model of the extent of anaerobic zones in aggregated soils and its potential application to estimates of denitrification. J. Soil Sci. 31:263-277.
Smith, L.P. 1937. Heat flow in an infinite solid bounded internally by a cylinder. J. Appl. Phys. 8:441-448.
Sparks, D.L. 1989. Kinetics of Soil Chemical Processes. Academic Press. San Diego, California.
Sutton, S.R., K.W. Jones, B. Gordon, M.L. Rivers, S. Bajt, and J.V. Smith. 1993. Reduced chromium in olivine grains from lunar basalt 15555: X-ray absorption near edge structure (XANES). Geochim. Cosmochim. Acta 57:461-468.
Sutton, S.R., M.L. Rivers, S. Bajt, and K.W. Jones. 1993a. Synchrotron x-ray fluorescence microprobe analysis with bend magnets and insertion devices. Nucl. Inst. Meth. B75:553-558.
Sutton, S.R., K.W. Jones, B. Gordon, M.L. Rivers, S. Bajt, and J.V. Smith. 1993b. Reduced chromium in olivine grains from lunar basalt 15555: X-ray absorption near edge structure (XANES). Geochim. Cosmochim. Acta 57:461-468.
Sutton, S.R., S. Bajt, D. Schulze, and T. Tokunaga. 1994. Oxidation state mapping using x-ray absorption near edge structure with synchrotron microbeams. Am. Geophys. Union, Fall 1994 Meeting, San Francisco, CA.
Thompson-Eagle, E.T., and W.T. Frankenberger. 1989. Volatilization of selenium from agricultural pond water. J. Environ. Qual. 19:125-131.
Tokunaga, T.K. 1992. The pressure response of the soil water sampler and possibilities for simultaneous soil solution sampling and tensiometry. Soil Sci. 154:171-183.
Tokunaga, T.K., I.J. Pickering, and G.E. Brown, Jr. submitted 1995. X-ray absorption spectroscopy studies of selenium transformations in ponded sediments. Submitted to Soil Sci. Soc. Am. J.
Tokunaga, T.K., S.R. Sutton, and S. Bajt. 1994b. Mapping of selenium concentrations in soil aggregates with synchrotron x-ray fluorescence microprobe. Soil Sci. 158:421-434.
Tokunaga, T.K., S.R. Sutton, and S. Bajt. 1994c. Reduction and diffusion of selenium in soil aggregates: Synchrotron x-ray fluorescence microprobe studies of intra-aggregate chemical heterogeneity formation. Am. Geophys. Union, Chapman Conference on Hydrogeologic Processes: Building and Testing Atomistic- to Basin-scale Models. Lincoln, New Hampshire, June, 1994.
Tokunaga, T.K, P.T. Zawislanski, P.W. Johannis, S. Benson, and D.S. Lipton. 1994. Field investigations of selenium speciation, transformation, and transport in soils from Kesterson Reservoir and Lahontan Valley. In, Selenium in the Environment. W.T. Frankenberger and S. Benson, eds. Marcel Dekker. New York. pp. 119-138.
Tokunaga, T.K., and S.M. Benson. 1992. Selenium in Kesterson Reservoir ephemeral pools formed by groundwater rise: 1. Field studies. J. Environ. Qual. 21:246-251.
Tokunaga, T.K., D.S. Lipton, S.M. Benson, A.Y. Yee, J.M. Oldfather, E.C. Duckart, P.W. Johannis, and K.H. Halvorsen. 1991. Soil selenium fractionation, depth profiles and time trends in a vegetated site at Kesterson Reservoir. Water, Air, and Soil Pollut. 57-58:31-41.
Tu, Q., X.-Q. Shan, and Z.-M. Ni. 1994. Evaluation of a sequential extraction procedure for the fractionation of amorphous iron and manganese oxides and organic matter in soils. Sci. Total Environ. 151:159-165.
USBR 1994 Annual Report to State Water Quality Control Board, in preparation.
USBR (United States Bureau of Reclamation) 1986. Final Environmental Impact Statement. Volume 2. Kesterson Program, Sacramento, Ca.
USBR (United States Bureau of Reclamation). 1984. San Luis Unit, Central Valley Project, Ca. Information Bulletin 1, 2, 3, and 4. USBR. Mid-Pacific Region, Sacramento, Ca.
Warrick, A.W and D.R. Nielsen. 1980. Application of Soil Physics. Academic Press. NY.
Waychunas, G.A., J. Apted, and G.E. Brown, Jr. 1983. X-ray K-edge absorption spectra of Fe minerals in model compounds: near edge structure. Phys. Chem. Minerals 10:1-9.

Waychunas, G.A. 1987. Synchrotron radiation XANES spectroscopy of Ti in minerals: Effects of Ti bonding distances, Ti valence, and site geometry on absorption edge structure. Am. Mineralogist 72:89-101.

Weres, O., A.-R. Jaouni, and L. Tsao. 1989a. The distribution, speciation and geochemical cycling of selenium in a sedimentary environment, Kesterson Reservoir, California, U.S.A. Applied Geochemistry 4:543-563.

Weres, O., G.A. Cutter, A. Yee, R. Neal, H. Moehser, and L. Tsao. 1989b. Section 3500-Se. pp. 3-128 to 3-141. In L.S. Clesceri et al. (ed.0 Standard Methods for the Examination of Water and Wastewater. 17th ed. Am. Public Health Assoc., Washington, D.C.

White, A.F., S.M. Benson, A.W. Yee, H.A. Wollenberg, and S. Flexser. 1991. Groundwater contamination at Kesterson Reservoir, California, Part 2. Geochemical parameters influencing selenium mobility. Water Resour. Res. 27:1085-1098.

Wong, J., F.W. Lytle, R.P. Messmer, and D.H. Maylotte. 1984. K-edge absorption spectra of selected vanadium compounds. Phys. Rev. B Condens. Matter 30:5596-5610.

Wu, Y., A.C. Thompson, J.H. Underwood, R.D. Giauque, K. Chapman, M.L. Rivers, and K.W. Jones. 1990. A tunable x-ray microprobe using synchrotron radiation. Nucl. Instrum. Methods Phys. Res. A291:146-151.

Xu, X, J.L. Nieber, and S.C. Gupta. 1992. Compaction effect on the gas diffusion coefficient in soils. Soil Sci. Soc. Am. J. 56:1743-1750.

Zawislanski, P.T., T.K. Tokunaga, S.M. Benson, J.M. Oldfather, and T.N. Narasimhan. 1992. Bare soil evaporation and solute movement of selenium in contaminated soils at Kesterson Reservoir. J. Environ. Qual. 21:447-457.

Zehr, J.P., and R.S. Oremland. 1987. Reduction of selenate to selenide by sulfate-respiring bacteria: Experiments with cell suspensions and estuarine sediments. Appl. Environ. Microbiol. 53:1365-1369.

Zieve, R., and P.J. Peterson. 1981. Factors influencing the volatilization of selenium from soil. Sci. Total Environ. 19:277-284.